New immunomodulatory roles of lymphatic endothelium and implications for immunotherapy

THÈSE N^{O} 6967 (2016)

PRÉSENTÉE LE 29 AVRIL 2016

À LA FACULTÉ DES SCIENCES DE LA VIE
LABORATOIRE DE RECHERCHE INTÉGRATIVE DU SYSTÈME LYMPHATIQUE ET DU CANCER
PROGRAMME DOCTORAL EN BIOTECHNOLOGIE ET GÉNIE BIOLOGIQUE

ÉCOLE POLYTECHNIQUE FÉDÉRALE DE LAUSANNE

POUR L'OBTENTION DU GRADE DE DOCTEUR ÈS SCIENCES

PAR

Efthymia VOKALI

acceptée sur proposition du jury:

Prof. F. Radtke, président du jury
Prof. M. Swartz, directrice de thèse
Prof. S. Turley, rapporteuse
Prof. A. Mondino, rapporteuse
Prof. C. Halin Winter, rapporteuse

ÉCOLE POLYTECHNIQUE
FÉDÉRALE DE LAUSANNE
Suisse
2016

Acknowledgements

The completion of a PhD thesis is not a one-woman show; it demands the contribution and help of several people whom I would like to wholeheartedly thank:

My advisor, Prof. Melody A. Swartz, for her scientific guidance, advice and support throughout this thesis. I would like to express my gratitude towards her for providing me with stimulating ideas, while also giving me the freedom to explore. Her endless energy and passion for science made this journey an exciting experience to navigate through.

Dr. Sachiko Hirosue for being with me since the very beginning of this adventure, teaching me how to properly do science, working with me, sharing her projects and ideas. Her limitless scientific curiosity and her well-guarded super-powers have been a source of motivation for me all the way to here. I would also like to thank her for being a great friend and for believing in me.

Prof. Susan Thomas, who was the first to welcome me into the lab and take me along her project although I hardly knew how to pipet (!). If it weren't for her patience and encouragement, I would probably not be writing these lines. Her smile and positive attitude, even when things went wrong, will always be on my mind.

Prof. Stéphanie Hugues, Prof. Dietmar Zehn, and Prof. Anna Mondino for kindly offering precious advice and feedback.

Prof. Vassily Hatzimanikatis for being a great mentor.

The members of my thesis committee, Prof. Cornelia Halin, Prof. Anna Mondino, Prof. Shannon Turley and Prof. Freddy Radtke, for taking the time to review my thesis.

Many thanks to the people I have worked with, Dr. Marcela Rincon, Dr. Shann Yu, Dr. Esra Guc, Dr. Fernanda Duraes, Stephanie Scherer, Dr. Valentina Triacca, Dr. Cara Buchanan, Lambert Potin, Léa Maillat, as well as the people who taught me how to ask questions and initiated intriguing (scientific or other) conversations, Dr. Amanda Lund and Dr. Witek Kilarski. Without your input, I would not have learnt so much!

Big thanks to the lab assistants: Patricia Corthésy, Yassin Ben Saida, Xavier Quaglia-Thermes, Giacomo Diaceri for making my life easier. Milles merci à Patricia,

for always being so willing to help. I would also like to acknowledge the assistance of all the personnel of the EPFL facilities, especially the people in FCCF.

Infinite thanks to Ingrid Margot for her invaluable administrative help, she is a life-saver.

I am more than grateful to Sachiko, Shann and Sylvie for reading, editing and providing feedback on my thesis draft.

The current and past members of LLCB and LMRP for their generosity in sharing knowledge and their positive spirits that generated such great atmosphere in the lab. Particularly, Vale, Marco, Marcela, Esra, Manuel, Laura, Sandeep for always being around and for trying to drag me out of the lab! Vasiliki, for her endless support, help and for being a great friend. And Scott, for all the little surprises on my desk! I feel very lucky to have been part of this lab!

My friends outside the lab for all the nice and funny moments we have shared, their support and for taking my mind off experiments. Special thanks to my friends back in Greece for the countless hours on skype, their visits, their love and encouragement, for always being there for me even though we are apart.

Finally, my family, my parents, Phaedra, Orestis, and Anna for their love and support during all my studies, for their trust, respect, and understanding.

And Yiannis, for arguing with me, bearing with my moods and making sure I eat and smile.

Σας ευχαριστώ!

Abstract

The lymphatic system serves a critical role in fluid homeostasis, lipid metabolism and immune surveillance. The growing appreciation of its implication in various diseases challenges the conventional view of lymphatics as a passive transport system.

Traditionally, the lymphatic endothelium has been perceived as a structural scaffold with certain immunological functions but no active involvement in immunomodulation. In the lymph nodes (LNs), the main sites of immune regulation in the periphery, lymphatic endothelial cells (LECs) come to close contact with immune cells, suggesting potential interactions. Indeed, LECs have been recently shown to suppress dendritic cell maturation and present peripheral tissue and tumor antigen for $CD8^+$ T cell deletion. While LECs have only begun to be acknowledged as active regulators of immunity, their function and relative contribution in shaping immune responses is as yet poorly understood.

This thesis aimed to elucidate the direct role of LECs in the induction of $CD8^+$ T cell immunity and tolerance. First, we demonstrated that murine LECs can actively scavenge and cross-present exogenous antigen to cognate $CD8^+$ T cells under non-inflamed conditions. By utilizing an *in vitro* coculture system and the model antigen ovalbumin, we investigated the antigen-specific interactions between LECs and $CD8^+$ T cells. LEC-educated $CD8^+$ T cells proliferated, exhibiting an activated phenotype, however, they displayed early-generation apoptosis and failed to produce effector cytokines. Our findings establish LECs as antigen-presenting cells and suggest that they may assist in the maintenance of peripheral tolerance during homeostasis.

The particular differentiation state of LEC-educated $CD8^+$ T cells prompted us to investigate whether they are terminally tolerized or they could escape the dysfunctional state. We demonstrated that LEC-educated $CD8^+$ T cells adopted a distinct phenotype with central memory-like characteristics and shared multiple functional properties with memory cells. Upon antigen re-encounter, LEC-educated $CD8^+$ T cells mounted proliferative responses and generated cytotoxic effector cells.

More importantly, they participated in anti-infectious immunity while preserving a secondary-memory persistent population. Our findings reveal a unique differentiation state of antigen-experienced $CD8^+$ T cells, generated under steady-state conditions, which remain inactive but can be functionally reactivated upon antigenic inflammatory challenge.

This previously unanticipated feature of LECs triggered questions for their antigen-presenting function in an inflammatory setting. We asked whether the previously observed extensive proliferation of LECs in the LN during inflammation might directly influence the induction of immunity. We employed an anti-VEGFR3 blocking antibody to inhibit LEC proliferation and thus, reduce the number of LECs following vaccine immunization. Alternatively, we generated the Prox1-Cre-DTR mouse model, allowing for specific ablation of LECs following administration of diphtheria toxin *in vivo*. Our findings advance our perception of the relative contribution of LECs in the establishment of adaptive immunity.

This thesis elucidates the multifaceted immunological role of LECs and strongly suggests the importance of harnessing their immunomodulatory function to enhance current vaccines and immunotherapeutic strategies. Looking forward, our work will contribute to future advances in the clinic.

Keywords: LEC, LN, cross-presentation, exogenous antigen, peripheral tolerance, $CD8^+$ T cell, non-terminal differentiation, memory, lymphangiogenesis, immunomodulation

Résumé

Le système lymphatique joue un rôle critique dans l'homéostasie des fluides tissulaires, le métabolisme des lipides et la surveillance immunitaire. L'augmentation croissante de son implication dans diverses maladies remet en question le point de vue conventionnel du réseau lymphatique comme étant un système de transport passif.

Généralement, l'endothélium lymphatique est perçu comme un élément structurel avec certaines fonctions immunologiques mais sans participation active dans l'immunomodulation. Dans les ganglions lymphatiques (GLs), les sites principaux de la régulation immunitaire dans la périphérie, les cellules endothéliales lymphatiques (CELs) entrent en contact étroit avec les cellules immunitaires, suggérant une interaction potentielle entre elles. En effet, il a été récemment montré que les CELs sont capables de stopper la maturation des cellules dendritiques et de présenter des antigènes provenant de tissus périphériques et tumoraux pour la délétion des cellules T $CD8^+$. Alors que les CELs commencent à être reconnues comme des acteurs actifs de l'immunité, leurs fonctions et leur importance relative dans l'élaboration de réponses immunitaires sont encore mal comprises.

Cette thèse vise à élucider le rôle direct des CELs dans l'induction de l'immunité cellulaire et de la tolérance des lymphocytes T $CD8^+$. Nous avons tout d'abord démontré que les CELs murines peuvent activement capter et cross-présenter des antigènes exogènes aux cellules T $CD8^+$ dans des conditions non inflammatoires. En utilisant un système de co-culture *in vitro* et l'ovalbumine comme l'antigène modèle, nous avons étudié les interactions spécifiques de l'antigène donné entre les CELs et les cellules T $CD8^+$. Les cellules T $CD8^+$ éduquées par les CELs ont proliféré et présenté un phénotype activé, cependant, elles ont affiché des signes d'apoptose précoce. De plus, elles étaient incapables de produire des cytokines induites par les cellules T $CD8^+$ effecteurs. Ces résultats établissent les CELs comme des cellules présentatrices d'antigènes et suggèrent qu'elles peuvent contribuer au maintien de la tolérance périphérique.

Cet état de différenciation particulier de cellules T $CD8^+$ éduquées par les CELs nous a incités à étudier si elles étaient rendues tolérantes ou si elles pouvaient échapper à cet état dysfonctionnel. Nous avons démontré que les cellules T $CD8^+$ éduquées par les CELs ont adopté un phénotype distinct, présentant des caractéristiques des cellules T de mémoire centrale et partageaient plusieurs propriétés fonctionnelles avec elles. Lors d'une nouvelle rencontre avec l'antigène, elles ont induit des lymphocytes T $CD8^+$ effecteurs qui pouvaient proliférer et produire des molécules cytotoxiques. Elles ont surtout contribué à l'établissement de l'immunité anti-infectieuse, tout en préservant une population persistante de mémoire secondaire. Ces résultats révèlent un état de différenciation unique de cellules T $CD8^+$, qui sont spécifiques à l'antigène qu'elles ont rencontré en premier en conditions non inflammatoires et qui restent inactives tout en gardant la capacité d'être réactivées en cas d'apparition d'un antigène inflammatoire.

Cette nouvelle propriété des CELs a posé des questions sur l'importance de leur fonction présentatrice dans le cadre de l'inflammation. Nous avons examiné si la prolifération excessive des CELs, précédemment observée dans le GL au cours de l'inflammation, pourrait influer directement sur l'induction de la réponse immunitaire. Nous avons utilisé un anticorps bloquant le récepteur VEGFR3 (anti-VEGFR3) pour limiter la prolifération des CELs et ainsi, réduire le nombre de CELs suivant l'immunisation. Parallèlement, nous avons généré un modèle de souris transgénique, Prox1-Cre-DTR, permettant d'éliminer précisément les CELs suite à l'administration de toxine diphtérique *in vivo*. Les résultats obtenus ont considérablement fait progresser notre perception de la contribution relative des CELs à l'établissement de l'immunité adaptative.

Cette thèse a permis de mettre en évidence les différents rôles immunologiques des CELs suggérant l'importance d'exploiter leurs fonctions immunomodulatrices afin d'améliorer les vaccins actuels et les stratégies immunothérapeutiques. Notre travail peut contribuer aux progrès de la recherche clinique future.

Mots-clés: Cellules endothéliales lymphatiques, ganglion lymphatique, cross-présentation de l'antigène (présentation croisée), antigène exogène, tolérance périphérique, cellule T CD8+, différenciation non-terminée, mémoire immunitaire, lymphangiogénèse, immunomodulation

Table of Contents

Chapter 3

List of figures

Common abbreviations

APC: Antigen presenting cell

aR3: Anti-VEGFR3

BEC: Blood endothelial cell

DC: Dendritic cell

dLN: Draining lymph node

DT: Diptheria toxin

DTR: Diptheria toxin receptor

FRC: Fibroblastic reticular cell

iDC: Immature dendritic cell

iLEC: Immortalized lymphatic endothelial cell

i.d.: Intradermal

I.p.: Intraperitoneal

I.v.: Intravenous

LEC: Lymphatic endothelial cell

L.m.: Listeria monocytogenes

LN: Lymph node

LNSC: Lymph node stromal cell

LSEC: Liver sinusoidal endothelial cell

mDC: Mature dendritic cell

MHC: Major histocompatibility complex

NP: Nanoparticle

OVA: Ovalbumin

PTA: Peripheral tissue-restricted antigen

T_{CM}: Central memory T cell

T_{eff}: Effector T cell

T_{EM}: Effector memory T cell

T_{SCM}: Stem cell-like memory T cell

TLR: Toll-like receptor

VEGFR3: Vascular endothelial growth factor receptor 3

Chapter 1

Introduction

The lymphatic system plays a crucial role in maintaining tissue homeostasis through the clearance of excess fluids from peripheral tissues and the absorption of dietary lipids from the intestine to return them into systemic circulation (1-3). Lymphatic vessels allow the continuous trafficking of immune cells as well as soluble antigen from the periphery to secondary lymphoid organs while lymph nodes (LNs) provide a place for antigen presentation and immune activation (4-6). Therefore, the lymphatic system represents a critical element for immune surveillance and the generation of immune responses.

The diversity in the physiological functions of the lymphatic system explains why they are known to contribute to the pathogenesis of various human diseases. These involve lymphedema, fat accumulation, inflammatory disorders such as rheumatoid arthritis, as well as solid organ transplant rejection (7, 8). Lymphatics are also implicated, through the mesenteric LN, in the regulation of local and systemic food tolerance, while they have been reported as the primary site of replication and dissemination of various pathogenic viruses inducing critical disease (1). Among the diseases involved, the vast majority triggers alterations in the lymphatic network with respect to lymph flow, lymphatic vessel size and architecture. Lymphangiogenesis, the expansion of lymphatic endothelium, is also observed in tumors allowing for increased drainage and transport of immune cells (9, 10). Immune cells and tumor antigen are transferred from the tumor to the draining lymph node (dLN) through lymphatic vessels and therefore, the dLN status reflects the tumor immune status. In addition, tumor associated lymphatics function as an escape route for tumor cells enabling their dissemination to the immunological network and subsequent metastasis (2, 11). More importantly, peritumoral lymphatic density as well as expression of the major lymphatic growth factor, vascular endothelial growth factor C (VEGF-C), are included among the prognostic indicators in many human cancers (12, 13).

The growing recognition of the key roles that the lymphatic system plays in health and disease challenges the established conventional view of lymphatics; Traditionally, the lymphatic network is portrayed as a passive transport system, with lymphatic endothelial cells (LECs) solely forming the structural scaffold for cell and antigen circulation. However, the anatomic distribution of the lymphatic system suggests several sites for close contact with immune cells (14, 15). In turn, this intimate physical contact indicates potential active interactions with immune cells and thus, introduces the possibility of regulating their function. Interestingly, LN LECs are situated in one of the prime anatomical sites for immunological sampling, being the first to get exposed to exogenous antigen arriving from the periphery through the lymph. The lymph bathes the LN in soluble foreign antigens as well as tissue-specific self-antigens mixed with other molecules present in the draining peripheral tissues and therefore, reflects their immunological state. During homeostasis, the lymph appears to be significantly enriched, compared to plasma, in proteins and peptides derived from tissue homeostatic turn-over (16). Human lymph has also been reported to display an expanded peptidome with respect to plasma (17). In the course of infection or tissue injury, exogenous antigens and self-peptides from damaged cells, along with homeostatic byproducts, all travel through the lymph to the local draining LN; hence, the lymph "communicates" to the LN the state of the tissue and LECs, positioned at the entrance of the LN, are the first to receive this "information".

Emerging evidence and thoughtful reexamination of the existing knowledge strongly suggest that LECs are not passive observers but may dynamically participate in the modulation of immune responses. While the appreciation for the immunological role of LECs grows, many exciting questions are raised and the answers are awaited with much anticipation.

1.1 Bridging the transport and immune functions of the lymphatic system

Viewing the elaborate structure of the lymphatic system through the lymphatic-driven journey of immune cells from the periphery to the LN

The lymphatic network displays a tree-like architecture that allows the unidirectional flow of the carried lymph from peripheral tissues to the blood circulation at the thoracic duct, passing through chains of LNs on its way (18). The anatomical distribution of lymphatic vessels, starting with initial lymphatics (lymphatic capillaries) in the periphery, leading to pre-collector vessels and collecting vessels that reach the LNs suggests diverse functional roles for LECs and different sites of physical contact with immune cells (19).

Following inflammation in the periphery, activated dermal dendritic cells (DCs) adhere firmly to the outer surface of initial lymphatics (15) to subsequently enter the vessels by passing through the flaps of oak-leaf shaped LECs that are connected by specialized discontinuous button-like junctions (Fig. 1.1A). At this level, the basement membrane around lymphatic vessels is almost totally missing, enabling them to be also highly endocytic and permeable to proteins (4). LECs of the initial lymphatics are characterized by the expression of LYVE-1, Prox-1, VEGFR-3, and podoplanin (gp38) and they are known to express the chemokine CCL21-Leu (containing a

leucine residue at position 65) (19, 20). Lymphatic-derived expression of CCL21-Leu in the periphery (Fig. 1.1B) is known to recruit the activated mature CCR7$^+$ DCs towards initial lymphatics via the generation of a chemotactic gradient (4).

Once in the lumen of initial lymphatics, dermal DCs originally move by active crawling, guided by sensing the flow. Later on, initial vessels converge into the larger collecting lymphatics, surrounded by smooth muscle cells with pumping activity, and from there on, lymph flow transfers DCs to the LN (15). The lymphatic vessels that actually reach the LN are thought to branch extensively into the so-called afferent lymphatics, as they terminate at, and within, the subcapsular sinus (4). The other form of CCL21, CCL21-Ser, is expressed in the LNs and terminal lymphatic vessels as opposed to lymphatics in the periphery, and is thought to favor CCR7$^+$ DC migration in the LN parenchyma (21) (Fig. 1.1C). The CCR7-CCL21 signaling axis is also important for the trafficking of naïve, memory and regulatory T cells from the periphery to the LN (22).

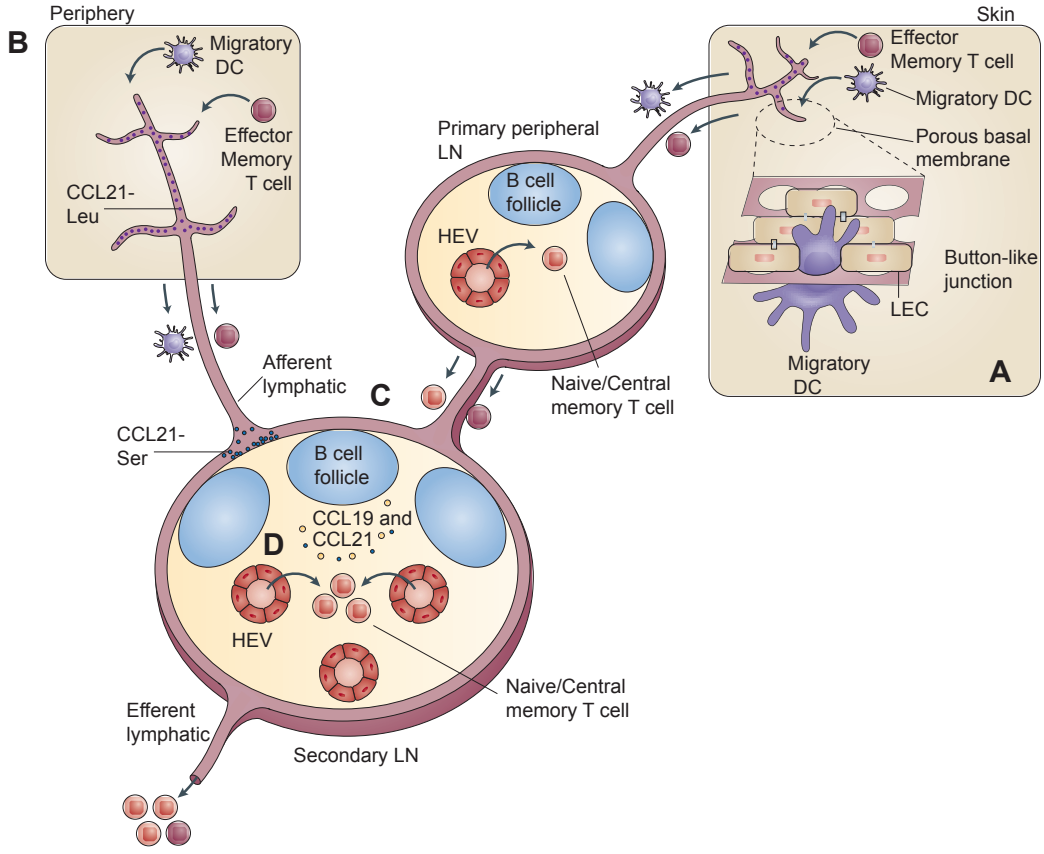

Figure 1.1 The lymphatic system regulates immune cell trafficking from the periphery to the LN. **(A)** Entry of DCs in initial lymphatic vessels through the loose button-like junctions of LECs. **(B)** Similar to CCR7$^+$ DCs, memory cells can also enter initial lymphatics in the periphery driven by the expression of CCL21 (CCL21-Leu). **(C)** DCs as well as memory T cells enter the LN via afferent lymphatics. Since LNs are frequently arranged in chains, naïve T cells derived from an upstream LN (Primary peripheral LN) can also arrive via afferent lymph. A CCL21 gradient (CCL21-Ser) also assists the directional migration of DCs from the subcapsular sinus (SCS) into the LN parenchyma. **(D)** Naïve T cells mainly arrive in the LN from the blood via specialized high endothelial venules (HEV). The expression of CCL19 and CCL21 in the T cell zone drives the intranodal migration and accumulation of T cells in the paracortical T cell areas of the LN. Figure adapted from Girard et al. (14).

CCL19, another ligand of CCR7, is also expressed by LECs and fibroblastic reticular cells (FRCs) and it is known to facilitate naïve T cell recruitment into the deep paracortex of the LN (23) (Fig. 1.1D).

Within the LN, LECs are divided in three different subgroups with respect to their anatomic location (24) (Fig. 1.2). Subcapsular sinus (SCS) LECs line the floor and the ceiling of the subcapsular region and come to contact with the residing SCS macrophages (Fig. 1.2A). Cortical LECs shape the vessels that emanate in between the B-cell follicles and into the T-cell zone and can cross the SCS and medullary LECs (Fig. 1.2B). Medullary LECs form the medullary sinuses at the LN exit within the medulla of the LN (Fig. 1.2C). While podoplanin (gp38) and PECAM-1 (CD31) are usually employed to define LECs and separate them from the other major lymph node stromal cell (LNSC) subsets by flow cytometry (25, 26), the expression of PD-L1, ICAM-1, MAdCAM-1 and LTβR allows for further subdivisions in the above described subgroups (27). SCS LECs have been recently shown to play a major role

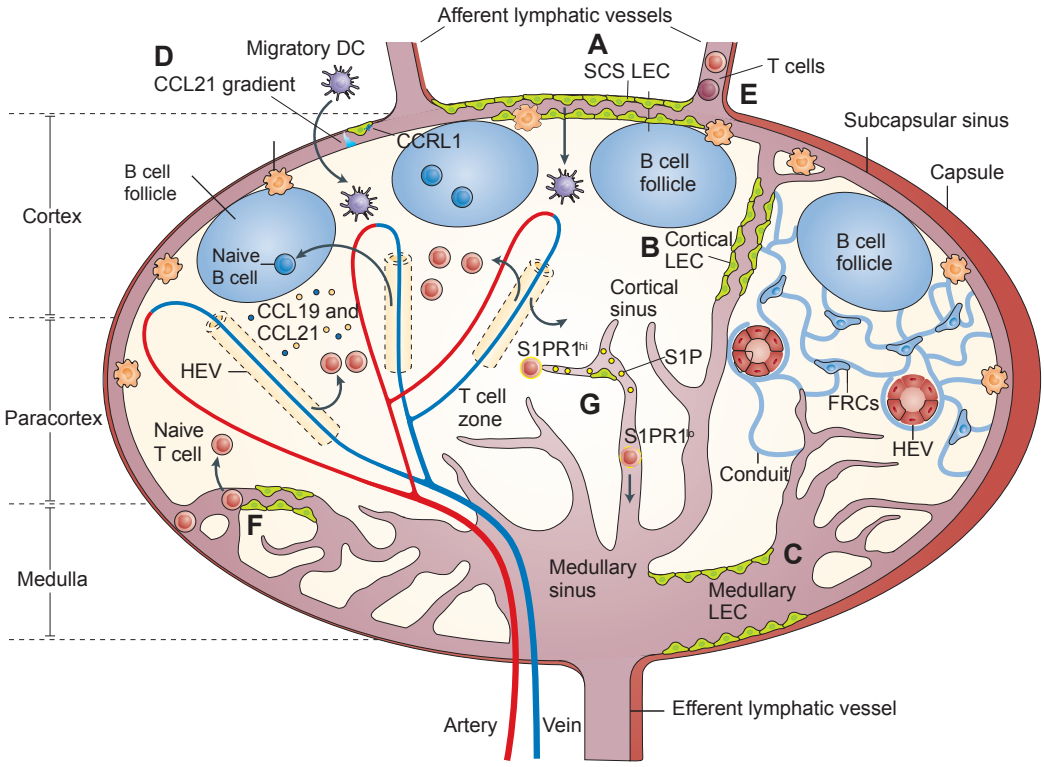

Figure 1.2 The subanatomical organization of the lymph node and the distinct sites of close contact between LECs and immune cells. LN LECs can be divided into three subgroups with regard to their localization in one of the three main regions of the LN: the cortex, the paracortex and the medulla. **(A)** Subcapsular sinus LECs line the floor and the ceiling of the subcapsular region of the LN. **(B)** Cortical LECs line the lymphatic vessels that branch between the B cell follicles into the T cell area. **(C)** LECs that form the sinuses at the medulla of the LN are called medullary LECs. **(D)** SCS LECs control the transmigration of DCs from the SCS into the LN parenchyma by driving a CCL21 chemokine gradient through the expression of CCRL1 scavenger receptor. **(E)** Naïve and memory T cells that reach the LN via the afferent lymph, come to close contact with LECs at the point of entry, in the SCS. **(F)** T cells are then channeled into the cortical and medullary sinuses. T cells can transmigrate from the medullary sinuses into the deep paracortex by sensing the expression of CCL21 and CCL19 in the T cell zone. **(G)** Secretion of S1P by LECs mediates the migration of T cells from the T cell areas into the sinuses through the S1P receptor (S1PR) on T cells. After their entry, T cells are flow-guided towards the medulla of the LN to exit via the efferent lymphatic vessels. Figure adapted from Girard et al. (14).

in the entry of activated DCs from the afferent lymphatic vessel into the LNs by driving the CCL21 chemokine gradient through the expression of the atypical CCRL1 scavenger receptor (28) (Fig. 1.2D).

Once they enter the LN, migrating DCs initially localize to the subcapsular region (15, 29) where they come to close contact with SCS LECs. In addition to DCs, T cells also interact intimately with LECs at distinct locations within the LN. Activated as well as naïve T cells encounter LECs in their route of entry in the LN (Fig. 1.2E) when migrating in from afferent lymphatic vessels (30, 31). T cells can then be directed into cortical and medullary sinuses, interacting with LECs while reaching the LN lumen (27) (Fig. 1.2F). Eventually, T cells are guided to exit the lymph node via efferent lymphatics. LECs have been also reported to facilitate T cell egress from the LN through secretion of sphingosine-1-phosphate (S1P), of which they are the main source (32) (Fig. 1.2G).

Therefore, it becomes apparent that LECs can dynamically regulate immune cell transport and thus, potentially modulate their downstream functions.

The lymphatic system controls antigen availability and regulates the kinetics of antigen presentation

Apart from the recruitment of immune cells, the lymphatic system also regulates the transport of soluble antigens carried in the lymph. In addition to cell-associated antigen that reaches the LN with a relative delay, free antigens can rapidly arrive to the SCS, through afferent lymphatics. Upon arrival, antigens are channeled to different compartments of the LN with respect to their size. Low-molecular weight antigens are promoted to FRC–lined conduits to subsequently reach the B and T cell zones (33, 34), whereas larger antigens and immune complexes can be directly taken up by SCS macrophages. The size-dependent antigen distribution is partially mediated by sieve-like diaphragms, composed of plasmalemma vesicle-associated protein (PLVAP) in the SCS LECs (35). The remaining high-molecular weight molecules will reach the next LN by exiting through the medullary sinuses. While passing through those LEC-covered structures, they can be sampled by resident DCs that extend their protrusions in the medullary sinuses (36). Smaller antigens can also be sampled by immature LN-resident DCs in the paracortex (37).

During homeostasis, lymph flow constantly supplies the LN with a pool of tissue self-antigens for the deletion of autoreactive T cells. Following infection or tissue injury, the lymph flow is vigorously altered in response to peripheral tissue inflammatory signaling, to accommodate increased lymph formation and accelerate the initiation of the immune response (38, 39). Additionally, the delayed arrival of DC-transported antigen, as opposed to the fast drainage of soluble antigen from the periphery and its subsequent capture by resident DCs, suggests an early onset of the adaptive immune response which is later amplified by migratory DCs (37, 40). Hence, the differential kinetics of lymph drainage, along with the spatial compartmentalization of the LN, may delicately orchestrate antigen presentation and in turn, powerfully influence the initiation and the magnitude of the immune response.

Evidently, the transport and immune functions of lymphatic vessels, which were previously thought to be distinct, are strongly interconnected. Lymphatics directly link

peripheral tissues to the central immune system and thus, constitute an important component of the body's immune defense.

1.2 LECs as direct participants in immune regulation: from simple bystanders to major players?

Modulation of DC-T cell interactions by LECs

As discussed earlier, LECs come into intimate contact with DCs and T cells, which suggests potential direct immunological interactions. Recent studies have shed some light on the functional influence that LECs might exert on DCs and T cells, along with the mechanisms implicated (41, 42). LECs have been reported to express diverse immunosuppressive molecules, such as the transforming growth factor beta (TGFβ), nitric oxide and indoleamine 2,3 dioxygenase (IDO) indicating their potential regulatory role (43-46) (Fig. 1.3A). Furthermore, LECs have been demonstrated to directly modulate DC differentiation status and function, via a cell contact – dependent mechanism (47). Inflamed human skin LECs were shown to induce down-regulation of the maturation marker CD86 on DCs, which subsequently resulted in reduced capacity of stimulating T cell proliferation in the absence of pathogen-derived signals. This immunosuppressive function required adhesive interactions between LECs and DCs and was dependent on binding of macrophage-1 antigen (MAC-1), on DCs, to intercellular adhesion molecule 1 (ICAM-1), on LECs (Fig. 1.3B). Subsequent findings revealed that the supernatant of IFN-γ - activated LECs abrogated the capacity of allogeneic DCs to induce T cell proliferation, pointing to IDO as the inhibitory mediator (45). Along the same lines, murine LN LECs, together with FRCs, were observed to inhibit $CD4^+$ and $CD8^+$ T cell proliferation via regulated expression of the nitric oxide synthase 2 (NOS2) enzyme, which catalyzes the production of nitric oxide (NO). The authors proposed a mechanism in which interferon-γ (IFN-γ), released from activated splenocytes, together with tumor necrosis factor (TNF) signaling, induced NO production in LECs which subsequently

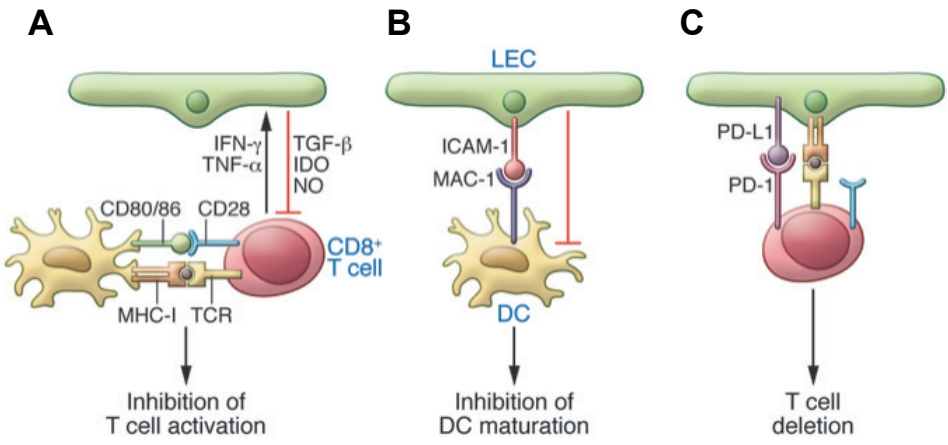

Figure 1.3 LECs employ different mechanisms to modulate immune responses. (A) LECs prohibit T cell proliferation via the secretion of immunosuppressive molecules. **(B)** LECs suppress DC maturation and thus, abrogate their ability to functionally activate T cells. **(C)** LECs can express PTAs and present them on MHC I to $CD8^+$ T cells to induce deletional tolerance. Image adapted from Card et al. (41).

resulted in down-regulation of T cell proliferation (48) (Fig. 1.3A). The suppressive effect also turned out to be cell-contact dependent, suggesting that bi-directional signaling is needed to sensitively fine-tune the outcome of T cell responses.

Taken together, it becomes evident that LECs can employ different mechanisms to modulate DC-T cell interactions.

Direct antigen presentation by LECs

LECs express various molecules associated with antigen presentation, which suggests that they could also themselves act as antigen presenting cells (APCs) and prime T cells. In addition, human and murine LECs express multiple functional Toll-like receptors (TLRs) (30, 49). Furthermore, LECs display several scavenging receptors, C-type lectins, and other known cross-presentation – related receptors, which implies that they might also be capable of antigen uptake and processing (42). The upregulation of many of these proteins under inflammatory conditions (44) further underlines the potential dynamic participation of LECs in shaping immune responses.

As all other nucleated cells, LECs express major histocompatibility complex (MHC) class I, which suggests that they can interact directly with $CD8^+$ T cells. Interestingly, LECs also display low-level expression of MHC class II in the steady state, which is further upregulated upon IFN-γ treatment (44, 50). In terms of costimulatory machinery components, LECs were shown to express low levels of CD40 and almost no CD80 or CD86 at steady state conditions (30). Expression of those molecules under inflammatory conditions was only slightly altered, if any. By contrast, LECs were demonstrated to express the coinhibitory programmed death ligand 1 (PD-L1), which was further enhanced following TLR-3 stimulation. In line with the murine model, HLA-A/B/C were reported to be constitutively expressed on human LN LECs, while HLA-DR/DQ/DP expression was induced after IFN-γ or PolyI:C treatment (45). Human LN LECs were also shown to express CD58 (LFA-I) although its expression was not increased upon IFN-γ or TNF-α stimulation or following treatment with several TLR ligands. Therefore, LECs seem to bear several activating and inhibitory elements of the antigen-presentation machinery. More importantly, LECs can dynamically tune the expression of those molecules in response to the immunological status of their microenvironment, similar to conventional APCs.

Strikingly, LECs, as well as other LNSCs, were found to express a wide variety of peripheral tissue-restricted antigens (PTAs), which they presented on MHC I molecules to primarily activate and subsequently delete $CD8^+$ T cells (51-53) (Fig. 1.3C). More specifically, distinct PTAs were found to be expressed among the four LNSC subsets (30). However, studies have been primarily focused on LECs and FRCs, which have been shown to mediate deletional tolerance. Interestingly, LECs were the only cell type among all LNSCs to express the melanocyte epitope tyrosinase (Tyr_{369}) and delete tyrosinase-specific $CD8^+$ T cells (54). This might have important clinical implications if the observed LEC-mediated induction of tolerance is confirmed in human melanomas. Thus, LECs might actively contribute to peripheral tolerance exerting non-redundant and biologically relevant regulatory functions.

LNSC-mediated induction of tolerance is considered to be reminiscent of the central tolerance mechanisms in the thymus, driven by medullary thymic epithelial cells (mTECs), which eliminate self-reactive T cells (55). The organized action of central versus peripheral tolerance is associated with distinct transcriptional regulators. PTA expression in mTECs has been reported to be dependent on the autoimmune regulator (Aire), (55) whereas it was found to be Aire-independent in LECs (30). Another transcriptional regulator, Deaf 1 (56), may be associated with LEC and FRC-mediated peripheral tolerance.

LECs, as well as FRCs, are not the only non-hematopoietic cells that have been shown to participate in the maintenance of peripheral tolerance (57). Unconventional APCs in the liver, skin, parenchymal tissues, and lymph nodes were found to efficiently present tissue-specific and exogenous antigens to naïve $CD8^+$ T cells participating in the regulation of immunity in the periphery (58). Hepatocytes and pancreatic islets have been suggested to directly present liver antigen to $CD8^+$ T cells. Liver sinusoidal endothelial cells (LSECs) constitutively display MHC class I and II, as well as low levels of co-stimulatory molecules and they can capture antigen for presentation to $CD4^+$ and $CD8^+$ T cells (59).

In addition to regulating tolerance via presentation of self-antigens, LECs also bear the required tools for cross-presentation of exogenous antigens. Indeed, our laboratory has recently shown that LECs in the tumor dLN can scavenge and cross-present tumor antigen on MHC I, to induce apoptotic and dysfunctional tumor-specific $CD8^+$ T cells, in a VEGF-C - overexpressing mouse B16/F10 melanoma tumor model (60). This mechanism is clearly distinct from the presentation of self-antigens by LNSCs, discussed above, and presents similarities with the scavenging function of LSECs, which were demonstrated to cross-present antigen to $CD8^+$ T cells with the immunological outcome characterized as rather tolerogenic (61-64). It is likely that tumors might harness a physiological ability of LECs (cross-presentation) to suppress cytotoxic anti-tumor responses and escape host immunity. However, it has not yet been verified whether LECs can exert similar function under steady-state conditions and what could be the immunological outcome. The specific mechanisms by which LECs capture antigens, as well as the trafficking pathways and processing mechanisms implicated remain largely unknown.

An open question that needs to be addressed is the functional outcome of interactions between LECs and $CD4^+$ T cells. Although MHC II expression in LECs has been reported (44, 65), it is unknown if this leads to proliferative responses in $CD4^+$ T cells. Human LN LECs failed to induce allogeneic, naïve or memory, $CD4^+$ T cell proliferation *in vitro* (45). In a different setting, DC-derived peptide:MHC II complexes in LECs did not induce T cell proliferation but instead, promoted cell death (50). Further studies should be conducted to clarify the contribution of MHC II presentation by LECs in $CD4^+$ T cell immune responses.

Signaling pathways governing direct LEC-$CD8^+$ T cell interactions

Our knowledge about the signaling mechanisms tipping LEC-$CD8^+$ T cell interactions towards the induction of tolerance is still quite limited. The overall picture of how LECs control and shape immune responses needs to be fully formulated. The outcome of $CD8^+$ T cell activation by professional APCs has been previously described to rely on three different signals; recognition of their cognate antigen

presented on an MHC-I molecule, costimulatory signaling, and cytokine or other inflammatory signaling (66, 67). In the absence of the appropriate costimulation, $CD8^+$ T cell activation is traditionally thought to result in anergy or deletion. Costimulatory signals are almost totally absent in LECs and are not enhanced following TLR stimulation (30); thus, in accordance with this concept, the observed tolerogenic outcome is not surprising (65).

One of the mechanisms that has been previously suggested to be associated with $CD8^+$ T cell impairment is the PD-1/PD-L1 pathway (68, 69). Earlier studies have highlighted the role of PD-L1 in the induction of $CD8^+$ T cell tolerance by intestinal epithelial cells (70). The same pathway has also been demonstrated to mediate deletional $CD8^+$ T tolerance by LSECs (64). Until recently, many of the significant immune check points (71), associated with dyfunctional $CD8^+$ T cells, such as Cytotoxic Lymphocyte Antigen-4 (CTLA-4), ICOS, LAG3 or TIM-3, have not been examined for their potential implication in LEC-mediated tolerance. In fact, Tewalt et al. have recently demonstrated, in a model of LEC-mediated tolerance against tyrosinase, that lack of costimulation via 4-1BB (CD137) induced up-regulation of PD-1 on activated T cells and subsequently resulted in reduced $CD8^+$ T cell survival *in vivo* (65). In the same model, blockade of the PD-1/PD-L1 pathway led to autoimmunity.

Collectively, multiple inhibitory mechanisms and regulatory molecules appear to be associated with LECs' immunomodulatory function. How all these combinatorial aspects might synergize or act independently in order to tightly drive LECs' behavior remains unresolved.

1.3 A place for LECs as APCs in the immune response

While the role of LECs as active regulators of immunity is gaining appreciation, this is still the beginning of the story.

The newly emerging concept of LECs' contribution as APCs to immunomodulation is primarily inclined towards the suppression of immune responses. Our current understanding and accumulating evidence point towards a complementary role in the maintenance of peripheral tolerance coupled to a safety mechanism for the preservation of the LN structure during immune responses or even the resolution of the immune response. Nevertheless, the potential capacity of exogenous antigen presentation in LECs introduces another layer of complexity. If LECs can capture, process and present exogenous antigens during homeostasis to sustain peripheral tolerance, how does this function influence the initiation of immunity following pathogenic infection?

While the contribution of LECs' exogenous antigen presentation in immunity is as yet poorly understood, what is not in question is the impact of the lymphatic endothelium in the modulation of immunity. With this picture as a context background basis, we set out to unwind the complex emerging role of LECs in the regulation of T cell immunity and tolerance.

1.4 Outline of the thesis

This thesis focuses on elucidating the direct role of LECs in the induction of $CD8^+$ T cell-mediated immunity and tolerance.

In **Chapter 2**, we explore the ability of LN LECs to capture and process exogenous antigen. We demonstrate that LECs can constitutively uptake and cross-present exogenous antigens on MHC I to $CD8^+$ T cells under steady-state conditions. We employed an *in vitro* coculture system and the model antigen ovalbumin to study antigen-specific LEC-$CD8^+$ T cell interactions. LEC-educated $CD8^+$ T cells proliferated, displaying an activated phenotype, however, they appeared to be more rapidly apoptotic and failed to produce effector cytokines, compared to T cells activated by professional antigen-presenting dendritic cells. The dysfunctionally activated state of LEC-educated $CD8^+$ T cells suggested that antigen presentation by LECs under steady state conditions might promote self-tolerance against draining peripheral antigens. Our findings establish LECs as *bona fide* APCs and reveal their contribution in the maintenance of peripheral tolerance.

Traditionally, the induction of peripheral tolerance has been assigned to immature cross-presenting DCs via different mechanisms, including T cell anergy, suppression or deletion. The surviving tolerized $CD8^+$ T cells should remain functionally impaired in response to any stimuli in order to sustain homeostasis and prevent autoimmunity. This prompted us to further investigate the phenotype and function of LEC-educated $CD8^+$ T cells to identify whether those cells are terminally tolerized or whether they could escape the dysfunctional state. In **Chapter 3**, we demonstrate that steady-state LEC-educated $CD8^+$ T cells adopted a unique phenotype with central and stem cell memory-like characteristics, accompanied by additional functional memory-like properties. Following antigen re-encounter, LEC-educated $CD8^+$ T cells mounted proliferative responses and gave rise to effector cells. Most importantly, they participated in anti-infectious immunity while preserving a secondary-memory persistent population. Our findings reveal a distinct differentiation state of antigen-experienced $CD8^+$ T cells, generated under steady-state conditions, which survive in an inert state but can be functionally reactivated upon antigenic inflammatory challenge. This previously unanticipated function of LECs probably serves as a supplementary mechanism, which complements and amplifies $CD8^+$ T cell immune responses, and further highlights the diverse immunomodulatory features of LECs.

The generation of an antigen-experienced $CD8^+$ T cell pool by LN LECs during homeostasis triggered questions about the role of LECs in an inflammatory setting. Lymph nodes (LNs) undergo considerable expansion during inflammation induced by pathogen infection or following vaccination. In **Chapter 4**, we asked whether the observed proliferation and dynamic remodeling of lymphatic structures during inflammation might directly impact the induction of $CD8^+$ T cell immunity. We demonstrate that LN LECs can sense and integrate signals from their microenvironment to actively scavenge exogenous antigen under inflammatory conditions. We employed two different strategies in order to determine the contribution of antigen presentation by LN LECs in the initiation of immune responses. We first exploited an anti-VEGFR3 blocking antibody in order to abrogate LEC proliferation following immunization with a subunit vaccine. In an alternative approach, we developed the Prox1-Cre-DTR mouse model, which allows for specific

ablation of LECs *in vivo*. Our findings improved our perception of the immunological significance of LEC expansion following inflammatory antigenic challenge and gave us valuable hints for their active contribution in the establishment of adaptive immunity.

This thesis illuminates the multifaceted immunological role of LECs and highlights their dynamic involvement in the regulation of immunity and tolerance. As we acquire a deeper understanding of the impact of antigen presentation by LECs, a new challenge rises. In **Chapter 5**, we discuss whether and how we could potentially exploit LECs' function to improve protection against pathogens and tumors, or to prevent autoimmunity and transplant rejection.

1.5 References

1. Trevaskis, N. L., L. M. Kaminskas, and C. J. H. Porter. 2015. From sewer to saviour - targeting the lymphatic system to promote drug exposure and activity. *Nat Rev Drug Discov* 14: 781–803.
2. Cueni, L. N., and M. Detmar. 2008. The lymphatic system in health and disease. *Lymphatic Research and Biology* 6: 109–122.
3. Oliver, G., and K. Alitalo. 2005. The lymphatic vasculature: recent progress and paradigms. *Annu. Rev. Cell Dev. Biol.* 21: 457–483.
4. Randolph, G. J., V. Angeli, and M. A. Swartz. 2005. Dendritic-cell trafficking to lymph nodes through lymphatic vessels. *Nat. Rev. Immunol.* 5: 617–628.
5. Angeli, V., and G. J. Randolph. 2006. Inflammation, lymphatic function, and dendritic cell migration. *Lymphatic Research and Biology* 4: 217–228.
6. Johnson, L. A., and D. G. Jackson. 2008. Cell traffic and the lymphatic endothelium. *Annals of the New York Academy of Sciences* 1131: 119–133.
7. Alitalo, K. 2011. The lymphatic vasculature in disease. *Nat. Med.* 17: 1371–1380.
8. Alitalo, K., T. Tammela, and T. V. Petrova. 2005. Lymphangiogenesis in development and human disease. *Nature* 438: 946–953.
9. Lund, A. W., and M. A. Swartz. 2010. Role of lymphatic vessels in tumor immunity: Passive conduits or active participants? *J Mammary Gland Biol Neoplasia* 15: 341–352.
10. Swartz, M. A., and A. W. Lund. 2012. Lymphatic and interstitial flow in the tumour microenvironment: linking mechanobiology with immunity. *Nat. Rev. Cancer* 12: 210–219.
11. Cao, Y. 2005. Opinion: Emerging mechanisms of tumour lymphangiogenesis and lymphatic metastasis. *Nat. Rev. Cancer* 5: 735–743.
12. Swartz, M. A. 2014. Immunomodulatory roles of lymphatic vessels in cancer progression. *Cancer Immunol Res* 2: 701–707.
13. Christiansen, A., and M. Detmar. 2011. Lymphangiogenesis and cancer. *Genes Cancer* 2: 1146–1158.
14. Girard, J.-P., C. Moussion, and R. Förster. 2012. HEVs, lymphatics and homeostatic immune cell trafficking in lymph nodes. *Nat. Rev. Immunol.* 12: 762–773.
15. Förster, R., A. Braun, and T. Worbs. 2012. Lymph node homing of T cells and dendritic cells via afferent lymphatics. *Trends Immunol.* 33: 271–280.
16. Hansen, K. C., A. D'Alessandro, C. C. Clement, and L. Santambrogio. 2015. Lymph formation, composition and circulation: a proteomics perspective. *Int. Immunol.* 27: 219–227.
17. Clement, C. C., E. S. Cannizzo, M.-D. Nastke, R. Sahu, W. Olszewski, N. E. Miller, L. J. Stern, and L. Santambrogio. 2010. An expanded self-antigen peptidome is carried by the human lymph as compared to the plasma. *PLoS ONE* 5: e9863.
18. Swartz, M. 2001. The physiology of the lymphatic system. *Advanced Drug Delivery Reviews* 50: 3–20.
19. Shields, J. D. 2011. Lymphatics: at the interface of immunity, tolerance, and tumor metastasis. *Microcirculation* 18: 517–531.

20. Gunn, M. D., K. Tangemann, C. Tam, J. G. Cyster, S. D. Rosen, and L. T. Williams. 1998. A chemokine expressed in lymphoid high endothelial venules promotes the adhesion and chemotaxis of naive T lymphocytes. *Proc. Natl. Acad. Sci. U.S.A.* 95: 258–263.
21. Vassileva, G., H. Soto, A. Zlotnik, H. Nakano, T. Kakiuchi, J. A. Hedrick, and S. A. Lira. 1999. The reduced expression of 6Ckine in the plt mouse results from the deletion of one of two 6Ckine genes. *J. Exp. Med.* 190: 1183–1188.
22. Förster, R., A. C. Davalos-Misslitz, and A. Rot. 2008. CCR7 and its ligands: balancing immunity and tolerance. *Nat. Rev. Immunol.* 8: 362–371.
23. Baekkevold, E. S., T. Yamanaka, R. T. Palframan, H. S. Carlsen, F. P. Reinholt, U. H. von Andrian, P. Brandtzaeg, and G. Haraldsen. 2001. The CCR7 ligand elc (CCL19) is transcytosed in high endothelial venules and mediates T cell recruitment. *J. Exp. Med.* 193: 1105–1112.
24. Kedl, R. M., and B. A. Tamburini. 2015. Antigen archiving by lymph node stroma: A novel function for the lymphatic endothelium. *Eur. J. Immunol.* 45: 2721–2729.
25. Link, A., T. K. Vogt, S. Favre, M. R. Britschgi, H. Acha-Orbea, B. Hinz, J. G. Cyster, and S. A. Luther. 2007. Fibroblastic reticular cells in lymph nodes regulate the homeostasis of naive T cells. *Nat. Immunol.* 8: 1255–1265.
26. Fletcher, A. L., D. Malhotra, S. E. Acton, V. Lukacs-Kornek, A. Bellemare-Pelletier, M. Curry, M. Armant, and S. J. Turley. 2011. Reproducible isolation of lymph node stromal cells reveals site-dependent differences in fibroblastic reticular cells. *Front. Immunol.* 2: 1–15.
27. Cohen, J. N., E. F. Tewalt, S. J. Rouhani, E. L. Buonomo, A. N. Bruce, X. Xu, S. Bekiranov, Y.-X. Fu, and V. H. Engelhard. 2014. Tolerogenic properties of lymphatic endothelial cells are controlled by the lymph node microenvironment. *PLoS ONE* 9: e87740.
28. Ulvmar, M. H., K. Werth, A. Braun, P. Kelay, E. Hub, K. Eller, L. Chan, B. Lucas, I. Novitzky-Basso, K. Nakamura, T. Rülicke, R. J. B. Nibbs, T. Worbs, R. Förster, and A. Rot. 2014. The atypical chemokine receptor CCRL1 shapes functional CCL21 gradients in lymph nodes. *Nat. Immunol.* 15: 623–630.
29. Andrian, Von, U., and T. Mempel. 2003. Homing and cellular traffic in lymph nodes. *Nat. Rev. Immunol.*
30. Fletcher, A. L., V. Lukacs-Kornek, E. D. Reynoso, S. E. Pinner, A. Bellemare-Pelletier, M. S. Curry, A. R. Collier, R. L. Boyd, and S. J. Turley. 2010. Lymph node fibroblastic reticular cells directly present peripheral tissue antigen under steady-state and inflammatory conditions. *J. Exp. Med.* 207: 689–697.
31. Braun, A., T. Worbs, G. L. Moschovakis, S. Halle, K. Hoffmann, J. Bölter, A. Münk, and R. Förster. 2011. Afferent lymph-derived T cells and DCs use different chemokine receptor CCR7-dependent routes for entry into the lymph node and intranodal migration. *Nat. Immunol.* 12: 879–887.
32. Pham, T. H. M., P. Baluk, Y. Xu, I. Grigorova, A. J. Bankovich, R. Pappu, S. R. Coughlin, D. M. McDonald, S. R. Schwab, and J. G. Cyster. 2010. Lymphatic endothelial cell sphingosine kinase activity is required for lymphocyte egress and lymphatic patterning. *Journal of Experimental Medicine* 207: 17–27.
33. Sixt, M., N. Kanazawa, M. Selg, T. Samson, G. Roos, D. P. Reinhardt, R. Pabst, M. B. Lutz, and L. Sorokin. 2005. The conduit system transports soluble antigens from the afferent lymph to resident dendritic cells in the T cell area of the lymph node. *Immunity* 22: 19–29.
34. Roozendaal, R., T. R. Mempel, L. A. Pitcher, S. F. Gonzalez, A. Verschoor, R. E. Mebius, U. H. von Andrian, and M. C. Carroll. 2009. Conduits mediate transport of low-molecular-weight antigen to lymph node follicles. *Immunity* 30: 264–276.
35. Rantakari, P., K. Auvinen, N. Jäppinen, M. Kapraali, J. Valtonen, M. Karikoski, H. Gerke, I. Iftakhar-E-Khuda, J. Keuschnigg, E. Umemoto, K. Tohya, M. Miyasaka, K. Elima, S. Jalkanen, and M. Salmi. 2015. The endothelial protein PLVAP in lymphatics controls the entry of lymphocytes and antigens into lymph nodes. *Nat. Immunol.* 16: 386–396.
36. Gerner, M. Y., P. Torabi-Parizi, and R. N. Germain. 2015. Strategically localized dendritic cells promote rapid T cell responses to lymph-borne particulate antigens. *Immunity* 42: 172–185.

37. Itano, A. A., S. J. McSorley, R. L. Reinhardt, B. D. Ehst, E. Ingulli, A. Y. Rudensky, and M. K. Jenkins. 2003. Distinct dendritic cell populations sequentially present antigen to CD4 T cells and stimulate different aspects of cell-mediated immunity. *Immunity* 19: 47–57.
38. Miteva, D. O., J. M. Rutkowski, J. B. Dixon, W. Kilarski, J. D. Shields, and M. A. Swartz. 2010. Transmural Flow Modulates Cell and Fluid Transport Functions of Lymphatic Endothelium. *Circulation Research* 106: 920–931.
39. Zawieja, D. C. 2009. Contractile Physiology of Lymphatics. *Lymphatic Research and Biology* 7: 87–96.
40. Gerner, M. Y., W. Kastenmuller, I. Ifrim, J. Kabat, and R. N. Germain. 2012. Histo-Cytometry: A Method for Highly Multiplex Quantitative Tissue Imaging Analysis Applied to Dendritic Cell Subset Microanatomy in Lymph Nodes. *Immunity* 37: 364–376.
41. Card, C. M., S. S. Yu, and M. A. Swartz. 2014. Emerging roles of lymphatic endothelium in regulating adaptive immunity. *J. Clin. Invest.* 124: 943–952.
42. Hirosue, S., and J. Dubrot. 2015. Modes of Antigen Presentation by Lymph Node Stromal Cells and Their Immunological Implications. *Front. Immunol.* 6: 446.
43. Podgrabinska, S., P. Braun, P. Velasco, B. Kloos, M. S. Pepper, and M. Skobe. 2002. Molecular characterization of lymphatic endothelial cells. *Proc. Natl. Acad. Sci. U.S.A.* 99: 16069–16074.
44. Malhotra, D., A. L. Fletcher, J. Astarita, V. Lukacs-Kornek, P. Tayalia, S. F. Gonzalez, K. G. Elpek, S. K. Chang, K. Knoblich, M. E. Hemler, M. B. Brenner, M. C. Carroll, D. J. Mooney, S. J. Turley, Immunological Genome Project Consortium. 2012. Transcriptional profiling of stroma from inflamed and resting lymph nodes defines immunological hallmarks. *Nat. Immunol.* 13: 499–510.
45. Nörder, M., M. G. Gutierrez, S. Zicari, E. Cervi, A. Caruso, and C. A. Guzman. 2012. Lymph node-derived lymphatic endothelial cells express functional costimulatory molecules and impair dendritic cell-induced allogenic T-cell proliferation. *FASEB J.* 26: 2835–2846.
46. Kriehuber, E., S. Breiteneder-Geleff, M. Groeger, A. Soleiman, S. F. Schoppmann, G. Stingl, D. Kerjaschki, and D. Maurer. 2001. Isolation and characterization of dermal lymphatic and blood endothelial cells reveal stable and functionally specialized cell lineages. *J. Exp. Med.* 194: 797–808.
47. Podgrabinska, S., O. Kamalu, L. Mayer, M. Shimaoka, H. Snoeck, G. J. Randolph, and M. Skobe. 2009. Inflamed Lymphatic Endothelium Suppresses Dendritic Cell Maturation and Function via Mac-1/ICAM-1-Dependent Mechanism. *J. Immunol.* 183: 1767–1779.
48. Lukacs-Kornek, V., D. Malhotra, A. L. Fletcher, S. E. Acton, K. G. Elpek, P. Tayalia, A.-R. Collier, and S. J. Turley. 2011. Regulated release of nitric oxide by nonhematopoietic stroma controls expansion of the activated T cell pool in lymph nodes. *Nat. Immunol.* 12: 1096–1104.
49. Pegu, A., S. Qin, B. A. Fallert Junecko, R. E. Nisato, M. S. Pepper, and T. A. Reinhart. 2008. Human lymphatic endothelial cells express multiple functional TLRs. *J. Immunol.* 180: 3399–3405.
50. Dubrot, J., F. V. Duraes, L. Potin, F. Capotosti, D. Brighouse, T. Suter, S. LeibundGut-Landmann, N. Garbi, W. Reith, M. A. Swartz, and S. Hugues. 2014. Lymph node stromal cells acquire peptide-MHCII complexes from dendritic cells and induce antigen-specific $CD4^+$ T cell tolerance. *Journal of Experimental Medicine* 211: 1153–1166.
51. Gardner, J. M., J. J. Devoss, R. S. Friedman, D. J. Wong, Y. X. Tan, X. Zhou, K. P. Johannes, M. A. Su, H. Y. Chang, M. F. Krummel, and M. S. Anderson. 2008. Deletional tolerance mediated by extrathymic Aire-expressing cells. *Science* 321: 843–847.
52. Magnusson, F. C., R. S. Liblau, H. von Boehmer, M. J. Pittet, J.-W. Lee, S. J. Turley, and K. Khazaie. 2008. Direct presentation of antigen by lymph node stromal cells protects against CD8 T-cell-mediated intestinal autoimmunity. *Gastroenterology* 134: 1028–1037.
53. Lee, J.-W., M. Epardaud, J. Sun, J. E. Becker, A. C. Cheng, A.-R. Yonekura, J. K. Heath, and S. J. Turley. 2006. Peripheral antigen display by lymph node stroma promotes T cell tolerance to intestinal self. *Nat. Immunol.* 8: 181–190.
54. Cohen, J. N., C. J. Guidi, E. F. Tewalt, H. Qiao, S. J. Rouhani, A. Ruddell, A. G. Farr, K. S. Tung, and V. H. Engelhard. 2010. Lymph node-resident lymphatic endothelial cells mediate peripheral tolerance via Aire-independent direct antigen presentation. *J. Exp.*

Med. 207: 681–688.

55. Anderson, G., and Y. Takahama. 2012. Thymic epithelial cells: working class heroes for T cell development and repertoire selection. *Trends Immunol.* 33: 256–263.
56. Yip, L., L. Su, D. Sheng, P. Chang, M. Atkinson, M. Czesak, P. R. Albert, A.-R. Collier, S. J. Turley, C. G. Fathman, and R. J. Creusot. 2009. Deaf1 isoforms control the expression of genes encoding peripheral tissue antigens in the pancreatic lymph nodes during type 1 diabetes. *Nat. Immunol.* 10: 1026–1033.
57. Mueller, S. N., and R. N. Germain. 2010. Stromal cell contributions to the homeostasis and functionality of the immune system. *Nat. Rev. Immunol.* 9: 618–629.
58. Reynoso, E. D., and S. J. Turley. 2009. Unconventional antigen-presenting cells in the induction of peripheral CD8(+) T cell tolerance. *J. Leukoc. Biol.* 86: 795–801.
59. Tiegs, G., and A. Lohse. 2010. ScienceDirect.com - Journal of Autoimmunity - Immune tolerance: What is unique about the liver. *Journal of autoimmunity*.
60. Lund, A. W., F. V. Duraes, S. Hirosue, V. R. Raghavan, C. Nembrini, S. N. Thomas, A. Issa, S. Hugues, and M. A. Swartz. 2012. VEGF-C promotes immune tolerance in B16 melanomas and cross-presentation of tumor antigen by lymph node lymphatics. *Cell Rep.* 1: 191–199.
61. Limmer, A., J. Ohl, C. Kurts, H. G. Ljunggren, Y. Reiss, M. Groettrup, F. Momburg, B. Arnold, and P. A. Knolle. 2000. Efficient presentation of exogenous antigen by liver endothelial cells to CD8+ T cells results in antigen-specific T-cell tolerance. *Nat. Med.* 6: 1348–1354.
62. Oppen, von, N., A. Schurich, S. Hegenbarth, D. Stabenow, R. Tolba, R. Weiskirchen, A. Geerts, W. Kolanus, P. Knolle, and L. Diehl. 2009. Systemic antigen cross-presented by liver sinusoidal endothelial cells induces liver-specific CD8 T-cell retention and tolerization. *Hepatology* 49: 1664–1672.
63. Schurich, A., J. P. Böttcher, S. Burgdorf, P. Penzler, S. Hegenbarth, M. Kern, A. Dolf, E. Endl, J. Schultze, E. Wiertz, D. Stabenow, C. Kurts, and P. Knolle. 2009. Distinct kinetics and dynamics of cross-presentation in liver sinusoidal endothelial cells compared to dendritic cells. *Hepatology* 50: 909–919.
64. Diehl, L., A. Schurich, R. Grochtmann, S. Hegenbarth, L. Chen, and P. A. Knolle. 2008. Tolerogenic maturation of liver sinusoidal endothelial cells promotes B7-homolog 1-dependent CD8+ T cell tolerance. *Hepatology* 47: 296–305.
65. Tewalt, E. F., J. N. Cohen, S. J. Rouhani, C. J. Guidi, H. Qiao, S. P. Fahl, M. R. Conaway, T. P. Bender, K. S. Tung, A. T. Vella, A. J. Adler, L. Chen, and V. H. Engelhard. 2012. Lymphatic endothelial cells induce tolerance via PD-L1 and lack of costimulation leading to high-level PD-1 expression on CD8 T cells. *Blood* 120: 4772–4782.
66. Sallusto, F., J. Geginat, and A. Lanzavecchia. 2004. Central memory and effector memory T cell subsets: function, generation, and maintenance. *Annu. Rev. Immunol.*
67. Mescher, M. F., P. Agarwal, K. A. Casey, C. D. Hammerbeck, Z. Xiao, and J. M. Curtsinger. 2007. Molecular basis for checkpoints in the CD8 T cell response: tolerance versus activation. *Seminars in Immunology* 19: 153–161.
68. Riley, J. L. 2009. PD-1 signaling in primary T cells. *Immunol. Rev.* 229: 114–125.
69. Leitner, J., K. Grabmeier-Pfistershammer, and P. Steinberger. 2010. Receptors and ligands implicated in human T cell costimulatory processes. *Immunology Letters* 128: 89–97.
70. Reynoso, E. D., K. G. Elpek, L. Francisco, R. Bronson, A. Bellemare-Pelletier, A. H. Sharpe, G. J. Freeman, and S. J. Turley. 2009. Intestinal Tolerance Is Converted to Autoimmune Enteritis upon PD-1 Ligand Blockade. *The Journal of Immunology* 182: 2102–2112.
71. Pardoll, D. M. 2012. The blockade of immune checkpoints in cancer immunotherapy. *Nat. Rev. Cancer* 12: 252–264.

Chapter 2

Steady-state antigen scavenging, cross-presentation and $CD8^+$ T cell priming: a new role for LECs*

Until recently, the known roles of lymphatic endothelial cells (LECs) in immune modulation were limited to directing immune cell trafficking and passively transporting peripheral antigens to lymph nodes. Recent studies have demonstrated that LECs can directly suppress dendritic cell maturation and present peripheral tissue and tumor antigens for autoreactive T cell deletion. We asked whether LECs play a constitutive role in T cell deletion under homeostatic conditions. Here, we demonstrate that murine LECs under non-inflamed conditions actively scavenge and cross-present foreign exogenous antigens to cognate $CD8^+$ T cells. This cross-presentation was sensitive to inhibitors of lysosomal acidification and ER-golgi transport and was TAP1-dependent. Furthermore, LECs up-regulated MHC I and the PD-1 ligand PD-L1, but not the co-stimulatory molecules CD40, CD80, or CD86, upon antigen-specific interactions with $CD8^+$ T cells. Finally, antigen-specific $CD8^+$ T cells that were activated by LECs underwent proliferation with early-generation apoptosis and dysfunctionally-activated phenotypes that could not be reversed by exogenous IL-2, indicating that LEC-mediated $CD8^+$ T cell tolerance is not simply T cell exhaustion. These findings help establish LECs as antigen-presenting cells, capable of scavenging and cross-presenting exogenous antigens, in turn causing dysfunctional activation of $CD8^+$ T cells under homeostatic conditions. We suggest that steady-state lymphatic drainage may thus contribute to peripheral tolerance not only by delivering self-antigens to lymph node-resident leukocytes, but also by providing constant exposure of draining peripheral antigens to LECs, which maintain tolerogenic cross-presentation of such antigens.

* adapted from the original manuscript Hirosue, S., E. Vokali, *et al*., 2014, The Journal of Immunology 192: 5002–5011.

2.1 Introduction

The lymphatic system transports interstitial fluid, antigens, solutes and immune cells from the periphery and returns them to the blood circulation after surveillance through lymph nodes (LNs), thereby initiating adaptive immune responses (1-3). In addition to effector immune responses, LNs are important sites for the maintenance of peripheral tolerance. Lymph node stromal cells, which include lymphatic and blood endothelial cells (LECs and BECs) as well as fibroblastic reticular cells (FRCs) in the T cell zone, are thought to contribute to tolerance induction of autoreactive T cells that escape central memory (4) as well as regulate the contraction of inflammatory responses (5). Indeed, the lymphatic endothelium is emerging as an important player in shaping immunity and tolerance (1-3, 6-10). For example, LECs have been shown to suppress maturation of DCs (1, 4, 11) and their subsequent priming of $CD8^+$ T cells in a contact-dependent manner (4, 5, 9). In addition, LECs as well as FRCs can directly prime $CD8^+$ T cells (5); they express components of the antigen presentation machinery including major histocompatibility complex (MHC) I and II molecules (6-9, 12) and have been shown to directly contribute to peripheral tolerance by expression and presentation of endogenous peripheral tissue-restricted antigens (PTAs), leading to compromised $CD8^+$ T cell activation (6-9). They are also sensitive to pathogen-associated molecular patterns via the expression of various members of the toll-like receptor (TLR) family (8, 11). Together, these studies have established LECs as contributors to maintaining peripheral tolerance to endogenously expressed self-antigens.

However, little is known about whether LECs as antigen-presenting cells (APCs) have the ability to capture and process exogenous antigens for $CD8^+$ T cell deletion. While so-called professional APCs such as $CD8a^+$ DCs can process exogenous antigens for cross-presentation to $CD8^+$ T cells, some non-hematopoietic cell types have also been shown to be capable of cross-presentation (13). For example, liver sinusoidal endothelial cells (LSECs) are thought to capture and cross-present circulating antigen to $CD8^+$ T cells, leading to $CD8^+$ T cell deletion and the establishment of a tolerogenic environment (14). This is especially important in the liver, where LSECs are amongst the first cells to encounter the large diversity of foreign antigens from food as well as TLR agonists from commensal sources (15). Similarly, LECs are the first cells to contact extracellular antigens that arise in the periphery and drain into lymphatic vessels after e.g., tissue damage, inflammation, or infection. We recently showed that a foreign antigen (OVA) expressed by an orthotopically implanted tumor could be cross-presented by tumor-associated LECs which, when isolated, could drive dysfunctional activation of cognate $CD8^+$ T cells and promote tumor progression (16). As tumors utilize physiological mechanisms to promote tolerance for their survival (17), we hypothesized that a similar mechanism of antigen cross-presentation by LECs may exist under steady-state conditions to promote tolerance against self-antigens.

Here, we demonstrate that under homeostatic conditions, LECs constitutively uptake and cross-present exogenous antigens to $CD8^+$ T cells. We further show that LEC-activated T cells are more rapidly apoptotic, upregulate so-called exhaustion markers (PD-1, CTLA-4, and CD80), secrete less IFNγ and IL-2, and express lower levels of the activation markers CD25, CD44, and CD69 compared to T cells activated by

DCs. Together, these data suggest that LECs help maintain $CD8^+$ T cell tolerance to exogenous antigens that are encountered in lymph under steady-state conditions, which may be important for preventing autoimmune reactions against self-antigens after infection or injury.

2.2 Materials and Methods

Reagents

All chemicals were from Sigma-Aldrich (Buchs, CH) unless otherwise noted. The mature MHC I epitope, $OVA_{256-264}$ (SIINFEKL) peptide, was from GenScript (Piscataway, NJ, US). Endotoxin-free OVA was from Hyglos GmbH, (Bernried am Starnberger See, DE). Antibodies used in flow cytometry were from eBioscience (Vienna, AT) or BioLegend (Luzern, CH) unless otherwise noted.

Mice

The following mice strains were used in this study at age 6-12 weeks unless noted otherwise. Female C57BL/6 wild-type mice and OT-I transgenic mice, C57BL/6- Tg(TcraTcrb)1100Mjb/J, were purchased from Harlan Laboratories (Gannat, FR). $TAP1^{-/-}$ mice (B6.129S2-*Tap1tm1Arp*/J), were purchased from Jackson Laboratories (Farmington, CT, US). Animals were housed in pathogen-free facilities and all procedures were approved by the Cantonal Veterinary Committee of Vaud, Switzerland (Protocol number 2518).

Cell lines

Conditionally immortalized dermal LECs (iLECs) from Immortomice were isolated and cultured as previously described (18). Cell culture surfaces used in all assays were coated with collagen (10µg/ml PureCol, Advanced Biomatrix, San Diego, CA, US) and 10µg/ml human fibronectin (Millipore, Billerica, MA, US) prior to seeding. Cells were grown in 40% DMEM low glucose, 40% F12, 20% Fetal Bovine Serum (FBS) (all from Invitrogen, Zug, CH), supplemented with 10µg/ml native bovine endothelial mitogen (AbD Serotec, Düsseldorf, DE) and 56µg/ml heparin sodium salt from porcine intestinal mucosa (Sigma-Aldrich). To induce large T antigen expression, IFNγ (R&D, Abingdon, UK) was added to the media at 100U/ml and cells were propagated at 33°C. Prior to all experiments, cells were grown for 72h in the absence of IFNγ at 37°C and maintained as such.

Primary cell isolation

To obtain primary LN LECs, LNs were digested with 0.25mg/ml Liberase DH and 100µg/ml DNase (both from Roche, Basel, CH) to obtain a single cell suspension and cultured as described (19). Cells were cultured for 5 days until confluent, removed by Accutase (Biological Industries, Lucerna-Chem AG, Lucerne CH), and stained with mAbs against gp38 (clone 8.1.1), CD31 (clone 390), and CD45 (clone 30-F10) and FACS sorted (FACS Aria II, BD, Basel, CH) into the following subpopulations: FRCs ($gp38^+CD31^-$) LECs ($gp38^+CD31^+$), BECs ($gp38^-CD31^+$), and DN ($gp38^-CD31^-$) as described (20). Bone marrow-derived DCs (BMDCs) were harvested from C57Bl/6 mice, differentiated in GM-CSF as described (21) and used at day 7 of culture.

Synthesis of peptide-conjugated nanoparticles (NPs)

To explore the mechanisms of cross-presentation poly(propylene sulfide)-nanoparticles (NPs) with ~30nm diameter were synthesized and characterized as described (22). The long peptide containing the mature MHC I epitope SIINFEKL – Cys-$OVA_{250-264}$ ($COVA_{250-264}$) was synthesized in-house and activated with a 2-pyridylthiol as previously described (22). Core sulfhydryls on NPs were reacted with the activated peptide and purified on a Sepharose

CL6B column (Sigma-Aldrich). To fluorescently label the NPs, NPs were exposed to Dy-649 maleimide (Dyomics GmbH, Jena, DE) after dialysis in a 1:60 molar ratio of dye to NP sulfydryl groups in phosphate buffered saline (PBS) at RT for 24 h (22). Free dye was removed by gel filtration in as above but in endotoxin-free water (B. Braun Medical AG, Sempach Switzerland) as eluent. Endotoxin levels of antigens were routinely assessed by a colorimetric assay based on the HEK-Blue ™ TLR4 cell line (InvivoGen, San Diego, CA, USA) according to the manufacturer's protocol using a standard curve generated from the E-Toxate ™ endotoxin standard (Sigma).

In vivo antigen drainage

To determine whether LN LECs can actively capture antigens *in vivo*, we injected fluorescently labeled OVA protein into the limbs of mice and determined its distribution within various cells in the LN after 90 min. Endotoxin-free OVA was labeled with AlexaFluor 647 NHS (Dyomics GmbH, Jena, DE) (OVA AF-647) and purified by size exclusion chromatography using a Sephadex G-25 column with PBS as eluent. C57BL/6 mice were injected intradermally (i.d.) with 15 µg OVA AF-647 in the limbs. After 90 min, mice were transcardially perfused with a heparinized saline solution containing 1g/L glucose and 20mM HEPES, pH 7.2. For immunostaining, brachial LNs were removed and fixed overnight in 2% PFA in PBS pH 7.4. After three washes in PBS, LNs were embedded in a block of 2% agarose, and sectioned (150µm) using a using a vibratome (Leica, Wetzlar DE). Sections were blocked in 0.5% of casein, and further labeled using antibodies against CD3e (BD Pharmingen, clone 500A2) and LYVE-1 (Reliatech, San Pablo, CA US). Images were acquired on a Leica SP5 confocal microscope using 20x or 60x objectives, and processed using Imaris software (Bitplane, Zürich, CH). For flow cytometric analysis, brachial LNs from individual mice were pooled and digested with 1mg/ml Collagenase D and 200 kunitz/ml DNase I (Sigma Aldrich). After LNs were fully digested as described (19) the single cell preparations were enriched for non-hematopoietic stromal cells by CD45 cell depletion using CD45 microbeads (Miltenyi Biotec, Bergisch Gladbach, DE). Enriched stroma and the $CD45^+$ fraction were then counted, stained with (gp38, CD31, CD45, LYVE-1) and (CD45, CD11c, CD11b, MHC II), respectively, and analyzed by flow cytometry.

Intracellular localization studies

To determine the intracellular pathways of antigen trafficking, we incubated iLECs with fluorescently labeled OVA and stained for different cellular components. Cells were seeded on glass coverslips (15mm round, Karl Hecht KG, DE) coated as above at 2×10^5 cells/well in 12-well plates. NP-Dy649 or OVA-AF647 at final concentrations of no more than 5 mg/ml, 10µg /ml, respectively, were added to the cells for 1 hour on ice in buffered (25mM Hepes) reduced serum (2% FBS) culture media, then transferred to 37^oC for 15 or 90 min. Cells were fixed in 4% paraformaldehyde in PBS, permeabilized in permeabilization buffer (3% bovine serum albumin and 0.1% saponin) in PBS overnight at 4^oC. Primary antibody incubations were 1h followed by species-matched secondary antibodies for 30min at room temperature. The 15min time point was stained for clathrin, while the 90min time point was stained for LAMP-1. All antibody dilutions were made in permeabilization buffer. Coverslips were mounted with Citifluor (Citifluor Ltd., UK), imaged with a 63x oil immersion lens on a LSM 700 or 710 inverted, or upright confocal microscope (Carl Zeiss, Feldbach, CH) respectively. After deconvolution (Huygens Deconvolution software, Scientific Volume Imaging, NL), Fiji software (NIH, Bethesda, MD US) applying the Image 5D plugin was used to generate the figures. To quantify fluorescent NP or OVA colocalization within clathrin-positive vesicles, single z-planes from deconvolved images were analyzed using a script that determines the statistical significance of object-based colocalization by comparison of the colocalization occurences on actual images as compared to colocalization by chance (23). To determine whether NP^+ or OVA^+ spots were within or outside of $LAMP\text{-}1^+$ surfaces, the ImarisXT matlab plugin "split spots onto surface objects" was used. Spots were defined as ≤0.2µm in diameter,

and LAMP-1$^+$ surfaces were drawn within a resolution of 0.1µm from the immunofluorescence signal. Intravesicular spots were defined as spots within this surface.

In vitro antigen cross-presentation

To determine whether LECs can cross-present antigen *in vitro*, cells were plated at 5x10^4 cells per well in 24 well plates and stimulated with either 2.5µM $OVA_{257-264}$ (SIINFEKL), 2.5µM NP-ss-$COVA_{250-264}$, or equivalent concentrations of unconjugated NP for 18h in medium buffered with 25mM HEPES (pH7.4) at 4° or 37°C. Cell surface H2-K^b –$OVA_{257–264}$ complexes were detected by the antibody 25d1.16 by flow cytometry. To characterize the kinetics of OVA accumulation in LECs, cells were stimulated with 1µM OVA-AF647 for up to 90min, washed, and analyzed for OVA uptake by flow cytometry. To demonstrate CD8$^+$ T cell priming, APCs were seeded at 10^4 cells per well in 96 well round-bottom (BMDCs) or flat-bottom (LECs) plates.

In vitro T cell co-culture assays

To determine the outcome of CD8$^+$ T cell interaction with cross-presenting LECs, we performed coculture assays. CD8α$^+$ T-cells were purified from the spleen of an OT-I mouse by negative selection (CD8α Kit II, Miltenyi Biotec, Bergisch Gladbach, DE). For LEC-T cell or DC-T cell coculture studies, 10^4 LECs or DCs were cocultured with naïve CD8$^+$ T-cells from OT-I mice in 96-well plates for 72h at a ratio of 1:10 APC:T cells in 200 µl of coculture media (IMDM with 10% FBS and 1% penicillin/streptomycin). To inhibit antigen uptake and processing, cells were pre-treated with either dynasore, LY294002, or lactacystin (inhibitors of dynamin, phosphoinositide 3-kinase, and proteasome activity, respectively) 1h prior to addition of antigen (SIINFEKL or NP-ss-$COVA_{250-264}$, 1nM peptide concentration) in APC-specific media. For drugs that inhibit intracellular antigen trafficking, we applied the antigen for 1h prior to addition of brefeldin A (BFA) and chloroquine, which inhibit protein transport from the endoplasmic reticulum (ER) to the golgi apparatus and endosome acidification, respectively. After 24h incubation at 37^{o}C, cells were washed and fixed with 2% paraformaldehyde in PBS (pH7.4) for 10min on ice. After washing, CFSE-labeled CD8$^+$ OT-I T cells were added as above. Supernatants were harvested and frozen for cytokine analysis by ELISA (R&D Systems, Minneapolis, MN, US). Cells were then processed and stained for immunological markers to be analyzed flow cytometry. Cellular proliferation was monitored by CFSE dilution and apoptosis was determined by Annexin V staining (BioVision, Milpitas, CA, US). OT-I T cell proliferation was determined by assessing CFSE intensity using the automated tool in FlowJo 9.4.11 and reported as a division index (i.e., the average number of divisions that a cell has undergone; division index = proliferation index (average number of divisions) × percent dividing cells). Intracellular IFNγ was determined after 2h of PMA/Ionomycin and 2h of BFA treatment. In some experiments, to determine the effect of exogenous IL-2 on LEC-T cell interactions, cocultures were supplemented with 50U/ml IL-2 (Roche, Mannheim, DE) in the co-culture media.

Flow cytometry

Cells were washed and stained with a cocktail of surface antibodies in staining buffer, containing HBSS (Life Technologies) supplemented with 0.5 % bovine serum albumin. Cell viability was determined by propidium iodide incorporation in staining buffer after surface antibody staining or with live/dead fixable cell viability reagent (Life Technologies) in PBS before surface antibody staining. Apoptosis was determined by annexin V staining (BioVision, Milpitas, CA). Finally, cells were resuspended in staining buffer and analyzed by flow cytometry (CyAn ADP Flow Cytometer, DAKO). Data analysis was performed using FlowJo (v9.4, Tree Star Inc., Ashland, OR, USA).

Statistical analysis

Statistical analysis was performed using one-way analysis of variance (ANOVA) followed by Bonferroni post-test with Prism software (Graphpad, San Diego, CA, US) unless otherwise stated. Results are shown as mean ± standard deviation with significance indicated as *p≤0.05, **p≤0.01, and ***p≤0.001.

2.3 Results

Lymphatic endothelial cells scavenge exogenous antigen *in vivo* and *in vitro*

While LECs transport antigens from the periphery to the lymph, we asked whether LECs could also scavenge and process antigens as well. To this end, we injected intradermally (i.d.) fluorescently labeled OVA protein (OVA-AF647) in the forearm and after 90 min observed its distribution in the brachial draining LN. The use of a foreign protein allowed us to determine specifically the immune response against an exogenous versus self-expressed PTA. Using confocal microscopy of thick sections of the brachial LN, we observed OVA in the lymphatic-rich, LYVE-1^+ sinuses of the LN (Fig. 2.1A). Upon magnification of the LYVE-1^+ regions, we observed that much of the OVA was contained within LYVE-1^+ cells, suggesting intracellular accumulation in LECs (Fig. 2.1B, C). Flow cytometric analysis validated the observed scavenger activity and demonstrated that LN LECs ($CD45^-gp38^+CD31^+$LYVE-1^+ cells), as well as professional APCs contained soluble OVA (Fig. 2.1D, E and Fig. 2.6). Among the $CD45^-$ stromal cells, LECs took up the most OVA (50±8%). When considered as a percentage of each cell population that took up OVA, LECs were on par with DCs for their scavenging ability (30±20% vs. 30±5%, respectively).

In vitro, we could follow the accumulation of fluorescent OVA by immortalized murine LECs (iLECs) (18). The degree of OVA-AF647 accumulation by iLECs was similar to that of bone marrow-derived dendritic cells (DCs) over 90 minutes at 37°C, reaching a plateau within 40 min, as observed by flow cytometry (Fig. 2.1F, G and Fig. 2.6C). This exogenous antigen uptake was an active or energy-dependent process, since OVA uptake at 4°C by iLECs was minimal compared to that at 37°C (Fig. 2.1G and Fig. 2.6D). These results confirm that exogenous proteins are actively scavenged by LECs, both *in vivo* and *in vitro*.

Lymphatic endothelial cells process and route antigen for cross-presentation on MHC I in a TAP1-dependent manner

Accumulation of exogenous proteins inside LECs allows for the possibility of antigen processing and cross-presentation on MHC I by these cells. We asked if under controlled in *vitro* conditions, hallmarks of cross-presentation could be observed in LECs.

First, we determined whether uptake of exogenous antigens could lead to peptide loading onto MHC I molecules and presentation on the cell surface by immunostaining cells with the monoclonal antibody 25d1.16, which specifically binds the MHC I-bound $CD8^+$ dominant epitope of OVA, SIINFEKL ($OVA_{257-264}$). In order to avoid SIINFEKL peptide binding directly to surface MHC I and thus bypass the need for intracellular processing and cross-presentation, we used a N-terminally elongated

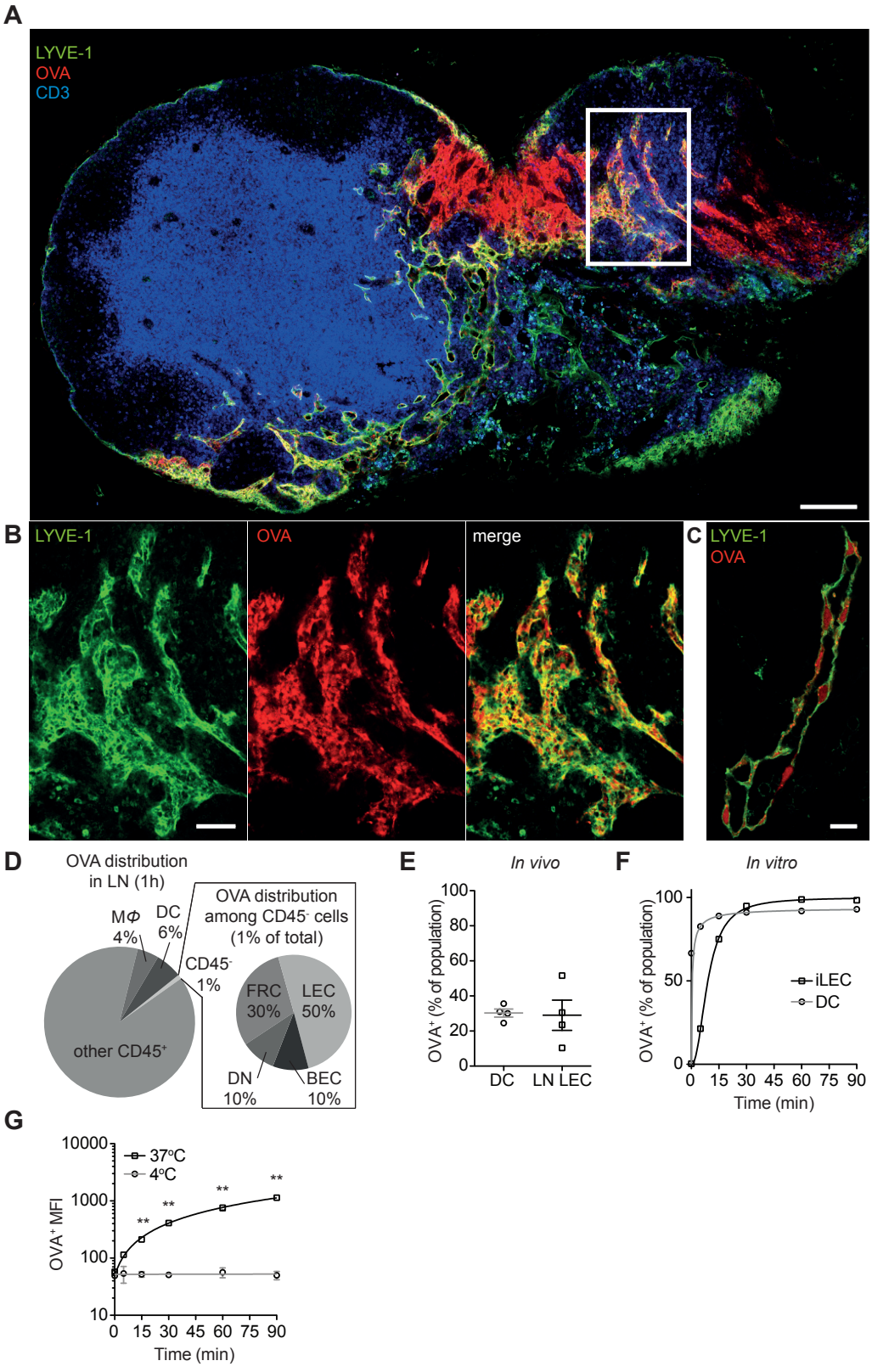

Figure 2.1 LECs scavenge exogenous protein, *in vivo* and *in vitro*. (A-E) After intradermal injection into the footpads, lymphatic endothelial cells (LECs) in the draining lymph node (LN) take up ovalbumin rapidly. **(A)** Brachial lymph node section showing LEC (Lyve-1, green) associated distribution of AlexaFluor 647 (AF-647)-labeled ovalbumin (OVA, red) after 90min; T cells (CD3e, blue) are shown for orientation. Bar, 150µm. **(B)** Close-up image from region indicated by white box in (A) shows

colocalization of OVA with LYVE-1$^+$ LECs. Bar, 75µm. **(C)** Further zoom into a LYVE-1$^+$ lymphatic vessel shows OVA$^+$ vesicles within the LECs; bar, 10µm. **(D)** Cellular distribution of OVA in the draining LN after 90 min i.d. injection, as analyzed by flow cytometry. Of all OVA$^+$ cells, 6% and 4% were dendritic cells (DCs, CD11b$^{-/+}$CD11c$^+$) and macrophages (MΦ, CD11b$^+$CD11c$^-$), respectively, while 1% of OVA$^+$ cells in the LN were stromal cells (CD45$^-$). Amongst these (inset), LECs (gp38$^+$CD31$^+$) scavenged the most compared to fibroblastic reticular cells (FRCs, gp38$^+$CD31$^-$), blood endothelial cells (BECs, gp38$^-$CD31$^+$), and double negative cells (DN, gp38$^-$CD31$^-$). **(E)** Shown as percentages of each LN cell population positive for OVA, LECs were similar to CD11b$^-$CD11c$^+$MHC II^{mid+} DCs in their scavenging capabilities and these two cell populations represented the highest %OVA$^+$ amongst all LN cell types. Data are from 2 independent experiments (n=4). **(F-G)** To demonstrate *in vitro* OVA accumulation, immortalized dermal LECs (iLECs) and bone marrow-derived dendritic cells (DCs) were incubated over 90min at 4 or 37^{o}C with 1µM OVA AF-647. Cells were washed and analyzed for OVA uptake by flow cytometric analysis. **(F)** Percent of OVA-AF-647$^+$ cells plotted for gp38$^+$CD31$^+$ gated iLECs and CD11c$^+$ gated DCs at 37^{o}C over time. **(G)** Geometric mean of OVA fluorescence is plotted for iLECs at 4^{o}C versus 37^{o}C. The data are representative from 2 independent experiments (n=3).

SIINFEKL-peptide conjugated onto synthetic poly(propylene sulfide) 30nm nanoparticles (NPs), a tool that we recently developed in our laboratory for more efficient SIINFEKL/ MHC I cross-presentation by 25d1.16 as compared to OVA (22). While SIINFEKL peptide can bind to MHC I without cell internalization and processing, this 16aa peptide on the NPs (NP-ss-COVA$_{250\text{-}264}$) minimally binds to surface MHC I, and instead requires uptake and intracellular processing for MHC I loading in BMDCs (22). Exogenously applied NP-ss-COVA$_{250\text{-}264}$ resulted in the detection of MHC I peptide complexes in an energy-dependent manner in both iLECs and *ex-vivo* cultured primary LN LECs (Fig. 2.2A, B). By conducting this study at both 4^{o}C and 37^{o}C, we confirmed that the cross-presentation of NP-ss-COVA$_{250\text{-}264}$ by LECs requires active processing, as only cells that received SIINFEKL and not NP-bound peptide antigen showed elevated 25d1.16 staining at 4^{o}C (Fig. 2.2A, B).

We then applied inhibitors of antigen uptake and intracellular trafficking to elucidate the relevant steps in LEC cross-presentation. We co-cultured inhibitor-treated, antigen-loaded LECs with OT-I CD8$^+$ T cells and measured T cell proliferation by CFSE dilution as a measure of MHC I/SIINFEKL presentation on the LEC surface. To confirm that LEC-induced T cell stimulation was dependent on intracellular uptake of NP-ss-COVA$_{250\text{-}264}$, we pre-treated iLECs with dynasore, an inhibitor of dynamin that affects both clathrin and caveolin mediated uptake (24), or LY294002, a PI-3K inhibitor that affects macropinocytosis (25). Both inhibitors led to reduced OT-I T cell proliferation in a concentration-dependent manner when LECs were treated with NP-conjugated antigen, but not free SIINFEKL peptide (Fig. 2.2C), confirming active uptake mechanisms contributing to MHC I presentation.

We next asked whether intracellular transport processes were important in LEC cross-presentation. To this end, we treated iLECs with BFA, which inhibits antigen transport from the endoplasmic reticulum (ER) to golgi (26), or chloroquine, which inhibits acidification and vesicle fusion to late endosomes/lysosomes (27). LECs pretreated with either of these agents also resulted in concentration-dependent inhibition of T cell proliferation (Fig. 2.2C).

Since ER-golgi transport as well as endosome acidification were observed to be important in cross-presentation by LECs, we next asked whether exogenous antigen processing in LECs depends on the canonical TAP1 pathway, where cytoplasmic peptide fragments are loaded onto MHC I in the ER after translocation by TAP1 (28).

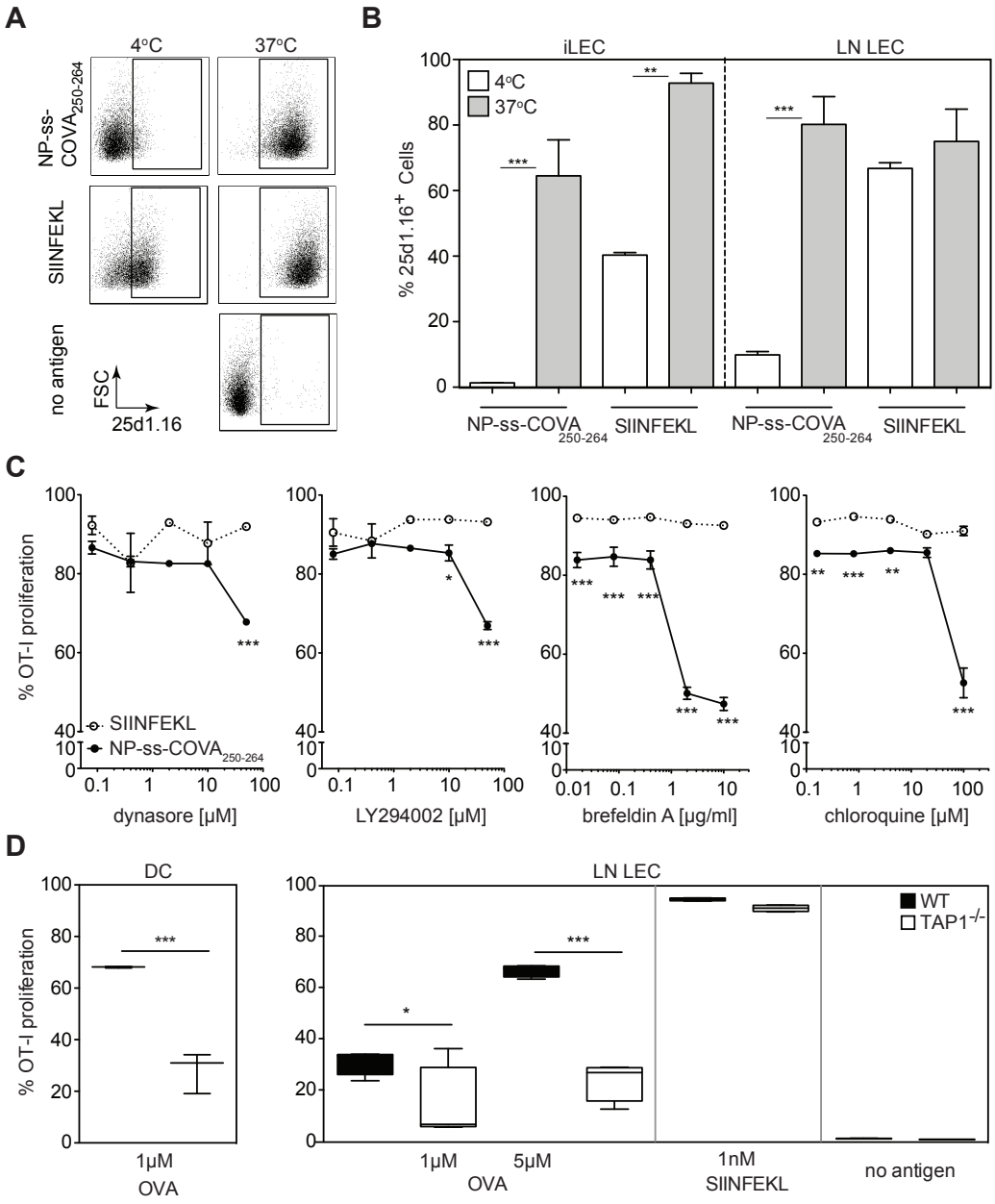

Figure 2.2 LECs process and cross-present exogenous antigen, resulting in priming naïve CD8$^+$ T cells. (A) Detection of the MHC I-SIINFEKL complex using the antibody 25d1.16 on *ex-vivo* expanded lymph node lymphatic endothelial cells (LN LEC; CD45$^-$ CD31$^+$ gp38$^+$) after exposure to N-term elongated OVA MHC I peptide conjugated to synthetic poly(propylene sulfide) 30 nm particles (NPssCOVA$_{250\text{-}264}$). Unlike the free peptide OVA$_{257\text{-}264}$ (SIINFEKL), the NPssCOVA$_{250\text{-}264}$ cannot bind extracellularly to MHC I; rather, the antigen must be processed intracellularly as seen by the lack of presentation at 4°C. **(B)** Expression of OVA peptide (SIINFEKL)-MHC I complex by LN LECs and cultured immortalized LECs (iLECs) after 18h incubation with NPssCOVA$_{250\text{-}264}$ or SIINFEKL at 2.5µM for 18h at 4 or 37°C. Pooled data from 2 independent experiments (n=3 each). **(C)** Proliferation of CFSE-labeled OT-I CD8$^+$ T cells after 3 days of co-culture with iLECs is impaired in the presence of dynasore and LY294002, which block antigen uptake pathways, as well as with Brefeldin A and chloroquine, which block ER-golgi membrane trafficking and endosome acidification, respectively. 1nM SIINFEKL peptide or NPssCOVA$_{250\text{-}264}$ was used as antigen; the data shown are representative of 2 experiments (n=3). **(D)** The ability of LECs to cross-prime OT-I CD8$^+$ T cells after OVA uptake depends on TAP1, which is required for intra-ER loading of peptides onto MHC I molecules. Percentages of proliferation of CFSE-labeled OT-I CD8$^+$ T cells after 3 days of co-culture with LN LECs or DCs derived from WT or TAP1$^{-/-}$ mice in the presence of OVA or SIINFEKL. Representative data from one out of 3 independent experiments (n=3). **p< 0.01 using two-way ANOVA followed by Bonferroni post-test.

Using LN LECs and DCs isolated from TAP1-null mice exposed to whole OVA protein, we found substantial reduction in OT-I T cell proliferation after coculture compared to those exposed to LECs or DCs isolated from WT mice (Fig. 2.2D). As expected, T cell proliferation was not significantly altered between WT and TAP1$^{-/-}$ with SIINFEKL stimulation, which binds externally to MHC I, suggesting that the density of SIINFEKL/MHC I complexes on LECs derived from both strains were comparable (Fig. 2.2D and Fig. 2.7). Together, these data suggest that cross-presentation pathways are active in LECs.

Collectively, these *in vitro* studies establish that exogenous antigens such as OVA and NPs can be internalized and trafficked to intracellular compartments. Subsequently, LECs efficiently process antigens for cross-presentation through TAP1 dependent cytoplasmic-ER import of peptides. Both ER-golgi transport of peptide loaded MHC I, or endosome acidification dependent MHC I trafficking are important for LEC cross-presentation. This suggests that some internalized antigen traffics and is loaded onto MHC I through acidified vesicles, while others reach the cytosol to be imported by TAP1 for loading onto MHC I (29).

Direct antigen-specific CD8$^+$ T cell interactions drive upregulation of MHC I and PD-L1 on lymphatic endothelial cells

Having demonstrated the scavenger activity of LECs and efficient processing and cross-presentation of exogenous antigens, we next explored the costimulatory functions of steady-state LECs in the presence of naïve CD8$^+$ T cells. We compared LEC expression of antigen-presentation molecules and costimulatory molecules with those of professional antigen presenting cells (DC). As expected, DCs clearly demonstrated constitutive expression of CD40, CD86, CD80, and MHC I that were further upregulated upon addition of the mature epitope peptide SIINFEKL and OT-I CD8$^+$ T cells (Fig. 2.3A bottom panel, OT-I and OT-I + SIINFEKL peptide, respectively). The increase in the expression levels of costimulatory molecules and receptors on DC surface upon antigen-specific interactions with OT-I CD8$^+$ T cells might appear surprising in the absence of TLR stimulation; however, there exist TLR-independent pathways that can drive maturation, and it has been reported that cognate interactions between DC and CD8$^+$ T cells can alone induce an upregulation of CD80 and CD86 expression on DCs (30).Furthermore, the transport of peptide-loaded MHC I to the cell surface has been suggested to be accompanied by an increased expression of costimulatory molecules (31).Thus, peptide loading of MHC I and subsequent engagement of TCR and T cell activation can indirectly upregulate costimulatory molecules on DCs. Since our peptide was not contaminated with endotoxin and the observed changes in maturation markers were not induced when DCs were incubated with the cognate peptide in the absence of CD8$^+$ T cells (Fig. 2.3A, bottom panel, SIINFEKL), our data suggest that it is the antigen presentation by the APC and subsequent recognition by T cell that leads to the altered expression. In contrast to expression by DCs, *ex-vivo* cultured primary LN LECs expressed low levels of CD40 and CD80 and undetectable levels of CD86 in either the presence or absence of antigen-specific interactions with CD8$^+$ T cells (Fig. 2.3A top panel). Similarly, constitutive expression of costimulatory molecules in human LECs was lower than that of human blood-derived DCs (data not shown). However,

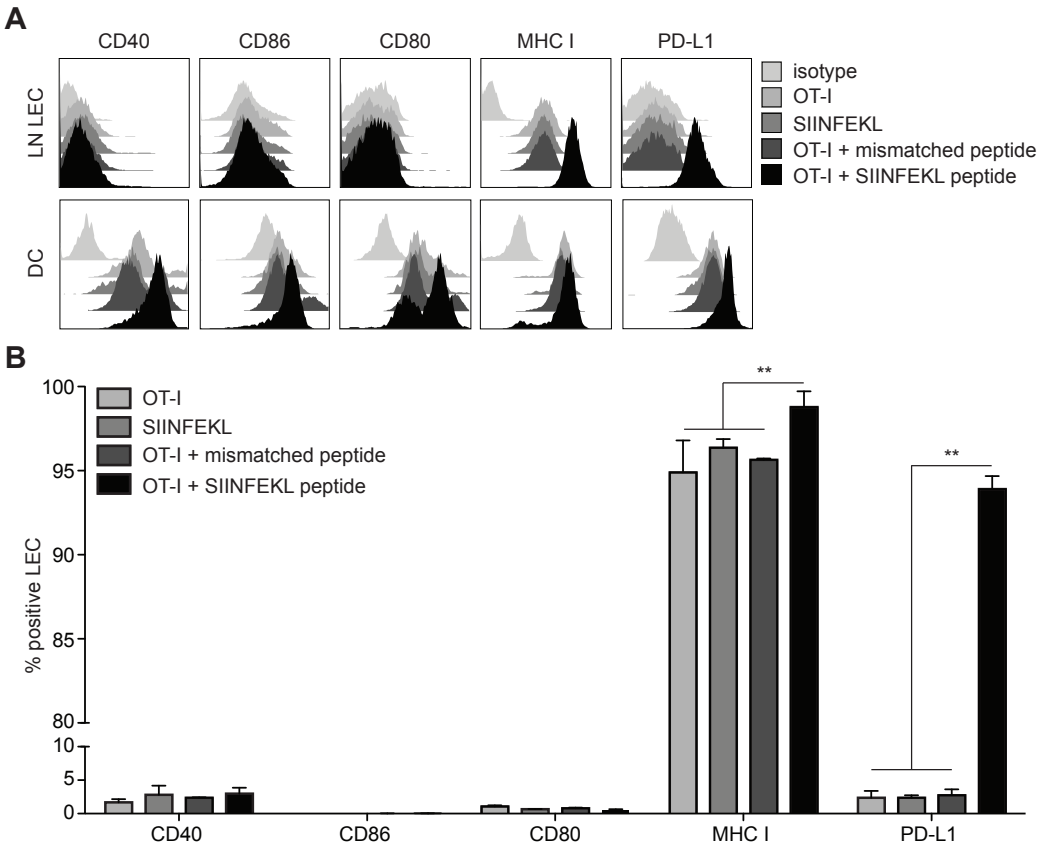

Figure 2.3 Antigen-specific interactions with naïve CD8$^+$ T cells result in upregulation of MHC I and PD-L1 expression on LECs. (A-B) In the presence of antigen-specific CD8$^+$ T cells *in vitro*, the lymphatic endothelial cell (LEC) phenotype suggests coinhibitory signaling. Naïve OVA-specific OT-I CD8$^+$ T cells were co-cultured with *ex-vivo* expanded lymph node LECs (LN LECs) or bone marrow-derived dendritic cells (DCs) from C57/Bl6 mice in the presence (OT-I +SIINFEKL peptide) or absence (OT-I) of 1nM SIINFEKL, the immunodominant MHC I peptide of OVA, or 1nM AMQMLKETI peptide (OT-I + mismatched peptide). As an additional control, DCs or LN LECs were also incubated with 1nM SIINFEKL in the absence of CD8$^+$ T cells (SIINFEKL). After 24h of T cell/LEC or T cell/DC co-culture, the relative expression levels of costimulatory molecules CD40, CD86 (B7-2), CD80 (B7-1), MHC I and Programmed Death Ligand 1 (PD-L1 or B7-H1) were determined by flow cytometric analysis. **(A)** Representative histograms for each marker are shown on gp38$^+$CD31$^+$ gated LN LECs or CD11c$^+$ gated DCs incubated with, from filled black to light gray, OT-I+SIINFEKL, OT-I+mismatched peptide, SIINFEKL only, OT-I only, and isotype control. **(B)** Percentages of CD40, CD86, CD80, MHC I and PD-L1$^+$ cells in gp38$^+$CD31$^+$ gated LN LECs in each case; shades of gray are assigned as in (A). Representative data from one of 2 independent experiments (n=3). **p< 0.01 using two-way ANOVA followed by Bonferroni post-test.

LECs significantly upregulated MHC I (**p<0.01) in a manner that was dependent on antigen-specific CD8$^+$ T cell interactions (Fig. 2.3A, B).

Consistent with previous reports (32, 33) both LECs and DCs constitutively expressed the inhibitory ligand programmed cell death ligand-1 (PD-L1 or B7.H-1, Fig. 2.3A), which has been reported to attenuate T cell proliferation and abrogate effector T cell differentiation (34). Furthermore, both LECs and DCs expressed higher levels of cell surface PD-L1 upon cognate interactions with CD8$^+$ T cells (Fig. 2.3A, OT-I + SIINFEKL peptide). Although DCs expressed higher baseline levels of PD-L1 compared to LECs, the upregulation of PD-L1 upon cognate antigen-specific CD8$^+$ T cell interaction was much more pronounced in LECs than in DCs (Fig. 2.3A, B and Fig. 2.8). More importantly, this change was not accompanied by increased

costimulatory molecule expression in LECs, as it clearly did in DCs. The same trends were also observed in cultured iLECs (data not shown), Collectively, these data demonstrate an evidently different balance between costimulatory and coinhibitory ligand expression in LECs versus DCs, and further suggest that antigen-specific interactions between LECs and $CD8^+$ T cells result in dynamic regulation of LEC phenotype to favor coinhibitory signaling.

Cross-presentation of exogenous antigen by lymphatic endothelial cells leads to impaired activation of naïve $CD8^+$ T cells in an antigen-specific manner.

Having shown that antigen-presenting LECs can upregulate PD-L1 in the presence of antigen-specific $CD8^+$ T cells *in vitro,* we next asked whether cross-presentation by LECs and engagement of antigen-specific T cell receptors could lead to a tolerized phenotype of $CD8^+$ T cells under steady-state conditions. To this end, we investigated the functional capacity of $CD8^+$ T cells after cross-priming by LECs compared to cross-priming by DCs *in vitro*. Upon incubation with iLECs in the presence of 1nM NP-ss-$COVA_{250-264}$, OT-I $CD8^+$ T cells proliferated strongly (Fig. 2.4A), but these iLEC-primed $CD8^+$ T cells displayed a dysfunctionally activated phenotype characterized by high levels of the apoptotic marker Annexin V in early generations of proliferating T cells compared to DC-stimulated T cells (Fig 2.4A).

The upregulation of PD-L1 on LECs upon antigen-specific interactions with $CD8^+$ T cells (Fig. 2.3) led us to analyze the expression of PD-L1 binding partners PD-1 and CD80 on co-cultured $CD8^+$ T cells. PD-1 is a member of the B7/CD28 superfamily and plays a central role in the regulation of T cell immunity; its activation results in decreased proliferation, reduced IFNγ and IL-2 production, and increased apoptosis (34). We observed that PD-1 expression was consistently high on iLEC-stimulated $CD8^+$ T cells from the early proliferative generations, while only later generations of DC-stimulated $CD8^+$ T cells expressed elevated levels of PD-1 (Fig. 2.4A). In addition to PD-1, recent studies have shown that PD-L1 also binds CD80 at a distinct site (35) to deliver inhibitory signals to T cells (36, 36); in those studies, CD80 expression was observed on anergic T cells and was further upregulated after re-exposure to the antigen. In contrast to DC-stimulated $CD8^+$ T cells, we detected a high percentage of CD80 expression on proliferating iLEC-primed $CD8^+$ T cells (Fig. 2.4A). In addition to PD-1, CTLA-4 was also substantially upregulated in early generations of $CD8^+$ T cells stimulated by LECs vs. DCs (Fig. 2.4A). CTLA-4 is another member of the CD28/B7 superfamily implicated in tolerogenic responses with a distinct, non-redundant regulatory role (34, 37), which competes with CD28 for binding to CD80 and CD86 on APCs to impede costimulatory signaling and increase CD86 degradation, resulting in impaired T cell activation (38). CTLA-4 also disrupts positive signaling through recruitment of phosphatases to the immunological synapse and subsequent dephosphorylation of key signaling molecules without direct engagement to CD80 and 86 (38). In addition to CTLA-4 upregulation, we found reduced expression of the surface activation markers CD25, CD44 and CD69 in iLEC-primed T cells compared to DC-primed T cells (Fig. 2.4B). Finally, OT-I $CD8^+$ T cells primed with iLECs in the presence of NP-ss-$COVA_{250-264}$ produced significantly less IFNγ and IL-2 compared to T cells primed with DCs (Fig. 2.4C).

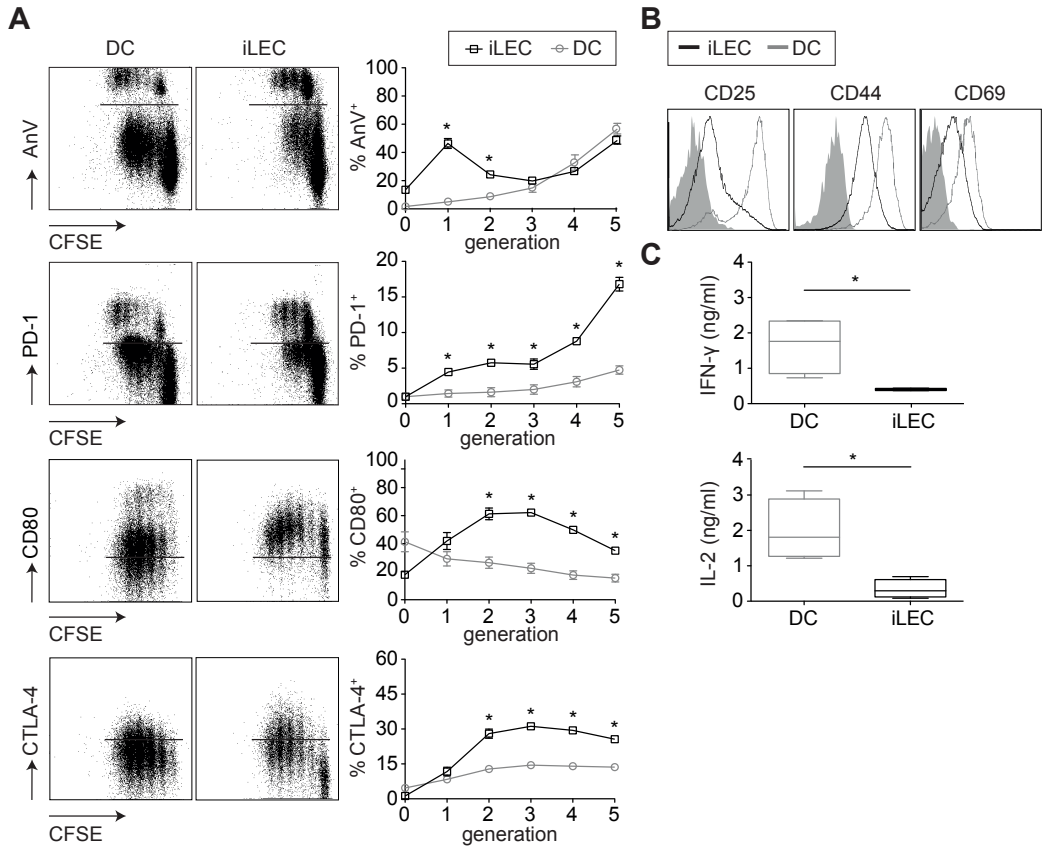

Figure 2.4 Cross-presentation by LECs induces impaired CD8$^+$ T cell proliferation. Naïve CFSE-labeled OVA-specific OT-I CD8$^+$ T cells were co-cultured with immortalized skin lymphatic endothelial cells (iLECs) or bone marrow-derived dendritic cells (DCs) from C57/Bl6 mice in the presence of N-term elongated OVA MHC I peptide disulfide conjugated to NPs (NPssCOVA$_{250\text{-}264}$) at 1nM and analyzed after 3 days. **(A)** Phenotypes of OT-I CD8$^+$ T cells after priming by cross-presenting DCs or iLECs as analyzed by flow cytometric evaluation of Annexin V, Programmed Death 1 (PD-1), CD80 (B7-1), and Cytotoxic T-Lymphocyte Antigen 4 (CTLA-4) surface marker expression. Left, representative dot plots from live-gated cells; right, percentages of positive cells per generation from one representative out of 3-5 independent experiments (n=3-4). **(B)** Representative flow cytometry histograms showing activation marker expression on OT-I CD8$^+$ cells after 3 days cross-priming by iLECs (black line) or DCs (gray line); filled gray area shows naïve (non-educated) OT-I CD8$^+$ T cells. **(C)** Cytokine secretion by iLEC- or DC-educated OT-I CD8$^+$ T cells as assessed by ELISA; Representative data from one of 4 experiments (n=4). *p< 0.05 using two-way ANOVA followed by Bonferroni post-test.

Taken together, these data indicate that iLECs can efficiently cross-present antigen and directly interact with CD8$^+$ T cells to induce antigen-specific proliferating T cells with a tolerized phenotype *in vitro*. The functional outcome of T cell priming differs significantly from that of T cells primed by conventional APCs, suggesting a tolerizing role for LECs under steady-state conditions.

IL-2 does not rescue the dysfunctional phenotype of CD8$^+$ T cells activated by lymphatic endothelial cells

Since we observed diminished levels of IL-2 by LEC- vs. DC-stimulated T cells (Fig. 2.4C), and since IL-2 is essential for CD8$^+$ T cell expansion, we asked whether the T cell phenotype could be rescued by exogenous IL-2, as has been shown for exhausted T cells in chronic viral infection (39). Interestingly, supplementation of the iLEC-T cell co-cultures with IL-2 (50U/ml) resulted in increased expression of the activation markers CD25, CD44, and CD69 on CD8$^+$ T cells (Fig. 2.5A). However, no

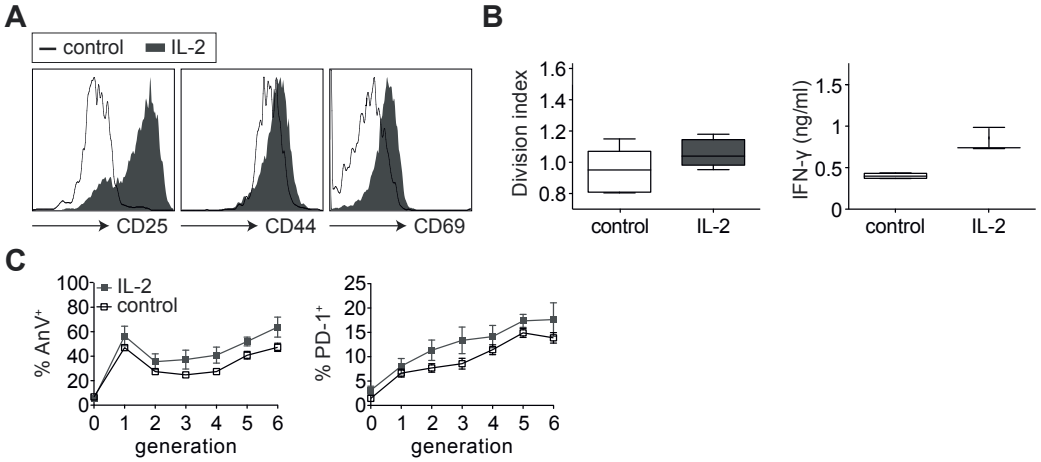

Figure 2.5 The LEC-educated T cell phenotype is only partially reversed by IL- 2. Naïve CFSE-labeled OVA-specific OT-I CD8$^+$ T cells were co-cultured with immortalized lymphatic endothelial cells (iLECs) for 3 days in the presence of antigen (1nM NPssCOVA$_{250-264}$) and supplemented with 50U/ml IL-2. **(A)** Representative flow cytometry histograms showing OT-I surface expression of activation markers after 3 days of priming by iLECs in the absence or presence of IL-2 (solid line vs. filled histograms, respectively). Representative data from one of 3 independent experiments (n=4). **(B)** Division index of proliferating OT-I CD8$^+$ T cells (left) and IFN-γ release (right) were only slightly affected by IL-2. Representative data from one of 4 independent experiments (n=4). **(C)** Percentage of Annexin V$^+$ and PD-1$^+$ OT-I CD8$^+$ T cells per generation after 3 days of co-culture with iLECs is unaffected by IL-2. Pooled data from two independent experiments (n=7).

effect was seen on T cell proliferation or IFNγ production (Fig. 2.5B), nor did IL-2 significantly decrease the percentages of Annexin V$^+$ or PD-1$^+$ cells per generation (Fig. 2.5C). These trends were similar when LN LECs treated with NP-ss-COVA$_{250-264}$ and when iLECs were stimulated with 1µM OVA protein instead of NP-ss-COVA$_{250-264}$ (data not shown). Together, these data suggest that the phenotype of T cells cross-primed by LECs were not merely exhausted, as they could not be rescued by IL-2.

2.4 Discussion

In addition to carrying antigens to the LN for uptake by immature DCs for immune surveillance, this study highlights an important role of lymphatic drainage for maintaining peripheral tolerance: the constant exposure of LECs to lymph-borne peripheral antigens, which they scavenge and cross-present for tolerance induction under steady-state conditions. Antigen cross-presentation was dependent on ER-golgi trafficking, endosome acidification, and TAP1. We observed that antigen-specific interactions with CD8$^+$ T cells resulted in upregulation of MHC I and PD-L1 on LECs and dysfunctional activation of CD8$^+$ T cells, which displayed early apoptosis and diminished cytokine production. Thus, in addition to the previously-described role of LECs in presenting endogenous peripheral tissue antigens for autoreactive CD8$^+$ T cell deletion (6-8), the present study demonstrates that LECs can efficiently scavenge and cross-present foreign antigen draining from the periphery, and thus play an immunoprotective role against a broader range of peripheral antigens.

Until recently, the cross-presentation mechanism in the induction of peripheral tolerance to exogenous antigens by non-hematopoietic stromal cells has been nearly exclusively attributed to LSECs, which line the hepatic sinusoidal wall and come into

close contact with foreign antigens and leukocytes passing through the liver (40). Similarly, LECs are positioned in a strategic anatomical site where crucial interactions determining the fate of an immune response take place. Here, we have demonstrated that antigen scavenging by LECs occurs under non-inflammatory steady-state conditions, adding to our previous observation that tumor-associated LECs cross-present OVA expressed by B16-F10 tumors (16). Murine LECs in the skin-draining LN actively took up peripherally administered OVA protein under steady-state conditions (Fig. 2.1A, B, C), consistent with an earlier study (41), and could be mediated through LEC expression of the mannose receptor (42, 43). This was further supported by our data showing that LN LECs were as effective as DCs in taking up OVA (Fig. 2.1D and Fig. 2.6). This is consistent with continual scavenging of inflammatory CC-chemokines (44) by D6 on afferent and subcapsular LECs, which results in intracellular degradation and reduction of inflammatory chemokines entering the LN under homeostatic conditions (45). Together with the data presented here, we conclude that LECs constitutively scavenge molecules to sample the peripheral lymph entering the LN.

We turned to *in vitro* studies to characterize the details of exogenous antigen cross-presenting mechanisms in LECs and found strong dependencies on temperature, dynamin-mediated uptake, intracellular antigen transporters, and TAP1 (Fig. 2.2), implicating similar cross-presentation pathways as those seen in DCs. Specifically, inhibitor sensitivity data suggested both dynamin (clathrin/ caveolin) and PI3K (phagocytosis/ macropinocytosis) pathways contribute to cross-presentation and T cell priming by LECs (Fig. 2.2C). This is in agreement with confocal microscopy studies (Fig. 2.9) showing OVA colocalization with clathrin heavy chain in LECs at early times after exposure. Similar observations have been made with LSECs (14), and are consistent with early endosome colocalization observed in BMDCs (46). At later time points, OVA was found in LAMP-1$^+$ vesicles, supporting the data showing chloroquine inhibition of antigen cross-presentation (Fig. 2.9).

A hallmark of cross-presentation of exogenous antigens by professional APCs is the dependence on TAP1 (47). As described for other murine stromal cells, such as LSECs (14, 48), aortic endothelial cells (49), and thymic stromal cells (50), we found that the TAP1-dependent transport of cytoplasmic peptides into the ER (Fig. 2.2D) and ER-golgi trafficking (Fig. 2.2C) was important in antigen specific CD8$^+$ T cell proliferation upon LEC cross-presentation. Furthermore, our data indicate that TAP1-independent pathways may be also active in LECs (Fig. 2.2D). In APCs, more than one pathway for loading of mature peptide epitopes on MHC I have been described, including loading in phagolysosomes or recycling endosomes (29, 51, 52). Intra-phagosome or lysosome release and MHC I loading of peptides in LAMP-1$^+$ MHC I$^+$ compartments have been described for DCs (53), which would be consistent with chloroquine sensitivity observed (Fig. 2.2C) and antigen presence in LAMP-1$^+$ vesicles in LECs (Fig. 2.9).

Although LECs displayed several similarities to LSECs with regard to Ag processing and cross-presenting capacity, LECs exhibited some phenotypic differences to LSECs. For example, under steady-state conditions, while LSECs were shown to express the costimulatory molecules CD40, CD80, and CD86 (30), LECs lack an immunostimulatory phenotype with remarkably low expression of costimulatory

molecules (Fig. 2.3). As the endotoxin levels found in portal blood under physiological conditions are presumably higher than in peripheral lymph, it is not surprising that the steady-state set point of co-stimulatory molecules in LSECs are higher than those of LECs. The inability of LECs to upregulate the costimulation machinery, together with PD-L1 upregulation upon antigen-specific T cell interactions (Fig. 2.3 and Fig. 2.8), indicated to us that LEC cross-presentation may be non-activating, since lack of costimulation is one mechanism of a dysfunctional $CD8^+$ T cell response that is reminiscent of the classical mechanism of peripheral tolerance induction by immature DCs under non-inflammatory conditions by T cell anergy and deletion (54).

The functional discrepancy and fate of LEC-educated vs. DC-educated $CD8^+$ T cells (Fig. 2.4C) was coupled with the reciprocal upregulation of inhibitory molecular partners on $CD8^+$ T cells: the PD-L1 partners PD-1 and CD80, as well as CTLA-4 (Fig. 2.4A). In accordance with our observations, Tewalt et al. recently demonstrated a key role for the PD-L1/PD-1 signaling pathway in the absence of costimulation in LEC-induced peripheral tolerance of endogenously expressed PTAs, where blocking PD-1 in LEC-educated, tyrosinase-specific $CD8^+$ T cells resulted in autoimmune vitiligo (6). While in LSEC-T cell co-cultures, exogenous IL-2 compensated for PD-L1-mediated coinhibitory signalling in the absence of costimulatory molecules (55), supplementation of LEC-T cell cocultures with IL-2 did not alter the phenotype of LEC-primed $CD8^+$ T cells (Fig. 2.5). Our data suggest that other regulatory pathways might be involved, such as the engagement of PD-1 by CD80 or signaling through CTLA-4, or additional ligands reported to be expressed on LEC surface, including the B and T lymphocyte attenuator (BTLA) molecule or the lymphocyte activation gene 3 (LAG-3) (6). Interestingly, there may be more than one differentiation state of $CD8^+$ T cells; apparently tolerized LSEC cross-primed $CD8^+$ T cells (30), upon inflammatory recall, were capable of becoming effector cells, reminiscent of central memory T cell activity (56). This may also apply in steady-state LEC cross-primed $CD8^+$ T cells. Further detailed mechanistic studies must be conducted on the coordination (57) of antigen processing, presentation and co-stimulatory/coinhibitory molecule pathways to shape the fate of these cells.

Because LECs are situated in one of the prime anatomical sites for immunological sampling, our findings support the idea that organ-draining LECs are the first to sample and present the exogenous peptides (3, 58), proteins and particulates present in lymph. Thus LECs may play an important role in the context of immunomodulation. Several findings from the literature support this concept that flow from the periphery, and the presence of lymphatics is important in shaping the adaptive immune responses in the LN. For example, Friedlaender and Baer showed in 1972 that alymphatic skin was more readily sensitized to dansyl chloride than intact skin (59), suggesting that presence of lymphatics in intact skin is contributing to a dampened delayed-type hypersensitivity response. Using the K14-VEGFR-3-Ig mice model, we have previously shown how impaired lymph drainage and absence of dermal LECs resulted in impaired acquired tolerance to contact hypersensitivity although these mice could mount a systemic T cell response (60). In the experimental autoimmune encephalomyelitis model, impaired lymphatic contraction and fluid drainage was reported to result in an autoimmune response (61). Together, this suggests that impaired lymphatic drainage translates to an inappropriately

activated immune response. Reciprocally, steady-state drainage of antigen to LN seems to favor tolerogenic responses. For example, the clinical success of allergen-specific immune therapy is based on a regimen of long-term s.c. low-dose allergen injection (62). We have shown that VEGF-C expanded tumor draining LN LECs impede a robust antigen-specific $CD8^+$ T cell response, which promotes tumor growth (16). In keeping with the idea that peripheral tolerance requires persistent antigen (63), continuous access to draining peripheral antigens newly establishes LECs as an active player in the maintenance of a tolerogenic LN environment. It implies that after injury or infection, where self-antigens drain to the LN together with TLRs and other danger signals, the steady-state tolerization by LECs can act as a dampening mechanism to prevent later potential autoimmune reactions. In other words, LEC cross-presentation of draining antigens helps amplify the signal-to-noise ratio between dangerous antigens and those that have been encountered under steady-state conditions.

This work demonstrates that priming by LEC via direct cross-presentation of scavenged exogenous antigens has a tolerizing effect on $CD8^+$ T cells. In addition to T cell tolerization against LEC expressed PTA (6-8), and contact-dependent immunosuppression of APCs (11), we establish LECs as a *bona-fide* APC, capable of sampling the peripheral antigen repertoire, by active internalization and cross-presentation of antigens in the MHC I context. This steady-state cross-presentation of scavenged peripheral antigens by LECs highlights the importance of lymphatic drainage and the role of LECs in immunomodulation, which may contribute an additional layer of control against self-reactive T cells in the context of maintaining self-tolerance against draining peripheral antigens during homeostasis or tissue injury. These findings help to explain why tumor-associated lymphatics promote tumor progression and metastasis to distant sites, and why dysfunctional lymphatic drainage is correlated with autoimmunity.

2.5 References

1. Oliver, G., and K. Alitalo. 2005. The lymphatic vasculature: recent progress and paradigms. *Annu. Rev. Cell Dev. Biol.* 21: 457–483.
2. Tal, O., H. Y. Lim, I. Gurevich, I. Milo, Z. Shipony, L. G. Ng, V. Angeli, and G. Shakhar. 2011. DC mobilization from the skin requires docking to immobilized CCL21 on lymphatic endothelium and intralymphatic crawling. *J. Exp. Med.* 208: 2141–2153.
3. Clement, C. C., E. S. Cannizzo, M.-D. Nastke, R. Sahu, W. Olszewski, N. E. Miller, L. J. Stern, and L. Santambrogio. 2010. An expanded self-antigen peptidome is carried by the human lymph as compared to the plasma. *PLoS ONE* 5: e9863.
4. Fletcher, A. L., D. Malhotra, and S. J. Turley. 2011. Lymph node stroma broaden the peripheral tolerance paradigm. *Trends Immunol.* 32: 12–18.
5. Graham, G. J. 2009. D6 and the atypical chemokine receptor family: novel regulators of immune and inflammatory processes. *Eur. J. Immunol.* 39: 342–351.
6. Tewalt, E. F., J. N. Cohen, S. J. Rouhani, C. J. Guidi, H. Qiao, S. P. Fahl, M. R. Conaway, T. P. Bender, K. S. Tung, A. T. Vella, A. J. Adler, L. Chen, and V. H. Engelhard. 2012. Lymphatic endothelial cells induce tolerance via PD-L1 and lack of costimulation leading to high-level PD-1 expression on CD8 T cells. *Blood* 120: 4772–4782.
7. Cohen, J. N., C. J. Guidi, E. F. Tewalt, H. Qiao, S. J. Rouhani, A. Ruddell, A. G. Farr, K. S. Tung, and V. H. Engelhard. 2010. Lymph node-resident lymphatic endothelial cells mediate peripheral tolerance via Aire-independent direct antigen presentation. *J. Exp. Med.* 207: 681–688.
8. Fletcher, A. L., V. Lukacs-Kornek, E. D. Reynoso, S. E. Pinner, A. Bellemare-Pelletier, M.

S. Curry, A. R. Collier, R. L. Boyd, and S. J. Turley. 2010. Lymph node fibroblastic reticular cells directly present peripheral tissue antigen under steady-state and inflammatory conditions. *J. Exp. Med.* 207: 689–697.

9. Lukacs-Kornek, V., D. Malhotra, A. L. Fletcher, S. E. Acton, K. G. Elpek, P. Tayalia, A.-R. Collier, and S. J. Turley. 2011. Regulated release of nitric oxide by nonhematopoietic stroma controls expansion of the activated T cell pool in lymph nodes. *Nat. Immunol.* 12: 1096–1104.
10. Swartz, M. A., and A. W. Lund. 2012. Lymphatic and interstitial flow in the tumour microenvironment: linking mechanobiology with immunity. *Nat. Rev. Cancer* 12: 210–219.
11. Podgrabinska, S., O. Kamalu, L. Mayer, M. Shimaoka, H. Snoeck, G. J. Randolph, and M. Skobe. 2009. Inflamed Lymphatic Endothelium Suppresses Dendritic Cell Maturation and Function via Mac-1/ICAM-1-Dependent Mechanism. *J. Immunol.* 183: 1767–1779.
12. Nörder, M., M. G. Gutierrez, S. Zicari, E. Cervi, A. Caruso, and C. A. Guzman. 2012. Lymph node-derived lymphatic endothelial cells express functional costimulatory molecules and impair dendritic cell-induced allogenic T-cell proliferation. *FASEB J.* 26: 2835–2846.
13. Reynoso, E. D., and S. J. Turley. 2009. Unconventional antigen-presenting cells in the induction of peripheral CD8(+) T cell tolerance. *J. Leukoc. Biol.* 86: 795–801.
14. Schurich, A., J. P. Böttcher, S. Burgdorf, P. Penzler, S. Hegenbarth, M. Kern, A. Dolf, E. Endl, J. Schultze, E. Wiertz, D. Stabenow, C. Kurts, and P. Knolle. 2009. Distinct kinetics and dynamics of cross-presentation in liver sinusoidal endothelial cells compared to dendritic cells. *Hepatology* 50: 909–919.
15. Oppen, von, N., A. Schurich, S. Hegenbarth, D. Stabenow, R. Tolba, R. Weiskirchen, A. Geerts, W. Kolanus, P. Knolle, and L. Diehl. 2009. Systemic antigen cross-presented by liver sinusoidal endothelial cells induces liver-specific CD8 T-cell retention and tolerization. *Hepatology* 49: 1664–1672.
16. Lund, A. W., F. V. Duraes, S. Hirosue, V. R. Raghavan, C. Nembrini, S. N. Thomas, A. Issa, S. Hugues, and M. A. Swartz. 2012. VEGF-C promotes immune tolerance in B16 melanomas and cross-presentation of tumor antigen by lymph node lymphatics. *Cell Rep.* 1: 191–199.
17. Shields, J. D., I. C. Kourtis, A. A. Tomei, J. M. Roberts, and M. A. Swartz. 2010. Induction of lymphoidlike stroma and immune escape by tumors that express the chemokine CCL21. *Science* 328: 749–752.
18. Jat, P. S., M. D. Noble, P. Ataliotis, Y. Tanaka, N. Yannoutsos, L. Larsen, and D. Kioussis. 1991. Direct derivation of conditionally immortal cell lines from an H-2Kb-tsA58 transgenic mouse. *Proc. Natl. Acad. Sci. U.S.A.* 88: 5096–5100.
19. Fletcher, A. L., D. Malhotra, S. E. Acton, V. Lukacs-Kornek, A. Bellemare-Pelletier, M. Curry, M. Armant, and S. J. Turley. 2011. Reproducible isolation of lymph node stromal cells reveals site-dependent differences in fibroblastic reticular cells. *Front. Immunol.* 2: 1–15.
20. Link, A., T. K. Vogt, S. Favre, M. R. Britschgi, H. Acha-Orbea, B. Hinz, J. G. Cyster, and S. A. Luther. 2007. Fibroblastic reticular cells in lymph nodes regulate the homeostasis of naive T cells. *Nat. Immunol.* 8: 1255–1265.
21. Lutz, M. B., N. Kukutsch, A. L. Ogilvie, S. Rössner, F. Koch, N. Romani, and G. Schuler. 1999. An advanced culture method for generating large quantities of highly pure dendritic cells from mouse bone marrow. *J. Immunol. Methods.* 223: 77–92.
22. Hirosue, S., I. C. Kourtis, A. J. van der Vlies, J. A. Hubbell, and M. A. Swartz. 2010. Antigen delivery to dendritic cells by poly(propylene sulfide) nanoparticles with disulfide conjugated peptides: Cross-presentation and T cell activation. *Vaccine* 28: 7897–7906.
23. Fletcher, P. A., D. R. L. Scriven, M. N. Schulson, and E. D. W. Moore. 2010. Multi-image colocalization and its statistical significance. *Biophys. J.* 99: 1996–2005.
24. Macia, E., M. Ehrlich, R. Massol, E. Boucrot, C. Brunner, and T. Kirchhausen. 2006. Dynasore, a Cell-Permeable Inhibitor of Dynamin. *Dev. Cell* 10: 839–850.
25. Araki, N., M. T. Johnson, and J. A. Swanson. 1996. A role for phosphoinositide 3-kinase in the completion of macropinocytosis and phagocytosis by macrophages. *J. Cell Biol.* 135: 1249–1260.
26. Fujiwara, T., K. Oda, S. Yokota, A. Takatsuki, and Y. Ikehara. 1988. Brefeldin A causes

disassembly of the Golgi complex and accumulation of secretory proteins in the endoplasmic reticulum. *J. Biol. Chem.* 263: 18545–18552.

27. Steinman, R., I. Mellman, and W. Muller. 1983. Endocytosis and the recycling of plasma membrane. *J. Cell Biol.* 96: 1–27.
28. Brossart, P., and M. J. Bevan. 1997. Presentation of exogenous protein antigens on major histocompatibility complex class I molecules by dendritic cells: pathway of presentation and regulation by cytokines. *Blood* 90: 1594–1599.
29. Grommé, M., F. G. UytdeHaag, H. Janssen, J. Calafat, R. S. van Binnendijk, M. J. Kenter, A. Tulp, D. Verwoerd, and J. Neefjes. 1999. Recycling MHC class I molecules and endosomal peptide loading. *Proc. Natl. Acad. Sci. U.S.A.* 96: 10326–10331.
30. Diehl, L., A. Schurich, R. Grochtmann, S. Hegenbarth, L. Chen, and P. A. Knolle. 2008. Tolerogenic maturation of liver sinusoidal endothelial cells promotes B7-homolog 1-dependent CD8+ T cell tolerance. *Hepatology* 47: 296–305.
31. Schmidt, S., and A. Nino-Castro. 2012. Regulatory dendritic cells: there is more than just immune activation. *Front. Immunol.* 3: 1–17.
32. Freeman, G. J., A. J. Long, Y. Iwai, K. Bourque, T. Chernova, H. Nishimura, L. J. Fitz, N. Malenkovich, T. Okazaki, M. C. Byrne, H. F. Horton, L. Fouser, L. Carter, V. Ling, M. R. Bowman, B. M. Carreno, M. Collins, C. R. Wood, and T. Honjo. 2000. Engagement of the PD-1 immunoinhibitory receptor by a novel B7 family member leads to negative regulation of lymphocyte activation. *J. Exp. Med.* 192: 1027–1034.
33. Keir, M., M. Butte, and G. Freeman. 2008. PD-1 and its ligands in tolerance and immunity. *Annu. Rev. Immunol.*
34. McGrath, M. M., and N. Najafian. 2012. The role of coinhibitory signaling pathways in transplantation and tolerance. *Front. Immunol.* 3: 1–17.
35. Butte, M. J., M. E. Keir, T. B. Phamduy, A. H. Sharpe, and G. J. Freeman. 2007. Programmed death-1 ligand 1 interacts specifically with the B7-1 costimulatory molecule to inhibit T cell responses. *Immunity* 27: 111–122.
36. Park, J.-J., R. Omiya, Y. Matsumura, Y. Sakoda, A. Kuramasu, M. M. Augustine, S. Yao, F. Tsushima, H. Narazaki, S. Anand, Y. Liu, S. E. Strome, L. Chen, and K. Tamada. 2010. B7-H1/CD80 interaction is required for the induction and maintenance of peripheral T-cell tolerance. *Blood* 116: 1291–1298.
37. Chen, L., and D. B. Flies. 2013. Molecular mechanisms of T cell co-stimulation and co-inhibition. *Nat. Rev. Immunol.* 13: 227–242.
38. Rudd, C. E., A. Taylor, and H. Schneider. 2009. CD28 and CTLA-4 coreceptor expression and signal transduction. *Immunol. Rev.* 229: 12–26.
39. Blattman, J. N., J. M. Grayson, E. J. Wherry, S. M. Kaech, K. A. Smith, and R. Ahmed. 2003. Therapeutic use of IL-2 to enhance antiviral T-cell responses in vivo. *Nat. Med.* 9: 540–547.
40. Crispe, I. 2003. Hepatic T cells and liver tolerance. *Nat. Rev. Immunol.* 3: 51–62.
41. Sixt, M., N. Kanazawa, M. Selg, T. Samson, G. Roos, D. P. Reinhardt, R. Pabst, M. B. Lutz, and L. Sorokin. 2005. The conduit system transports soluble antigens from the afferent lymph to resident dendritic cells in the T cell area of the lymph node. *Immunity* 22: 19–29.
42. Irjala, H., K. Alanen, R. Grénman, P. Heikkilä, H. Joensuu, and S. Jalkanen. 2003. Mannose receptor (MR) and common lymphatic endothelial and vascular endothelial receptor (CLEVER)-1 direct the binding of cancer cells to the lymph vessel endothelium. *Cancer Research* 63: 4671–4676.
43. Marttila-Ichihara, F., R. Turja, M. Miiluniemi, M. Karikoski, M. Maksimow, J. Niemela, L. Martinez-Pomares, M. Salmi, and S. Jalkanen. 2008. Macrophage mannose receptor on lymphatics controls cell trafficking. *Blood* 112: 64–72.
44. Lee, K. M., R. J. B. Nibbs, and G. J. Graham. 2013. D6: the “crowd controller” at the immune gateway. *Trends Immunol.* 34: 7–12.
45. Nibbs, R. J. B., P. Mclean, C. McCulloch, A. Riboldi-Tunnicliffe, E. Blair, Y. Zhu, N. Isaacs, and G. J. Graham. 2009. Structure-function dissection of D6, an atypical scavenger receptor. *Meth. Enzymol.* 460: 245–261.
46. Burgdorf, S., A. Kautz, V. Böhnert, P. A. Knolle, and C. Kurts. 2007. Distinct pathways of antigen uptake and intracellular routing in CD4 and CD8 T cell activation. *Science* 316:

612–616.

47. Joffre, O. P., E. Segura, A. Savina, and S. Amigorena. 2012. Cross-presentation by dendritic cells. *Nat. Rev. Immunol.* 12: 557–569.
48. Limmer, A., J. Ohl, C. Kurts, H. G. Ljunggren, Y. Reiss, M. Groettrup, F. Momburg, B. Arnold, and P. A. Knolle. 2000. Efficient presentation of exogenous antigen by liver endothelial cells to CD8+ T cells results in antigen-specific T-cell tolerance. *Nat. Med.* 6: 1348–1354.
49. Bagai, R., A. Valujskikh, D. H. Canaday, E. Bailey, P. N. Lalli, C. V. Harding, and P. S. Heeger. 2005. Mouse endothelial cells cross-present lymphocyte-derived antigen on class I MHC via a TAP1-and proteasome-dependent pathway. *J. Immunol.* 7711–7715.
50. Merkenschlager, M., M. O. Power, H. Pircher, and A. G. Fisher. 1999. Intrathymic deletion of MHC class I-restricted cytotoxic T cell precursors by constitutive cross-presentation of exogenous antigen. *Eur. J. Immunol.* 29: 1477–1486.
51. Guermonprez, P., L. Saveanu, M. Kleijmeer, J. Davoust, P. Van Endert, and S. Amigorena. 2003. ER-phagosome fusion defines an MHC class I cross-presentation compartment in dendritic cells. *Nature* 425: 397–402.
52. Houde, M., S. Bertholet, E. Gagnon, S. Brunet, G. Goyette, A. Laplante, M. F. Princiotta, P. Thibault, D. Sacks, and M. Desjardins. 2003. Phagosomes are competent organelles for antigen cross-presentation. *Nature* 425: 402–406.
53. Lizée, G., G. Basha, J. Tiong, J.-P. Julien, M. Tian, K. E. Biron, and W. A. Jefferies. 2003. Control of dendritic cell cross-presentation by the major histocompatibility complex class I cytoplasmic domain. *Nat. Immunol.* 4: 1065–1073.
54. Steinman, R. M., D. Hawiger, K. Liu, L. Bonifaz, D. Bonnyay, K. Mahnke, T. Iyoda, J. Ravetch, M. Dhodapkar, K. Inaba, and M. Nussenzweig. 2003. Dendritic cell function in vivo during the steady state: a role in peripheral tolerance. *Ann. N.Y. Acad. Sci.* 987: 15–25.
55. Schurich, A., M. Berg, D. Stabenow, J. Bottcher, M. Kern, H. J. Schild, C. Kurts, V. Schuette, S. Burgdorf, L. Diehl, A. Limmer, and P. A. Knolle. 2010. Dynamic Regulation of CD8 T Cell Tolerance Induction by Liver Sinusoidal Endothelial Cells. *J. Immunol.* 184: 4107–4114.
56. Böttcher, J. P., O. Schanz, D. Wohlleber, Z. Abdullah, S. Debey-Pascher, A. Staratschek-Jox, B. Höchst, S. Hegenbarth, J. Grell, A. Limmer, I. Atreya, M. F. Neurath, D. H. Busch, E. Schmitt, P. Van Endert, W. Kolanus, C. Kurts, J. L. Schultze, L. Diehl, and P. A. Knolle. 2013. Liver-primed memory T cells generated under noninflammatory conditions provide anti-infectious immunity. *Cell Rep.* 3: 779–795.
57. Nair, P., D. Amsen, and J. M. Blander. 2011. Co-ordination of incoming and outgoing traffic in antigen-presenting cells by pattern recognition receptors and T cells. *Traffic* 12: 1669–1676.
58. Clement, C. C., O. Rotzschke, and L. Santambrogio. 2011. The lymph as a pool of self-antigens. *Trends Immunol.* 32: 6–11.
59. Friedlaender, M. H., and H. Baer. 1972. Immunologic tolerance: role of the regional lymph node. *Science* 176: 312–314.
60. Thomas, S. N., J. M. Rutkowski, M. Pasquier, E. L. Kuan, K. Alitalo, G. J. Randolph, and M. A. Swartz. 2012. Impaired humoral immunity and tolerance in K14-VEGFR-3-Ig mice that lack dermal lymphatic drainage. *J. Immunol.* 189: 2181–2190.
61. Liao, S., G. Cheng, D. A. Conner, Y. Huang, R. S. Kucherlapati, L. L. Munn, N. H. Ruddle, R. K. Jain, D. Fukumura, and T. P. Padera. 2011. Impaired lymphatic contraction associated with immunosuppression. *Proc. Natl. Acad. Sci. U.S.A.* 108: 18784–18789.
62. Frew, A. J. 2010. Allergen immunotherapy. *J. Allergy Clin. Immunol.* 125: S306–13.
63. Redmond, W. L., and L. A. Sherman. 2005. Peripheral Tolerance of CD8 T Lymphocytes. *Immunity* 22: 275–284.

2.6 Appendix

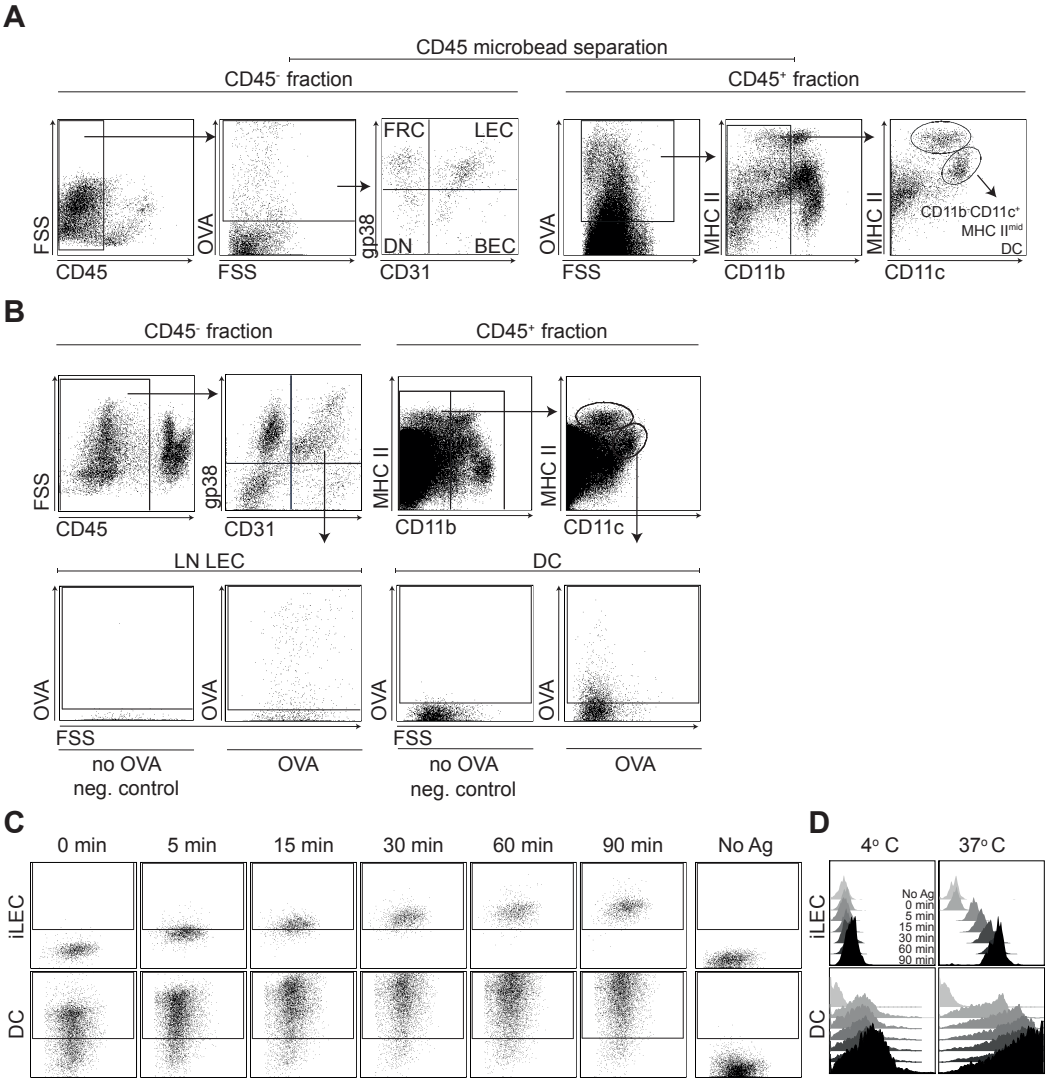

Figure 2.6 Gating strategy and representative flow cytometry plots for assessing OVA uptake by cells in the lymph node and for showing intracellular accumulation of fluorescent OVA in cultured cells. 90 min after i.d. injection of OVA AF-647, brachial LNs were digested and the single cell preparation was first magnetically separated using anti-CD45 microbeads before analyzing each fraction by flow cytometry for data shown in Fig. 1D-E. **(A)** Using CD45 staining, any remaining $CD45^+$ cells in the magnetically sorted $CD45^-$ fraction were excluded from analysis before the OVA+ subsets were determined for the different populations, with the use of a naive non-injected control. The $CD45^-OVA^+$ populations were further subdivided in the 4 stromal subsets using gp38, CD31. The $CD45^+OVA^+$ population was further subdivided in various APC subsets using the CD11b, CD11c and MHC II surface markers. To determine the percentage of each cell population out of all OVA^+ cells, the counts of OVA^+ $gp38^+CD31^+$ gated LECs, $gp38^+CD31^-$ gated fibroblastic reticular cells (FRCs), $gp38^-CD31^+$ gated blood endothelial cells (BECs), $gp38^-CD31^-$ gated double negative cells (DNs) in the $CD45^-$ fraction and OVA^+ APCs in the $CD45^+$ fraction were separately calculated and subsequently, divided to the overall (added) counts of OVA^+ cells in both fractions. Here, the gating for the resident $CD11b^-CD11c^+$MHC II^{mid} DCs is shown. **(B)** The $CD45^-$ stroma was divided in the four LNSC subpopulations using the gp38, CD31 antibodies and OVA fluorescence was determined in LEC ($gp38^+CD31^+$). LECs from a naive non-injected mouse (no OVA) were used as eference for the OVA gating. The $CD45^+$ fraction was divided in $CD11b^-$ and $CD11b^+$ cells and the $CD11b^-$ subpopulation was further separated with the use of MHC II and CD11c surface markers in the MHC $II^{mid/hi}CD11c^+$ DC subpopulations. The fluorescence of OVA was determined for the resident $CD11b^-CD11c^+$MHC II^{mid} DC subpopulation. The same DC subset from a naive non-injected mouse (no OVA) was used as a reference for the OVA gating. Representative flow cytometry plots showing intracellular accumulation of fluorescent ovalbumin (OVA) in cultured cells. **(C)**

Representative dot plots of immortalized lymphatic endothelial cells (iLEC) or bone marrow-derived dendritic cells (DC) after incubation with 1µM OVA AF-647 for the data shown in Fig. 1F-G. Shown on the far right is the no-antigen control (No Ag) used to determine the positive OVA gating. **(D)** Representative histograms for the OVA fluorescence are shown for iLECs (top) and DCs (bottom) at 4°C versus 37°C showing different time points as indicated. Data shown are representative of 2 independent experiments, n=3 eac**h.**

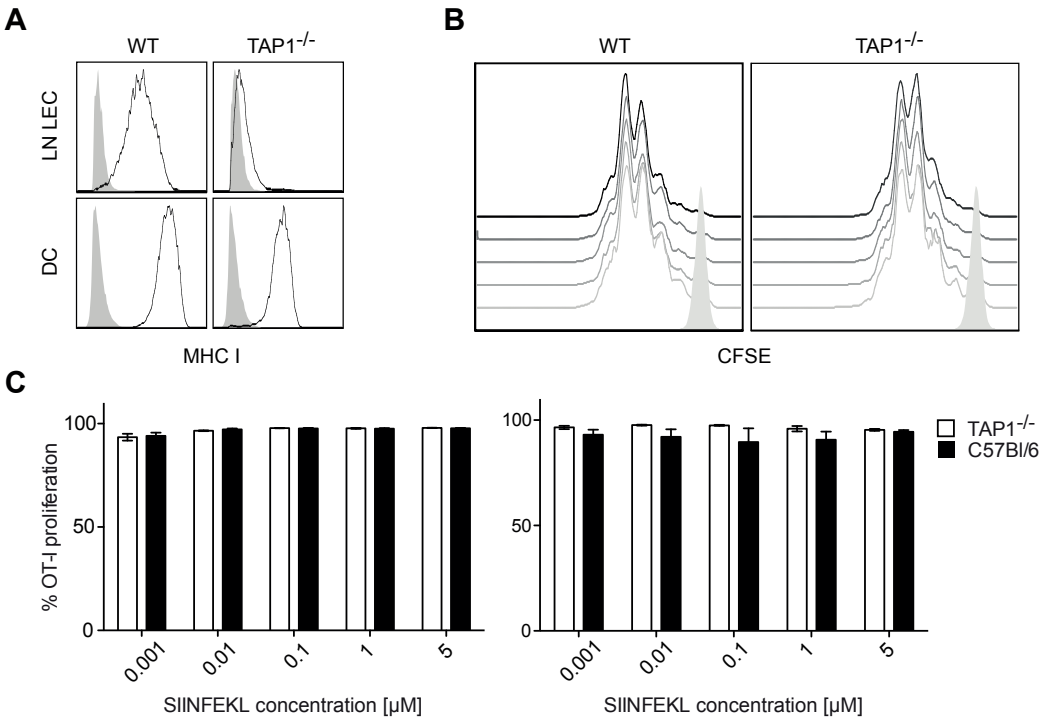

Figure 2.7 TAP1$^{-/-}$ LECs can equally trigger OT-I proliferation at 1 and 5µM SIINFEKL compared to WT LECs despite lower MHCI levels. (A) MHC I levels by flow cytometry analysis, with isotype control (filled histogram). Lymph node lymphatic endothelial cells (LN LEC) and bone marrow derived dendritic cells (DC) from wild type C57Bl/6 (WT) or TAP1$^{-/-}$ mice. Representative histograms of n=3 mice. **(B)** CFSE labeled OT-I CD8 T cells were co-cultured with LN LECs or DCs derived from WT or TAP1$^{-/-}$ mice, pulsed with no peptide to 0.001, 0.01, 0.1, 1, and 5µM SIINFEKL peptide. Histogram of CFSE dilution after 3 days shows LEC and OT-I T cell co-cultures, with gray filled histogram representing no peptide, and the respective concentrations from light to dark gray. **(C)** Percent OT-I proliferation, n=3 in 2 independent experiments.

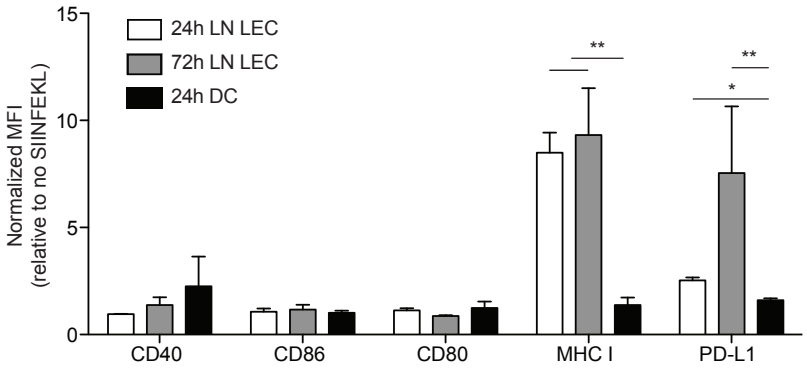

Figure 2.8 MHC I and PD-L1 expression levels in the presence versus absence of antigen are higher in LN LEC compared to DC. Naïve OVA-specific OT-I CD8+ T cells were co-cultured with ex-vivo expanded lymph node lymphatic endothelial cells (LN LEC) or bone marrow derived DCs (DC) from C57/Bl6 mice in the presence (+ SIINFEKL) or absence (no SIINFEKL) of 1nM immunodominant MHC I peptide of OVA (SIINFEKL). After 24h or 72h of T cell/LEC, or after 24h of T cell/DC co-culture, the expression levels of costimulatory molecules CD40, CD86 (B7-2), CD80 (B7-1), major histocompatibility complex class I (MHC I) and Programmed Death Ligand 1 (PD-L1 or B7-H1) were determined by flow cytometric analysis. The Mean Fluorescent Intensity (MFI) was determined for CD40, CD86, CD80, MHC I and PD-L1 in the respective positive populations in LN LECs and DCs. Normalized MFI was calculated as follows: (MFI + SIINFEKL) / (MFI no SIINFEKL). Values depict mean ± SD from two representative experiment (n=3-4). ** $p<0.01$ and * $p<0.05$, two-way ANOVA followed by Bonferroni post-test.

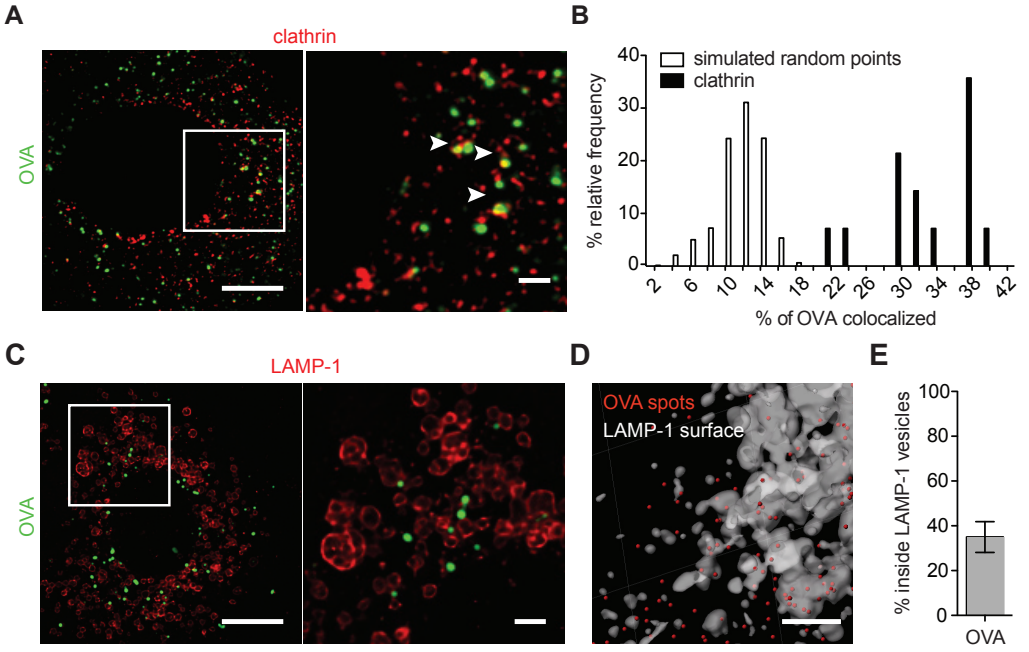

Figure 2.9 Ovalbumin colocalization analysis shows clathrin colocalization is not by chance, and that OVA can be found within the LAMP1 vesicles. (A, C) Cells were exposed to AF647-labeled OVA for 15 min or 90 min and stained for clathrin heavy chain or Lysosomal-Associated Membrane Protein 1 (LAMP-1), respectively. Images were acquired by confocal microscopy. Arrowheads indicate co-localizing pixels. The regions of interest shown to the right are indicated as white squares on the cell. The scale bar corresponds to 4 and 2µm, respectively. **(B)** Object-based colocalization method of Fletcher et al. (2010) was used to determine that those OVA+ vesicles, which are also clathrin$^+$ occur more than by chance by comparison to a randomly generated spots. % relative frequency is plotted against %OVA$^+$ vesicles. 14 images were analyzed. **(D)** A typical Imaris analysis for quantifying LAMP-1 enclosed OVA. Spots (red) were assigned to OVA fluorescence maxima, and the white surfaces were drawn around LAMP-1 fluorescence structures. The ImarisXT plugin "split spots into surface objects" was used to determine the % OVA inside LAMP-1+ surfaces. Scale bar = 3µm. **(E)** The result of such analysis for 5 images shows that approximately 30% of OVA can be found within LAMP-1$^+$ vesicles.

Chapter 3

Phenotype and function of $CD8^+$ T cells activated by pMHCI-bearing LECs: The multifaceted immunomodulatory role of LECs

Over the last decade, there has been accumulating evidence on the dynamic contribution of the lymphatic endothelium to the regulation of immune responses. In addition to expressing self-antigens and presenting them for autoreactive T cell deletion, we established lymphatic endothelial cells (LECs) as *bona fide* antigen presenting cells (APCs), which are capable of scavenging and cross-presentation of foreign exogenous antigens. We previously reported that antigen-specific interactions led to naïve $CD8^+$ T cell proliferation albeit with a dysfunctionally activated phenotype. Here, we examined the function of LEC-educated $CD8^+$ T cells and asked whether they could escape the dysfunctional state. We demonstrated that steady-state LEC-educated $CD8^+$ T cells adopted a unique phenotype with central memory-like characteristics, distinct from naïve or dendritic cell (DC)-activated effector cells. The phenotypic diversification was coupled with functional properties and allowed them to preferentially home to the lymph node (LN) and survive long-term in the absence of the antigen. Once they re-encountered the antigen, LEC-educated $CD8^+$ T cells mounted proliferative responses and gave rise to effector cells, producing cytokines (IFN-γ, TNF-α) and displaying killing activity. In the setting of *Listeria monocytogenes*-expressing-OVA infection, LEC-educated cells not only participated in anti-infectious immunity but also preserved a persistent secondary-memory population. Our findings suggest a previously unanticipated role for LECs in immunomodulation: the generation of antigen-experienced $CD8^+$ T cells which survive in an inactive state but can be functionally reactivated upon antigenic inflammatory challenge, likely acting as a supplementary mechanism that complements and enhances immune responses.

3.1 Introduction

Recently, rising evidence has revealed that the lymphatic endothelium is more actively involved in the modulation of immunity, shaping T cell responses, both directly and indirectly (1-6). Lymphatic endothelial cells (LECs) were shown to endogenously express and present peripheral tissue-restricted antigens (PTAs) on MHC class I molecules to tolerize $CD8^+$ T cells and thus, participate in the induction of peripheral tolerance against self-antigens (7-9). In addition to endogenous antigen presentation, we previously showed that LECs can actively scavenge and cross-present foreign exogenous antigens, both in the context of a tumor (10) as well as under homeostatic conditions [Chapter 2 and (11)], to compromise $CD8^+$ T cell activation. The interactions of LECs with $CD8^+$ T cells were accompanied by low-level costimulatory signaling together with increased levels of the inhibitory ligand PD-L1 on LECs, and resulted in activated $CD8^+$ T cells displaying early-generation apoptosis and dysfunctionally activated phenotypes. LECs have, therefore, been established as APCs that can sample the peripheral antigen repertoire inducing dysfunctional activation of $CD8^+$ T cells under homeostatic conditions.

The induction of peripheral tolerance is primarily assigned to professional antigen-presenting cells (12). Immature DCs obtain self-antigens from peripheral tissues and cross-present them in the absence of costimulation (13) to induce T cell anergy, suppression or deletion (14). Ensuring that the immune system is restrained from attacking self-antigens is critical for the maintenance of homeostasis. Rescued $CD8^+$ T cells, which were tolerized against a self-antigen under steady state conditions, remained functionally impaired even in response to pathogenic challenge, shielding the host from autoimmune reactions (15). By contrast, in the iFABP-tOVA PTA model, in which OVA is endogenously expressed under control of the intestinal fatty acid binding promoter (iFABP), tolerized $CD8^+$ T cells, which were primed by non-hematopoietic intestinal epithelial cells, were reactivated upon viral challenge (16). Tissue destruction, triggered by the reactivated cells, was dependent on antigen density and the presence of inflammatory molecules. Additionally, $CD8^+$ T cells tolerized by liver sinusoidal endothelial cells (LSEC) were recently demonstrated to exit the non-responsive state once reactivated under inflammatory conditions (17). Originally, LSECs were shown to cross-present exogenous antigens on MHC I and induce tolerogenic $CD8^+$ T cells (18, 19). Similar to antigen presentation by LECs, LSEC-mediated induction of $CD8^+$ T cell tolerance was governed by the PD-L1 – PD-1 inhibitory signaling. Considering the similarities between LSECs and LECs, the question arises whether LEC-educated $CD8^+$ T cells might exhibit similar functional properties to LSEC-educated T cells. In other words, whether they can recover from the dysfunctional non-responsive state in response to inflammatory challenge.

The differentiation state of $CD8^+$ T cells following cognate APC-T cell interaction is tightly governed by the integration of various signals, including the antigen load, costimulation, cytokines and other inflammatory mediators (20-22). The relative balance among such signals strongly influences the differentiation fate, leading to the generation of different effector and/or memory T cell subsets. An emerging concept suggests that T cells educated under conditions of increased inflammation and high antigen load are more prone to differentiate into terminal effectors rather than memory cells (23, 24). Alternatively, reduced exposure to antigenic and inflammatory

signals might favor the generation of memory cells. Among the different inflammatory signals that crucially impact T cell responses are various cytokines. IL-12 has been shown to suppress memory formation (25, 26) whereas high levels of IL-2 have been associated with the generation of short-lived effectors (27, 28). This new understanding raises important considerations with regard to $CD8^+$ T cell priming by non-hematopoietic cells. Education by LECs and LSECs, orchestrated by decreased costimulation and very low levels of pro-inflammatory cytokines, would rather mirror the setting of reduced, short-lived inflammation and therefore, disfavor the generation of terminally differentiated cells. Indeed, LSEC-educated T cells displayed an antigen-experienced phenotype with central memory-like characteristics and homed to secondary lymphoid organs (17). However, it is still unknown whether LEC-education may also promote $CD8^+$ T cells with memory-like phenotypes, as well as functional, properties. Furthermore, it remains an open question whether LEC-education may lead to more than one T cell differentiation state or how plastic that fate might be.

Here, we describe a new role for LECs in the induction of immune responses and the development of immunological memory. First, we demonstrate that surviving antigen-specific $CD8^+$ T cells educated by LECs under steady state conditions are phenotypically distinct from naïve or mDC-educated cells and display central-memory like features. Following *in vivo* transfer, LEC-educated $CD8^+$ T cells primarily homed to the LN, while mDC-educated T cells migrated to the periphery, and survived for long periods of time in the absence of the antigen. Upon antigen reencounter, LEC-educated $CD8^+$ T cells responded quickly and underwent extensive proliferation generating cytotoxic effector cells. Recapitulating a hallmark of memory cells, LEC-educated T cells participated in anti-infectious pathogenic immunity, not only by controlling bacterial load but also by retaining a secondary memory-persistent population. Our findings suggest that cross-priming of peripheral antigens to $CD8^+$ T cells by LECs under homeostatic conditions promotes a temporarily inert state while allowing them to respond in case of subsequent inflammatory challenge. Thus, while being employed for the maintenance of peripheral tolerance, they might also function as a reserve of antigen-experienced T cells, enhancing immune responses when needed.

3.2 Materials and Methods

Reagents

All chemicals were from Sigma-Aldrich (Buchs, CH) unless otherwise noted. The mature MHC I epitope, $OVA_{256\text{-}264}$ (SIINFEKL) peptide, was from GenScript (Piscataway, NJ, US) and the $gp100_{25–33}$ peptide was from Anaspec (Fremont, CA, US). The Endotoxin-free OVA was from Hyglos GmbH, (Bernried am Starnberger See, DE). Ultra-pure lipopolysaccharide (LPS, 01:11 B4) was from Invivogen (InvivoGen, San Diego, CA, USA). Recombinant murine GM-CSF and IL-15 were purchased from Peprotech (Oak Park, CA, USA), IL-10 from eBioscience (Vienna, AT), IL-12, IFN-α and recombinant human TGF-β1 from R&D systems (Minneapolis, MN, USA). Antibodies used in flow cytometry were from eBioscience or BioLegend (Luzern, CH) unless otherwise noted.

Mice

The following mice strains were used in this study at age 6-12 weeks unless noted otherwise. Female C57BL/6 (CD45.2 or CD45.1 Ly5) wild-type mice and OT-I CD45.2 transgenic mice, C57BL/6-Tg(TcraTcrb)1100Mjb/J, were purchased from Harlan Laboratories (Gannat, FR). Female transgenic OT-I CD45.1.2 mice were acquired from the group of Dietmar Zehn. Pmel transgenic mice, B6.Cg-Thy1a/Cy Tg(TcraTcrb)8Rest/J, were obtained from the group of Pedro Romero. $\beta 2m^{-/-}$ mice (lacking MHC class I) were obtained from H.R. MacDonald. Animals were housed in pathogen-free facilities and all procedures were approved by the Cantonal Veterinary Committee of Vaud, Switzerland (Protocol number 2518 and 2992).

Primary cell isolation

To obtain primary LN LECs and LN FRCs, LNs were digested with 0.25mg/ml Liberase DH and 100µg/ml DNase (both from Roche, Basel, CH) to obtain a single cell suspension and cultured as described (29). Cells were cultured for 5 days until confluent, removed by Accutase (Biological Industries, Lucerna-Chem AG, Lucerne CH), and stained with mAbs against gp38 (clone 8.1.1), CD31 (clone 390), and CD45 (clone 30-F10) and FACS sorted (FACS Aria II, BD, Basel, CH) into the following subpopulations: FRCs ($gp38^{+}CD31^{-}$) LECs ($gp38^{+}CD31^{+}$), BECs ($gp38^{-}CD31^{+}$), and DN ($gp38^{-}CD31^{-}$) as described (30). Bone marrow-derived DCs (BMDCs) were harvested from C57Bl/6 mice, differentiated in GM-CSF as described (31) and used at day 7 of culture. When indicated, BMDCs were matured (mDCs) by being cultured in the presence of LPS (10 ng/ml) for another 12h.

Synthesis of peptide-conjugated nanoparticles (NPs)

To explore the mechanisms of cross-presentation poly(propylene sulfide)-nanoparticles (NPs) with ~30nm diameter were synthesized and characterized as described (32). The long peptide containing the mature MHC I epitope SIINFEKL – Cys-$OVA_{250-264}$ ($COVA_{250-264}$) was synthesized in-house and activated with a 2-pyridylthiol as previously described (32). Core sulfhydryls on NPs were reacted with the activated peptide and purified on a Sepharose CL6B column (Sigma-Aldrich). To fluorescently label the NPs, NPs were exposed to Dy-649 maleimide (Dyomics GmbH, Jena, DE) after dialysis in a 1:60 molar ratio of dye to NP sulfydryl groups in phosphate buffered saline (PBS) at RT for 24 h (32). Free dye was removed by gel filtration as above but in endotoxin-free water (B. Braun Medical AG, Sempach Switzerland) as eluent. Endotoxin levels of antigens were routinely assessed by a colorimetric assay based on the HEK-Blue ™ TLR4 cell line (InvivoGen, San Diego, CA, USA) according to the manufacturer's protocol using a standard curve generated from the E-Toxate ™ endotoxin standard (Sigma).

Generation of bone marrow chimeras

Bone marrow (BM) was recovered from tibia and femurs by flushing with PBS-EDTA and dissociated by repeated passages through a 20-gauge needle. To generate bone marrow chimeras, recipient mice (C57BL/6 wild-type or $\beta 2m^{-/-}$ mice) were gamma-irradiated twice with 450 rad (4h apart) and reconstituted by tail vein injection with $8x10^{6}$ bone marrow cells from wild-type or $\beta 2m^{-/-}$ donor mice. Reconstitution was assessed by analyzing blood cells by flow cytometry and used after 8 weeks.

$CD8^{+}$ T cell purification

Splenic $CD8^{+}$ T cells from OT-I mice or pmel mice were isolated by immunomagnetic CD8 negative selection using the EasySep Mouse $CD8^{+}$ T Cell Isolation Kit from Stemcell Technologies (Vancouver, BC, Canada).

Generation of *ex vivo* LN LEC/mDC-educated CD8$^+$ T cells

Naïve CD8α$^+$ T-cells from OT-I or pmel mice were purified and directly cocultured with LN LECs or mDCs in the presence of 1nM NPssCOVA$_{250-264}$ or 1nM SIINFEKL peptide or 1μM of gp100 peptide. More specifically, 10^4 LECs or DCs were cocultured with naïve CD8$^+$ T cells in 96-well plates for 72h for OT-I and for 6 days for pmel CD8$^+$ T cells at a ratio of 1:10 APC:T cells in 200 μl of co-culture media (IMDM with 10% FBS and 1% penicillin/streptomycin - all from Life Technologies, Carlsbad, CA, USA). Supernatants were harvested and frozen for cytokine analysis. Cells were then processed and stained for immunological markers to be analyzed by flow cytometry. Cellular proliferation was monitored by CFSE dilution and apoptosis was determined by Annexin V staining (BioVision, Milpitas, CA, US). OT-I T cell proliferation was determined by assessing CFSE intensity using the automated tool in FlowJo 9.4.11.

In vitro reactivation

LEC/mDC-educated OT-I CD8$^+$ T cells were harvested on day 3 of coculture, washed at least twice with basal medium and counted. 10^5 LEC-educated or mDC-educated CD8$^+$ T cells were subsequently cocultured with 10^4 mDCs loaded, or not, with the SIINFEKL peptide (1 nM) for 24h in 200 μl of co-culture media (mDC-recall). Supernatants were harvested and frozen for cytokine analysis. Cells were then processed and stained for immunological markers to be analyzed by flow cytometry. The levels of intracellular cytokines were determined after 3h reactivation and 2h of Brefeldin A (BFA) treatment. In some cases, only when indicated, LEC-educated or mDC-educated CD8$^+$ T cells were reactivated by non-LPS-treated DCs (immature DCs, iDCs) loaded, or not, with the SIINFEKL peptide (1nM) for 24h in the presence or absence of the following cytokines: rmIL-12 (5ng/ml), rmIFN-α (2kU/ml), rmIL-10 (20ng/ml), rhTGF-β1 (20ng/ml). In some experiments, reactivation of LEC-educated or mDC-educated CD8$^+$ T cells was also conducted with plate-bound anti-CD3 antibody (145.2C11) at 5μg/ml and/or soluble anti-CD28 (37.51) at 2μg/ml (aCD3/CD28, eBioscience). The same procedures, described above, were performed to analyze the phenotype and function of the reactivated cells.

In vitro homeostatic proliferation

To determine whether LEC-educated CD8$^+$ T cells can respond to homeostatic signals and proliferate, we exposed them to IL-15 for different time periods. LEC/mDC-educated CD8$^+$ T cells were harvested on day 3 of coculture, washed at least twice with basal medium and counted. 10^5 LEC-educated or mDC-educated CD8$^+$ T cells were subsequently cultured in the presence, or absence, of IL-15 (100ng/ml). 24-72h later, the cells were harvested and stained for immunological markers to be analyzed by flow cytometry.

Adoptive CD8$^+$ T cell transfer

Following CD8$^+$ T cell purification, for the naïve groups, or following 3-day *in vitro* LEC/mDC – CD8$^+$ T cell coculture, cells were collected, washed in basal medium (IMDM, Life Technologies, Carlsbad, CA, USA) and resuspended in 100μl volume prior to tail vein injection. To assess proliferation of LNSC-educated cells *in vivo*, 10^6 naïve OT-I CD8$^+$ T cells (CD45.1.2) were adoptively transferred in chimeric mice (CD45.2). To determine the homing potential of LN LEC/mDC-educated CD8$^+$ T cells, 10^6 cells (CD45.1) were adoptively transferred in naïve host mice (CD45.2). For the *in vivo* antigen reencounter experiments, 10^6 LEC/mDC-educated cells (CD45.2) were adoptively transferred in naïve host mice (CD45.1). For the studies including challenge with bacterial pathogen, $5x10^4$ LN LEC/mDC-educated CD8$^+$ T cells (CD45.1 or CD45.1.2) were adoptively transferred in naïve host mice (CD45.2).

Antigenic challenge

In order to determine whether exogenous antigen uptake by LNSCs can drive $CD8^+$ T cell proliferation *in vivo*, we intradermally (i.d.) administered 50µg of endotoxin-free OVA in all four limbs at a volume of 10µl/limb, or saline as a control. To test the capacity of LN LEC/mDC-educated T cells to respond to secondary antigen encounter *in vivo*, we subcutaneously administered 50µg of endotoxin-free OVA plus 100µg of ultrapure LPS.

Infection with *Listeria monocytogenes* – expressing OVA (*L.m.*-OVA)

In order to assess the functional potential of LN LEC/mDC-educated $CD8^+$ T cell upon pathogenic challenge, mice were infected i.v. with *L.m.*-OVA (33) (10^3 colony forming units, cfu) acquired from log phase of growth in brain heart infusion (BHI) (Sigma-Aldrich) medium. The mice were challenged at least 5 weeks following adoptive transfer of LN LEC/mDC-educated $CD8^+$ T cells. The mice were sacrificed either eight days after challenge to analyze T cell responses or, three weeks after challenge to assess the formation of secondary memory. For the analysis of bacterial load in the spleen, mice were infected with 10^4 cfu *L.m.*-OVA at least nine weeks following adoptive transfer of LN LEC/mDC-educated $CD8^+$ T cells and sacrificed three days after. Spleens were collected, homogenized and resuspended in 10ml sterile PBS. Cell suspensions were diluted 1:10, 1:100, 1:500, 1:2000 and 100µl per respective dilution were plated on BHI agar plates and incubated overnight at 37°C. The following day, colony-forming units were counted and the amounts of *L.m.*-OVA were calculated with respect to the relative dilutions.

Tissue and cell preparation

Spleens, LNs (brachial, axillary, inguinal, popliteal), as well as lungs, liver and BM when indicated, were harvested at time of killing. LNs were digested 45min, in DMEM supplemented with 1mg/ml collagenase D (Roche, Basel, CH). Single-cell suspensions were obtained by gently disrupting the spleen and LNs through a 70-µm cell strainer. BM was recovered from tibia and femurs by flushing with medium through a 20-gauge needle and passed through a 70-µm cell strainer. Lungs were perfused with 10ml PBS, digested in medium with collagenase D for 45 min and the remaining tissue disrupted as described above. Afterwards, a 30% Percoll (VWR, Dietikon, Switzerland) gradient was applied to the cells to isolate lung leukocytes. Liver was perfused with 10ml PBS and gently disrupted through a 100-µm and subsequently, 70-µm cell strainer. A 37.5% Percoll gradient was then applied to the cells to isolate liver leukocytes. Spleen, BM, liver and blood RBCs were lysed with NH_4Cl for 4 min. Cells were counted and resuspended in co-culture media.

Ex vivo restimulation

Up to $3x10^6$ cells were plated in 96-well plates and cultured in co-culture media for 2 hours at 37°C in the presence of 1µg/mL SIINFEKL peptide, followed by additional 3h treatment with BFA (5µg/mL). Stimulation with PMA/ionomycin served as a control. For CD107a staining, the monoclonal antibody against CD107a was added in the culture together with Monensin at 5µg/mL for 5 hours. Finally, cells were washed in PBS prior to intracellular staining for flow cytometric analysis.

In vitro killing assay

To assess the specific killing capacity of reactivated LEC-educated and mDC-educated $CD8^+$ T cells, the cells were cultured, following *in vivo* or *in vitro* antigen reencounter, with a 1:1 mixture of $CFSE^{high}$- labelled (5µM) SIINFEKL-loaded and $CFSE^{low}$- labelled (0.1µM) mismatched-peptide-loaded DCs (mixed target cells) at different effector over target cell ratios. We kept the number of mixed target cells stable at $5x10^4$ cells. Mixed target cells alone served as a control for non-specific death. After 12-16 hours, the ratio of the surviving $CFSE^{high}$ and $CFSE^{low}$ cell populations was assessed by flow cytometry to calculate the

percentage of specific killing as follows: % specific killing: 100-[100*($CFSE^{high}/CFSE^{low}$)$_{sample}$ /($CFSE^{high}/CFSE^{low}$)$_{control}$].

LN localization studies – Immunofluorescence

To determine the specific localization of LEC-educated $CD8^+$ T cells in the LN, we adoptively cotransferred naïve and LEC-educated $CD8^+$ T cells at a ratio of 1:1 ($5x10^6$ total cells). Prior to transfer, naïve cells were labeled with CFSE and LEC-educated $CD8^+$ T cells with eFluor670 Cell Proliferation Dye (Ebioscience). 24-48h later brachial LNs were removed and fixed overnight in 2% PFA in PBS pH 7.4. After three washes in PBS, LNs were embedded in a block of 2% agarose, and sectioned (150µm) using a using a vibratome (Leica, Wetzlar DE). Sections were blocked in 0.5% of casein, and further labeled using antibodies against B220 (Invitrogen, Auckland, NZ, USA) and LYVE-1 (Reliatech, San Pablo, CA US). Images were acquired on a Leica SP5 confocal microscope using 20x or 60x objectives, and processed using Imaris software (Bitplane, Zürich, CH).

Flow cytometry

Cells were washed and stained with a cocktail of surface antibodies in staining buffer, containing HBSS (Life Technologies) supplemented with 0.5% bovine serum albumin. Cell viability was determined by propidium iodide incorporation in staining buffer after surface antibody staining or with live/dead fixable cell viability reagent (Life Technologies) in PBS before surface antibody staining. For intracellular/intranuclear staining, cells were fixed and permeabilized with the Foxp3/Transcription Factor Fixation/Permeabilization kit (eBiosciences) according to the manufacturer's instructions. Cells were stained in permeabilization buffer with a cocktail of monoclonal antibodies. The following anti-mouse antibodies were used: CD62L (MEL-14), CD44 (IM7), KLRG-1 (2F1/KLRG1), PD-1 (RMP1-30), CXCR3 (CXCR3-173), CD43 (1B11), CD27 (LG.3A10), CD122 (TM-b1), CCR7 (4B12), CD127 (A7R34), T-bet (eBio4B10), Eomes (Dan11mag), LFA-1 (H155-78), Sca-1 (D7), Bcl-2 (BCL/10C4), CD45.1 (F20), CD45.2 (104), CD8 (53-6.7), CD3e (145-2C11), IFN-γ (XMG1.2), IL-2 (JES6-5H4), TNF-α (MP6-XT22), CD107 (1D4B), Granzyme-B (NGZB), ki-67 (SolA15). Finally, cells were resuspended in staining buffer and analyzed by flow cytometry (CyAn ADP Flow Cytometer, DAKO). Data analysis was performed using FlowJo (v9.4, Tree Star Inc., Ashland, OR, USA).

Cytokine ELISAs

Ready-SET-go! ELISA kits for cytokine detection were purchased from eBioscience, except from the IL-7 mouse ELISA kit that was purchased from Abcam (Cambridge, UK), and used according to the manufacturer's instructions.

Statistical analysis

Statistical analysis was performed using one-way or two-way analysis of variance (ANOVA) followed by Bonferroni post-test with Prism software (Graphpad, San Diego, CA, US) unless otherwise stated. Results are shown as mean ± standard deviation with significance indicated as *p≤0.05, **p≤0.01, and ***p≤0.001.

3.3 Results

LNSCs can prime $CD8^+$ T cells under steady state conditions *in vivo* and the LNSC-education favors the generation of $CD8^+$ T cells with a central memory rather than effector-like phenotype

We previously showed that LN LECs can actively scavenge exogenous antigens *in vivo* under steady state conditions and cross-present it on MHC I inducing $CD8^+$ T cell proliferation *in vitro* [Chapter 2 and (11)]. We asked whether exogenous antigen

uptake in LECs can also drive $CD8^+$ T cell proliferation *in vivo* under homeostatic conditions. To this end, we generated bone marrow (BM) chimeric mice in which $CD45^+$ cells lacked MHC class I (β2m:WT) and therefore, presentation of the Kb-restricted SIINFEKL epitope was limited only to radioresistant lymph node stromal cells (LNSCs). To further elucidate the contribution of LNSC education in $CD8^+$ T cell priming, we also generated reciprocal chimeras (WT:β2m), in which LNSCs were excluded from antigen presentation. To address the question of whether non-hematopoietic LNSCs cross-present the antigen and directly induce proliferation *in vivo*, we transferred naïve CFSE-labeled OT-I $CD8^+$ T cells ($CD45.1.2^+$) in the chimeric mice and one day after, we intradermally (i.d.) administered OVA protein or saline (PBS), as a control (Fig. 3.1A). Five days after OVA administration, we were able to detect the transferred $CD8^+$ T cells in the skin-draining LNs and we observed notable levels of proliferation in β2m:WT mice (Fig. 3.1B, bottom panel, on the very left), suggesting that indeed, LNSCs can drive antigen-specific $CD8^+$ T cell proliferation under steady state-conditions *in vivo*. As expected, OVA administration induced remarkable levels of proliferation in the control WT:WT mice (Fig. 3.1B, bottom panel, second from the left) while there was no expansion of the transferred $CD8^+$ T cells in β2m:β2m control mice, in which both hematopoietic and non-hematopoietic cells lack MHC class I (Fig. 3.1B, bottom panel, on the very right). The mice that received saline (PBS) served as controls and allowed us to confirm that the observed proliferation was antigen-specific, resulting from MHC class I/SIINFEKL presentation on the cell surface. We further used the saline controls to separate the proliferating cells (g>0) (Fig. 3.1B, top panel, on the very left) from the ones that stayed undivided (generation 0, g=0) and determine the levels of non-specific background proliferation (Fig. 3.1B, top panel). We quantified the levels of $CD8^+$ T cell proliferation by assessing CFSE dilution (Fig. 3.1C). The analysis confirmed that OVA administration resulted in $CD8^+$ T cell proliferation at levels significantly higher than the background (PBS) when LNSCs, but not $CD45^+$ cells, were able to present the antigen (β2m:WT). As anticipated, the transferred cells proliferated more robustly in case both hematopoietic and non-hematopoietic cells were capable of MHC class I presentation (WT:WT). Interestingly, we detected notably lower levels of proliferation, compared to WT:WT mice, when stromal cells did not contribute in antigen presentation (WT:β2m), suggesting that LNSCs not only participate, but also might be appreciably involved in the induction of $CD8^+$ T cell proliferation in the LN. In the β2m:β2m mice, the difference in proliferation levels between PBS and OVA-treated mice was not statistically significant, as expected, since in these mice, neither LNSCs nor $CD45^+$ cells can present antigen on MHC class I. Next, we wanted to evaluate the phenotype of the LNSC-educated $CD8^+$ T cells in terms of activation and effector potential. By day 5 after OVA administration, the majority of the transferred $CD8^+$ T cells in the LN of β2m:WT , WT:WT and WT:β2m mice were activated, as indicated by the expression of CD44 marker (Fig. 3.1D, plots in the middle, OVA). In the β2m:β2m mice (Fig. 3.1D, bottom row), as well as in the control mice of any group that received saline (Fig. 3.1D, plots on the left, PBS), the cells expressed high levels of CD62L and low levels of CD44, preserving a naïve phenotype ($CD62L^+CD44^-$), as expected. Assessing the phenotype of the proliferating T cells, specifically, (Fig. 3.1D, plots on the right, g>0, OVA), we detected both subsets of central memory (T_{CM}), defined as $CD44^+CD62L^+$, and effector or effector memory ($T_{eff/EM}$), defined as $CD44^+CD62L^-$, $CD8^+$ T cells in all the groups (β2m:WT , WT:WT and WT:β2m mice),

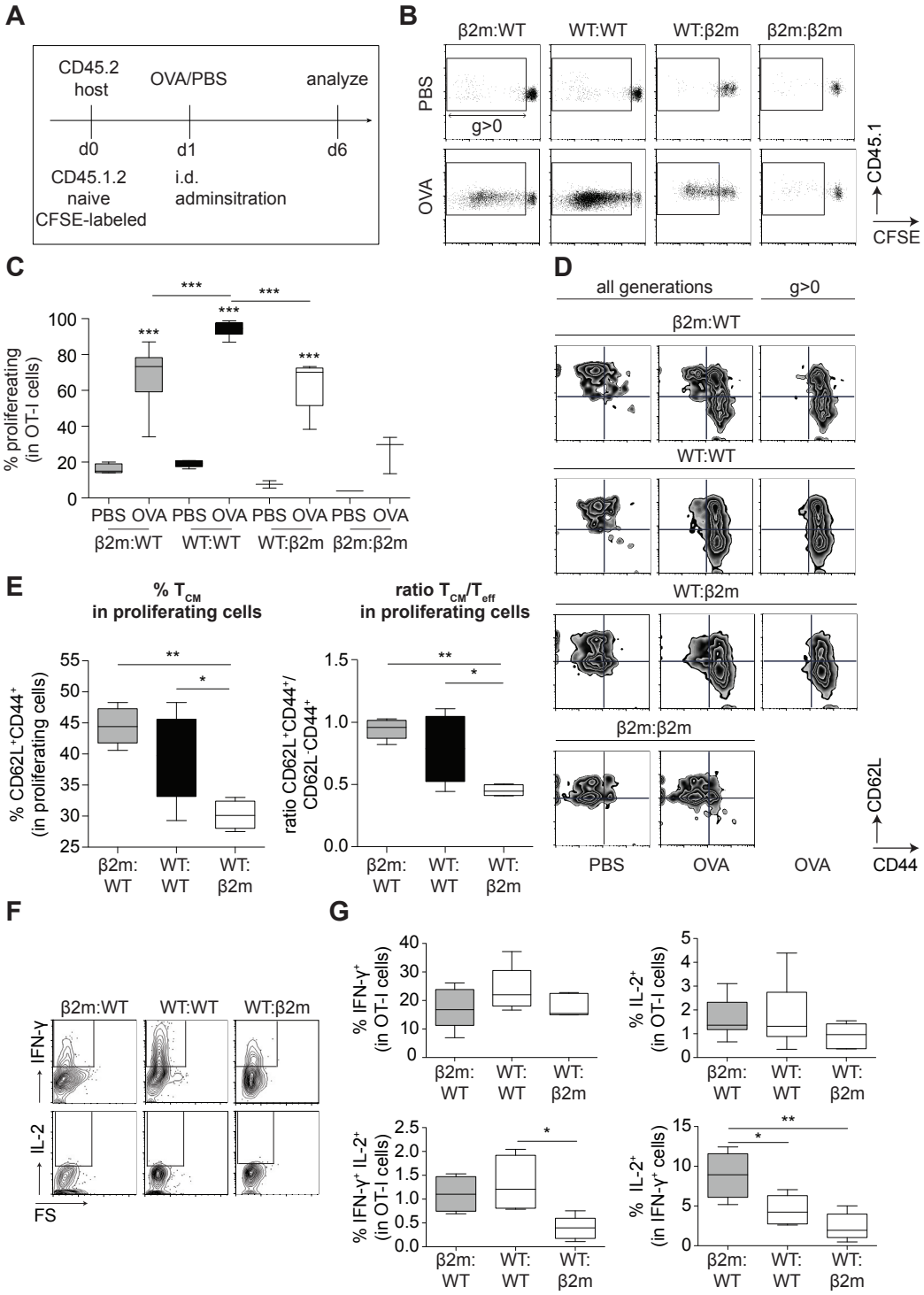

Figure 3.1 LNSCs can prime CD8$^+$ T cells under steady state conditions *in vivo* and the LNSC-educated CD8$^+$ T cells display memory-like characteristics. To evaluate the contribution of LNSCs in CD8$^+$ T cell proliferation, we generated BM chimeric mice using β2m$^{-/-}$ (lacking MHC I) mice, as described in Materials and Methods. β2m:WT, irradiated C57/Bl6 mice reconstituted with β2m$^{-/-}$ BM; WT:β2m, irradiated β2m$^{-/-}$ mice reconstituted with WT BM; WT:WT and β2m:β2m served as controls. Naïve CFSE-labeled OT-I cells were adoptively transferred and one day after, the mice were vaccinated i.d. with OVA or saline control (PBS). 5 days after vaccination, the mice were sacrificed and skin-dLNs collected. Cell suspensions were generated and analyzed by flow cytometry. **(A)** Experimental timeline. LNSCs cross-present the antigen and directly induce proliferation *in vivo*. **(B)** Representative dot plots of transferred cells displaying CD45.1 (y-axis) and CFSE dye (x-axis) in OVA (bottom) or PBS (top) - treated mice. Lower levels of expansion when presentation is limited to LNSCs or when they are

eliminated from presentation. **(C)** Percentage of proliferating cells in response to vaccination (gated on transferred cells). The stars on top of whiskers indicate statistically significant difference between PBS and OVA treatment in the same group. The T_{CM}-like subset appears larger when presentation is limited to LNSCs compared to WT:WT controls and smaller when LNSCs are eliminated from presentation. **(D)** Representative zebra plots of the phenotype of transferred cells with regard to CD44 (x-axis) and CD62L (y-axis) in response to OVA or PBS for all cells (left and middle column, all generations) or for proliferating cells (right column, g>0). **(E)** Left, the percentage of T_{CM} ($CD44^+CD62L^+$) in proliferating cells; right, the ratio of T_{CM} ($CD44^+CD62L^+$) over T_{eff} ($CD44^+CD62L^-$) in proliferating cells in response to OVA. LNSC-educated $CD8^+$ T cells induce IFN-γ and IL-2 expression and the levels of IFN-γ^+IL-2^+ cells appear to be lower when LNSCs are excluded from priming. The cells were ex-vivo restimulated with SIINFEKL followed by intracellular staining. **(F)** Representative contour plots displaying cytokine expression (in response to OVA) with IFN-γ (top) or IL-2 (bottom) on y-axis and the side scatter on x-axis. **(G)** The percentage of IFN-γ^+ (top left) or IL-2^+ (top right) or IFN-γ^+IL-2^+ (bottom left) cells (gated on transferred cells) in OVA-treated mice. Bottom right, the percentage of IL-2^+ cells gated on IFNγ^+ cells. Representative data from one of two independent experiments (n=5-6, except B-C, PBS group, n=3). *p≤0.05, **p≤0.01, ***p≤0.001 by one-way ANOVA followed by Bonferroni posttest.

with the $T_{eff/EM}$ subset being always the dominant one. However, when we compared the relative distribution of these two subsets among the different groups, we observed that the percentage of the T_{CM} subset appeared greater in β2m:WT mice, when only LNSCs were responsible for the education of $CD8^+$ T cells, in comparison to that of WT:WT mice (Fig. 3.1E, on the left). Even though this trend was not statistically significant, it suggested that LNSCs might favor the induction of the T_{CM} subset. More importantly, we observed that in the absence of LNSC-education (WT:β2m mice), the T_{CM} subset was remarkably lower compared to that of β2m:WT or WT:WT mice. This indicated that LNSC-education favors the induction of central memory-like $CD8^+$ T cells. We noted a similar trend when we examined the ratio of T_{CM} versus $T_{eff/EM}$ in the proliferating cells (Fig. 3.1E, on the right), which further suggested that LNSC-educated $CD8^+$ T cells are more biased towards a T_{CM}-like rather than $T_{eff/EM}$ phenotype.

To further characterize the effector potential of LNSC-educated $CD8^+$ T cells, we analyzed their capacity to produce cytokines upon *ex vivo* peptide restimulation. LNSC-educated $CD8^+$ T cells did express IFN-γ and IL-2 cytokines (Fig. 3.1F, G) at levels similar to those observed when $CD8^+$ T cells were educated only by $CD45^+$ cells or to those detected in WT:WT mice. More specifically, we did not detect any significant differences in the percentage of IFN-γ positive or IL-2 positive cells among the groups (Fig. 3.1G, top graphs, left and right respectively and Fig. 3.9A). However, we observed a trend for lower levels of IFN-γ in the absence of LNSC (WT:β2m) or $CD45^+$ (β2m:WT) cells MHC I presentation compared to WT:WT mice, which matched the trend that we noted for its expression in a per cell basis, by assessing the mean fluorescence intensity (MFI) (Fig. 3.9B), still not significant though. Additional analysis revealed lower levels of IFN-γ and IL-2 double positive cells when LNSCs were eliminated from T cell priming (WT:β2m) (Fig. 3.1G, bottom graphs, left). Moreover, the percentage of IL-2 positive cells among the IFN-γ producing ones was significantly higher for exclusively LNSC-educated $CD8^+$ T cells (β2m:WT) while in the absence of LNSC-education, the percentage displayed was the lowest. The expression of IL-2 has been traditionaly related to the T_{CM} subset (20, 21, 23, 34). Even though the levels of IL-2 expression were very low to comfortably arrive to a safe conclusion, it is intriguing to speculate that the enhanced levels of IL-2 in IFN-γ producing LNSC-educated $CD8^+$ T cells might be related to the central memory-like phenotype that we observed in LNSC-educated $CD8^+$ T cells.

By using the β2m$^{-/-}$ BM chimeric mice we cannot exclusively attribute our findings to LN LECs and exclude the contribution of the other LNSC subsets, including fibroblastic reticular cells (FRCs), blood endothelial cells (BECs) or double negative (DN) cells (follicular DCs cannot present antigen to CD8$^+$ cells (35)). Indeed, FRCs have been also reported to induce antigen-specific CD8$^+$ T cell priming (9). We, and others, have recently demonstrated that LN LECs were the most effective, among stromal cells, in the uptake of peripherally administered OVA [Chapter 2 and (11, 36)], potentially due to its mannosylated pattern (37). Thus, it is likely that CD8$^+$ T cell proliferation in this setting might be mainly governed by LECs.

Collectively, these data demonstrate that LNSCs can prime CD8$^+$ T cells under steady state conditions *in vivo* and that the LNSC-educated CD8$^+$ T cells display memory-like characteristics and are able to produce cytokines.

LECs induce apoptosis but the non-apoptotic CD8$^+$ T cells go into a central memory-like phenotype

To determine the contribution of LEC-educated CD8$^+$ T cells in LNSC-priming, we decided to turn to *in vitro* studies and characterize *ex vivo* generated LN LEC-educated CD8$^+$ T cells. Motivated by our *in vivo* findings of LNSC-educated CD8$^+$ T cells being more biased towards a central memory-like phenotype, we sought to assess their profile with regard to CD44 and CD62L expression, compared to that of mature, bone marrow derived, dendritic cell (mDC)-educated CD8$^+$ T cells. To this end, we cocultured LN LEC or mDC together with transgenic OVA-specific OT-I CD8$^+$ T cells in the presence (education: LEC/mDC) or absence (education: none) of 1nM NP-ss-COVA$_{250–264}$. This 16-aa peptide on the NPs (NP-ss-COVA$_{250–264}$) requires uptake and intracellular processing for MHC class I loading in BMDCs (32) and in LECs (11). It is a very efficient tool for cross-presentation studies, that we have extensively used and characterized (32). Upon incubation with LN LECs in the presence of NP-ss-COVA$_{250–264}$, OT-I CD8$^+$ T cells proliferated strongly and increased in size compared to naive cells, which is consistent with their activated state, although they did not develop as large a blastoid size as mDC-educated CD8$^+$ T cells (Fig. 3.2A, top panel). Interestingly, when we assessed the expression of CD44 and CD62L in LEC/mDC-educated cells on day 3 of the coculture, we observed a very particular profile for LEC-educated CD8$^+$ T, characterized by high levels of CD62L and CD44 (Fig. 3.2A, bottom panel, middle). This profile was totally different from the one of uneducated cells, which maintained a naive CD62L$^+$CD44$^-$ phenotype (Fig. 3.2A, bottom panel, left), and clearly distinct from the effector-like profile of mDC-educated CD8$^+$ T cells, which displayed mainly high levels of CD44 but mid to low levels of CD62L. CD62L (L-selectin) is a marker widely used to distinguish central memory from effector memory T cells. It is shed from the T cell membrane following TCR activation (38) and its regulation plays an important role in T cell trafficking, since it functions as a homing receptor, facilitating entry to secondary lymphoid organs. Recent studies have demonstrated that CD62L shedding might also reflect a physiological role in regulating the differentiation and function of effector cells (39, 40). We asked whether activation of CD8$^+$ T cells by LECs induced CD62L downregulation or whether CD62L has been maintained in the course of a three day coculture. We observed that CD62L was actually downregulated for both LEC and mDC-educated CD8$^+$ T cells on the first day of the

co-culture (Fig. 3.2B, top), consistent with the cleavage of CD62L from the cell surface following TCR engagement reported previously (41). On day 2, we detected both CD62L$^+$ as well as CD62L$^-$ cells in the LEC-educated population of CD8$^+$ T cells

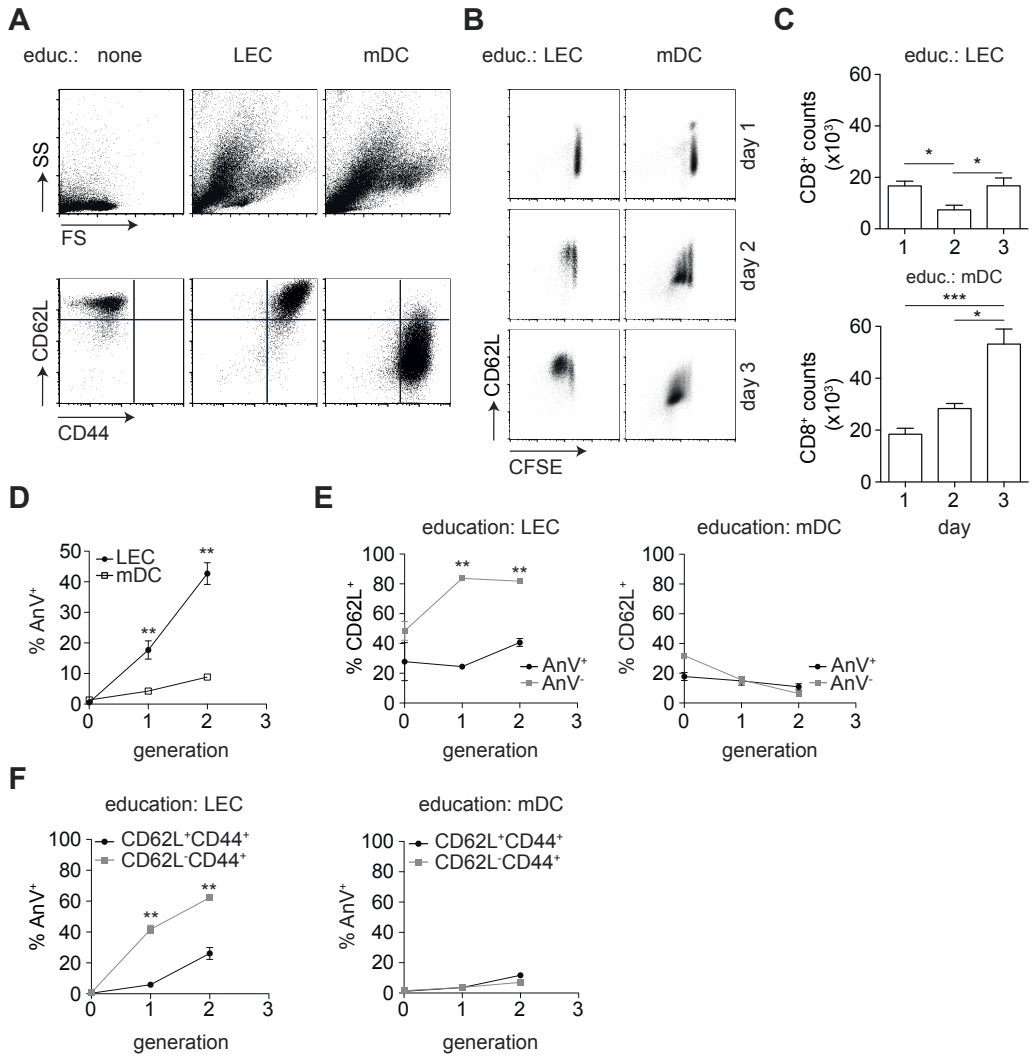

Figure 3.2 LEC education induces apoptosis but the non-apoptotic CD8$^+$ T cells go into a central memory-like phenotype *in vitro*. Naive CFSE-labeled OT-I cells were cocultured in the presence of NPssCOVA$_{250\text{-}264}$ (1nM) with LN LEC or mature BMDC (mDC). At different time points, LEC/mDC-educated CD8$^+$ T cells were harvested and evaluated for apoptosis, by assessing the apoptotic marker Annexin V (AnV), and expression of CD44 and CD62L. **(A)** LEC-educated CD8$^+$ T cells display a distinctive CD44$^+$CD62L$^+$ phenotype similar to T_{CM} cells. Top, representative dot plots of the size of LEC/mDC-educated (LEC/mDC educ.) or non-educated (naïve, none) CD8$^+$ T cells with the forward scatter on x-axis and side scatter on y-axis. Bottom, representative dot plots with CD62L on y-axis and CD44 on x-axis on day 3 of coculture. **(B)** Proliferating cells in LEC-educated CD8$^+$ T cells are mainly CD62L$^+$ whereas in mDC-educated they are mainly CD62L$^-$. Representative dot plots of CD62L expression per generation in a 3-day coculture with CFSE on x-axis and CD62L on y-axis. **(C)** Counts of live LEC/mDC-educated CD8$^+$ T cells on day 1, 2, and 3 of coculture. **(D)** Percentage of AnV positive cells per generation on day 2 of coculture. **(E)** In LEC-educated CD8$^+$ T cells, AnV$^-$ cells display increasing levels of CD62L per generation whereas AnV$^+$ cells display lower CD62L levels. Percentage of CD62L$^+$ cells per generation, gated on AnV$^+$ (black lines) or AnV$^-$ (grey lines) cells on day 2 of coculture. **(F)** Levels of apoptosis per generation in T_{eff}-like (CD44$^+$ CD62L$^-$, grey lines) and T_{CM}-like (CD44$^+$CD62L$^+$, black lines) subset of LEC/mDC-educated CD8$^+$ T cells on day 2 of coculture. Representative data from one of two independent experiments (n=3). (D-F), stars indicate significant difference between groups in the same generation. *p≤0.05, **p≤0.01 by one-way ANOVA (C) or two-way ANOVA (D-F) followed by Bonferroni posttest.

whereas most of the cells maintained mid to low levels of CD62L in the mDC-educated population (Fig. 3.2B, middle). By day 3, as stated above, almost all LEC-educated $CD8^+$ T cells expressed high levels of CD62L while DC-educated cells were mainly $CD62L^-$ (Fig. 3.2B, bottom). Interestingly, by analyzing the expression of CD62L with regard to proliferation, we noticed that in LEC-educated $CD8^+$ T cells, proliferating cells were mainly $CD62L^+$ during the 3-day coculture, whereas in the mDC-educated population there was the opposite trend with proliferating cells being mainly $CD62L^-$ (Fig. 3.2B). This observation can be interpreted in different ways: either LEC-educated $CD8^+$ T cells downregulate or transiently lose CD62L and then re-express it, or the gradual predominance of $CD62L^+$ cells is mainly a result of an increased proliferation rate relative to $CD62L^-$ cells which might have a lower turnover rate or even die. In order to better interpret these findings, we assessed viability and expansion of $CD8^+$ T cells during the 3 days of coculture (Fig. 3.1C). mDC-educated $CD8^+$ T cells expanded continously after priming with a more than 2-fold increase on day 3. However, we detected a decrease in LEC-educated $CD8^+$ T cells on day 2 of the coculture compared to day 1 and the cells expanded to levels similar to day 1 on day 3. The fact that we do observe proliferation in LEC-educated $CD8^+$ T cells but the overall expansion (from day 3 to day 1) is not significant favors the scenario of a lower proliferation rate as well as apoptosis.

These findings were not surprising since we have previously shown that skin-derived, immortalized, LEC-educated $CD8^+$ T cells display a dysfunctionally activated phenotype characterized by increased levels of the apoptotic marker annexin V in early generations compared to DC-stimulated T cells. In order to address the question of whether the difference in expansion in the LEC-educated population can be attributed to apoptosis and more specifically, define whether there is an apparent predominance of $CD62L^+$ cells due to higher apoptotic levels in the $CD62L^-$ subset, we sought to evaluate the levels of Annexin V in LN-LEC-educated $CD8^+$ T cells on day 2 of the coculture. We thought that the second day of the coculture would be the most appropriate time point since it allowed us to detect both the $CD62L^+$ and $CD62L^-$ subets in LEC-educated and mDC-educated populations. In agreement with our previous findings, LN-LEC-educated $CD8^+$ T cells displayed higher levels of apoptosis from the early generations compared to mDC-educated ones (Fig. 3.1D). More importantly, when we analyzed the expression of CD62L per generation in the Annexin V^+ or the Annexin V^- subset for LN LEC-educated (Fig. 3.1E, left) and mDC-educated (Fig. 3.1E, right) $CD8^+$ T cells, we found that that the apoptotic cells (annexin V^+, black line) displayed lower levels of CD62L compared to the non-apoptotic cells (grey line) in LEC-educated, while there was not much difference in CD62L expression between the two subsets in mDC-educated cells. This observation supports the rationale that $CD62L^-$ effector-like cells tend to be more apoptotic relative to $CD62L^+$ central memory-like cells, which therefore, dominate the LEC-educated population. Indeed, monitoring the levels of apoptosis per generation in the T_{eff}-like $CD62L^-CD44^+$ (Fig. 3.1F, grey line) and T_{CM}-like $CD62L^+CD44^+$ (Fig. 3.1F, black line) subsets revealed that even though both subsets displayed increasing levels of apoptosis per generation, LEC-educated $CD8^+$ T_{eff}-like cells are significantly more apoptotic from the early generations compared to the T_{CM}-like subset, which displays similar levels of apoptosis to mDC-educated $CD8^+$ T cells with either phenotype.

Taken together, these data suggest that in agreement to our previous studies, antigen-specific education of $CD8^+$ T cells by LN LECs under steady-state conditions *in vitro* induces apoptosis, but the non-apoptotic cells seem to adopt a particular, T_{CM}-like phenotype, which is clearly distinct from the profile of conventional APC-educated cells.

LEC-educated $CD8^+$ T cells display a divergent phenotype sharing characteristics with central memory and stem cell memory cells

Having shown that LEC-educated $CD8^+$ T cells display a central memory-like phenotypic profile ($CD44^+CD62L^+$), we wanted to further characterize how they related to known memory subsets. We compared the expression of surface markers, intracellular proteins, as well as transciption factors in LN LEC-educated OT-I $CD8^+$ T cells with those of mDC-educated or naive $CD8^+$ T cells on day 3 of our *in vitro* coculture system. As described above, LEC-educated T cells diplayed high levels of CD44 (pink line) similar to those of mDC-educated cells (blue line), but they also expressed high levels of CD62L matching the expression of non-educated (black line) naive cells (Fig. 3.3). Since most of the cells in the LEC-educated population were $CD44^+CD62L^+$ and the majority of cells in mDC-educated $CD44^+CD62L^-$, we decided to compare these two subsets to better illustrate the phenotypic variation. LEC-educated $CD8^+$ T cells expressed CD127 (IL-7R), CD122 (IL-2Rβ) and CCR7 at levels similar or slightly higher to mDC-educated cells (Fig. 3.3A, B and Fig. 3.10A). They also expressed Eomes and T-bet, two transcription factors that have been shown to dynamically regulate effector and memory cells (42, 43). More specifically LEC-educated $CD8^+$ T cells presented higher levels of Eomes compared to mDC-educated ones, while their expression of T-bet was slightly lower.

Interestingly, we found that LEC-educated $CD8^+$ T cells express additional markers, which have been reported to delineate the newly-described subset of stem cell memory T cells (T_{SCM}) in humans (44) and mice (45). T_{SCM} cells phenotypically resemble both naive cells, being $CD44^-CD62L^+$ in mice, as well as antigen-experienced cells, since they express CD122, CXCR3 and CD27 (46). The expression of additional molecules, such as CD95 (FAS), stem cell antigen 1 (Sca-1) and the B cell lymphoma 2 (Bcl-2) protein further portray their phenotypic profile. LEC-educated $CD8^+$ T cells were positive for Sca-1 and CD27, as well as partly positive for Bcl-2, CD95 and CXCR3 at levels greater than mDC-educated $CD8^+$ T cells. Surprisingly, LEC-educated $CD8^+$ T cells also expressed CD43 in the same range as mDC-educated cells, which has been described to be expressed on effector but not memory $CD8^+$ T cells (47). Furthermore, LEC-educated and mDC-educated cells also expressed LFA-1 with LEC-educated ones expressing higher levels.

Trying to better illustrate the divergence in the $CD8^+$ T cell differentiation state induced upon antigen-specific interaction with LN LEC or mDC, we analyzed the distribution of diverse T cell subsets detected with respect to various markers (Fig. 3.3C). We observed that the subsets of LN LEC-educated cells fell mostly in the $CD44^+CD62L^+$ subpopulation (CM-like and SCM-like). The largest subset among this population, was the one that also displayed expression of CD127, CD122, Sca-1 and medium levels of Bcl-2. The distribution of subsets in LEC-educated cells differed clearly from the one of mDC-educated cells that were dominated by the $CD44^+CD62L^-CD127^+$ (EM-like) subset.

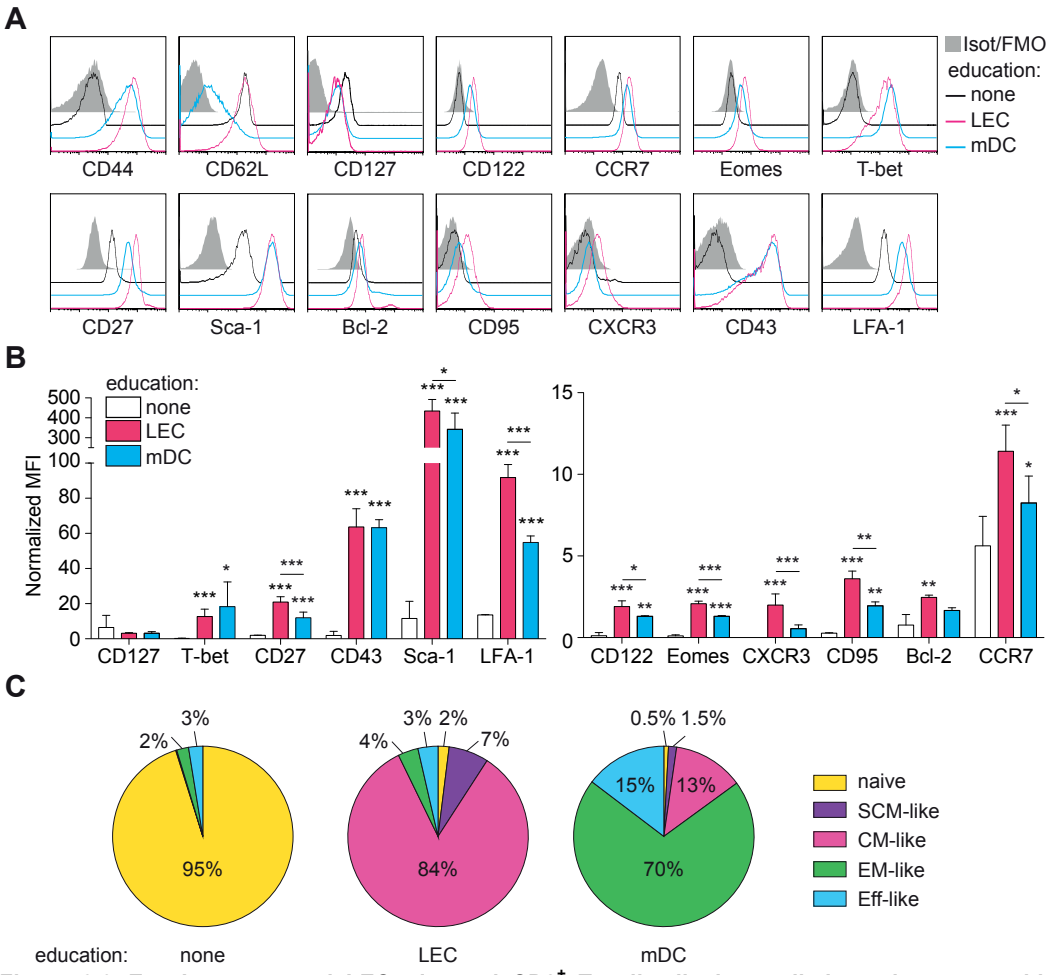

Figure 3.3 *Ex vivo* generated LEC-educated CD8$^+$ T cells display a distinct phenotype with central memory-like and stem cell memory-like characteristics. Naïve OT-I cells were *in vitro* educated in the presence of NPssCOVA$_{250\text{-}264}$ (1nM) by LN LEC or mDC (education) or not educated (none). On day 3 of co-culture, LEC/mDC-educated CD8$^+$ T cells were stained for different surface, intracellular and intranuclear markers and analyzed by flow cytometry. **(A)** CD44$^+$CD62L$^+$ LEC-educated cells are also CCR7$^+$, CD127$^+$, CD122$^+$, T-bet$^+$ and Eomes$^+$ but they also display Sca-1, a typical marker for stem-cells. They were also partly positive for other markers related to T_{SCM} cells (Bcl-2, CD95, CXCR3). Representative histograms of various surface (CD44, CD62L, CD127, CD122, CCR7, etc) markers or intracellular proteins (Bcl-2) or transcription factors (T-bet, Eomes) for non-educated (black line), mDC-educated (blue line) and LEC-educated (pink line) CD8$^+$ T cells. **(B)** Normalized mean fluorescence intensity (MFI) for the markers shown in (A), in CD44$^-$CD62L$^+$ non-educated (empty bars), in CD44$^+$CD62L$^+$ LEC-educated (pink bars), or in CD44$^+$CD62L$^-$ DC-educated (blue bars) CD8$^+$ T cells. Normalized MFI was determined as $(MFI_{sample}\text{-}MFI_{isotype})/MFI_{isotype}$. **(C)** Pie charts representing the distribution of various T cell subsets in naïve (left), LN LEC-educated (middle) and mDC-educated (right) CD8$^+$ T cells, defined as follows: CD44$^-$CD62L$^+$, naïve; CD44$^+$CD62L$^+$CD127$^+$CD122$^+$Sca-1$^+$Bcl-2^{high}, stem cell memory (SCM)-like; CD44$^+$CD62L$^+$CD127$^+$CD122$^+$Sca-1$^+$Bcl-2$^{mid/low}$, central memory (CM)-like; CD44$^+$CD62L$^-$CD127$^+$, effector memory (EM)-like; CD44$^+$CD62L$^-$CD127$^-$, effector (Eff)-like. Representative data from one of three independent experiments (n=3). *p≤0.05, **p≤0.01, ***p≤0.001 by one-way ANOVA followed by Bonferroni posttest.

Although it is hard to ultimately classify LN LEC-educated CD8$^+$ T cells among one of the known T cell subsets, we can observe that their phenotypic profile appeared to lie somewhere between the T_{CM} and T_{SCM} subsets, and it was distinct from the one of mDC-educated cells that resembled more with the $T_{EM/eff}$ subset. It is important to note that the particular phenotypic profile described here for LN LEC-educated CD8$^+$

T cells was not specific to the model antigen and TCR transgenic system used, nor it was dependent on the cross-presentation mechanism; By altering NP-ss-COVA$_{250–264}$ with the SIINFEKL peptide (Fig. 3.10C, D), as well as using the pmel transgenic mice bearing the TCR specific for the gp100 peptide, yielded the same profile (Fig. 3.10E). In any case, the extensive phenotypic complexity and diversity among T cell subsets reflects also their functional heterogeneity. Therefore, the phenotypic profile constitutes only one of the steps towards the identification of the differentiation state of LN LEC-educated CD8$^+$ T cells.

CD62L expression in LEC-educated CD8$^+$ T cells reflects their LN homing ability and the memory-like phenotype is preserved upon *in vivo* transfer

The characterization of the T cell differentiation state also involves the evaluation of tissue-homing properties. One of the very distinct characteristics of LEC-educated CD8$^+$ T cells was the enhanced expression of CD62L. Since naive T cells and T_{CM} engage CD62L to localize to lymphoid tissue, we next investigated whether *ex vivo* generated LN LEC-educated CD8$^+$ T cells can migrate to secondary lymphoid organs. To address this question, we adoptively transferred *ex vivo* generated LEC/mDC-educated or naive OT-I CD8$^+$ T cells and subsequently analyzed their distribution among lymphoid and non-lymphoid organs (Fig. 3.4A). LEC-educated CD8$^+$ T cells homed primarily to secondary lymphoid organs (LN, spleen) whereas mDC-educated cells migrated mainly to the periphery (lung, liver) (Fig. 3.4B). More specifically, although we observed LEC-educated cells in both lymphoid and non-lympoid organs, 53% of the transferred LEC-educated cells were detected in the LN and spleen, while only 33% of the mDC-educated cells were found in the same organs. As expected, naive CD8$^+$ T cells were almost exclusively detected in lymphoid tissue (91%).

Additionally, analyzing the phenotype of the detected cells, we observed that LEC-educated CD8$^+$ T cells retained their central memory-like phenotype after *in vivo* transfer (Fig. 3.4C, D). Precisely, the CD44$^+$CD62L$^+$ T_{CM}-like subset dominated in the population of LEC-educated cells detected in the LN (77.0±3.5) and spleen (56.5±9.4) (Fig. 3.4D, left), as well as in the rest of the organs examined (Fig. 3.11A), one week after the transfer. In mDC-educated cells, the subset of CD44$^+$CD62L$^+$ was the predominant one in the LN (67.5±0.3) but not in the spleen (Fig. 3.4D) or any of the other organs, where it was actually much smaller (Fig. 3.11A). Evaluating the ratio of CD44$^+$CD62L$^+$ T_{CM}-like versus CD44$^+$CD62L$^-$ T_{eff}-like (Fig. 3.4D, right) nicely illustrated the polarization of LEC-educated CD8$^+$ T cells versus a T_{CM}-like rather than $T_{eff/EM}$-like phenotype. Those ratios were found to be greater than one in LEC-educated for all the organs examined (Fig. 3.4D and Fig. 3.11B, C) whereas in mDC-educated cells, the ratios were always lower than one, except from the LN. Yet in the LN, where both LEC and mDC-educated were more inclined to the T_{CM}-like subset, the indicative ratio was significantly higher in LEC-educated, highlighting the phenotypic differences between the two populations. Interestingly, the predominance of the T_{CM}-like subset in LEC-educated CD8$^+$ T cells was much more pronounced in the LN (Fig. 3.4D and Fig. 3.11B, C), suggesting a specific enrichment at this location compared to other organs. Furthermore, these findings suggest that the differentiation state might be flexible to some extent and dynamically reprogrammed in response to the local microenvironment.

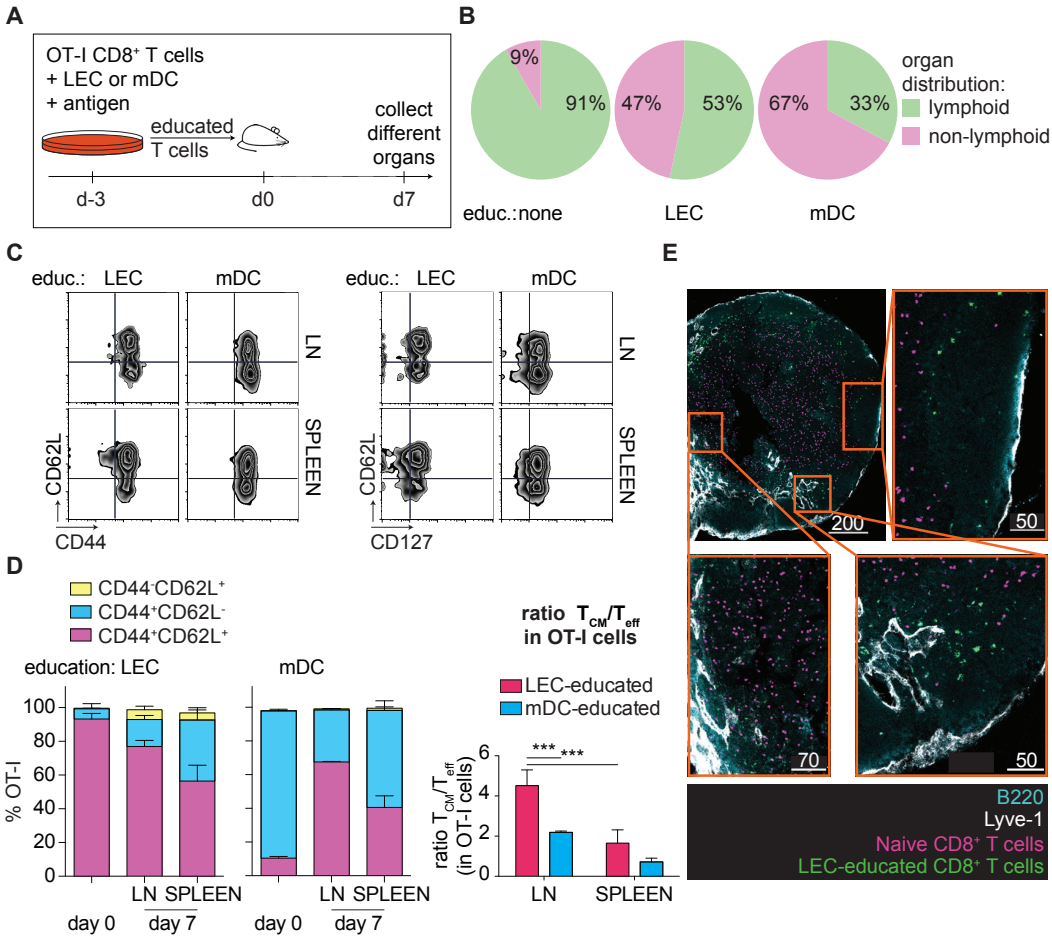

Figure 3.4 CD62L expression in LEC-educated CD8$^+$ T cells translates to LN homing where they retain their memory-like phenotype. (A) CD45.1$^+$ OT-I cells were educated in the presence of NPssCOVA$_{250-264}$ (1nM) by LN LEC or mDC (educated T cells). On day 3 of coculture, LEC/mDC-educated or naive OT-I CD8$^+$ T cells were transferred i.v. in C57/Bl6 WT mice. One week after, mice were sacrificed; spleen, skin-dLNs, liver and lungs were collected and analyzed by flow cytometry. **(B)** LEC-educated CD8$^+$ T cells home primarily to secondary lymphoid organs (LN, spleen) whereas DC-educated cells home mainly to non-lymphoid tissues (liver and lungs). Pie charts displaying the distribution of transferred cells in lymphoid versus non-lymphoid organs. Percentages are calculated as number of cells detected in lymphoid or non-lymphoid organs over total cells in all organs analyzed. LEC-educated CD8$^+$ T cells retain the T$_{CM}$-like phenotype after *in vivo* transfer. **(C)** Representative zebra plots of transferred LEC/mDC-educated cells in LN and spleen with CD44 on x-axis and CD62L on y-axis (left) or with CD127 on the x-axis and CD62L on the y-axis (right). **(D)** Left, percentage of T$_{CM}$-like (CD44$^+$CD62L$^+$, pink), T$_{eff/EM}$-like (CD44$^+$CD62L$^-$, blue) and naïve (CD44$^-$CD62L$^+$, yellow) cells in LEC/mDC-educated cells before transfer (day 0) and one week after (day 7) in LN and spleen. Right, ratio of T$_{CM}$-like (CD44$^+$CD62L$^+$) over T$_{eff}$-like (CD44$^+$CD62L$^-$) cells in each organ in transferred LEC/mDC-educated CD8$^+$ T cells. Representative data from one of two independent experiments (n=3). **p≤0.01, ***p≤0.001 by two-way ANOVA followed by Bonferroni posttest. **(E)** LEC-educated CD8$^+$ T cells are situated at the outermost regions of the LN, in the subcapsular sinus area, close to B cell follicles and the interfollicular areas of the LN. LEC-educated (green) and naive (pink) OT-I CD8$^+$ T cells were cotransfered in C57/Bl6 WT mice. Mice were sacrificed 24-48h later and brachial LNs were collected. Top left, brachial lymph node section stained with Lyve-1 (white), marking lymphatic structures, and B220 (cyan) marking B cells for orientation. The orange frames indicate regions of close-up images. Top right and bottom right, close-up images showing the particular distribution of LEC-educated cells on the edges of B cell follicles compared to broadly-distributed naive cells in the T cell zone (bottom left and top left images). Scale bars in µm.

This particular pattern of homing and distribution among the different organs prompted us to explore the specific sub-anatomical sites in the LN, in which LEC-educated cells reside. To this end, we co-transferred differentially fluorochrome-labeled LEC-educated or naive CD8$^+$ T cells and analyzed their localization pattern

using confocal microscopy of thick sections of the brachial LN. The cotransfer of the two populations allowed us to identify whether there was a difference in distribution in the different LN compartments. We observed the naive population residing mainly around the T cell zone, in the paracortex, (Fig. 3.4E, top left, bottom left), consistent with previous reports (48, 49) describing the localization of naive $CD8^+$ T cells in the LN. Noticeably, most of the LEC-educated $CD8^+$ T cells were found close to the cortical and medullary sinuses, around B cell follicles and particularly in the interfollicular areas (Fig. 3.4E, top left, top right, bottom right), in a position similar to the one recently described for central memory $CD8^+$ T cells (48, 49).

Collectively, these data suggest that CD62L expression in LEC-educated $CD8^+$ T cells is functional and is actually employed for preferential homing to secondary lymphoid organs. The migrating cells retain their memory-like phenotype and display a characteristic sublocalization pattern in the LN, similar to that of $CD8^+$ T_{CM} cells.

Upon antigen re-encounter on mature DCs *in vitro*, LEC-educated $CD8^+$ T cells can be reactivated and generate effector cells

Having demonstrated that LEC-educated $CD8^+$ T cells display a memory-like phenotype with lymphoid tissue homing properties, we asked whether they can be reactivated upon antigen re-encounter, a property ascribed to memory cells. To this end, we educated OT-I $CD8^+$ T cells with LECs or mDCs (in the presence of NP-ss-$COVA_{250–264}$), labeled them with CFSE and incubated them with mDCs loaded with the SIINFEKL peptide (mDC-recall, + antigen) for 24h (Fig. 3.5A). We subsequently analysed their proliferation and differentiaton potential. Reactivation with mDCs not bearing the SIINFEKL peptide served as control (- antigen). By assessing CFSE dilution, we detected proliferation upon mDC-recall in LEC-educated $CD8^+$ T cells (Fig. 3.5B), even though at low levels likely due to the short length of the reactivation period. mDC-educated cells did not manage to proliferate at higher levels compared to control during the same period, indicating lower proliferative potential upon antigen re-encounter compared to LEC-educated cells. We have previously characterized $CD8^+$ T cells educated by LECs as dysfunctionally activated since we detected very low levels of cytokines in the supernatant of a 3-day coculture, much lower than mDC-educated cells [Chapter 2 and (11)]. Therefore, we sought to investigate whether the cells maintain this dysfunctional state or whether they can respond, displaying functional potential. Interestingly, LEC-educated $CD8^+$ T cells exited the non-responsive state and produced cytokines (Fig. 3.5C). More specifically, (upon 5h mDC-recall) we detected slightly lower levels of IFN-γ but significantly higher levels of TNF-α and IL-2 in LEC-educated compared to mDC-educated cells, as determined by intracellular staining. Naïve OT-I $CD8^+$ T cells were also stimulated with SIINFEKL-bearing DCs, as a control. We failed to detect significant cytokine expression in naïve cells at this time interval, suggesting that antigen-experienced cells can respond more quickly, as previously anticipated. In agreement with these data, we observed the same trends when we assessed the secretion of cytokines in the supernatant of the 24h mDC-recall assay (Fig. 3.12). The enhanced proliferation potential and the increased levels of IL-2 production upon reactivation in LEC-educated $CD8^+$ T cells add up to their memory-like characteristics and suggest a less differentiated state compared to mDC-educated ones.

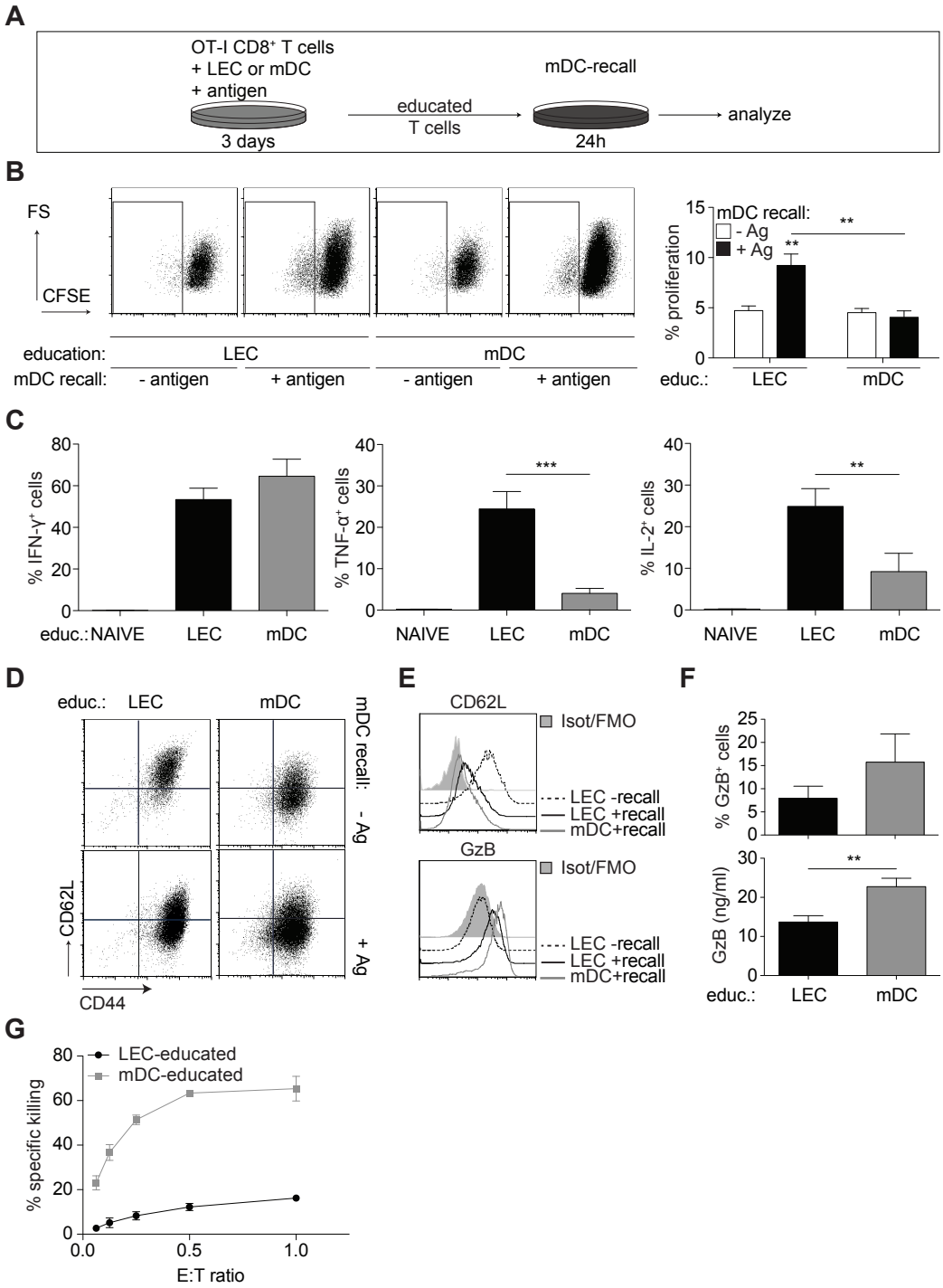

Figure 3.5 LEC-educated CD8$^+$ T cells can be reactivated by mature DCs *in vitro*, giving rise to effector cells. OT-I cells were cultured in the presence of NPssCOVA$_{250\text{-}264}$ (1nM) with LN LEC or mDC for 3 days (education). LEC/mDC-educated CD8$^+$ T cells were subsequently harvested, labeled with CFSE and re-plated in the presence of mDCs (mDC recall), bearing or not the SIINFEKL peptide **(A)** Schematic of the experiment. **(B)** Upon 24h restimulation with SIINFEKL-loaded DCs, LEC-educated CD8$^+$ T cells rapidly proliferate, as determined by flow cytometry. Left, representative dot plots with CFSE on x-axis and the forward scatter on y-axis. Right, percentage of proliferating cells in CD8$^+$ T cells upon DC recall with (+Ag) or without (-Ag) SIINFEKL. **(C)** LEC-educated CD8$^+$ T cells can exit the non-responsive state and produce cytokines upon mDC-recall. From left to right: percentage of IFN-γ$^+$, TNF-α$^+$, and IL-2$^+$ cells (gated on CD8$^+$ T cells) after 5h mDC-recall. **D)** LEC-educated CD8$^+$ T cells downregulate CD62L and turn to more T$_{eff}$-like phenotype after mDC recall. Representative flow cytometry dot plots with CD62L on y-axis and CD44 on x-axis for LEC/mDC-educated cells re-activated

by DCs bearing the SIINFEKL peptide (+Ag), or not (-Ag). LEC-educated $CD8^+$ T cells display cytotoxic effector characteristics upon mDC recall. **(E)** Representative histograms of CD62L (top) and Granzyme B (GzB, bottom) in LEC-educated $CD8^+$ T cells before (black dotted line) or after mDC-recall (black line) and in mDC-educated $CD8^+$ T cells after mDC-recall (grey line). Isotype/FMO control in solid grey. **(F)** LEC-educated $CD8^+$ T cells express cytolytic molecules upon mDC recall. Top, percentage of GzB^+ cells (gated on $CD8^+$ T cells) upon recall, as determined by intracellular staining. Bottom, secreted GzB (ng/ml) in the supernatant after 24h mDC recall. **(G)** LEC-educated $CD8^+$ T cells display specific killing capacity. Reactivated LEC/mDC-educated OT-I $CD8^+$ T cells were cultured on top of DCs loaded with SIINFEKL or non-congenic peptide for 16-20h at different effector to target ratios. Percent specific killing for LEC-educated versus mDC-educated cells. E:T; effector to target ratio. **p≤0.01, ***p≤0.001 by two-way ANOVA (B) or one-way ANOVA (C) followed by Bonferroni posttest or by two-tailed unpaired Student's t test (F).

We further investigated the differentiation potential of LEC-educated $CD8^+$ T cells by assessing the phenotype of the cells upon reactivation. LEC-educated T cells downregulated CD62L and turned to a more effector-like phenotype ($CD44^+CD62L^-$) after DC-recall, similar to the one of mDC-educated cells (Fig. 3.5D, E). However, they still preserved a $CD44^+CD62L^+$ subset. We also detected Granzyme-B (GzB) expression upon reactivation (Fig. 3.5E, F), as determined by intracellular staining (Fig. 3.5F top) as well as by assessing the amount secreted in the supernatant by ELISA (Fig. 3.5F bottom), at lower levels though compared to mDC-educated cells. The production of cytolytic molecules upon DC-recall suggests that the differentiated cells display cytotoxic effector characteristics. Consistent with the acquisition of effector function, LEC-educated $CD8^+$ T cells also displayed specific killing activity (Fig. 3.5G), although they appeared less potent compared to their DC-educated counterparts.

Taken together, these data suggest that LEC-educated $CD8^+$ T cells can escape the non-responsive state and retrieve their functional potential upon antigen re-encounter *in vitro*. They are situated higher than the terminal effector stage in the scale of differentiation and, similar to T_{CM} $CD8^+$ T cells, they can differentiate and give rise to effector cells.

LEC-educated $CD8^+$ T cells undergo rapid expansion following re-exposure to the antigen *in vivo*, even after prolonged periods in the absence of encounter, and differentiate into effector CTLs upon recall

The next step was to assess the ability of LEC-educated $CD8^+$ T to undergo rapid recall responses to secondary antigen exposure under inflammatory conditions *in vivo*. For that purpose, we transferred *ex vivo* generated CFSE-labeled LEC/mDC-educated OT-I $CD8^+$ T cells in mice and shortly after (short-term recall), we administered OVA plus LPS (+RECALL), or not (-RECALL) (Fig. 3.6A). Three days following antigen plus adjuvant administration, we observed robust expansion of the transferred cells in the LN and the spleen for LEC-educated as well as mDC-educated $CD8^+$ T cells (Fig. 3.6B, C). More specifically, we detected a significant 4-fold increase in the percentage of transferred LEC-educated cells in the LN and the spleen upon recall, suggesting that similar to our *in vitro* findings, the cells can respond to secondary exposure to the antigen. The relative increase in mDC-educated cells was lower than the one in LEC-educated cells. In addition to that, we found LEC-educated cells at a higher percentage (out of live cells) in the LN, compared to the spleen, whereas mDC-educated cells appeared at higher levels in the spleen. We attributed this finding to the early time point following the challenge as well as to the different homing properties that we previously described, since the

fold increase in expansion was similar in both organs. We also noticed that LEC-educated cells were detected at lower numbers in both the spleen and the LN in the mice that did not receive the antigen recall, suggesting that LEC-educated $CD8^+$ T cells might not engraft as well as their mDC-educated counterparts upon *in vivo* transfer.

Along with the vigorous expansion, and in agreement with our *in vitro* observations, LEC-educated $CD8^+$ T cells also exhibited functional potential, inducing the expression of cytokines. Upon *ex vivo* restimulation, we noted increased production of IFN-γ and TNF-α upon recall (Fig. 3.6D, E), and the transferred cells acquired effector function expressing GzB (Fig. 3.6E, right), and being capable of direct specific cytolysis (Fig. 3.6F). mDC-educated $CD8^+$ T cells displayed greater potency in specific killing, similar to what we observed *in vitro*.

Next, we sought to assess the survival properties of LEC-educated $CD8^+$ T cells in the absence of antigen encounter and confirm their expansion capacity in this setting. To this end, we let the mice rest for more than five weeks before we administered OVA+LPS. Yet, LEC-educated cells were able to expand (Fig. 3.6G) showing more than a 2-fold increase, while their mDC-educated counterparts displayed a 4-fold expansion in the LN. Furthermore, LEC-educated $CD8^+$ T cells generated effector-like cells after the challenge with the majority of the detected cells being $CD62L^-$ (Fig. 3.6H, I). The phenotype of LEC-educated cells upon recall appeared similar to the one of mDC-educated cells, however, they still maintained a clear $CD44^+CD62L^+$ subset (Fig. 3.6H). Indeed, the percentage of $CD44^+CD62L^-$ effector/memory effector cells in the LN and spleen was about 60% in LEC-educated upon recall, yet significantly lower to the one of mDC-educated that displayed about 80% effector cells (Fig. 3.6I, left). This was better illustrated by assessing the ratio of T_{CM} ($CD44^+CD62L^+$) over T_{eff} ($CD44^+CD62L^-$); The ratio was lower than one in LEC-educated cells, manifesting the polarization versus an effector phenotype after recall, but still significantly higher than the relative ratio in mDC-educated cells (Fig. 3.6I, middle). Additionally, LEC-educated and mDC-educated cells displayed similar levels of short-lived effector cells (T_{SLEC}, KLRG-1^+CD127^-) with a trend for more T_{SLEC} in mDC-educated cells in the spleen, where the T_{SLEC} subset was the predominant one for both populations (Fig. 3.6H, I, left). There were also no significant differences observed between the two populations with regard to the memory precursor effector subset (T_{MPEC}, KLRG-1^-CD127^+).

Taken together, these data confirm the ability of LEC-educated $CD8^+$ T cells to proliferate and differentiate into functional effectors that produce cytokines and display specific killing activity upon antigen re-encounter in an inflammatory setting *in vivo*. The ability of antigen-experienced T cells to undergo rapid recall responses upon antigen reexposure constitutes a hallmark of immunological memory, allowing for protective immunity.

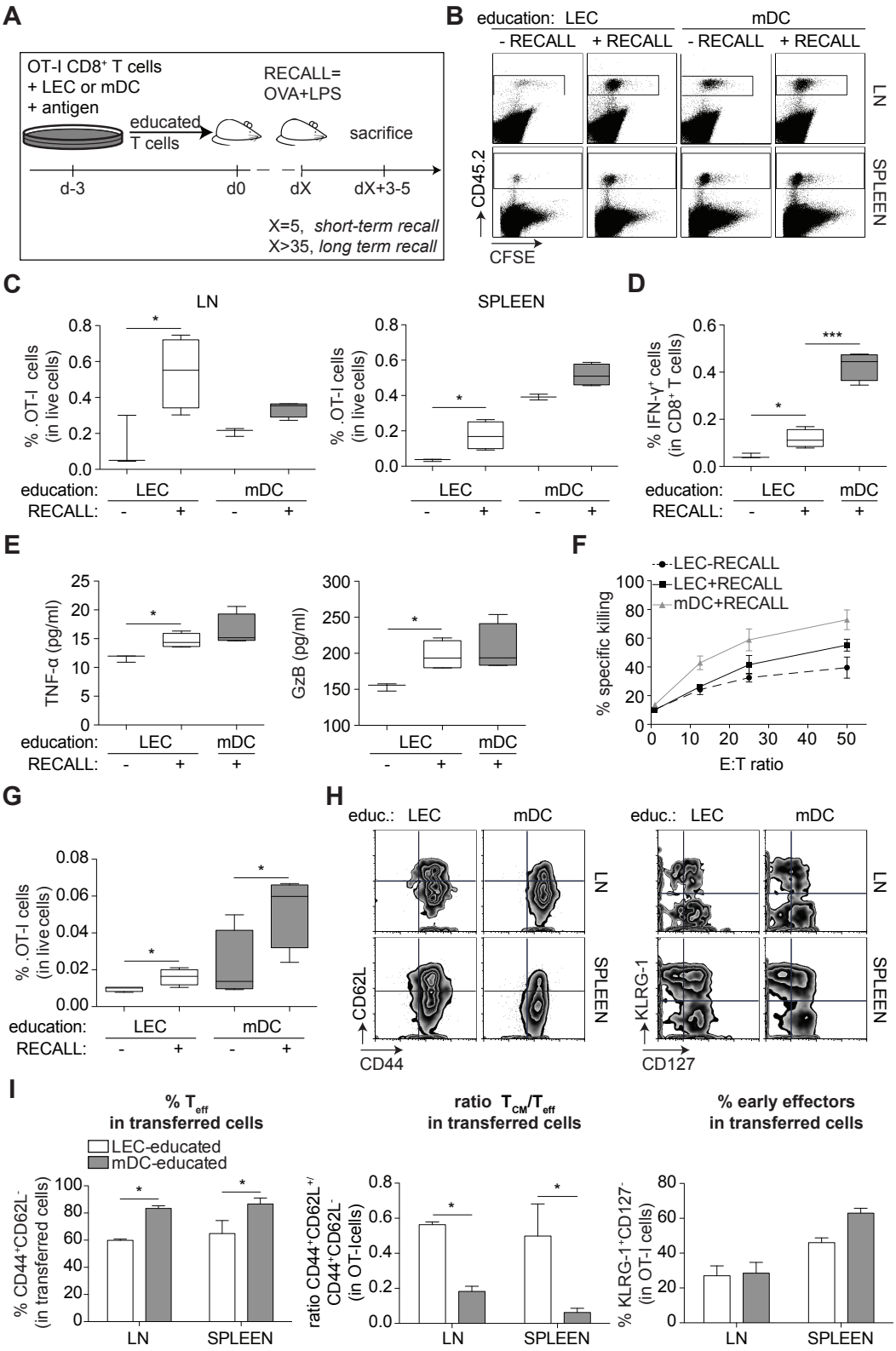

Figure 3.6 LEC-educated CD8$^+$ T cells expand rapidly upon short and long-term antigen re-encounter *in vivo* and differentiate into effector CTLs upon recall. *Ex vivo* generated LEC/mDC-educated OT-I cells (CD45.2$^+$) were CFSE-labeled and transferred in C57/Bl6 mice (CD45.1$^+$). Two days (short-term recall) or at least 5 weeks (long-term recall) after transfer, mice were administered

(+recall) OVA+LPS, or not (- recall), and sacrificed 3-5 days after challenge. Cell suspensions of the spleen and skin-dLNs were generated and analyzed by flow cytometry. **(A)** Experimental timeline. LEC-educated $CD8^+$ T cells proliferate rapidly and expand when they re-encounter the antigen *in vivo*. **(B)** Representative dot plots with CD45.2 on y-axis and CFSE on x-axis in spleen and LN 3 days after short-term recall. **(C)** Percentage of OT-I cells (gated on live cells) in LN (left) and spleen (right). **(D)** Percentage of IFN-γ^+ cells (gated on $CD8^+$ T cells) after short-term recall, following 5h *ex vivo* restimulation. **(E)** TNF-α (left) and GzB (right) detected in the supernatant (pg/ml) after 3-day *ex vivo* restimulation. **(F)** LEC-educated $CD8^+$ T cells display higher levels of specific killing activity after recall. 3 days after short-term recall, spleen cell suspensions were cultured on top of splenocytes loaded with SIINFEKL or non-congenic peptide for 16-20h at different effector to target ratios to assess killing activity. Percent specific killing in LEC-educated that received (black line) or not (black dotted line) the recall vaccine versus mDC-educated cells after recall (grey line). Even after prolonged absence of the antigen, LEC-educated $CD8^+$ T cells survive and display effector phenotype when they re-encounter the antigen *in vivo*. More than 5 weeks (long-term recall) after transfer, mice were challenged with OVA+LPS and sacrificed 5 days later. **(G)** Percentage of OT-I cells (gated on live cells) in LN. LEC-educated $CD8^+$ T cells generate T_{eff}-like cells after challenge with the majority of cells being $CD62L^-$. **(H)** Representative dot plots of LEC/mDC-educated cells displaying CD44 on x-axis and CD62L on y-axis (right), or CD127 on x-axis and KLRG-1 on y-axis (left) in LN and spleen. **(I)** From left to right: percentage of T_{eff} ($CD44^+CD62L^-$), ratio of T_{CM} ($CD44^+CD62L^+$) over T_{eff} ($CD44^+CD62L^-$) and percentage of early short-lived effector cell ($KLRG\text{-}1^+CD127^-$) in OT-I cells in LN and spleen. Representative data from one of two independent experiments (n=3-4). *p≤0.05, ***p≤0.001 by two-tailed unpaired Student's t test (C-E, G) or by one-way ANOVA followed by Bonferroni posttest (F, I).

LEC-educated $CD8^+$ T cells not only contribute to anti-infectious protection but also preserve a secondary memory persistent population

Our findings raised the question whether LEC-educated $CD8^+$ T cells can mediate protective immunity. Therefore, we sought to assess their contribution to immune responses against a real pathogen as well as evaluate their protective ability in direct competition to mDC-educated T cells. To this end, we co-transferred *ex vivo* generated LEC-educated OT-I $CD8^+$ T cells together with mDC-educated cells in mice at a 1:1 ratio. We let the mice rest for five weeks and then, we challenged the mice with *Listeria Monocytogenes* (*L.m.*)-expressing OVA (Fig. 3.7A). Tracking the transferred cells in the blood at different time points after bacterial infection, we noticed that LEC-educated $CD8^+$ T cells expanded after challenge with a 15-20–fold increase, as a percentage of total $CD8^+$ T cells, from day 4 to day 6 or day 8 (Fig. 3.7B). mDC-educated $CD8^+$ T cells exhibited a greater expansion in the blood during the same time period. We also detected slightly higher numbers of mDC-educated $CD8^+$ T cells in the spleen on day 8 after challenge (Fig. 3.7C), while the two populations were detected at similar levels in the LN (Fig. 3.13A). Both populations appeared at much lower numbers in the LN, which was expected at this time point since *L.m.*-OVA infection acts primarily in the spleen and liver. Most importantly, LEC-educated cells exhibited effector function with cytotoxic potential, since they expressed cytokines (Fig. 3.7D, 7E and Fig. 3.13B) and underwent cytolytic granule release. More specifically, upon *ex vivo* restimulation, LEC-educated $CD8^+$ T cells displayed similar levels of IFN-γ (Fig. 3.7E), as well as TNF-α and IL-2 (Fig. 3.13B), with their mDC-educated counterparts and they were on par in the expression of CD107, a marker of cytolytic granule exocytosis (Fig. 3.7E) in the spleen. By assessing the percentage of single, double or triple positive cells for IFN-γ, TNF-α and IL-2 in order to evaluate the polyfunctionality of the cells, we observed a similar distribution between the two populations (Fig. 3.7F). In LEC-educated cells, we detected a dominant subset of cells positive for one of the three cytokines (42.18±5.35), a subset of cells positive for two of the three cytokines (30.37±6.25), a smaller subset of triple positive cells (2.85±0.60), while 25.11% (±6.75) of the cells

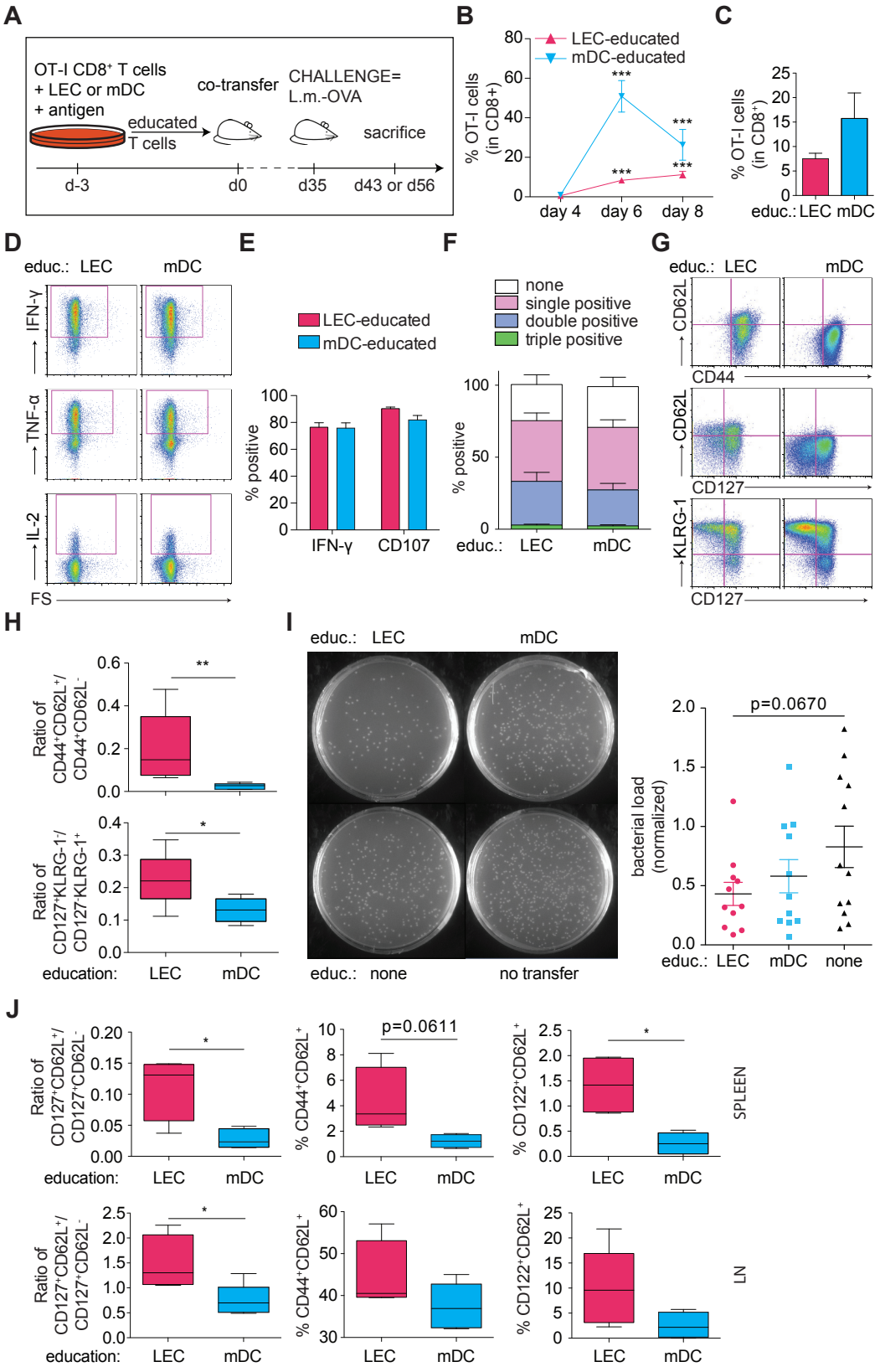

Figure 3.7 LEC-educated CD8$^+$ T cells can participate in anti-infectious immunity and might give rise to a persistent secondary-memory population. To evaluate the functional potential of LEC-educated CD8$^+$ T cells, we assessed expansion, phenotype and functionality after bacterial pathogen encounter, in competition to DC-educated CD8$^+$ T cells. *Ex vivo* generated (CD45.1.2) LEC-educated

together with (CD45.1) DC-educated OT-I $CD8^+$ T cells were mixed at 1:1 ratio and transferred in C57/Bl6 mice ($5x10^4$ total cells/mouse). 5 weeks after, mice were i.v. challenged with *L.m.*-OVA (10^3 cfu) and sacrificed either on day 8 or 3 weeks after. Cell suspensions of the spleen were generated and analyzed by flow cytometry. **(A)** Experimental timeline. LEC-educated $CD8^+$ T cells expand after challenge. **(B)** Percentage of OT-I cells (gated on $CD8^+$ T cells) in blood on day 4, 6 and 8 following infection. **(C)** Percentage of OT-I cells (gated on $CD8^+$ T cells) in spleen on day 8 after infection. LEC-educated $CD8^+$ T cells can induce cytokines and cytolysis-related molecules at levels similar to mDC-educated $CD8^+$ T cells. **(D)** Representative dot plots of OT-I cells in spleen showing IFN-γ (top plots), TNF-α (middle plots) and IL-2 (bottom plots) on y-axis and forward scatter on x-axis upon 5h *ex vivo* restimulation. **(E)** Percentage of IFN-γ^+ and $CD107^+$ cells (gated on OT-I cells) in spleen. **(F)** Percentage of single, double, triple positive cells for IFN-γ, TNF-α, and IL-2 in spleen. On day 8 after infection, most LEC-educated $CD8^+$ T cells display effector phenotype , as well as a T_{CM}-like subset at levels higher compared to mDC-educated cells. **(G)** Representative dot plots of OT-I cells displaying CD62L on y-axis and CD44 on x-axis (top), CD62L on y-axis and CD127 on x-axis (middle) and KLRG-1 on y-axis and CD127 on x-axis (bottom) in spleen. **(H)** Ratio of T_{CM} ($CD44^+CD62L^+$) over T_{eff} ($CD44^+CD62L^-$) cells (top) and ratio of short-lived effector cells ($CD44^+CD127^-KLRG1^+$) over memory precursor effector cells ($CD44^+CD127^+KLRG1^-$) in OT-I cells in spleen. LEC-educated $CD8^+$ T cells not only contribute to CTL generation against infectious pathogens but also control bacterial load. *Ex vivo* generated LEC-educated or mDC-educated or naïve OT-I $CD8^+$ T cells were transferred in C57/Bl6 mice ($5x10^4$ total cells/mouse). Mice that did not receive any cells served as positive control (no transfer). 9 weeks after, mice were i.v. challenged with *L.m.*-OVA (10^4 cfu/mouse) and sacrificed 3 days later. Spleens were collected, homogenized and resuspended in sterile PBS. Different dilutions of the cell suspensions were generated, plated on BHI plates and incubated overnight at 37°C. The day after, cfu were counted and the amounts of *L.m.*-OVA were calculated with respect to the relative dilutions. **(I)** Left, representative images of bacterial culture plates for the differentially educated cells. Right, bacterial burden in spleen; the number of cfu in each group normalized to the one in the "no transfer" group. LEC-educated $CD8^+$ T cells may give rise to a persistent memory subset upon challenge. To evaluate the formation of secondary memory, we assessed the expression of phenotypic markers in OT-I cells 3 weeks after challenge. **(J)** From left to right: ratio of T_{CM} ($CD44^+CD127^+CD62L^+$) over T_{EM} ($CD44^+CD127^+CD62L^-$) cells, percentage of T_{CM} ($CD44^+CD62L^+$) cells, percentage of $CD122^+CD62L^+$ cells, in OT-I cells in the spleen (top) and LN (bottom). Pooled data from two independent experiments (B-I, n=10) or data from one experiment (J, n=5). *p≤0.05, **p≤0.01, ***p≤0.001 by one-way ANOVA (B) or by two-way ANOVA (F) followed by Bonferroni posttest or by two-tailed unpaired Student's t test (C, E, H-J).

did not produce any cytokine. Interestingly, there was a trend for a greater subset of double positive and triple positive cells (p=0.07) in LEC-educated compared to mDC-educated. Furthermore, by assessing the actual cell number of the same subsets in LEC/mDC-educated cells, we observed a trend for more of the double positive cells in LEC-educated cells (Fig. 3.13C), suggesting that after *ex vivo* restimulation, LEC-educated cells might generate more of the polyfunctional effector cells in absolute numbers.

In agreement with our findings following *in vivo* antigen administration, on day 8 after pathogen infection, the majority of LEC-educated $CD8^+$ T cells displayed a predominant effector phenotype (Fig. 3.7G, H). Most of the cells exhibited low levels of CD62L ($CD44^+CD62L^-$, $CD127^{+/-}$) and analyzing their distribution with respect to KLRG-1 and CD127, the majority of cells were found in the T_{SLEC} ($KLRG\text{-}1^+CD127^-$) subset. Remarkably, we also identified a noteworthy T_{CM}-like ($CD44^+CD62L^+$) subset in LEC-educated cells at the peak of the immune response. Evaluating the ratio of T_{CM} ($CD44^+CD62L^+$) over T_{eff} ($CD44^+CD62L^-$), we remarked a consistent trend for this ratio to be significantly higher in LEC-educated cells than in mDC-educated cells (Fig. 3.7H, top). Along the same lines, the ratio of T_{MPEC} ($KLRG\text{-}1^-CD127^+$) over T_{SLEC} ($KLRG\text{-}1^+CD127^-$) was enhanced in the LEC-educated population compared to the relative ratio in DC-educated cells. Similar trends were observed in the LN (Fig. 3.13D).

Most importantly, LEC-educated $CD8^+$ T cells not only contributed to the generation of effector CTLs against infectious pathogens but also controlled the bacterial load during infection with *L.m.*-OVA (Fig. 3.7I). To assess the protective capacity of LEC-

educated cells, we adoptively transferred *ex vivo* generated (CD45.1.2) LEC-educated or mDC-educated or naïve OT-I $CD8^+$ T cells. Mice that did not receive any cells served as a positive control (no transfer). Nine weeks after, we challenged the mice with a high dose of *L.m.*-OVA and sacrificed them three days later to assess bacterial burden in the spleen. LEC-educated $CD8^+$ T cells exhibited a trend for lower bacterial load compared to control mice, allowing for protection. Surprisingly, they also appeared to display greater protective capacity compared to mDC-educated cells, although the difference was not statistically significant. This might be attributed to the generation of greater numbers of polyfunctional effector cells in LEC-educated $CD8^+$ T cells and it might be associated with the less differentiated state of the cells compared to the mDC-educated ones.

The observation that LEC-educated $CD8^+$ T cells manifested a persistent T_{CM}-like ($CD44^+CD62L^+$) population at the peak of the infection raised the question whether LEC-educated cells might not only generate effector cells upon challenge but also give rise to a secondary T_{CM}-like subset. In order to evaluate the establishment of a secondary T_{CM} subset in LEC-educated $CD8^+$ T cells, we assessed the expression of different phenotypic markers three weeks after the *L.m.*-OVA challenge in the spleen and LN, while we also tracked the transferred cells in the blood during this time. We observed that already between day 7 and day 9, the percentage of $CD44^+CD62L^+$ cells in the blood significantly increased in LEC-educated cells, with the subset being always greater than the relative one in mDC-educated cells (Fig. 3.13E, F). Interestingly, during this time period, the percentage of cytotoxic effector-like cells ($CD44^+GzB^+$) in the blood gradually decreased at the same rate between LEC and mDC-educated cells (Fig. 3.13F). This suggested that the increase in $CD44^+CD62L^+$ cells might be subset-specific and not an overall population trend. Furthermore, LEC-educated cells in the spleen and the LN, presented a higher T_{CM} ($CD127^+CD62L^+$) to T_{EM} ($CD127^+CD62L^-$) ratio at this time point (Fig. 3.7J). Actually, this ratio was greater in the LN, where T_{CM} cells preferentially home, with the T_{CM} subset being the principal among antigen-experienced cells. We observed similar trends for the ratio of T_{CM} over T_{Eff} as well as the ratio of T_{MPEC} over T_{SLEC} (Fig. 3.13G). In addition to that, there was a noticeable trend for a larger subset of $CD44^+CD62L^+$ in LEC-educated compared to mDC-educated while the subset of $CD44^+CD62L^+$ cells that also expressed CD122 was significantly higher in LEC-educated cells both in LN and spleen. These data are consistent with our hypothesis that LEC-educated $CD8^+$ T cells might also favor the maintenance of a secondary central memory-like subset following reactivation.

Overall, our findings indicate that LEC-educated $CD8^+$ T cells can participate in protective immunity, being at least equally potent to mDC-educated cells in fighting the infection. Additionally, memory-like LEC-educated $CD8^+$ T cells might display self-renewing capacity, giving rise to a secondary memory persistent population.

LN LEC-educated $CD8^+$ T cells require CD28 costimulation and proinflammatory signals in order to generate polyfunctional effector cells

Finally, we sought to determine the necessary signals for functional reactivation of LEC-educated $CD8^+$ T cells. To this end, we replaced mDCs from our previous studies with an artificial APC system and assessed the response of LEC- educated

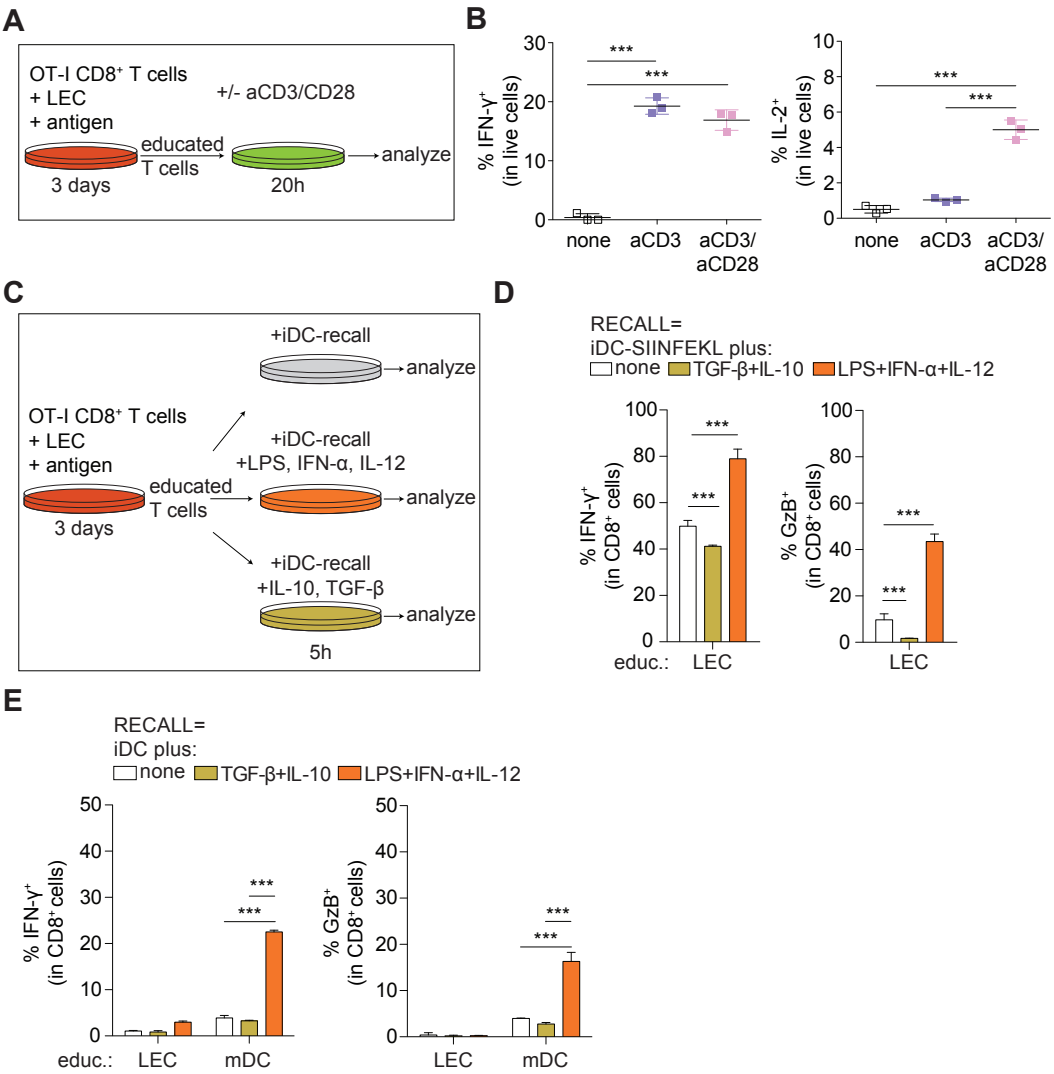

Figure 3.8 LN LEC-educated CD8$^+$ T cells need to be reactivated in the presence of CD28 costimulation and proinflammatory signals in order to generate functional effector cells. To determine the required signals for functional reactivation of LEC-educated CD8$^+$ T cells, we assessed their response upon stimulation with an artificial APC, aCD3/CD28 system. OT-I CD8$^+$ T cells were cultured in the presence of NPssCOVA$_{250-264}$ (1nM) with LN LEC for 3 days (education). LEC-educated CD8$^+$ T cells were then harvested, washed and cultured in the presence or absence of plate-bound anti-CD3 (5µg/ml) and soluble anti-CD28 (2µg/ml). **(A)** Schematic of the assay. LEC-educated cells fail to induce polyfunctional effectors in the absence of costimulation. **(B)** From left to right: percentage of IFN-γ$^+$ and IL-2$^+$ cells (gated on live cells) after 20h restimulation, as determined by intracellular staining followed by flow cytometric analysis. To evaluate the physiological conditions under which LEC-educated CD8$^+$ T cells may give rise to CTLs, we assessed their response following reactivation with immature DCs (iDCs) loaded with SIINFEKL (iDC-recall), in the presence or absence of different immunogenic (LPS, IFN-α and IL-12) or immunosuppressive (IL-10 and TGF-β) molecules or none of the aforementioned for 5h. **(C)** Schematic of the assay. Reactivated LEC-educated CD8$^+$ T cells give rise to cytotoxic effectors only when reactivation takes place under inflammatory conditions. **(D)** From left to right: percentage of IFN-γ$^+$ and GzB$^+$ positive cells (gated on CD8$^+$ cells) after reactivation with iDCs loaded with SIINFEKL. **(E)** From left to right: percentage of IFN-γ$^+$ and GzB$^+$ cells (gated on CD8$^+$ cells) after 5h reactivation with iDCs in the absence of SIINFEKL. The data are representative from one of two independent experiments (n=3-4). ***p≤0.001 using two-way ANOVA followed by Bonferroni posttest.

cells upon anti-CD3/CD28 stimulation. *Ex vivo* generated LEC-educated CD8$^+$ T cells were cultured in the presence or absence of plate-bound anti-CD3 and soluble anti-CD28 (Fig. 3.8A). LEC-educated CD8$^+$ T cells that were stimulated neither with anti-

CD3 nor with anti-CD28 (none) served as controls. After 20h, we observed that anti-CD3 stimulation alone was enough to induce IFN-γ production, however, both anti-CD3 and anti-CD28 were required to induce polyfunctional IFN-γ and IL-2 producing cells (Fig. 3.8B).

We moved forward to investigate the physiological conditions under which LEC-educated $CD8^+$ T cells might give rise to CTLs. To address this question, we assessed their functional profile following reactivation with immature DCs (iDCs) loaded with antigen in the presence or absence of different immunogenic or immunosuppressive molecules. LEC/mDC-educated $CD8^+$ T cells were cultured together with iDCs (iDC-recall), bearing or not the SIINFEKL peptide, in the presence of either LPS together with IFN-α and IL-12 or IL-10 together with TGF-β, or none of the aforementioned (Fig. 3.8C). Interestingly, reactivated LEC-educated $CD8^+$ T cells gave rise to cytotoxic effectors only when reactivation took place under inflammatory conditions (LPS+IFN-α+IL-12) (Fig. 3.8D). In contrast, they failed to induce functional effectors in a more suppressive setting (IL-10+TGF-β), as indicated by the lower levels of IFN-γ and the absence of GzB production. mDC-educated $CD8^+$ T cells that were restimulated under the same conditions displayed similar trends; we observed decreased levels of effector cytokines in the presence of immunosuppressive molecules. However, the effect of the different treatments was much more pronounced in LEC-educated $CD8^+$ T cells, which required proinflammatory cytokines in order to induce effectors producing noticeable levels of GzB. Importantly, restimulation with iDCs in the absence of the cognate peptide failed to induce significant levels of IFN-γ or GzB production in LEC-educated $CD8^+$ T cells under any of the conditions described above. On the contrary, LPS with IFN-α and IL-12 stimulation was enough to induce both IFN-γ and GzB in mDC-educated $CD8^+$ T cells, similar to conventional memory cells (Fig. 3.8E). Our observations suggest that LEC-educated $CD8^+$ T cells might display a higher threshold of reactivation compared to conventional memory cells in order to display effector function.

3.4 Discussion

Recently, there has been mounting evidence on the active involvement of the lymphatic system in the regulation of immune responses. In addition to expressing self-antigens or scavenging and cross-presenting exogenous antigens on MHC I for the maintenance of peripheral tolerance, this study highlights a previously unanticipated role for LECs in immunomodulation: the generation of antigen-experienced $CD8^+$ T cells, which survive in an inactive state but can escape and be functional upon antigenic inflammatory challenge.

The temporarily inert state of LEC-educated $CD8^+$ T cells can be interpreted as an indication of tolerance or senescence and may act as a tolerizing mechanism against self-reactive T cells [Chapter 2 and (11)]. Our current findings do not challenge this notion but rather put it in a different perspective. We propose a model in which LECs constantly sample peripheral antigens present in the lymph, of both self and foreign origin. LECs then educate naïve antigen-specific $CD8^+$ T cells to remain silent as apoptotic or dysfunctionally activated effectors, but also as surviving memory-like cells. This is until they are re-activated by professional APCs in the presence of

danger signals and/or proinflammatory cytokines. In this broader perspective, LN LECs can contribute to the maintenance of peripheral tolerance without eliminating antigen-specific $CD8^+$ T cells from the T cell repertoire.

The generation of antigen-experienced $CD8^+$ T cells by LECs introduces the possibility that LECs may also participate in the induction of immunological memory. The ability of non-hematopoietic APCs to induce the formation of memory has been reported in an earlier study (50). The generation and persistence of long-lived immunological memory, which can provide life-long protection against pathogens is one of the hallmarks of adaptive immunity. It is intriguing to speculate that along with professional APCs, LECs educate $CD8^+$ T cells to further supplement the memory pool following pathogenic infection.

Our findings support this possibility, as LEC-educated $CD8^+$ T cells displayed diverse molecules related to the development of T_{CM} cells, such as CD62L, CD127 (IL-7R), CD122 (IL-2Rβ), CCR7, CD27, LFA-1 and CXCR3 (Fig. 3.3). The relative expression of some of the transcriptional regulators that are known to balance effector versus memory $CD8^+$ T-cell development (51, 52), such as T-bet and Eomes, was also in favor of a T_{CM}-like differentiation state in LEC-educated cells.

Apart from the phenotypic and molecular characteristics, LEC-educated $CD8^+$ T cells also manifested functional properties of T_{CM} cells. Behaving similar to T_{CM} cells, in accordance with their $CD62L^{hi}$ phenotype, they preferentially migrated to secondary lymphoid organs (LN, spleen), in which they mainly preserved their $CD44^+CD62L^+$ memory-like phenotype (Fig. 3.4B-D). In addition to the specific homing pattern, we also observed that LEC-educated $CD8^+$ T cells resided to particular locations inside the LN (Fig. 3.4E), distinct from naive cells, in which $CD8^+$ T_{CM} cells have been previously described to localize (48, 49): in the outermost regions of medullary, interfollicular, and subcapsular areas and beneath B cell follicles, at sites with potential direct contact with lymph-borne pathogens or infected cells under stready-state (48) and/or during infection (48, 49). Interestingly, regulation of this localization pattern involved signalling via CXCR3 expressed on T_{CM} cells (48, 49), a chemokine receptor also expressed in LEC-educated $CD8^+$ T cells (Fig. 3.3).

The ability to produce IL-2 is a well-established functional characteristic of central memory T cells (34, 46, 53). Consistent with this, LEC-educated $CD8^+$ T cells mounted proliferative responses and produced increased levels of IL-2 upon secondary stimulation *in vitro* (Fig. 3.5B-C). This was also in agreement with our *in vivo* data showing that LNSC-education might be involved in the induction of IL-2 – producing cells (Fig. 3.1F-G). Furthermore, *ex vivo* generated LN FRC-educated $CD8^+$ T cells, which also displayed a $CD44^+CD62L^+$ phenotype, however less polarized towards the T_{CM} subset with lower levels of CD62L (Fig. 3.14A, B), failed to produce cytokines at levels similar to LEC-educated ones following reactivation (Fig. 3.14C, D). *In vivo* inflammatory antigenic stimulation confirmed our *in vitro* findings and LEC-educated $CD8^+$ T cells showed high proliferative and survival capacity, even when they had not encountered the antigen for long periods of time, a key characteristic of memory cells (Fig. 3.6). Most importantly, LEC-educated $CD8^+$ T cell generated highly potent CTL effectors following pathogenic challenge with *L.m.*-OVA (Fig. 3.7B-F) and controlled the bacterial load providing protection to the host (Fig. 3.7I). Interestingly, LEC-educated $CD8^+$ T cells also appeared to sustain a persistent

secondary T_{CM}-like population indicating that they may display self-renewing capacity (Fig. 3.7G-H, J and Fig. 3.13E-G).

It follows that LEC-educated $CD8^+$ T cells also displayed expression of molecules that are known to characterize the T_{SCM} subset (Fig. 3.3), such as Sca-1, Bcl-2 and CD95 (44, 45, 54). T_{SCM} cells share a lot of characteristics with naïve cells but they also have properties of antigen-experienced cells. More importanly, they can self-renew and further differentiate into T_{CM} and T_{EM} cells (44). We observed that LEC-educated $CD8^+$ T cells underwent homeostatic turnover and displayed increased survival in response to IL-15 stimulation *in vitro* (Fig. 3.15B), an attribute of both T_{CM} and T_{SCM} cells (44, 55, 56). In contrast, $T_{eff/EM}$-like, mDC-educated cells showed lower sensitivity to IL-15 signaling. Interestingly, following IL-15 dependent proliferation, LEC-educated cells retained their initial $CD44^{hi}CD62L^{hi}$ phenotype (Fig. 3.15C), which may indicate self-renewal capacity, whereas mDC-educated ones did not enhance their relative subset. Aditionally, Cieri et al. recently demonstrated the generation of T cells resembling the T_{SCM} population by activating naive T cells with anti-CD3 and anti-CD28 antibody-conjugated beads in the presence of low doses of IL-7 and IL-15 (57), which are also produced by LN LECs.

Nevertheless, the T_{SCM} subset in mice has been only described in the setting of chronic antigen exposure (graft-versus-host disease, GVHD) (45) and it has not been yet identified in a traditional infection model. Instead, Graef et al. have recently demonstrated, conducting a set of very elegant serial single-cell adoptive transfer experiments, that adult tissue stem cells reside within the $CD62L^+CD44^+$ T_{CM} cell subset (58). The T_{CM} cells described in this study and ascribed stemness, displayed a similar phenotypic profile to LEC-educated $CD8^+$ T cells being positive for CXCR3, CD122, CD27, CD127, T-bet and Eomes. Further studies should be performed to determine whether LEC-educated $CD8^+$ T cells can exhibit multipotency and self-renewal potential at the level of individual cells.

The traditional model of $CD8^+$ T cell differentiation dictates that, following pathogen elimination, a small percentage of antigen-specific $CD8^+$ T cells survives to form the memory pool (59-61). Alternatively, the developmental model suggests that memory cells can arise directly from naive cells based on signal strength and the extent of activation (52, 62, 63). This model includes the generation of antigen-specific $CD8^+$ T cells with a wide spectrum of differentiation states.

Along this spectrum, cell differentiation and the acquisition of effector function are accompanied by the gradual loss of memory potential and longevity, leading eventually to senescence (52, 63). The unique differentiation state of LEC-educated $CD8^+$ T cells finds its place in the intermediate range of the two extremes, that being T_{SCM}/T_{CM} cells and terminal effector T cells: LEC-educated $CD8^+$ T cells appeared to be in a more differentiated position than T_{SCM} cells, since they expressed CD44, while they also evidently differed from mDC-educated $CD8^+$ T which displayed characteristics closer to an effector profile (Fig. 3.3).

The divergence in differentiation states reflects the conditions under which $CD8^+$ T cells are educated by LECs compared to those by professional APCs, such as mDCs. This is apparent in the molecular interactions between APCs and $CD8^+$ T cells, such as the LEC education under low costimulation coupled with inhibitory signaling via the PD-L1 – PD-1 pathway [Chapter 2 and (7, 11)]. Antigenic

stimulation in the absence of costimulatory signals is traditionally considered to induce a tolerogenic outcome (23, 53). Besides costimulation, a variety of signals, including the strength of TCR, the duration of antigen exposure, the type of APCs, cytokines and many more factors regulate the outcome of T cell differentiation (64-67). For instance, it has been shown that high levels of TCR stimulation can overcome the requirement for costimulation in the induction of efficient $CD8^+$ T cell responses and the generation of memory (68).

Furthermore, the conditions during LEC-education, as described above, may relate to the setting of reduced inflammatory signaling. Transient inflammation has been correlated to favoring a memory rather than terminal effector differentiation; IL-12 is a key regulator of effector T cell generation and can negatively regulate memory generation (25, 26) while low levels of IL-2 during priming have been associated with the induction of a memory rather than effector phenotype (27, 69). LEC-educated $CD8^+$ T cells produce very low amounts of cytokines (IFN-γ, IL-2), as detected in the supernatant of LEC-$CD8^+$ T cell cocultures [Chapter 2 and (11)], in which we have also failed to detect significant levels of IL-12 (data not shown). Moreover, $CD25^{low}$ $CD8^+$ T cells have been shown to preferentially upregulate CD127 and CD62L generating long-lived memory cells (28). LEC-educated $CD8^+$ T cells express CD25, though at lower levels compared to their DC-educated counterparts [Chapter 2 and (11)].

Two cytokines, which are well known for mediating survival and self-renewal of memory $CD8^+$ T cells, IL-7 and IL-15, have been previously shown to support the preferential generation of functional T_{CM} (69, 70). While we are currently trying to evaluate their production by qPCR analysis, as we have not detected significant secreted amounts of IL-7 and IL-15 in the supernatant of LEC-$CD8^+$ T cell cocultures (Fig. 3.10B), LN LECs have been demonstrated to be a primary source of IL-7, in human and mouse LNs, as well as IL-15, under steady-state and/or inflammatory conditions (71-74). All the above suggest that the conditions during LEC-education may support the generation of memory cells and thus, endorse our observations for the T_{CM}-like differentiation state of LEC-educated $CD8^+$ T cells.

It is important to note that we observed an evident heterogeneity within the mDC-educated population, displaying different levels of CD62L, similar to what has been previously demonstrated for mature DCs in the context of infectious inflammation generating a wide range of T cell subsets (52, 75). This may further explain some of the discrepancies in the expression of different phenotypic markers. However, the observed variation may be also related to the heterogeneity of the *in vitro* generated BMDC population itself (76). Nevertheless, the phenotypic and functional characteristics of LEC- and mDC-educated $CD8^+$ T cells reflect distinct differentiation states, with the former approaching more T_{CM} cells and the latter $T_{eff/EM}$.

LEC-educated $CD8^+$ T cells do not replace, but add diversity to the memory T cell states. As much as they have in common, they differ in some functional properties of conventional T_{CM} cells. Conventional T_{CM} cells are known to produce IFN-γ upon stimulation with IL-12 (or IL-18) in the absence of antigen-specific TCR stimulation, as a bystander effect during inflammation (77-79). By contrast, LEC-educated $CD8^+$ T cells failed to do so and instead, required the combination of TCR cross-linking, costimulatory signals and proinflammatory cytokines to generate functional effector

cells (Fig. 3.8). Although the need for CD28-mediated costimulation to induce memory recall responses has been under debate (68), our findings suggest that LEC-educated $CD8^+$ T cells have a stricter threshold of reactivation and they appear to require all three signals, similar to naïve cells, to display effector function. Further mechanistic studies should be performed to quantify the reactivation threshold requirements in LEC-educated versus conventional T_{CM} cells. Along the same lines, LSEC cross-primed $CD8^+$ T cells required combinatorial signaling via TCR, CD28 and IL-12 to exhibit functional effector function (17). In the setting of the iFABP-tOVA mouse model, in which $CD8^+$ T cells are tolerized to OVA, OVA-specific OTI-I $CD8^+$ T cells were reactivated upon VSV-OVA infection and the amount of antigen as well as the presence of virally-induced inflammatory signaling dictated the outcome of the reactivation (16). Such stringent prerequisites to reactivation may safeguard undesired reactions and restrict the harmful prospect of autoimmunity.

At least two scenarios can be imagined for these antigen recognizing LEC-educated $CD8^+$ T_{CM}-like cells. They may be very important in containing systemic spread of antigen before innate immunity kicks in. Both viral and bacterial pathogens employ different strategies to avoid detection by the innate immune system, which can result in serious disease (80). Therefore, LEC-education may act as a reserve mechanism that spares pathogen-specific T cells in the absence of inflammation, while contributing to self-tolerance. A very similar function has been recently suggested for $CD8^+$ T cells cross-primed by LSEC that share many common characteristics as non-professional APCs with LECs (17).

In addition, LEC-education may act as an early trigger for the generation of antigen-experienced $CD8^+$ T cells following an infection. Antigens arrive to the LN much earlier than the migrating DCs bearing the antigen. Early after vaccinia virus (VV) or vesicular stomatitis virus (VSV) infection, virions were reported to drain to the LN and infect cells resident in the SC region (50, 81), close to the interfollicular ridges, at the same location in which viral antigen was found to be archived in LECs (36). Being situated in one of the prime anatomical sites for antigen sampling, LECs may provide a supplementary pool of antigen-experienced T cells, awaiting to expand following interaction with professional APCs. When LNSCs could not participate in antigen presentation, we observed a significant decrease in $CD8^+$ T cell proliferation, indicating that LECs may significantly contribute to the expansion of $CD8^+$ T cells in an antigen-specific manner. Previous reports have also highlighted the contribution of antigen presentation by non-hematopoietic stromal cells in $CD8^+$ T cell immune responses (50, 82, 83). Along with the pathogenic stimuli, differences in kinetics of the infection model as well as other parameters may balance antigen presentation by professional APCs versus LECs. In line with our hypothesis for an early trigger, radioresistant stromal cells were able to induce recruitment and activation of naïve T cells during the early stages of VV-OVA, VSV-OVA and *L.m.*-OVA infection, even though their sustained expansion examined at later time points was markedly limited (82).

These differentiation states and the strict reactivation requirements are also consistent with the tolerizing role of cross-presenting LECs in the tumor stroma and tumor-draining LN, as we previously reported (10). In a VEGF-C-overexpressing tumor model, education by tumor-draining LN LECs resulted in the proliferation of

tumor-specific $CD8^+$ T cells, which were dysfunctional and apoptotic, and thus, promoted tumor growth. Efficient reactivation of LEC-educated $CD8^+$ T cells and subsequent generation of cytotoxic effectors would be quite unlikely due to the strong regulatory factors present in the suppressive microenvironment of the tumor-draining LN. On the contrary, the local microenvironment rather resembles the reactivation, which failed to induce functional IFN-γ and GzB expressing effector cells, as we described earlier in the presence of IL-10 and TGF-β. Alternatively, in the setting of chronic inflammation or following transplants, with the microenvironment being rich in inflammatory cytokines and danger signals, reactivation would likely favor the generation of cytotoxic effectors. Indeed, while still being under debate, lymphangiogenesis has been frequently associated with inflammatory diseases and transplant rejection (84, 85).

Site-specific immune responses and antigen targeting to modulate T cell differentiation fate offer a potential therapeutic benefit in the design of prophylactic and therapeutic vaccines. Thus, a better understanding of the relative importance of $CD8^+$ T cell education by LN LECs as opposed to professional APCs may be useful in identifying novel strategies to advance effective immunomodulation and pathogen-specific immunity. LEC-education may allow the generation of antigen-specific $CD8^+$ T cells with direct acquisition of memory characteristics, specific homing features and the ability to respond to boost immunization. In this context, it may be exploited to enhance protection against infectious pathogens and cancer.

Our findings demonstrate a new role for LN LECs in the modulation of immune responses; exogenous antigen presentation by LN LECs can induce an expandable pool of memory-like T cells, leading to the generation of effector cells under inflammatory conditions to fight an ongoing infection while preserving a subset of long-lived memory cells to combat future pathogen encounter. In addition to the maintenance of peripheral tolerance via presentation of PTAs (7-9) or scavenged exogenous antigens (11) under homeostatic conditions and contact-dependent immunosuppression of APCs (86), LECs can also participate in anti-infectious immunity. Our work reveals the multifaceted function of LEC education and highlights its dynamic role in response to the local microenvironment for the regulation of immunity. These findings also help to explain and reconcile the seemingly contradictory effects of lymphangiogenesis in tumors versus chronic inflammatory diseases or transplants, with lymphangiogenesis being tumor-promoting while at the same time being associated with aggravation of chronic inflammation as well as transplant rejection (84, 85). As we begin to better understand the impact of antigen presentation by LECs in immunomodulation and unravel the various signals implicated, the new challenge that emerges is how we can harness this function to improve protection against pathogens and tumors, or to prevent autoimmunity and transplant rejection.

3.5 References

1. Hirosue, S., and J. Dubrot. 2015. Modes of Antigen Presentation by Lymph Node Stromal Cells and Their Immunological Implications. *Front. Immunol.* 6: 446.
2. Malhotra, D., A. L. Fletcher, and S. J. Turley. 2013. Stromal and hematopoietic cells in secondary lymphoid organs: partners in immunity. *Immunol. Rev.* 251: 160–176.
3. Card, C. M., S. S. Yu, and M. A. Swartz. 2014. Emerging roles of lymphatic endothelium in

regulating adaptive immunity. *J. Clin. Invest.* 124: 943–952.

4. Turley, S. J., A. L. Fletcher, and K. G. Elpek. 2010. The stromal and haematopoietic antigen-presenting cells that reside in secondary lymphoid organs. *Nat. Rev. Immunol.* 10: 813–825.
5. Fletcher, A. L., D. Malhotra, and S. J. Turley. 2011. Lymph node stroma broaden the peripheral tolerance paradigm. *Trends Immunol.* 32: 12–18.
6. Rouhani, S. J., J. D. Eccles, E. F. Tewalt, and V. H. Engelhard. 2014. Regulation of T-cell Tolerance by Lymphatic Endothelial Cells. *J Clin Cell Immunol* 5.
7. Tewalt, E. F., J. N. Cohen, S. J. Rouhani, C. J. Guidi, H. Qiao, S. P. Fahl, M. R. Conaway, T. P. Bender, K. S. Tung, A. T. Vella, A. J. Adler, L. Chen, and V. H. Engelhard. 2012. Lymphatic endothelial cells induce tolerance via PD-L1 and lack of costimulation leading to high-level PD-1 expression on CD8 T cells. *Blood* 120: 4772–4782.
8. Cohen, J. N., C. J. Guidi, E. F. Tewalt, H. Qiao, S. J. Rouhani, A. Ruddell, A. G. Farr, K. S. Tung, and V. H. Engelhard. 2010. Lymph node-resident lymphatic endothelial cells mediate peripheral tolerance via Aire-independent direct antigen presentation. *J. Exp. Med.* 207: 681–688.
9. Fletcher, A. L., V. Lukacs-Kornek, E. D. Reynoso, S. E. Pinner, A. Bellemare-Pelletier, M. S. Curry, A. R. Collier, R. L. Boyd, and S. J. Turley. 2010. Lymph node fibroblastic reticular cells directly present peripheral tissue antigen under steady-state and inflammatory conditions. *J. Exp. Med.* 207: 689–697.
10. Lund, A. W., F. V. Duraes, S. Hirosue, V. R. Raghavan, C. Nembrini, S. N. Thomas, A. Issa, S. Hugues, and M. A. Swartz. 2012. VEGF-C promotes immune tolerance in B16 melanomas and cross-presentation of tumor antigen by lymph node lymphatics. *Cell Rep.* 1: 191–199.
11. Hirosue, S., E. Vokali, V. R. Raghavan, M. Rincon-Restrepo, A. W. Lund, P. Corthésy-Henrioud, F. Capotosti, C. Halin Winter, S. Hugues, and M. A. Swartz. 2014. Steady-state antigen scavenging, cross-presentation, and CD8+ T cell priming: a new role for lymphatic endothelial cells. *The Journal of Immunology* 192: 5002–5011.
12. Steinman, R. M., D. Hawiger, K. Liu, L. Bonifaz, D. Bonnyay, K. Mahnke, T. Iyoda, J. Ravetch, M. Dhodapkar, K. Inaba, and M. Nussenzweig. 2003. Dendritic cell function in vivo during the steady state: a role in peripheral tolerance. *Ann. N.Y. Acad. Sci.* 987: 15–25.
13. Belz, G. T., G. M. N. Behrens, C. M. Smith, J. F. A. P. Miller, C. Jones, K. Lejon, C. G. Fathman, S. N. Mueller, K. Shortman, F. R. Carbone, and W. R. Heath. 2002. The CD8alpha(+) dendritic cell is responsible for inducing peripheral self-tolerance to tissue-associated antigens. *J. Exp. Med.* 196: 1099–1104.
14. Redmond, W. L., and L. A. Sherman. 2005. Peripheral Tolerance of CD8 T Lymphocytes. *Immunity* 22: 275–284.
15. Schietinger, A., J. J. Delrow, R. S. Basom, J. N. Blattman, and P. D. Greenberg. 2012. Rescued Tolerant CD8 T Cells Are Preprogrammed to Reestablish the Tolerant State. *Science* 335: 723–727.
16. Vezys, V., S. Olson, and L. Lefrançois. 2000. Expression of intestine-specific antigen reveals novel pathways of CD8 T cell tolerance induction. *Immunity* 12: 505–514.
17. Böttcher, J. P., O. Schanz, D. Wohlleber, Z. Abdullah, S. Debey-Pascher, A. Staratschek-Jox, B. Höchst, S. Hegenbarth, J. Grell, A. Limmer, I. Atreya, M. F. Neurath, D. H. Busch, E. Schmitt, P. Van Endert, W. Kolanus, C. Kurts, J. L. Schultze, L. Diehl, and P. A. Knolle. 2013. Liver-primed memory T cells generated under noninflammatory conditions provide anti-infectious immunity. *Cell Rep.* 3: 779–795.
18. Diehl, L., A. Schurich, R. Grochtmann, S. Hegenbarth, L. Chen, and P. A. Knolle. 2008. Tolerogenic maturation of liver sinusoidal endothelial cells promotes B7-homolog 1-dependent CD8+ T cell tolerance. *Hepatology* 47: 296–305.
19. Schurich, A., M. Berg, D. Stabenow, J. Bottcher, M. Kern, H. J. Schild, C. Kurts, V. Schuette, S. Burgdorf, L. Diehl, A. Limmer, and P. A. Knolle. 2010. Dynamic Regulation of CD8 T Cell Tolerance Induction by Liver Sinusoidal Endothelial Cells. *J. Immunol.* 184: 4107–4114.
20. Harty, J. T., and V. P. Badovinac. 2008. Shaping and reshaping CD8+ T-cell memory. *Nat. Rev. Immunol.* 8: 107–119.

21. Sallusto, F., J. Geginat, and A. Lanzavecchia. 2004. Central memory and effector memory T cell subsets: function, generation, and maintenance. *Annu. Rev. Immunol.*
22. Mueller, S. N., T. Gebhardt, F. R. Carbone, and W. R. Heath. 2013. Memory T Cell Subsets, Migration Patterns, and Tissue Residence. *Annu. Rev. Immunol.* 31: 137–161.
23. Cui, W., and S. M. Kaech. 2010. Generation of effector CD8+ T cells and their conversion to memory T cells. *Immunol. Rev.* 236: 151–166.
24. Joshi, N. S., and S. M. Kaech. 2008. Effector CD8 T cell development: a balancing act between memory cell potential and terminal differentiation. *J. Immunol.* 180: 1309–1315.
25. Cui, W., N. Joshi, A. Jiang, and S. Kaech. 2009. Effects of Signal 3 during CD8 T cell priming: Bystander production of IL-12 enhances effector T cell expansion but promotes terminal differentiation. *Vaccine*.
26. Pearce, E. L., and H. Shen. 2007. Generation of CD8 T cell memory is regulated by IL-12. *J. Immunol.* 179: 2074–2081.
27. Pipkin, M. E., J. A. Sacks, F. Cruz-Guilloty, M. G. Lichtenheld, M. J. Bevan, and A. Rao. 2010. Interleukin-2 and inflammation induce distinct transcriptional programs that promote the differentiation of effector cytolytic T cells. *Immunity* 32: 79–90.
28. Kalia, V., S. Sarkar, S. Subramaniam, W. N. Haining, K. A. Smith, and R. Ahmed. 2010. Prolonged Interleukin-2Rα Expression on Virus-Specific CD8+ T Cells Favors Terminal-Effector Differentiation In Vivo. *Immunity* 32: 91–103.
29. Fletcher, A. L., D. Malhotra, S. E. Acton, V. Lukacs-Kornek, A. Bellemare-Pelletier, M. Curry, M. Armant, and S. J. Turley. 2011. Reproducible isolation of lymph node stromal cells reveals site-dependent differences in fibroblastic reticular cells. *Front. Immunol.* 2: 1–15.
30. Link, A., T. K. Vogt, S. Favre, M. R. Britschgi, H. Acha-Orbea, B. Hinz, J. G. Cyster, and S. A. Luther. 2007. Fibroblastic reticular cells in lymph nodes regulate the homeostasis of naive T cells. *Nat. Immunol.* 8: 1255–1265.
31. Lutz, M. B., N. Kukutsch, A. L. Ogilvie, S. Rössner, F. Koch, N. Romani, and G. Schuler. 1999. An advanced culture method for generating large quantities of highly pure dendritic cells from mouse bone marrow. *J. Immunol. Methods.* 223: 77–92.
32. Hirosue, S., I. C. Kourtis, A. J. van der Vlies, J. A. Hubbell, and M. A. Swartz. 2010. Antigen delivery to dendritic cells by poly(propylene sulfide) nanoparticles with disulfide conjugated peptides: Cross-presentation and T cell activation. *Vaccine* 28: 7897–7906.
33. Pope, C., S. K. Kim, A. Marzo, D. Masopust, K. Williams, J. Jiang, H. Shen, and L. Lefrançois. 2001. Organ-specific regulation of the CD8 T cell response to Listeria monocytogenes infection. *J. Immunol.* 166: 3402–3409.
34. Wherry, E. J., V. Teichgräber, T. C. Becker, D. Masopust, S. M. Kaech, R. Antia, U. H. von Andrian, and R. Ahmed. 2003. Lineage relationship and protective immunity of memory CD8 T cell subsets. *Nat. Immunol.* 4: 225–234.
35. McCloskey, M. L., M. A. Curotto de Lafaille, M. C. Carroll, and A. Erlebacher. 2011. Acquisition and presentation of follicular dendritic cell-bound antigen by lymph node-resident dendritic cells. *Journal of Experimental Medicine* 208: 135–148.
36. Tamburini, B. A., M. A. Burchill, and R. M. Kedl. 2014. Antigen capture and archiving by lymphatic endothelial cells following vaccination or viral infection. *Nat Comms* 5.
37. Harvey, D. J., D. R. Wing, B. Küster, and I. B. Wilson. 2000. Composition of N-linked carbohydrates from ovalbumin and co-purified glycoproteins. *J. Am. Soc. Mass Spectrom.* 11: 564–571.
38. Kahn, J., R. H. Ingraham, F. Shirley, G. I. Migaki, and T. K. Kishimoto. 1994. Membrane proximal cleavage of L-selectin: identification of the cleavage site and a 6-kD transmembrane peptide fragment of L-selectin. *J. Cell Biol.* 125: 461–470.
39. Richards, H., M. P. Longhi, K. Wright, A. Gallimore, and A. Ager. 2008. CD62L (L-selectin) down-regulation does not affect memory T cell distribution but failure to shed compromises anti-viral immunity. *The Journal of Immunology* 1: 198–206.
40. Yang, S., F. Liu, Q. J. Wang, S. A. Rosenberg, and R. A. Morgan. 2011. The shedding of CD62L (L-selectin) regulates the acquisition of lytic activity in human tumor reactive T lymphocytes. *PLoS ONE* 6: e22560.
41. Obar, J. J., and L. Lefrançois. 2010. Memory CD8+ T cell differentiation. *Annals of the New York Academy of Sciences* 1183: 251–266.

42. Lazarevic, V., L. H. Glimcher, and G. M. Lord. 2013. T-bet: a bridge between innate and adaptive immunity. *Nat. Rev. Immunol.* 13: 777–789.
43. Li, G., Q. Yang, Y. Zhu, H.-R. Wang, X. Chen, X. Zhang, and B. Lu. 2013. T-Bet and Eomes Regulate the Balance between the Effector/Central Memory T Cells versus Memory Stem Like T Cells. *PLoS ONE* 8: e67401.
44. Gattinoni, L., E. Lugli, Y. Ji, Z. Pos, C. M. Paulos, M. F. Quigley, J. R. Almeida, E. Gostick, Z. Yu, C. Carpenito, E. Wang, D. C. Douek, D. A. Price, C. H. June, F. M. Marincola, M. Roederer, and N. P. Restifo. 2011. A human memory T cell subset with stem cell-like properties. *Nat. Med.* 17: 1290–1297.
45. Zhang, Y., G. Joe, E. Hexner, J. Zhu, and S. G. Emerson. 2005. Host-reactive CD8+ memory stem cells in graft-versus-host disease. *Nat. Med.* 11: 1299–1305.
46. Farber, D. L., N. A. Yudanin, and N. P. Restifo. 2014. Human memory T cells: generation, compartmentalization and homeostasis. *Nat. Rev. Immunol.* 14: 24–35.
47. Harrington, L. E., M. Galvan, L. G. Baum, J. D. Altman, and R. Ahmed. 2000. Differentiating between memory and effector CD8 T cells by altered expression of cell surface O-glycans. *J. Exp. Med.* 191: 1241–1246.
48. Kastenmüller, W., M. Brandes, Z. Wang, J. Herz, and J. Egen. 2013. Peripheral Prepositioning and Local CXCL9 Chemokine-Mediated Guidance Orchestrate Rapid Memory CD8+ T Cell Responses in the Lymph Node. *Immunity*.
49. Sung, J. H., H. Zhang, E. A. Moseman, D. Alvarez, M. Iannacone, S. E. Henrickson, J. C. de la Torre, J. R. Groom, A. D. Luster, and U. H. von Andrian. 2012. Chemokine guidance of central memory T cells is critical for antiviral recall responses in lymph nodes. *Cell* 150: 1249–1263.
50. Bassett, J. D., T. C. Yang, D. Bernard, J. B. Millar, S. L. Swift, A. J. R. McGray, H. VanSeggelen, J. E. Boudreau, J. D. Finn, R. Parsons, C. Evelegh, D. Damjanovic, N. Grinshtein, M. Divangahi, L. Zhang, Z. Xing, Y. Wan, and J. L. Bramson. 2011. CD8+ T-cell expansion and maintenance after recombinant adenovirus immunization rely upon cooperation between hematopoietic and nonhematopoietic antigen-presenting cells. *Blood* 117: 1146–1155.
51. Chang, J. T., E. J. Wherry, and A. W. Goldrath. 2014. Molecular regulation of effector and memory T cell differentiation. *Nat. Immunol.* 15: 1104–1115.
52. Kaech, S. M., and W. Cui. 2012. Transcriptional control of effector and memory CD8+ T cell differentiation. *Nat. Rev. Immunol.* 12: 749–761.
53. Parish, I. A., and S. M. Kaech. 2009. Diversity in CD8(+) T cell differentiation. *Current Opinion in Immunology* 21: 291–297.
54. Gattinoni, L., X.-S. Zhong, D. C. Palmer, Y. Ji, C. S. Hinrichs, Z. Yu, C. Wrzesinski, A. Boni, L. Cassard, L. M. Garvin, C. M. Paulos, P. Muranski, and N. P. Restifo. 2009. Wnt signaling arrests effector T cell differentiation and generates CD8+ memory stem cells. *Nat. Med.* 15: 808–813.
55. Berard, M., K. Brandt, S. Bulfone-Paus, and D. F. Tough. 2003. IL-15 promotes the survival of naive and memory phenotype CD8+ T cells. *J. Immunol.* 170: 5018–5026.
56. Papatriantafyllou, M. 2011. T cell memory: the stem of T cell memory. *Nat. Rev. Immunol.* 11: 716.
57. Cieri, N., B. Camisa, F. Cocchiarella, M. Forcato, G. Oliveira, E. Provasi, A. Bondanza, C. Bordignon, J. Peccatori, F. Ciceri, M. T. Lupo-Stanghellini, F. Mavilio, A. Mondino, S. Bicciato, A. Recchia, and C. Bonini. 2013. IL-7 and IL-15 instruct the generation of human memory stem T cells from naive precursors. *Blood* 121: 573–584.
58. Graef, P., V. R. Buchholz, C. Stemberger, M. Flossdorf, L. Henkel, M. Schiemann, I. Drexler, T. Höfer, S. R. Riddell, and D. H. Busch. 2014. Serial Transfer of Single-Cell-Derived Immunocompetence Reveals Stemness of CD8+ Central Memory T Cells. *Immunity* 41: 116–126.
59. Youngblood, B., J. S. Hale, and R. Ahmed. 2013. T-cell memory differentiation: insights from transcriptional signatures and epigenetics. *Immunology* 139: 277–284.
60. Ahmed, R., M. J. Bevan, S. L. Reiner, and D. T. Fearon. 2009. The precursors of memory: models and controversies. *Nat. Rev. Immunol.* 9: 662–668.
61. Lefrançois, L., and A. L. Marzo. 2006. The descent of memory T-cell subsets. *Nat. Rev. Immunol.* 6: 618–623.

62. Gattinoni, L., C. A. Klebanoff, and N. P. Restifo. 2012. Paths to stemness: building the ultimate antitumour T cell. *Nat. Rev. Cancer* 12: 671–684.
63. Restifo, N. P., and L. Gattinoni. 2013. Lineage relationship of effector and memory T cells. *Current Opinion in Immunology* 25: 556–563.
64. Williams, M. A., and M. J. Bevan. 2007. Effector and memory CTL differentiation. *Annu. Rev. Immunol.* 25: 171–192.
65. Ahmed, R., and B. Rouse. 2006. Immunological memory. *Immunol. Rev.*
66. Buchholz, V. R., P. Gräf, and D. H. Busch. 2013. The smallest unit: effector and memory CD8(+) T cell differentiation on the single cell level. *Front. Immunol.* 4: 31.
67. Zehn, D., S. Roepke, K. Weakly, M. J. Bevan, and M. Prlic. 2014. Inflammation and TCR signal strength determine the breadth of the T cell response in a bim-dependent manner. *The Journal of Immunology* 192: 200–205.
68. Boesteanu, A. C., and P. D. Katsikis. 2009. Memory T cells need CD28 costimulation to remember. *Seminars in Immunology* 21: 69–77.
69. Manjunath, N., P. Shankar, J. Wan, W. Weninger, M. A. Crowley, K. Hieshima, T. A. Springer, X. Fan, H. Shen, J. Lieberman, and U. H. von Andrian. 2001. Effector differentiation is not prerequisite for generation of memory cytotoxic T lymphocytes. *J. Clin. Invest.* 108: 871–878.
70. Kaneko, S., S. Mastaglio, A. Bondanza, M. Ponzoni, F. Sanvito, L. Aldrighetti, M. Radrizzani, S. La Seta-Catamancio, E. Provasi, A. Mondino, T. Nagasawa, K. Fleischhauer, V. Russo, C. Traversari, F. Ciceri, C. Bordignon, and C. Bonini. 2009. IL-7 and IL-15 allow the generation of suicide gene-modified alloreactive self-renewing central memory human T lymphocytes. *Blood* 113: 1006–1015.
71. Onder, L., P. Narang, E. Scandella, Q. Chai, M. Iolyeva, K. Hoorweg, C. Halin, E. Richie, P. Kaye, J. Westermann, T. Cupedo, M. Coles, and B. Ludewig. 2012. IL-7-producing stromal cells are critical for lymph node remodeling. *Blood* 120: 4675–4683.
72. Hara, T., S. Shitara, K. Imai, H. Miyachi, S. Kitano, H. Yao, S. Tani-ichi, and K. Ikuta. 2012. Identification of IL-7-producing cells in primary and secondary lymphoid organs using IL-7-GFP knock-in mice. *The Journal of Immunology* 189: 1577–1584.
73. Miller, C. N., D. J. Hartigan-O'Connor, M. S. Lee, G. Laidlaw, I. P. Cornelissen, M. Matloubian, S. R. Coughlin, D. M. McDonald, and J. M. McCune. 2013. IL-7 production in murine lymphatic endothelial cells and induction in the setting of peripheral lymphopenia. *Int. Immunol.* 25: 471–483.
74. Cui, G., T. Hara, S. Simmons, K. Wagatsuma, A. Abe, H. Miyachi, S. Kitano, M. Ishii, S. Tani-ichi, and K. Ikuta. 2014. Characterization of the IL-15 niche in primary and secondary lymphoid organs in vivo. *Proceedings of the National Academy of Sciences* 111: 1915–1920.
75. Chang, J. T., V. R. Palanivel, I. Kinjyo, F. Schambach, A. M. Intlekofer, A. Banerjee, S. A. Longworth, K. E. Vinup, P. Mrass, J. Oliaro, N. Killeen, J. S. Orange, S. M. Russell, W. Weninger, and S. L. Reiner. 2007. Asymmetric T lymphocyte division in the initiation of adaptive immune responses. *Science* 315: 1687–1691.
76. Helft, J., J. Böttcher, P. Chakravarty, S. Zelenay, J. Huotari, B. U. Schraml, D. Goubau, and C. Reis e Sousa. 2015. GM-CSF Mouse Bone Marrow Cultures Comprise a Heterogeneous Population of CD11c(+)MHCII(+) Macrophages and Dendritic Cells. *Immunity* 42: 1197–1211.
77. Kambayashi, T., E. Assarsson, A. E. Lukacher, H.-G. Ljunggren, and P. E. Jensen. 2003. Memory CD8+ T cells provide an early source of IFN-gamma. *J. Immunol.* 170: 2399–2408.
78. Berg, R. E., E. Crossley, S. Murray, and J. Forman. 2003. Memory CD8+ T cells provide innate immune protection against Listeria monocytogenes in the absence of cognate antigen. *J. Exp. Med.* 198: 1583–1593.
79. Haluszczak, C., A. D. Akue, S. E. Hamilton, L. D. S. Johnson, L. Pujanauski, L. Teodorovic, S. C. Jameson, and R. M. Kedl. 2009. The antigen-specific CD8+ T cell repertoire in unimmunized mice includes memory phenotype cells bearing markers of homeostatic expansion. *Journal of Experimental Medicine* 206: 435–448.
80. Finlay, B. B., and G. McFadden. 2006. Anti-immunology: evasion of the host immune system by bacterial and viral pathogens. *Cell* 124: 767–782.

81. Hickman, H. D., K. Takeda, C. N. Skon, F. R. Murray, S. E. Hensley, J. Loomis, G. N. Barber, J. R. Bennink, and J. W. Yewdell. 2008. Direct priming of antiviral CD8+ T cells in the peripheral interfollicular region of lymph nodes. *Nat. Immunol.* 9: 155–165.
82. Thomas, S., G. A. Kolumam, and K. Murali-Krishna. 2007. Antigen presentation by nonhemopoietic cells amplifies clonal expansion of effector CD8 T cells in a pathogen-specific manner. *J. Immunol.* 178: 5802–5811.
83. Grinshtein, N., T. C. Yang, R. Parsons, J. Millar, G. Denisova, D. Dissanayake, J. Leitch, Y. Wan, and J. Bramson. 2006. Recombinant adenovirus vaccines can successfully elicit CD8+ T cell immunity under conditions of extreme leukopenia. *Mol Ther* 13: 270–279.
84. Swartz, M. A. 2014. Inflammatory lymphangiogenesis in postpartum breast tissue remodeling. *J. Clin. Invest.* 124: 3704–3707.
85. Angeli, V., and G. J. Randolph. 2006. Inflammation, lymphatic function, and dendritic cell migration. *Lymphatic Research and Biology* 4: 217–228.
86. Podgrabinska, S., O. Kamalu, L. Mayer, M. Shimaoka, H. Snoeck, G. J. Randolph, and M. Skobe. 2009. Inflamed Lymphatic Endothelium Suppresses Dendritic Cell Maturation and Function via Mac-1/ICAM-1-Dependent Mechanism. *J. Immunol.* 183: 1767–1779.

3.6 Appendix

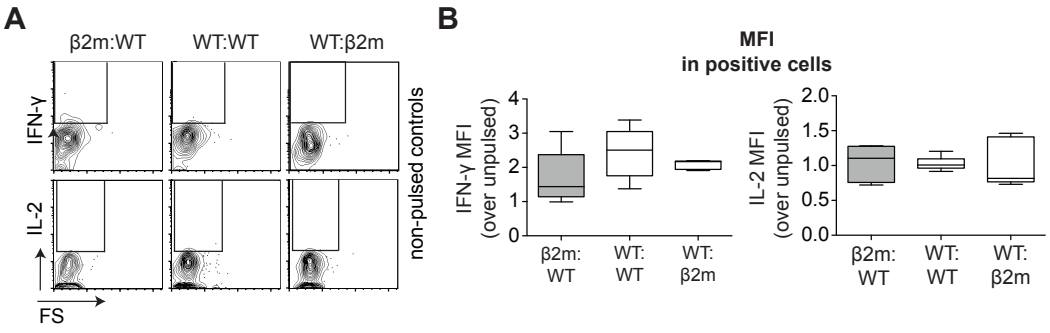

Figure 3.9 (Related to Fig. 3.1), LNSC-educated CD8$^+$ T cells can induce expression of IFN-γ and IL-2 and the per cell expression levels of IL-2$^+$ cells tend to be lower when stromal cells are excluded from CD8$^+$ T cell priming. We generated BM chimeric mice using β2m$^{-/-}$ (β2 microglobulin knockout, lacking MHC class I) mice, as described in the Materials and Methods. Irradiated C57/Bl6 WT mice were reconstituted with β2m$^{-/-}$ BM to limit presentation of the Kb-restricted SIINFEKL epitope to radioresistant lymph node stromal cells (β2m:WT); Irradiated β2m$^{-/-}$ mice were reconstituted with BM from C57/Bl6 WT mice (WT:β2m) to exclude LNSCs cells from antigen presentation; the relative (positive and negative) control mice (WT:WT, β2m: β2m) were also generated. Naïve CFSE-labeled OT-I CD8$^+$ T cells (CD45.1.2$^+$) were transferred in the chimeric mice and one day after, the mice were vaccinated intradermally with OVA or saline control (PBS). 5 days after vaccination, the mice were sacrificed and the skin-draining LNs were collected. To determine the capacity of LNSC-educated cells to produce cytokines, the cells were ex-vivo restimulated with SIINFEKL peptide (or not) for 5h followed by intracellular staining for flow cytometric analysis. **(A)** Representative contour plots displaying IFN-γ top) or IL-2 (bottom) on y-axis and the side scatterer on x-axis, in the controls samples in which the cells were not restimulated with SIINFEKL (unpulsed controls). **(B)** Normalized mean fluorescence intensity (MFI) of IFN-γ$^+$ cells (top) or IL-2$^+$ (bottom) cells. The normalized MFI was determined as ($MFI_{pulsed\ sample}$)/$MFI_{unpulsed\ control}$. Representative data from one of two independent experiments (n=5).

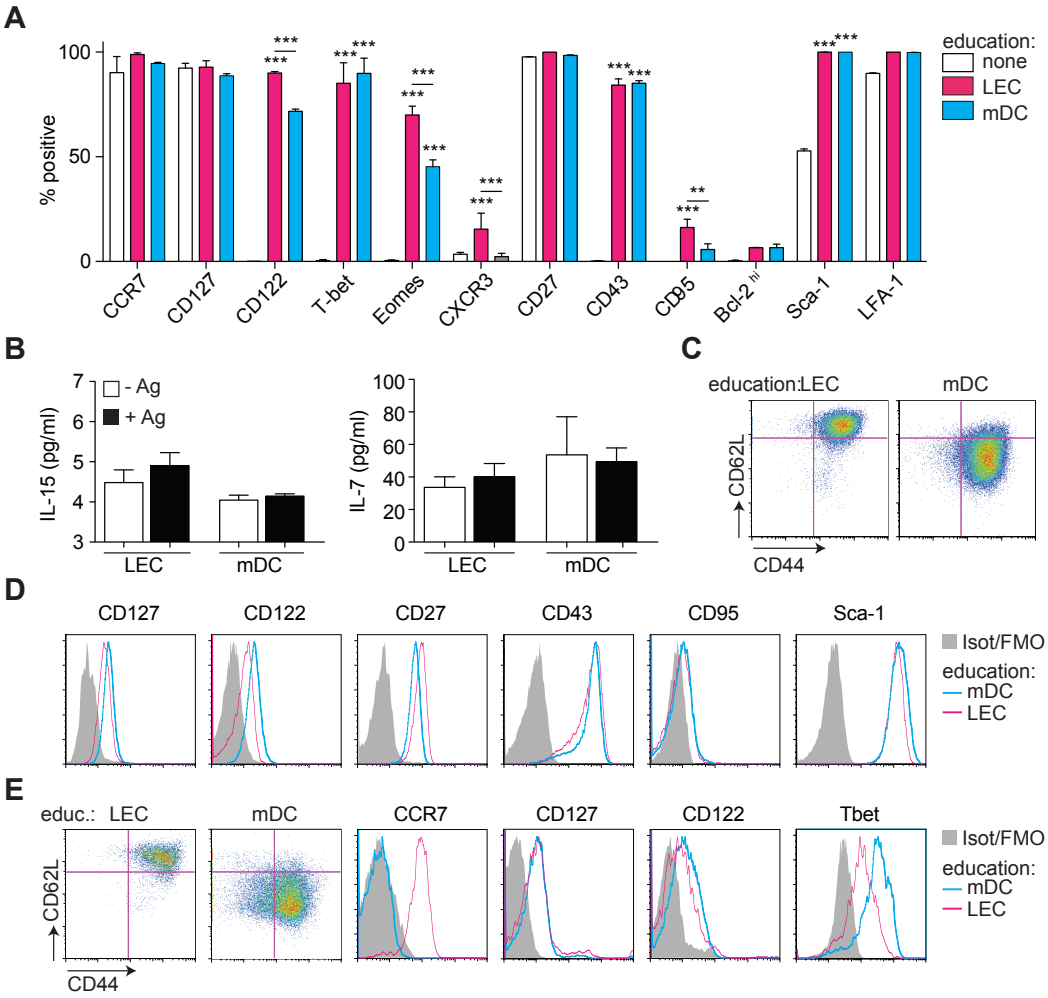

Figure 3.10 (Related to Fig. 3.3), LEC-educated CD8$^+$ T cells display a particular phenotype with central memory-like and stem cell memory-like characteristics, distinct from the one of mDC-educated cells. OT-I CD8$^+$ T cells were educated in the presence of NPssCOVA$_{250-264}$ (1nM) by LN LEC or mDC (education) or not educated (none). On day 3 of co-culture, LEC/mDC-educated CD8$^+$ T cells were harvested, stained for different surface, intracellular and intranuclear markers and analyzed by flow cytometry. **(A)** Percent positive expression of surface markers (CD44, CD62L, CD127, CD122, CCR7, etc) or intracellular proteins (Bcl-2) or transcription factors (T-bet, Eomes) in naive CD44$^-$CD62L$^+$ (empty bars), CD44$^+$CD62L$^+$ LEC-educated (black bars), or CD44$^+$CD62L$^-$ DC-educated (white bars) CD8$^+$ T cells. **(B)** Low levels of IL-15 and IL-7 in the supernatant of LEC/mDC - CD8$^+$ T cell coculures. Levels of IL-15 and IL-7 secreted in the supernatant (pg/ml), as assessed by ELISA. The CD44$^+$CD62L$^+$ phenotypic profile of LN LEC-educated CD8$^+$ T cells is neither specific to the model antigen and TCR transgenic system used, nor it is dependent on the cross-presentation mechanism. **(C)** OT-I CD8$^+$ T cells educated by LN LECs in the presence of SIINFEKL (1nM) display a similar phenotype to those educated in the presence of NP-ss-COVA$_{250–264}$. Representative dot plots with CD44 on x-axis and CD62L on y-axis. **(D)** Representative histograms of various surface markers (CD127, CD122, CD27, CD43, CD95, Sca-1). **(E)** pmel CD8$^+$ T cells educated by LN LECs in the presence of gp100$_{25–33}$ peptide displayed a similar CD44$^+$CD62L$^+$ phenotype to OT-I LEC-educated CD8$^+$ T cells in the presence of NP-ss-COVA$_{250–264}$. Representative dot plots with CD44 on x-axis and CD62L on y-axis and representative histograms of various surface and intranuclear markers (CCR7, CD127, CD122, T-bet). Representative data from one of three independent experiments (A, n=3) Representative data from one of three independent experiments (A, n=3) or out of two experiments (C-E, n=3). **p≤0.01, ***p≤0.001 by two-way ANOVA (A) or one-way ANOVA (B) followed by Bonferroni posttest.

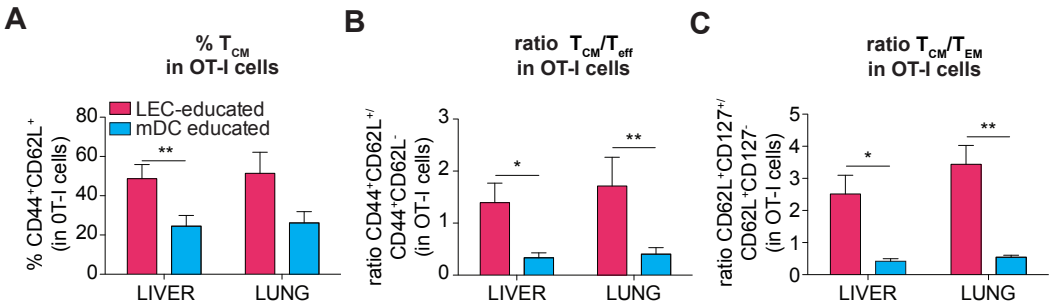

Figure 3.11 (**Related to Fig. 3.4**), ***Ex vivo*** **generated LEC-educated CD8$^+$ T cells mainly preserve their central memory-like phenotype after *in vivo* transfer, even when they migrate in the periphery.** OT-I CD8$^+$ T cells were educated in the presence of NPssCOVA$_{250-264}$ (1nM) by LN LEC or mDC. After 3 days of coculture, *ex vivo* LEC/mDC-educated were transferred i.v. in C57/Bl6 WT mice. One week after the transfer, the mice were sacrificed; the liver and lungs were collected and analyzed by flow cytometry. The CD44$^+$CD62L$^+$ T_{CM}-like subset dominates in LEC-educated cells in the liver and lung, even though at lower levels compared to LN. **(A)** Percentage of T_{CM} (CD44$^+$CD62L$^+$) in OT-I cells in liver and lung. LEC-educated CD8$^+$ T cells are more polarized to T_{CM}-like rather than $T_{eff/EM}$ phenotype, in constrast to mDC-educated cells. **(B)** Ratio of T_{CM} (CD44$^+$CD62L$^+$) over T_{eff} (CD44$^+$CD62L$^-$) in OT-I CD8$^+$ T cells. **(C)** Ratio of T_{CM} (CD44$^+$CD127$^+$CD62L$^+$) over T_{EM} (CD44$^+$CD127$^+$CD62L$^+$) in OT-I cells in liver and lung. Representative data from one of two independent experiments (n=3). *p≤0.05, **p≤0.01 by two-way ANOVA followed by Bonferroni posttest.

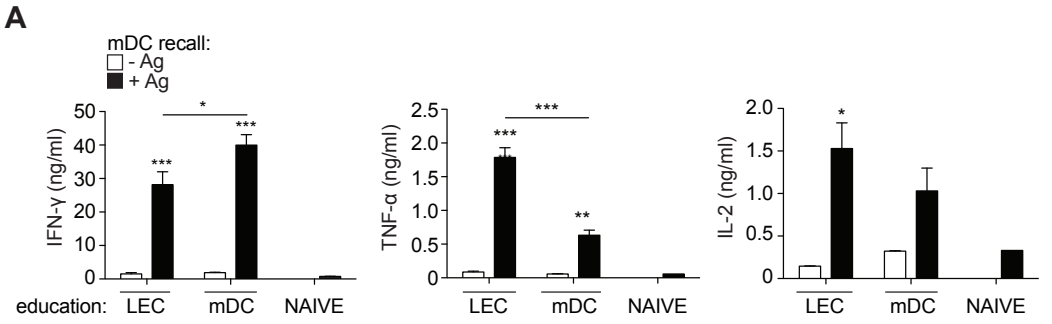

Figure 3.12 (Related to Fig. 3.5), Following reactivation, LEC-educated CD8$^+$ T cells exit the non-responsive state and release high levels of cytokines. OT-I CD8$^+$ T cells were cultured in the presence of NPssCOVA$_{250-264}$ (1nM) with LN LEC or mDC for 3 days . LEC/mDC-educated CD8$^+$ T cells were subsequently harvested and re-plated in the presence of mDCs (mDC recall), bearing (+Ag, white bars) or not (-Ag, black bars) the SIINFEKL peptide, for 24h. **(A)** Following mDC-recall, LEC-educated CD8$^+$ T cells produce IFN-γ, TNF-α, as well as IL-2. The graphs (from left to right) display the levels of IFN-γ, TNF-α, and IL-2 (ng/ml) secreted in the supernatant of the 24h reactivation coculture, as assessed by ELISA. The stars on top of the bars indicate significant difference compare to -Ag control. Pooled data from two independent experiments (n=6). **p≤0.01, ***p≤0.001 by one-way ANOVA followed by Bonferroni posttest.

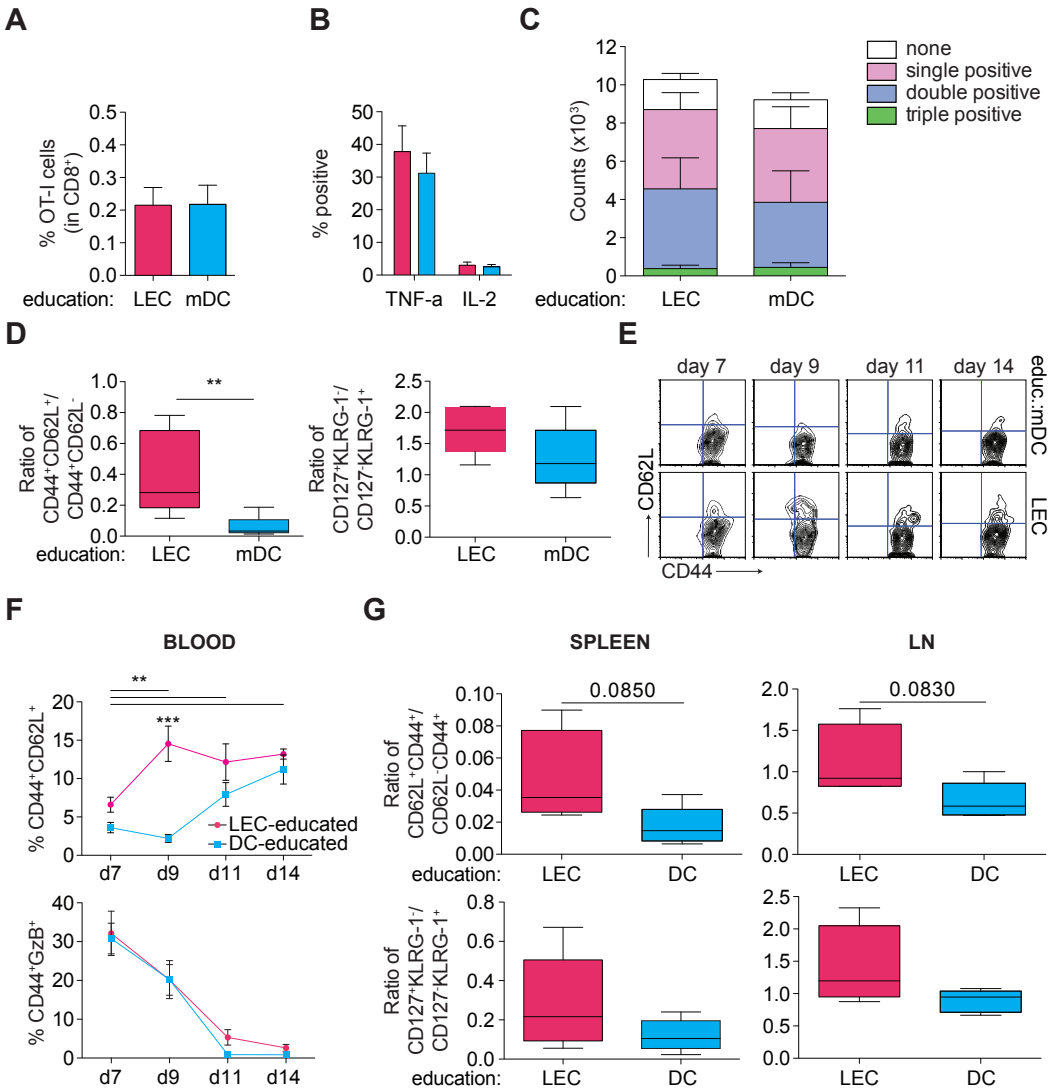

Figure 3.13 (Related to Fig. 3.7), LEC-educated CD8$^+$ T cells can mediate protection against infectious pathogens while preserving a secondary memory persistent population. *Ex vivo* generated (CD45.1.2) LEC-educated were transferred together with (CD45.1) DC-educated CD8$^+$ T cells a 1:1 ratio in C57/Bl6 mice (5x10^4 total cells/mouse). 5 weeks after, mice were i.v. challenged with *L.m.*-OVA (10^3 cfu) and sacrificed either on day 8 or 3 weeks after challenge. Cell suspensions of spleens and skin-dLNs were generated and analyzed by flow cytometry. **(A)** Percentage of OT-I cells (gated on CD8$^+$ T cells) in LN on day 8 after infection. **(B)** Percentage of TNF-a$^+$ and IL-2$^+$ cells (gated on OT-I cells) in spleen. **(C)** Counts of single, double or triple positive OT-I cells for IFN-γ, TNF-α and IL-2 **(D)** Left, ratio of T_{CM} (CD44$^+$CD62L$^+$) over T_{eff} (CD44$^+$CD62L$^-$) in OT-I cells on day 8 after challenge in the LN. Right, ratio of short-lived effector cells (CD44$^+$CD127$^-$KLRG1$^+$) over memory precursor effector cells (CD44$^+$CD127$^+$KLRG1$^-$). A secondary memory-subset in LEC-educated CD8$^+$ T cells persists upon challenge. In order to evaluate the formation of secondary memory in LEC-educated CD8$^+$ T cells, we assessed their phenotypic profile 3 weeks after challenge. **(E)** Representative dot plots displaying CD62L on y-axis and CD44 on x-axis at different time points following challenge in the blood. The T_{CM} subset increases in LEC-educated CD8$^+$ T cells after the peak of infection. **(F)** Top, percentage of CD44$^+$CD62L$^+$ cells in blood (gated on OT-I cells) at different time points following challenge. Bottom, percentage of CD44$^+$GzB$^+$ cytotoxic T_{eff}-like cells (gated on OT-I cells) in blood. **(G)** Top, ratio of T_{CM} (CD44$^+$ CD62L$^+$) over $T_{EM/eff}$, (CD44$^+$ CD62L$^-$) in OT-I cells in spleen and LN on day 21 after challenge. Bottom, ratio of memory precursor effector cells (CD127$^+$KLRG1$^-$) over short-lived effector cells (CD127$^-$ KLRG1$^+$) in spleen and LN on day 21 after challenge. Pooled data from two independent experiments (A-D, n=5) or data from one experiment (E-G, n=5). **p≤0.01, by two-way ANOVA followed by Bonferroni posttest (C, F) or by two-tailed unpaired Student's t test (D, G)

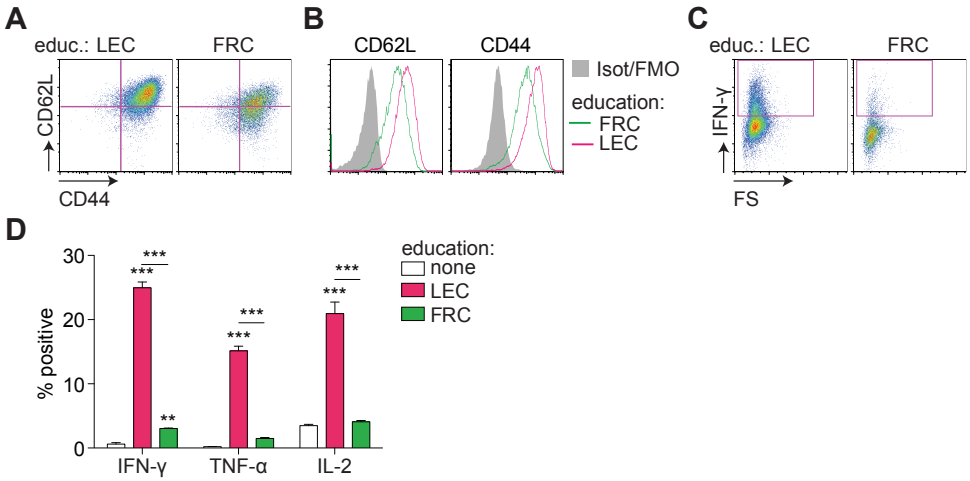

Figure 3.14 LN FRC-educated CD8$^+$ T cells display lower levels of CD62L, compared to LEC-educated ones, and fail to produce cytokines upon reactivation. OT-I CD8$^+$ T cells were educated in the presence of NPssCOVA$_{250-264}$ (1nM) by LN LEC or FRC (education) or not educated (none). After 3 days of co-culture, LEC/FRC-educated CD8$^+$ T cells were harvested, stained for different surface and analyzed by flow cytometry. FRC-educated CD8$^+$ T cells displayed a less «polarized» phenotype towards the T_{CM} subset, compared to LEC-educated, with lower levels of CD62L. **(A)** Representative dot plots with CD62L on y-axis and CD44 on x-axis on day 3 of coculture. **(B)** Representative histograms displaying the expression of CD44 and CD62L for LEC-educated (pink line) and FRC-educated (green line) CD8$^+$ T cells. FRC-educated CD8$^+$ T cells failed to produce cytokines upon mDC-recall. LEC/FRC-educated OT-I cells were harvested on day 3 of the coculture and re-plated in the presence of mDCs, bearing or not the SIINFEKL peptide. **(C)** Representative dot plots with IFN-γ on y-axis and forward scatter on x-axis after 5h restimulation with mDCs bearing the SIINFEKL peptide, as determined by intracellular staining followed by flow cytometric analysis. **(D)** Percentage of IFN-γ$^+$, TNF-α$^+$, and IL-2$^+$ cells (gated on CD8$^+$ cells). The stars on top of bars indicate significant difference with respect to naïve group. Data from one experiment (n=3). **p≤0.01, ***p≤0.001 by one-way ANOVA followed by Bonferroni posttest.

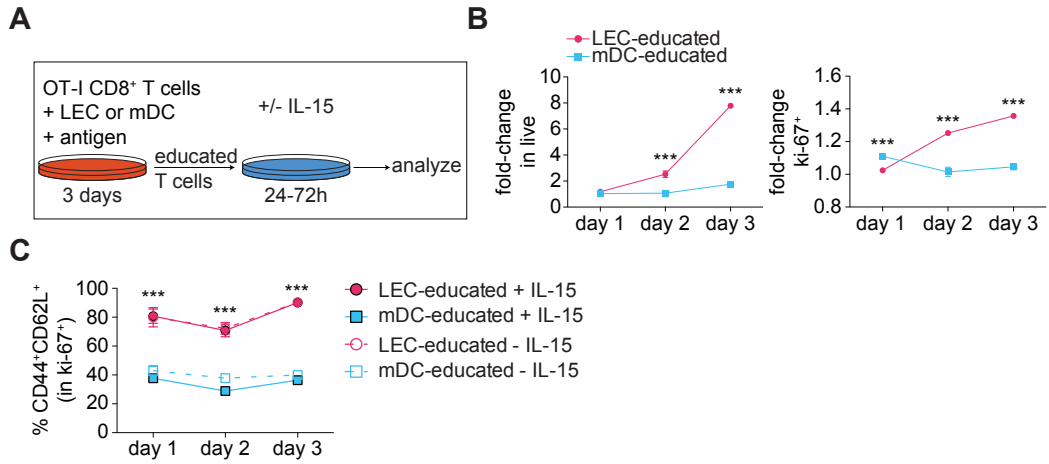

Figure 3.15 LN LEC-educated CD8$^+$ T cells display increased survival in response to homeostatic signals while retaining their phenotype. To determine whether LEC-educated CD8$^+$ T cells have the capacity to self-renew in response to homeostatic signals, we evaluated survival, proliferation and phenotype of LEC/mDC-educated CD8$^+$ T cells upon exposure to IL-15. OT-I CD8$^+$ T cells were educated in the presence of NPssCOVA$_{250-264}$ (1nM) by LN LEC or mDC. After 3 days of co-culture, LEC/mDC-educated CD8$^+$ T cells were harvested, washed and subsequently cultured in the presence (+ IL-15) or absence (- IL-15) of IL-15 (100ng/ml). At different time points (24h, 48h, 72h), the cells were harvested and assessed for viability, proliferation (ki-67) and T_{CM}–like phenotype (CD44$^+$CD62L$^+$) by flow cytometry. **(A)** Schematic of the experiment. LEC-educated CD8$^+$ T cells undergo homeostatic turnover and display increased survival in response to IL-15 stimulation, whereas mDC-educated cells appear less sensitive to IL-15 treatment. **(B)** Left, fold change in live cells in groups treated with IL-15 over non-treated, at different time points. Right, fold change in ki67$^+$ cells in groups treated with IL-15

over non-treated, at different time points. LEC-educated $CD8^+$ T cells preserve their T_{CM}–like phenotype. **(C)** Percentage of $CD44^+CD62L^+$ cells in LEC-educated cells (pink) or mDC-educated (blue), treated (filled symbols) or non-treated (empty symbols) with IL-15. Stars indicate significant difference between groups at the specific time point. Data from one experiment (n=3). ***p≤0.001 by two-way ANOVA followed by Bonferroni posttest.

Chapter 4

Investigating the contribution of antigen presentation by LECs in $CD8^+$ T cell immune responses

Lymph nodes (LNs) display remarkable enlargement during inflammation induced by pathogen infection or vaccination. The expansion and remodeling of the stromal elements has been previously claimed to accommodate the vigorous infiltration of lymphocytes and dendritic cells in the LN at the onset of the immune response. We asked whether proliferation of lymphatic endothelial cells (LECs) in the LN during inflammation might play a direct immunological role in the initiation of the response, via their antigen-presenting function. First, we demonstrated that LN LECs can perceive inflammatory signals, dynamically regulating their phenotype, and actively scavenge exogenous antigen under inflammatory conditions. To answer the questions raised, we pursued two different approaches to control the number of LECs. We exploited a VEGFR3 blocking antibody in order to inhibit LEC expansion following immunization with a subunit vaccine. However, it only partially induced LEC contraction and thus, minimally affected the frequency, phenotype and functional potential of antigen-specific $CD8^+$ T cells. As an alternative approach, we developed the Prox1-Cre-DTR mouse model, which allows for specific ablation of LECs *in vivo* following administration of diphtheria toxin (DT). We attained local ablation of lymphatic vessels in the ear as we tried to optimize the conditions for LEC deletion in the LN. Our findings contributed towards the development of models to investigate the immunological significance of LEC expansion following inflammatory antigenic challenge and advanced our understanding of it. Nevertheless, further studies need to be performed, integrating the knowledge obtained here, in order to elucidate the active role of LN LEC in the establishment of adaptive immunity.

4.1 Introduction

Lymph nodes (LNs) undergo considerable expansion during inflammation induced by infectious pathogen invasion or following vaccination. Lymphangiogenesis, the proliferation and remodeling of the lymphatic endothelium, has been widely observed in the LN draining the inflammatory site (1-5). Different cellular mediators, including immune and non-immune cells, orchestrate inflammatory lymphangiogenesis via the secretion of vascular endothelial growth factors (VEGFs) (6-8). Among them, VEGF-C and VEGF-D bind to the VEGFR3 receptor, which is primarily expressed on the lymphatic endothelium (9). Inflammation-induced NF-κB signaling has been suggested to further amplify the lymphangiogenic signals by upregulating VEGFR-3 expression on lymphatic endothelial cells (LECs) (10).

This expansion of the stromal elements in the LN has been primarily attributed to the need to support the robust infiltration of lymphocytes at the onset of immune responses (11-13) and has been associated with enhanced DC migration and antigen drainage to the LN (14). Additionally, remodeling of the lymphatic structures has been shown to facilitate lymphocyte egress during prolonged inflammation at later stages of the immune response (15). However, it still remains unknown whether proliferation of LECs during inflammation might also actively influence the outcome of the response. Accumulating evidence suggests a direct immunological role for LN LECs during immune responses. Supporting this hypothesis, LN LEC proliferation in the course of a vaccine-elicited immune response was demonstrated to be necessary for antigen archiving in LECs, which subsequently led to enhanced long-term protection (16).

We have previously demonstrated that LN LECs can actively scavenge exogenous antigen under steady-state conditions for MHC class I presentation to $CD8^+$ T cells [Chapter 2 and (17)], contributing to the generation of antigen-experienced $CD8^+$ T cells. LN LEC-educated $CD8^+$ T cells appear temporarily inactive but can be functionally reactivated following inflammatory antigenic challenge (Chapter 3). It is currently unclear whether LN LECs retain their capacity for antigen presentation under inflammatory conditions, and how they may interact with and impact the education of antigen-specific $CD8^+$ T cells in this setting.

Given our findings highlighting the active contributions of LN LEC-educated $CD8^+$ T cells in protective immunity, we hypothesized that LEC expansion during inflammation might be directly associated with the initiation of the immune response and act as an additional determinant of its outcome. To explore this hypothesis, we exploited the model of CpG-induced inflammatory LN lymphangiogenesis, and by incorporating CpG in a subunit vaccine, we triggered robust $CD8^+$ T cell responses while promoting significant LEC proliferation in the LN.

In this model, we investigated the scavenging ability of LN LECs during inflammation and evaluated the expression of the antigen presentation machinery components in response to inflammatory signals to confirm their APC function in the course of an inflammatory immune response. We also determined the phenotypic profile of $CD8^+$ T cells educated by LN LECs during inflammation, which was not significantly different from their homeostatic phenotype.

From here, we adopted two different strategies in order to evaluate the potential direct immunological function of LECs in the establishment of immune responses. We first exploited an anti-VEGFR3 blocking antibody to inhibit lymphangiogenesis following immunization and therefore, assess the impact of limited LEC-education in the outcome of immune responses. Alternatively, we attempted to identify the contribution of LECs in the induction of immune responses by evaluating the effect of their absence. To eliminate LECs, the LYVE-1-Cre-DTR mouse model had been previously developed for the ablation of LYVE-1 - expressing lymphatic vessels in an inducible, diphtheria toxin – dependent manner (18). However, following systemic diphtheria toxin administration, these mice died from sepsis due to distortion of blood capillaries in the intestine, induced by the loss of lymphatic lacteals. To counter the drawbacks of this model, we established the Prox1-DTR transgenic mouse model, in which Prox1-expressing LECs can be selectively ablated. Because of the potential lethality of a systemic ablation approach, we mainly focused on locally deleting LECs in the LN. Our findings provide valuable hints for the immunological significance of LN lymphangiogenesis and further studies on the established models might offer useful insight for the design of vaccines, as well as the treatment of inflammatory disorders.

4.2 Materials and Methods

Reagents

All chemicals were from Sigma-Aldrich (Buchs, CH) unless otherwise noted. The mature MHC I epitope for ovalbumin, $OVA_{256-264}$ (SIINFEKL) peptide, was from GenScript (Piscataway, NJ, US). The Endotoxin-free OVA was purchased from Hyglos GmbH, (Bernried am Starnberger See, DE). CpG-B 1826 oligonucleotide (CpG) was obtained from Microsynth (Balgach, CH). Recombinant murine IFN- γ was purchased from R&D systems (Abingdon, U.K.) and TNF-α from Invitrogen (Zug, CH). Diphtheria toxin (Corynebacterium diptheriae CALBIOCHEM) was acquired from Merck&Cie (Schaffhausen, CH). Tamoxifen (T5648) was purchased from Sigma-Aldrich (Buchs, CH) and was dissolved according to the manufacturer's instructions. Antibodies used in flow cytometry were from eBioscience or BioLegend (Luzern, CH) unless otherwise noted.

Mice

The following mice strains were used in this study at age 6-12 weeks unless noted otherwise. Female C57BL/6 (CD45.2 or CD45.1 Ly5) wild-type mice and OT-I CD45.2 transgenic mice, (C57BL/6-Tg(TcraTcrb)1100Mjb/J), were purchased from Harlan Laboratories (Gannat, FR). Transgenic OT-I CD45.1.2 mice were a kind gift of the laboratory of Prof. Dietmar Zehn (CHUV) and were bred in our SPF facilities. Prox1-CreERT2 mice (Prox1-Cre mouse) were a kind gift of the laboratory of Prof. Tatiana Petrova (UNIL) and were re-derived and bred in our SPF facility. C57BL/6-Gt(ROSA)26Sortm1(HBEGF)Awai/J mice (DTR-Floxed mouse) were from Jackson Laboratory (Bar Harbor, ME, USA). All experiments were conducted with age- or sex-matched mice, with the exception of the experiments involving Prox1-$Cre^{+/-}$-DTR mice. Animals were housed in pathogen-free facilities and all procedures were approved by the Cantonal Veterinary Committee of Vaud, Switzerland (Protocol number 2687 and 2992).

Cell lines

Conditionally immortalized dermal LECs (iLECs; Immortomice) were isolated and cultured as previously described (19). Cell culture surfaces used in all assays were coated with collagen (10µg/ml PureCol; Advanced Biomatrix, San Diego, CA) and human fibronectin (10µg/ml,

Millipore, Billerica, MA) prior to seeding. Cells were grown in 40% DMEM low glucose, 40% F12, 20% FBS (all from Invitrogen, Zug, CH), supplemented with 10 µg/ml native bovine endothelial mitogen (AbD Serotec, Dusseldorf, DE) and 56 µg/ml heparin sodium salt from porcine intestinal mucosa (Sigma-Aldrich). To induce large T Ag expression, IFN-γ (R&D Systems, Abingdon, U.K.) was added to the media at 100U/ml, and cells were propagated at 33℃. Prior to all experiments, cells were grown for 72h in the absence of IFN-γ at 37℃ and maintained as such.

Synthesis of OVA-conjugated nanoparticles (NP-OVA)

For the immunization studies, poly (propylene sulfide)-nanoparticles (NPs) were synthesized by emulsion polymerization, surface-functionalized and characterized as previously described (20, 21). Endotoxin-free OVA was incubated overnight at room temperature with NPs in the presence of guanidinium hydrochloride (GndHCl, Sigma-Aldrich) and subsequently purified on a Sepharose CL-6B column (Sigma-Aldrich). OVA concentration on NPs was determined by BCA protein assay (Thermo Fisher Scientific, Waltham MA, USA). The size of NPs, before and after protein conjugation, was determined by dynamic light scattering with a Nano ZS Zetasizer (Malvern Instruments) and was measured in the range of 35-40nm. Endotoxin levels of antigens were routinely assessed by a colorimetric assay based on the HEK-Blue ™ TLR4 cell line (InvivoGen, San Diego, CA, USA) according to the manufacturer's protocol using a standard curve generated from the E-Toxate ™ endotoxin standard (Sigma).

Primary LEC isolation

To obtain primary LN LECs, LNs were harvested and digested with 0.25mg/ml Liberase DH and 100µg/ml DNase (both from Roche, Basel, CH) to obtain a single cell suspension, and cultured as described (22). Cells were cultured for 5 days until confluent, detached by Accutase (Biological Industries, Kibbutz Beit-Haemek, Israel), and stained with mAbs against gp38 (clone 8.1.1), CD31 (clone 390), and CD45 (clone 30-F10) and FACS sorted (FACS Aria II, BD, Basel, CH) into the following subpopulations: FRCs ($gp38^+CD31^-$) LECs ($gp38^+CD31^+$), BECs ($gp38^-CD31^+$), and DN ($gp38^-CD31^-$) as described (23).

$CD8^+$ T cell purification

Splenic $CD8^+$ T cells from OT-I mice were isolated by immunomagnetic CD8 negative selection using the EasySep Mouse $CD8^+$ T Cell Isolation Kit from Stemcell Technologies (Vancouver, BC, Canada) according to the manufacturer's instructions.

Adoptive $CD8^+$ T cell transfer

Following $CD8^+$ T cell purification, cells were collected, washed in basal medium IMDM (Life Technologies, Carlsbad, CA, USA), and resuspended in 100µl volume prior to tail vein injection. To assess the effect of anti-VEGR3 treatment in the immune response, 10^6 naïve OT-I $CD8^+$ T cells (CD45.1.2) were adoptively transferred into C57Bl/6 mice (CD45.2).

Immunization studies

In order to induce inflammatory lymphangiogenesis, mice were injected intradermally with 15µg of CpG-B in all four limbs at a volume of 10µl/limb. As a negative control, saline (PBS) was administered instead. The subunit vaccine, consisting of 10µg of NP-OVA and 10µg of CpG-B was also administered intradermally in all four limbs. To inhibit LEC proliferation, the mice received intraperitoneally 500µg of a VEGFR-3 neutralizing antibody (mF4-31C1, ImClone/Eli Lilly), or the isotype control IgG one day prior to vaccination. Where stated, repeat administrations were injected at 3-day intervals between injections.

Tissue and cell preparation

Spleens and LNs (brachial, axillary, inguinal, popliteal) were harvested and weighed at time of killing. For lymphocyte collection, LNs were digested for 45min, in DMEM supplemented with

1mg/ml collagenase D (Roche, Basel, CH). Single-cell suspensions were obtained by gently disrupting the spleen and LNs through a 70µm cell strainer. Spleen red blood cells were lysed by treatment with ammonium chloride–potassium bicarbonate (ACK) buffer for 4min. To obtain lymph node stromal cells (LNSCs), LNs were processed as previously described (23, 24). Briefly, LNs were poked and slightly disrupted before digestion in DMEM (1.2mM $CaCl_2$, 2% FBS, Pen/Strep) containing collagenase IV (1mg/mL) and DNAse I (40µg/ml). This first fraction contained mainly $CD45^+$ cells and was collected for lymphocyte analysis. Undigested cells were further digested with 1mg/ml Collagenase D and 40µg/ml DNase I (Roche). The reaction was stopped by addition of 5mM EDTA. Following digestion, single-cell suspensions were obtained by filtering through a 70µm cell strainer. Cells were subsequently counted, stained and analyzed by flow cytometry.

In vivo antigen drainage during inflammation

To determine whether LN LECs can actively capture Ags under inflammatory conditions *in vivo*, we injected fluorescently labeled OVA protein into the limbs of mice that had been pretreated with CpG, and determined its distribution within stromal cells. Endotoxin-free OVA was labeled with Alexa Fluor 647 NHS (OVA-AF647; Dyomics) and purified by size-exclusion chromatography using a Sephadex G-25 column with PBS as eluent. Five days after CpG administration, C57BL/6 mice were injected intradermally (i.d.) with 15µg OVA-AF647 in the limbs. After 90min, mice were transcardially perfused with a heparinized saline solution containing 1g/l glucose and 20mM HEPES (pH 7.2). Brachial LNs were collected for immunostaining and flow cytometric analysis. For flow cytometric analysis, brachial LNs from individual mice were pooled and processed as described above to obtain LNSCs. Cells were counted, stained with gp38, CD31, CD45, and analyzed by flow cytometry.

Immunohistochemistry and confocal microscopy

Mice were transcardially perfused with a heparinized saline solution containing 1g/l glucose and 20mM HEPES (pH 7.2). Brachial LNs were removed and fixed overnight in 2% PFA in PBS pH 7.4. After three washes in PBS, LNs were embedded in a block of 2% agarose, and sectioned (150µm) using a using a Vibratome (Leica, Wetzlar DE). Sections were blocked in 0.5% of casein, and further labeled using antibodies against B220 (Invitrogen, Auckland, NZ, USA) and LYVE-1 (Reliatech, San Pablo, CA, US). Images were acquired on a Leica SP5 confocal microscope using 20x or 60x objectives, and processed using Imaris software (Bitplane, Zürich, CH).

In vitro LEC stimulation with inflammatory cytokines

iLECs were incubated for 24h in the presence of IFN-γ (100ng/ml) or IFN-γ and TNF-α (10ng/ml). The cells were subsequently stained for CD40, CD86, MHC I and MHC II and analyzed by flow cytometry.

In vitro $CD8^+$ T cell education by LN LECs

Naïve $CD8\alpha^+$ T-cells from OT-I mice were purified and directly cocultured with LN LECs in the presence of 1nM NP-ss-$COVA_{250\text{-}264}$. When indicated, the following molecules were also added in the coculture media (IMDM with 10% FBS and 1% penicillin/streptomycin - all from Life Technologies, Carlsbad, CA, USA): IFN-γ (100ng/ml), IFN-γ (100ng/ml) and TNF-α (10ng/ml) or CpG-B (100ng/ml). More specifically, 10^4 LECs were cocultured with naïve OT-I $CD8^+$ T cells in 96-well plates for 72h at a ratio of 1:10 APC:T cells in 200µl of co-culture media. Cells were then processed and stained for immunological markers to be analyzed by flow cytometry.

Ex vivo restimulation

Up to $3x10^6$ cells were plated in 96-well plates and cultured in coculture media for 2h at 37°C in the presence of 1µg/mL SIINFEKL peptide, followed by additional 3h treatment with

brefeldin-A (BFA, 5µg/mL). Stimulation with PMA (50ng/ml) and ionomycin (300ng/ml) served as a control. For CD107a staining, the monoclonal antibody against CD107a was added in the culture together with Monensin at 5µg/mL for 5 hours. Finally, cells were washed in PBS prior to intracellular staining for flow cytometric analysis.

Ablation of LECs *in vivo*

Prox1-CreERT2 mice were bred with *Rosa26-DTR* mice to generate Prox1-Cre-DTR mice. Prox1-Cre^{+}-DTR mice, in which Prox1^{+} cells expressed the diphtheria toxin receptor (DTR), and the Prox1-Cre^{-}-DTR littermate control mice were injected intraperitoneally with tamoxifen (TAM) daily for 3-5 days to induce expression of the Cre recombinase, two weeks prior the beginning of the study for all studies. For systemic LEC ablation, the mice received 100ng of diphtheria toxin (DT) intraperitoneally and were sacrificed 24h later to assess the efficiency of ablation in the skin-draining LNs by flow cytometry. For local ablation of LECs in the LN, the mice received either 15ng of DT intradermally in the upper footpads and sacrificed 48h later, or 1ng of DT and sacrificed at 24h, 48h and 72h following DT injection. The draining LNs were collected and analyzed by flow cytometry to evaluate LEC-specific ablation. For local ablation of lymphatic vessels in the ear, the mice were injected with 1ng of DT intradermally in the top of the ear dorsal skin, administered with a Hamilton syringe. The mice received three doses of DT with a two-day and three-day interval respectively. Three days after the last dose, the mice were sacrificed and the ear skin was collected to determine the efficiency of ablation by flow cytometry.

Lymphangiography

To assess the ablation of lymphatic vessels in the ear skin of live mice, we performed lymphangiography with the use of a fluorescent agent, followed by live imaging. The mice were anesthetized with 50mg/kg ketamine and 10mg/kg xylazine before the procedure. The head and the ears of the Prox1-Cre^{+}-DTR and the Prox1-Cre^{-}-DTR littermate control mice were depilated at the beginning of the study. Together with the administration of DT, the mice were injected with fluorescent streptavidin (SA-AF647) in the top of the ear skin and directly subjected to live imaging of the ear under a fluorescence stereomicroscope with a motorized stage (M250 FA, Leica Microsystems CMS GmbH, Wetzlar, DE) to visualize the network of the draining lymphatic vessels.

Flow cytometry

Cells were washed and stained with a cocktail of surface antibodies in staining buffer, consisting of HBSS (Life Technologies) supplemented with 0.5% bovine serum albumin. Cell viability was determined by propidium iodide incorporation in staining buffer (performed after surface antibody staining) or with live/dead fixable cell viability reagent (Life Technologies; performed according to manufacturer's instructions before surface antibody staining). Apoptotic cells were identified by annexin V staining (BioVision, Milpitas, CA, USA). Pentamer staining for H-2kb-SIINFEKL-PE (Proimmune, Oxford, UK) was performed according to manufacturer's guidelines. For VEGFR3 staining, the Goat Anti-Mouse VEGFR3 (Flt-4) polyclonal Antibody (R&D systems, Abingdon, U.K.) was used with donkey anti-goat secondary antibodies in AF647. For intracellular/intranuclear staining, cells were fixed and permeabilized with the Foxp3/Transcription Factor Fixation/Permeabilization kit (eBiosciences) according to the manufacturer's instructions. Cells were stained in permeabilization buffer with a cocktail of monoclonal antibodies. The following anti-mouse antibodies were used: CD40 (HM40-3), CD80 (16-10A1), CD86 (GL-1), MHC I (AF6-88.5), MHC II (M5/114.15.2), PD-L1 (MIH5), CD25 (PC61.5), CD69 (H1.2F3), CD4 (RM4-5), CD8a (53-6.7), B220 (RA3-6B2), CD11b (M1/70), CD11c (N418), CD62L (MEL-14), CD44 (IM7), KLRG-1 (2F1/KLRG1), CD127 (A7R34), CD45.1 (F20), CD45.2 (104), CD8 (53-6.7), CD3e (145-2C11), IFN-γ (XMG1.2), IL-2 (JES6-5H4), TNF-α (MP6-XT22), CD107 (1D4B), Granzyme-B (NGZB), ki-67 (SolA15). Finally, cells were resuspended in staining buffer and

analyzed by flow cytometry (CyAn ADP Flow Cytometer, DAKO). Data analysis was performed using FlowJo (v9.4, Tree Star Inc., Ashland, OR, USA).

Statistical analysis

Statistical analysis was performed using either unpaired Student's t test, or two-way analysis of variance (ANOVA) followed by Bonferroni post-test with Prism software (Graphpad, San Diego, CA, US) unless otherwise stated. Results are shown as mean ± standard deviation with significance indicated as *p≤0.05, **p≤0.01, and ***p≤0.001.

4.3 Results

CpG-B induces inflammatory lymph node lymphangiogenesis

In order to evaluate the direct effect of LN LEC proliferation in the induction and the outcome of immune responses, we employed a subunit vaccine model involving CpG-B as the adjuvant. We have previously observed that intradermal administration of the TLR-9 adjuvant CpG-B induces inflammatory LN lymphangiogenesis, characterized by a remarkable expansion of the LN coupled with increased proliferation and dynamic remodeling of the lymphatic structures in the draining LNs

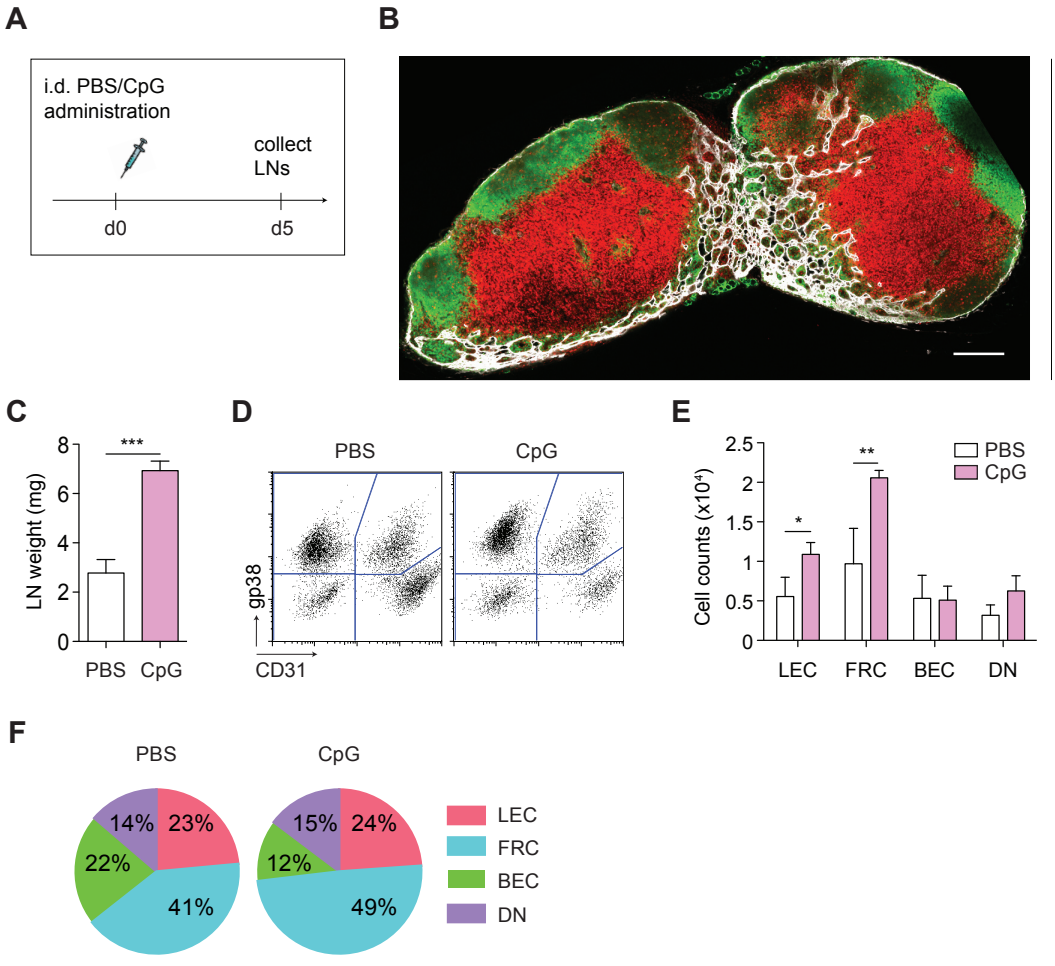

Figure 4.1 CpG-induced inflammatory lymph node lymphangiogenesis. Administration of the TLR-9 adjuvant CpG-B induces remarkable cellular expansion in the draining LN (dLN) coupled with remodeling of the lymphatic structures. 15µg of CpG-B or saline (PBS) were intradermally (i.d.) administered in the footpads of C57Bl/6 mice. 5 days after, we collected the skin-dLNs. Cell

suspensions were generated and analyzed by flow cytometry. **(A)** Experimental timeline. **(B)** Brachial lymph node section stained with LYVE-1 (white), marking lymphatic structures, CD3 (red) marking the T cel zone and B220 (green) marking B cell follicles, acquired by confocal microscopy. Scale bar, 200µm. CpG administration results in significant expansion of the LN. **(C)** Weights of LNs isolated from saline- or CpG-treated mice. CpG administration leads to expansion of LNSC populations. **(D)** Representative dot plots showing the distribution of LNSC subsets (FRCs gp38^{+}CD31^{-}, LECs gp38^{+}CD31^{+}, BECs gp38^{-} CD31^{+}, DNs gp38^{-}CD31^{-}) with gp38 on y-axis and CD31 on x-axis, gated on CD45^{-} cells. **(E)** Number of LNSCs within indicated subsets (LECs, FRCs, BECs, DNs) in saline (white bars) and CpG (pink bars) treated mice. **(F)** Pie charts displaying the distribution of LNSC subsets (LECs, pink; FRCs, blue; BECs, green; DNs, purple) in saline and CpG-treated mice as a percentage of CD45^{-} cells. Representative data from one of two independent experiments (n=4). *p≤0.05, **p≤0.01, ***p≤0.001, by two-tailed unpaired Student's t test (C) or by two-way ANOVA followed by Bonferroni posttest (E).

(dLNs). Indeed, five days following CpG administration in the footpads of C57Bl/6 mice (Fig. 4.1A), we noted a significant expansion of the dLNs, accompanied by a noticeable increase in LYVE-1^{+} structures, as determined by confocal imaging of LN sections (Fig. 4.1B). The observed expansion in size for the CpG-inflamed LNs translated to increased weight compared to the LNs of saline-treated control mice (Fig. 4.1C). Flow cytometric analysis (Fig. 4.1D, E) demonstrated a significant, two-fold, enhancement in the number of both LN LECs (determined as CD45^{-} gp38^{+}CD31^{+}) and fibroblastic reticular cells (FRCs, determined as CD45^{-}gp38^{+}CD31^{-}). The subset of blood endothelial cells (BECs, determined as CD45^{-}gp38^{-}CD31^{+}) was only slightly affected while the one of double negative cells (DNs, CD45^{-}gp38^{-} CD31^{-}) appeared enlarged but non-significantly (Fig. 4.1D). Interestingly, when we analyzed the overall distribution of the four LNSC subsets as a percentage of CD45^{-} cells in CpG-treated mice and compared to the one in control mice, the effect was much less pronounced, suggesting that the relative LNSC subset composition was maintained (Fig. 4.1F).

LN LECs can take up exogenous antigen under inflammatory conditions *in vivo*

We have previously shown that LN LECs can scavenge exogenous antigen *in vivo* under steady-state conditions [Chapter 2, (17)]. Here, we wanted to verify whether LECs in the CpG-inflamed LN would also exhibit such function.

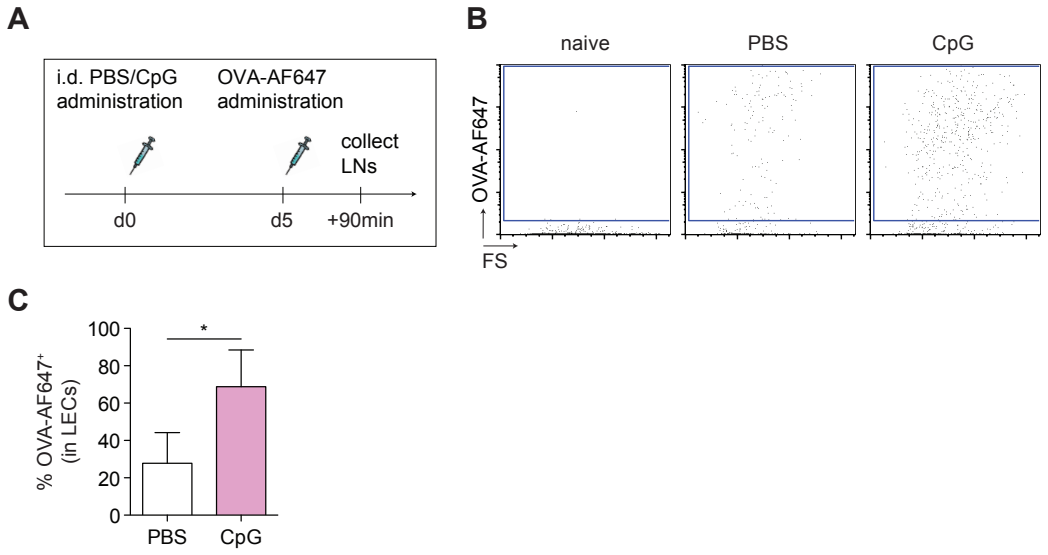

Figure 4.2 LN LECs take up exogenous antigen not only under steady-state but also under inflammatory conditions. Following i.d. injection into the footpads, inflamed LECs in the dLNs take up

OVA rapidly. 15μg of CpG-B or saline (PBS) were i.d. administered in the footpads of C57Bl/6 mice. Mice rested for five days before fluorescently-labeled OVA (OVA-AF647) was administered. 90 min after injection, the mice were sacrificed and skin-dLNs were collected. Cell suspensions of skin-dLNs were generated and analyzed by flow cytometry. Almost 3-fold higher uptake of OVA in LECs from CpG-inflamed LNs. **(A)** Experimental timeline. **(B)** Representative dot plots with OVA-AF647 on y-axis and the forward scatter on x-axis showing OVA positive cells gated on $gp38^{+}CD31^{+}$ LECs in saline (PBS, middle) and CpG-treated (right) mice. As a negative control, LECs from an untreated mouse are shown (naïve, left) and served to set the gate for OVA^{+} cells. **(C)** The graph displays the percentage of OVA^{+} LECs in saline and CpG-treated mice. Pooled data from 2 independent experiments (n=5). *p≤0.05, by two-tailed unpaired Student's t test.

To address this, we administered fluorescently labeled OVA protein (OVA-AF647) i.d. in the footpad of C57Bl/6 mice that have been injected with CpG five days earlier (Fig. 4.2A). Flow cytometric analysis revealed OVA uptake by LECs in the CpG-inflamed LN (Fig. 4.2B, C). More importantly, we observed that LN LECs ($CD45^{-}$ $gp38^{+}CD31^{+}$) in the CpG-treated (CpG) mice more avidly internalized OVA-AF647 compared to the LN LECs in saline-treated (PBS) control mice (Fig. 4.2C). Our findings validate that LN LECs can actively scavenge soluble exogenous antigen not only during homeostasis but also under inflammatory conditions.

LECs in the CpG-inflamed LN retain the low levels of costimulation and further upregulate MHC II, PD-L1 and VEGFR3

We have earlier demonstrated that Ag-specific interactions between LECs and $CD8^{+}$ T cells result in activated $CD8^{+}$ T cells, which appear temporarily inactive and display central memory-like characteristics [Chapter 3 and (17)]. Such an outcome was associated with the phenotypic profile of LECs characterized by high levels of the inhibitory ligand PD-L1 coupled to very low levels of costimulation. We asked whether the phenotype of LN LECs would be altered following CpG-administration. To this end, we assessed the expression of different costimulatory or coinhibitory molecules and receptors in LECs in the LNs of mice that had been treated with CpG five days earlier and compared it to that of control mice (Fig. 4.3A). Treatment with CpG only slightly affected the expression of the costimulatory molecules CD40, CD86 and CD80 in LN LECs (Fig. 4.3B, C), an effect that has been previously observed following administration of other adjuvants (25). More specifically, the expression of CD80 was three-fold increased relative to LECs from control saline-treated mice, although low levels were detected (Fig. 4.3C). Interestingly, we observed a notable increase in the levels of the MHC class II receptor, the inhibitory ligand PD-L1 as well as the lymphatic endothelium receptor, VEGFR3. Taken together, LEC phenotype is influenced by CpG administration, in a fashion that is similar to our previous findings following direct interactions of LN LECs with $CD8^{+}$ T cells *in vitro* [Chapter 2 and (17)].

In previous studies, in which we had assessed the cytokine microenvironment of the CpG-inflamed LN using an ELISA multiplex system (data not shown), we have observed abundance of inflammatory cytokines, including high levels of IFN-γ and TNF-α. By incubating skin-derived immortalized lymphatic endothelial cells (iLEC) for 24h in the presence of IFN-γ with or without TNF-a, we detected a similar phenotype to the one observed upon CpG treatment *in vivo* (Fig. 4.3D). We detected almost no expression of the costimulatory molecules CD40 and CD86 and increased levels of the MHC class I and II receptors following IFN-γ or combinatory IFN-γ plus TNF-a treatment. Taken together, our data suggest that the balance between costimulatory

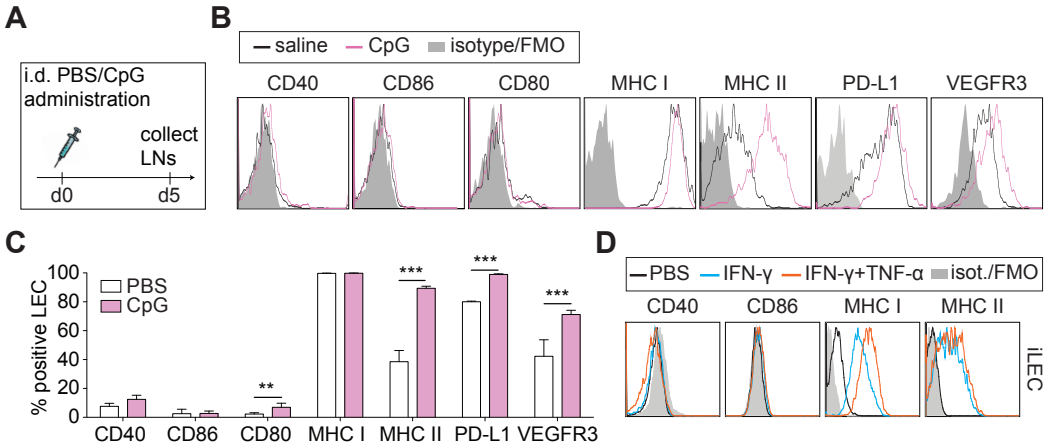

Figure 4.3 Immune status of inflamed LECs. LECs in the CpG-inflamed LN retain the low levels of costimulation and further upregulate MHC II, PD-L1 and VEGFR-3. 15μg of CpG-B or saline (PBS) were i.d. administered in the footpads of C57Bl/6 mice. 5 days after, the mice were sacrificed and dLNs collected. Cell suspensions were generated and the expression levels of CD40, CD86, CD80, MHC class I, MHC class II, PD-L1 and VEGFR-3 were determined by flow cytometric analysis. **(A)** Experimental timeline. **(B)** Representative histograms for each marker in gp38$^+$CD31$^+$-gated LN LECs from PBS (black line) or CpG (pink line) treated mice. **(C)** Percentage of positive cells for each marker within gp38$^+$CD31$^+$-gated LN LECs from saline (white bars) and CpG (pink bars) treated mice. **(D)** Treatment of LECs with IFN-γ or IFN-γ and TNF-α induces increase in the expression of MHC I and MHC II but does not alter the expression of costimulatory molecules *in vitro*. iLECs were incubated for 24h in the presence of IFN-γ (100ng/ml, blue line) or IFN-γ and TNF-α (10ng/ml, orange line). The expression levels of costimulatory molecules CD40, CD86, MHC I and MHC II were determined by flow cytometric analysis. Representative histograms for each marker in gp38$^+$CD31$^+$-gated LN LECs. Solid gray line: isotype/FMO control. Representative data from one of two independent experiments (n=4). **p≤0.01, ***p≤0.001, by two-way ANOVA followed by Bonferroni posttest (C).

and coinhibitory ligand expression in LECs is not altered under inflammatory conditions.

The phenotype of *in vitro* LEC-educated CD8$^+$ T cells is not altered in the presence of CpG or inflammatory cytokines

We next sought to determine whether the phenotype of CD8$^+$ T cells educated by inflamed LN LECs would be different than the one observed under steady-state conditions. To address this question, we cocultured OT-I CD8$^+$ T cells with LN LECs in the presence of NP-ss-COVA$_{250-264}$, as previously performed [Chapter 2 and (17)], adding IFN-γ, IFN-γ and TNF-α, or CpG in the coculture media (Fig. 4.4A). Following three days of coculture, we assessed the expression of different activation markers (CD25, CD44, CD69, CD62L) on the surface of LEC-educated CD8$^+$ T cells. We failed to detect any remarkable differences in the expression levels of CD25, CD44 and CD69 whether the cells were educated in the presence of IFN-γ, IFN-γ and TNF-α or CpG (Fig. 4.4B), compared to being cultured in the presence of the antigen alone (none). Adding to that, LEC-educated CD8$^+$ T cells cultured in the presence of IFN-γ or CpG displayed high levels of CD62L (Fig. 4.4C) with the percentage of the CD44$^+$CD62L$^+$ subset, among educated CD8$^+$ T cells, being maintained at levels similar to those observed following incubation with antigen alone (Fig. 4.4C, D). Collectively, our findings indicate that the activation status and the central memory-like phenotypic profile of LEC-educated CD8$^+$ T cells are retained under inflammatory conditions.

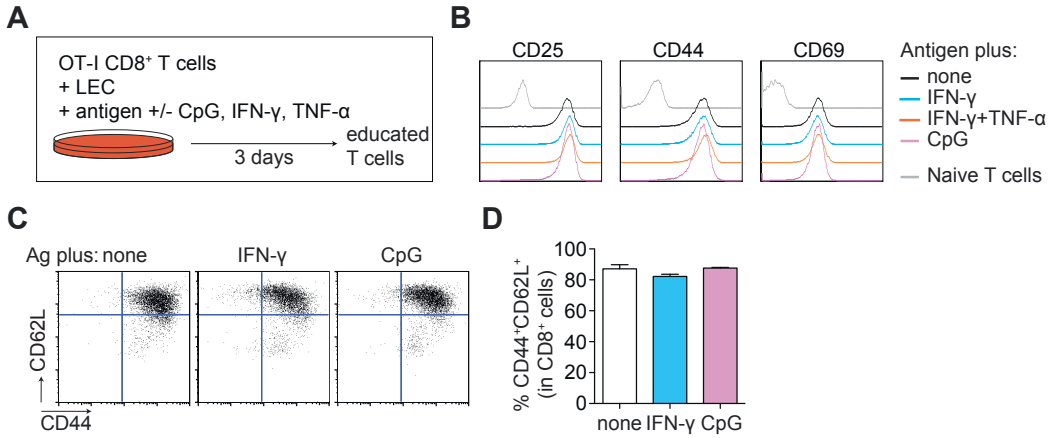

Figure 4.4 The phenotype of *in vitro* LEC-educated CD8$^+$ T cells is not altered in the presence of CpG or inflammatory cytokines. OT-I CD8$^+$ T cells were educated by LN LEC in the presence of NPssCOVA$_{250-264}$ (1nM) alone (black line) or together with either IFN-γ (100ng/ml, blue line), IFN-γ and TNF-α (10ng/ml, orange line) or CpG (100ng/ml, pink line). After 3 days of coculture, LEC-educated CD8$^+$ T cells were harvested, stained for different surface markers and analyzed by flow cytometry. **(A)** Experimental timeline. The expression levels of activation markers in LEC-educated CD8$^+$ T cells are not affected by the presence of inflammatory cytokines or CpG. **(B)** Representative histograms of T cell activation markers (CD25, CD44, CD69). Grey line: isotype/FMO control. **(C)** Representative flow cytometry dot plots with CD62L on y-axis and CD44 on x-axis on day 3 of the coculture in LEC-educated CD8$^+$ T cells in the presence of NPssCOVA$_{250-264}$ alone (none), or together with IFN-γ or CpG. **(D)** Percentage of T_{CM}-like CD44$^+$CD62L$^+$ cells within LEC-educated CD8$^+$ T cells. Representative data from one of two independent experiments (B, n=3) or data are from one experiment (C, D) n=3.

The cellular composition of the stromal and hematopoietic compartment in the lymph node following immunization is not greatly affected by treatment with the anti-VEGFR3 blocking antibody

Having confirmed that LN LECs can take up exogenous antigen under inflammatory conditions, as well as that the costimulatory/coinhibitory molecule balance on their surface is not reversed during inflammation, we moved forward to evaluate the direct impact of LEC-education in the induction of immune responses. For that purpose, we decided to employ a subunit vaccine model and exploit the anti-VEGFR3 antibody (aR3), which has been previously used in our laboratory and shown to reduce lymphangiogenesis in the context of solid tumors and ovarian follicles [(26, 27) and unpublished observations]. As a subunit vaccine model, we decided to combine the nanoparticle (NP) vaccine platform established in our laboratory (NP-OVA) together with the CpG-B adjuvant. This particular subunit vaccine induces remarkable expansion of the LN accompanied by robust CD8$^+$ T cell responses, while LN LECs can also take up and process the NP-OVA formulation for MHC I presentation, as previously shown (20).

We first sought to evaluate the effect of aR3 treatment on the cellular composition of the lymph node in the course of an immune response. We intraperitoneally administered the aR3 antibody or the IgG control into C57Bl/6 mice one day prior to intradermal immunization in the footpad with NP-OVA plus CpG-B. The mice received one more dose of the blocking antibody or the IgG control and were sacrificed five days after immunization (Fig. 4.5A) to analyze the cellular distribution in the dLNs. Immunofluorescence microscopy of LN sections demonstrated some noticeable changes in the morphology and organization of the lymphatic network following treatment with the aR3 blocking antibody (Fig. 4.5B), which might indicate a

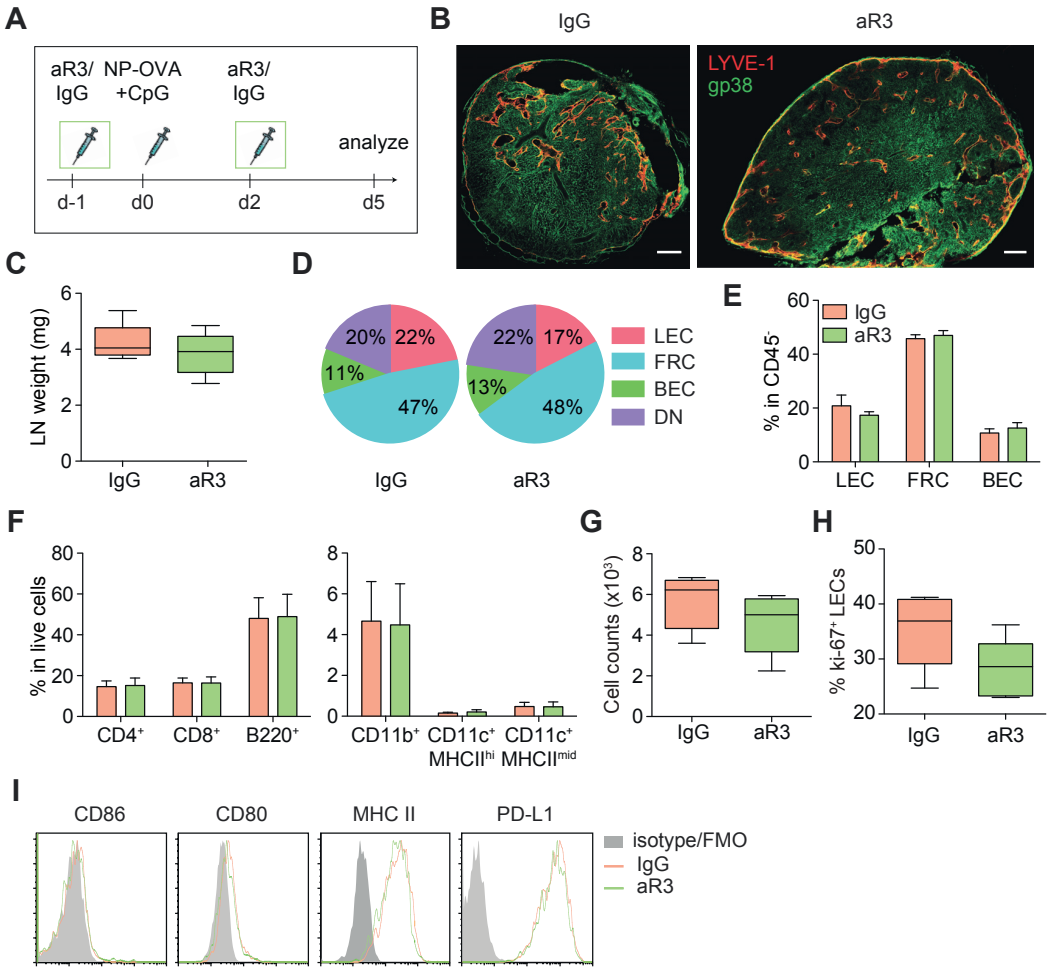

Figure 4.5 Treatment with anti-VEGFR3 does not significantly affect the relative cellular distribution of stromal and hematopoietic cells subsets in the LN following immunization. The anti-VEGFR3 (aR3) antibody or IgG control antibody (500µg) were administered intraperitoneally (i.p.) in C57Bl/6 mice one day prior to i.d. immunization in the footpads with CpG-B (10µg) and NP-OVA(10µg). 2 days after, the mice received a second dose of aR3 or IgG (i.p.). They were sacrificed 5 days after immunization and the dLNs were collected., Cell suspensions were generated and analyzed by flow cytometry. **(A)** Experimental timeline. **(B)** Popliteal LN sections from IgG or aR3 –treated mice stained with LYVE-1 (red) and gp38 (green), acquired by confocal microscopy. Scale bar, 150µm. **(C)** Weights of LNs isolated from IgG- (light orange) or aR3- (green) treated mice. Only slight changes were observed in the percentage and counts of LECs in response to aR3 treatment. **(D)** Pie charts showing the distribution of LNSC subsets, with respect to IgG or aR3 treatment, among $CD45^-$ cells, defined as: LEC (pink), $gp38^+CD31^+$; FRC (blue), $gp38^+CD31^-$; BEC (green), $gp38^-CD31^+$; DN (purple), $gp38^-CD31^-$. **(E)** Percentage of LECs, FRCs and BECs within $CD45^-$ cells in response to IgG (light orange bars) or aR3 (green bars) treatment. **(F)** Percentage of CD4 ($CD4^+$) and CD8 ($CD8^+$) T cells, B cells ($B220^+$) and different antigen-presenting cell subsets ($CD11b^+$, $CD11c^+$MHC II^{hi}, $CD11c^+$ MHC II^{mid}) in live cells in response to IgG or aR3 treatment. The various cells subsets are defined as it follows: $CD4^+$, $CD3^+CD8^-CD4^+$; $CD8^+$, $CD3^+CD4^-CD8^+$; $B220^+$, $CD3^-B220^+$; $CD11b^+$, MHC II^+CD11b^+; $CD11c^+$MHC II^{hi}, $CD11b^-CD11c^+$MHC II^{high}; $CD11c^+$MHC II^{mid}, $CD11b^-$ $CD11c^+$MHC II^{mid}. **(G)** Counts of LECs in IgG- or aR3-treated mice. **(H)** Percentage of ki-67 positive cells within LECs in response to IgG or aR3 treatment. **(I)** The expression levels of the costimulatory molecules CD86 and CD80, the MHC class II receptor and the coinhibitory ligand PD-L1 in LECs are not altered with respect to aR3 treatment. Representative histograms of each marker within $gp38^+CD31^+$-gated LN LECs in IgG (light orange line) or CpG (green line) treated mice. Solid grey line: isotype/FMO control . Pooled data from two (C, n=8) or three independent experiment (F, n=11) or representative data from one out of two independent experiments (D-E, n=3; G-H, n=5). Two-tailed unpaired Student's t test (C, G-H) or two-way ANOVA followed by Bonferroni posttest (D-F).

decrease in the density of LYVE-1 positive structures. However, systematic quantitative analysis should be performed in order to confirm those qualitative observations. We also detected a slight, non-statistically-significant, decrease in LN weight in mice treated with aR3 compared to the IgG-treated control mice (Fig. 4.5C).

Modest changes were also observed in the frequency of LECs ($gp38^+CD31^+$) and the other LNSC subsets among $CD45^-$ cells in response to aR3 treatment (Fig. 4.5D, E). More specifically, we noted a small decrease in the percentage of LECs while FRCs ($gp38^+CD31^-$) and BECs ($gp38^-CD31^+$) appeared slightly enhanced; however, these changes were not statistically significant. We also failed to detect any alteration in the composition of the hematopoietic cell compartment; there were no differences in the frequencies of CD4 ($CD4^+$) and CD8 ($CD8^+$) T cells, B cells ($B220^+$) or various professional antigen-presenting cell subsets ($CD11b^+$, $CD11c^+$MHC II^{hi}, $CD11c^+$ MHC II^{mid}) among all live cells (Fig. 4.5F) in aR3-treated relative to IgG-treated mice. Although VEGFR3 expression has been mainly known to be limited in the lymphatic endothelium in adult tissue, it has been also reported in activated macrophages (28) and specialized monocytic populations in the ocular region (29). Macrophages have been well described to drive lymphangiogenesis in inflamed tissues and dLNs via the secretion of VEGFs (7). Surprisingly, we did not observe any significant changes in the subset of $CD11b^+$ cells in response to aR3 treatment, but only slightly lower frequencies in aR3-treated mice (Fig. 4.5F, on the right). Further characterization of the macrophage subset in the inflamed LN, including the use of more detailed markers, might be necessary in order to verify our observations. Along with the observed trend for lower frequency of LECs in the aR3-treated mice, we further noted a trend for lower absolute LEC counts per LN (Fig. 4.5G) as well as lower levels of the ki-67 protein (Fig. 4.5H), which is indicative of cell proliferation. More specifically, while aR3 treatment reduced the number and proliferation levels of LECs by 11% and 20% respectively, relative to control-treated mice, none of these trends were statistically significant. Additional analysis of the phenotype of LN LECs in response to aR3 treatment revealed no effect in the expression of costimulatory molecules (CD86 and CD80), MHC class II receptor or PD-L1 (Fig. 4.5I).

Although we observed a consistent trend for a slight contraction of the LEC population as well as a decreased proliferation rate, treatment with aR3 did not seem to significantly inhibit LN lymphangiogenesis following subunit vaccine immunization.

Treatment with anti-VEGFR3 only moderately influences the induction and the functional outcome of the primary and secondary $CD8^+$ T cell immune response

Even though the effects of aR3 treatment in limiting lymphangiogenesis were mild at best, we attempted to evaluate its impact in the induction of immune responses. Yang et al. have very recently shown that FRC expansion in the LN following immunization relied primarily on trapping of naïve lymphocytes (13), while a pharmacologic inhibitor of VEGF-receptor signaling only partially affected the cellularity and proliferation of FRCs. Therefore, a variety of factors might affect the expansion of stromal cells in the dLN at the onset of immune responses and thus, mask the effects of aR3 treatment. However, we thought that we might still be able to detect its influence in the initiation of adaptive immunity, as reflected in antigen-specific $CD8^+$ T cells. To address this question, we adoptively transferred OT-I $CD8^+$

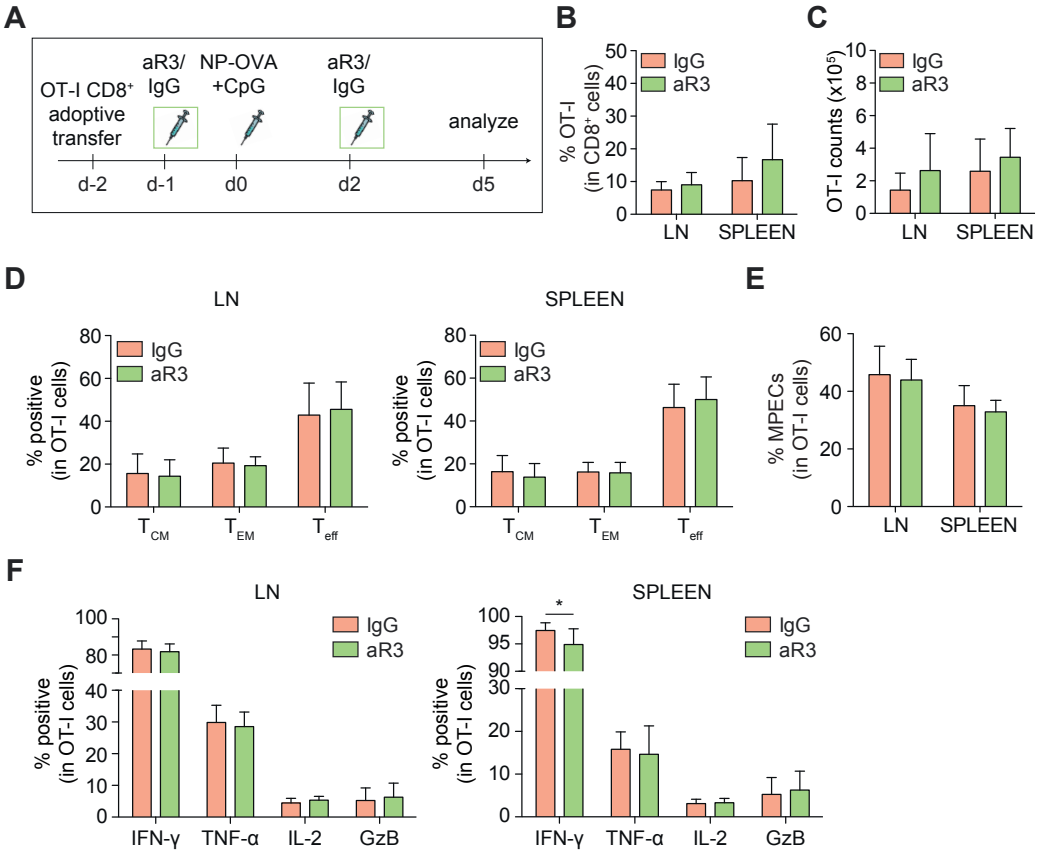

Figure 4.6 Anti-VEGFR3 treatment does not greatly impact the induction and the outcome of the primary CD8$^+$ T cell immune response in an adoptive transfer model. CD45.1.2 OT-I CD8$^+$ T cells (10^6 cells/mouse) were transferred i.v. in CD45.2 C57Bl/6 mice (day -2). The day after (day -1), aR3 or control IgG antibody (500µg) were administered i.p. After 24h, (day 0), the mice were immunized (i.d) with CpG-B (10µg) and NP-OVA (10µg) in the footpads. 2 days after immunization, the mice received a second dose of aR3 or IgG antibody (i.p.). The mice were sacrificed 5 days after immunization and the dLNs and spleen were collected. Cell suspensions were generated and analyzed by flow cytometry. The expansion and phenotype of OT-I CD8$^+$ T cells following immunization is not altered in response to aR3 treatment. **(A)** Experimental timeline. **(B)** Percentage of OT-I cells within CD8$^+$ T cells in the LNs and spleen of IgG (light orange bars) and aR3 (green bars) –treated mice. **(C)** Number of OT-I cells. **(D)** Percentage of T_{CM}-like (CD44$^+$CD62L$^+$CD127$^+$), T_{EM}-like (, CD44$^+$CD62L$^-$ CD127$^+$) and T_{eff}-like (CD44$^+$CD62L$^-$ CD127$^-$) cells in OT-I cells in the LNs (left) and spleen (right) of IgG/aR3-treated mice. **(E)** Percentage of memory precursor effector cells (MPECs, CD44$^+$KLRG-1$^-$CD127$^+$) among OT-I cells in the LNs and spleen of IgG/aR3-treated mice. The functional potential of OT-I CD8$^+$ T cells is not substantially affected by aR3 treatment. The cells were subjected to 5h *ex vivo* restimulation with SIINFEKL peptide, followed by intracellular staining. **(F)** Percentage of IFN-γ$^+$, TNF-α$^+$, IL-2$^+$ and GzB$^+$ cells (in OT-I cells) in the LNs (left) and spleen (right) of IgG/aR3-treated mice. Pooled data from two (F, n=10) or three (B-E, n=15) independent experiments. *p≤0.05, using two-tailed unpaired Student's t test.

T cells (CD45.1.2) in C57Bl/6 (CD45.2) mice (day -2) one day prior to treating the mice with the aR3 or IgG control antibody (day -1). The adoptive transfer system was selected because it provides a larger number of easily traceable antigen-specific CD8$^+$ T cells. We subsequently immunized the mice with the NP-OVA plus CpG subunit vaccine (day 0). Two days after immunization (day 2), the mice received a second dose of the aR3 or IgG antibody and we sacrificed the mice on day 5 after immunization to analyze the phenotype and function of the antigen-specific OT-I CD8$^+$ T cells (Fig. 4.6A). The cellular expansion of OT-I CD8$^+$ T cells following immunization was not altered in response to treatment with the aR3 antibody, as determined by analyzing the percent frequency of CD45.1$^+$ OT-I cells in total CD8$^+$

cells (Fig. 4.6B), as well as in terms of absolute OT-I cell counts in the LN and spleen (Fig. 4.6C). Adding to that, we failed to detect any significant differences in the phenotype of OT-I cells in the LNs and spleen of IgG/aR3-treated mice (Fig. 4.6D, E). More specifically, we assessed the percentage of central memory-like (T_{CM}, $CD44^+CD62L^+CD127^+$), memory effector-like (T_{EM}, $CD44^+CD62L^-$ $CD127^+$) and effector-like (T_{eff}, $CD44^+CD62L^-$ $CD127^-$) cell subsets within OT-I $CD8^+$ T cells in the LNs and spleen of IgG/aR3-treated mice and did not observe any significant differences between the two groups (Fig. 4.6D). Along the same lines, the percentage of memory precursor effector cells (MPECs, $CD44^+KLRG\text{-}1^-CD127^+$) among OT-I $CD8^+$ T cells in the LN and spleen of IgG/aR3-treated mice was similar (Fig. 4.6E). More importantly, the functional potential of OT-I $CD8^+$ T cells was also not substantially affected by aR3 treatment (Fig. 4.6F). Following *ex vivo* restimulation with the SIINFEKL peptide, the percentage of IFN-γ, TNF-α, IL-2 and GzB positive cells, among OT-I $CD8^+$ T cells, in the LN was quite similar in IgG versus aR3-treated mice with a trend for lower levels of IFN-γ and TNF-α positive cells in the aR3-treated. We observed identical trends in the spleen, in which the frequency of IFN-γ – producing cells in aR3-treated mice was decreased by approximately 3% relative to IgG-treated mice.

The next step was to determine whether aR3 treatment would impact the secondary immune response. The lower levels of IFN-γ positive cells might indicate a smaller pool of functional antigen-specific cells in aR3-treated mice. We speculated that the effect of aR3 treatment might be more pronounced following a recall response. To investigate this, we performed adoptive transfer studies following the same timeline described above, however this time, the mice received an additional dose of IgG/aR3 on day 5 and were left to rest for approximately 6 weeks following immunization (Fig. 4.7A). We then challenged the mice (day 45) with the re-administration of NP-OVA plus CpG (i.d.). We sacrificed the mice seven days after the challenge immunization and analyzed the cellular expansion and phenotypic profile of OT-I $CD8^+$ T cells in the LN and spleen. Similar to our observations in the course of the primary immune response, we did not detect any differences in the frequency of OT-I cells (Fig. 4.7B) or the OT-I counts (Fig. 4.7C) in the LN and spleen between IgG and aR3-treated mice following secondary challenge. In addition to that, there was no noticeable difference in the distribution of the T_{CM}, T_{EM}, and T_{eff} subsets among antigen-specific OT-I $CD8^+$ T cells in the LN and spleen (Fig. 4.7D) of IgG/aR3-treated mice. The cytokine-producing capacity of OT-I $CD8^+$ T cells following *ex vivo* antigen-specific restimulation was also analyzed and was not markedly affected by aR3 treatment. More specifically, the frequency of IFN-γ, IL-2 and GzB positive cells (among OT-I $CD8^+$ T cells) in the LN was identical in IgG/aR3-treated mice with a non-statistically-significant trend for lower levels of TNF-α positive cells in aR3-treated mice (Fig. 4.7E). A similar trend, still non-significant, for a smaller compartment of IFN-γ and TNF-α expressing cells in aR3-treated mice was observed whereas we noticed a two-fold decrease in the percentage of IL-2 producing cells in the mice that received the aR3 antibody (Fig. 4.7F). Along with the lower frequency, we further noted decreased counts of IL-2 positive cells in terms of absolute numbers in the spleen (Fig. 4.7G). The smaller IL-2 positive subset might reflect a smaller memory compartment established after the primary immune response.

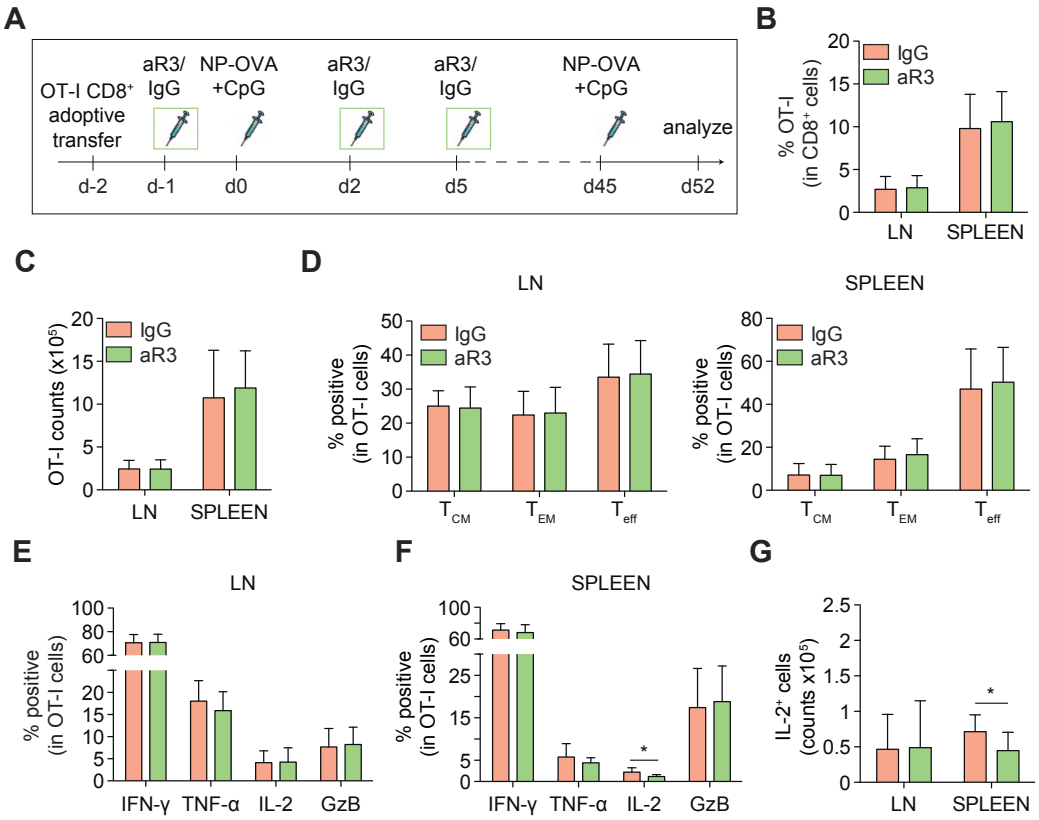

Figure 4.7 Treatment with anti-VEGFR3 only slightly influences the functional outcome of the secondary CD8$^+$ T cell response in an adoptive transfer model. CD45.1.2 OT-I CD8$^+$ T cells (10^6 cells/mouse) were transferred i.v. in CD45.2 C57Bl/6 mice (day -2). The day after (day -1), aR3 or control IgG antibody (500µg) were administered i.p. After 24h, (day 0), the mice were immunized (i.d) with CpG-B (10µg) and NP-OVA(10µg). 2 days and 5 days after immunization, the mice received a second dose of aR3 or IgG (i.p.). The mice rested for 6 weeks before they were challenged with the administration (i.d) of CpG-B (10µg) and NP-OVA (10µg). 7 days after challenge the mice were sacrificed and the dLNs and spleen collected. Cell suspensions were generated and analyzed by flow cytometry. The cellular expansion and phenotypic profile of OT-I CD8$^+$ T cells in a secondary response are not altered in response to aR3 treatment. **(A)** Experimental timeline. **(B)** Percentage of OT-I cells within CD8$^+$ T cells in the LN and spleen of IgG (light orange bars) and aR3 (green bars) –treated mice . **(C)** Number of OT-I cells. **(D)** Percentage of T_{CM}-like (CD44$^+$CD62L$^+$CD127$^+$), T_{EM}-like (CD44$^+$CD62L$^-$ CD127$^+$) and T_{eff}-like (CD44$^+$CD62L$^-$ CD127$^-$) cells within OT-I cells in the LNs (left) and spleen (right) of IgG/aR3-treated mice. The cytokine-producing capacity of OT-I CD8$^+$ T cells following a secondary challenge is not markedly affected by aR3 treatment. The cells were subjected to 5h *ex vivo* restimulation with SIINFEKL peptide, followed by intracellular staining. Percentage of IFN-γ$^+$, TNF-α$^+$, IL-2$^+$ and GzB$^+$ cells (within OT-I cells) in the LNs **(E)** and spleen **(F)** of IgG/aR3-treated mice. **(G)** Number of IL-2$^+$ OT-I cells in the LN and spleen of IgG/aR3-treated mice. Pooled data from two independent experiments (n=12). *p≤0.05, using two-tailed unpaired Student's t test.

We speculated that the adoptive transfer system might not allow us to clearly identify the differences between the aR3 and IgG-treated mice due to the great abundance of antigen-specific CD8$^+$ T cells available and thus, hinder the impact of aR3 treatment in immune responses. Therefore, we performed similar studies analyzing the capacity, phenotype and functional potential of endogenous antigen-specific CD8$^+$ T cells following primary immunization as well as secondary antigenic challenge. In the setting of a primary immune response (Fig. 4.8A), five days following immunization with the NP-OVA plus CpG subunit vaccine, we detected a non-significant trend for decreased levels of antigen-specific CD8$^+$ T cells in the LN and spleen of aR3-treated mice (Fig. 4.8B), as determined by staining with the H2kb-SIINFEKL pentamer. The absolute counts of pentamer positive cells in the LN and spleen

reflected the same trend (Fig. 4.8C). Analyzing the phenotype of the antigen-specific CD8$^+$ T cells, we observed a significantly lower frequency of the T_{EM} (CD44$^+$CD62L$^-$ CD127$^+$) subset in the LN of mice that received the aR3 antibody but not in the spleen (Fig. 4.8D).

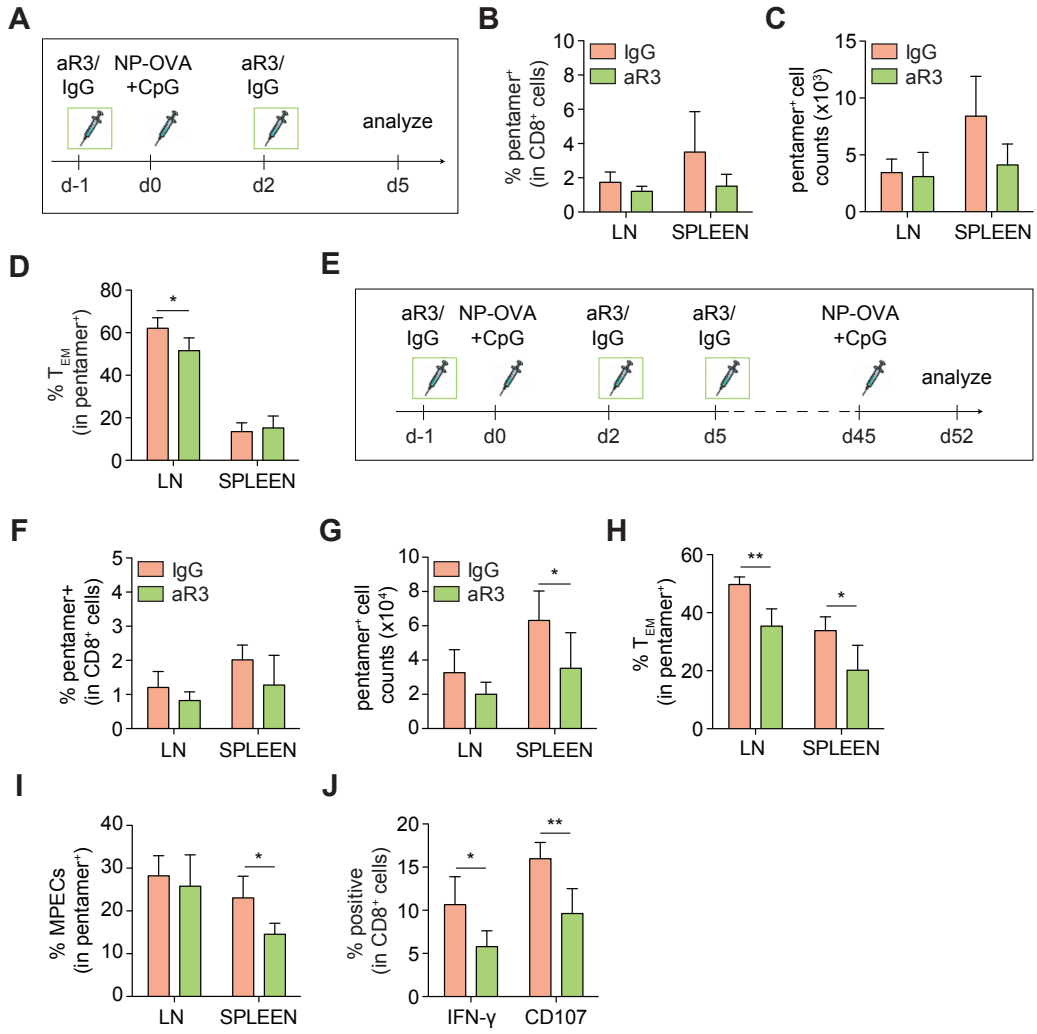

Figure 4.8 The expansion capacity, phenotype and functional potential of endogenous antigen-specific CD8$^+$ T cells are not remarkably altered in response to anti-VEGFR3 treatment following primary immunization as well as secondary antigenic challenge. The aR3 or the control IgG antibody (500μg) were administered (i.p.) in C57Bl/6 mice one day prior to i.d. immunization in the footpads with CpG-B (10μg) and NP-OVA (10μg). 2 days after immunization, the mice received a second dose of aR3 or IgG (i.p.). The mice were sacrificed 5 days after immunization and the dLNs and spleen were collected. Cell suspensions were generated and analyzed by flow cytometry. **(A)** Experimental timeline. **(B)** Percentage of antigen-specific cells (within total CD8$^+$ T cells) in the LNs and spleen of IgG (light orange bars) and aR3 (green bars) –treated mice, as determined by SIINFEKL-pentamer staining. **(C)** Number of antigen-specific CD8$^+$ T cells. **(D)** Percentage of T_{EM}-like (CD44$^+$CD62L$^-$ CD127$^+$) cells in pentamer$^+$ cells. Treatment with aR3 only moderately affects the phenotypic and functional profile of endogenous CD8$^+$ T cells in a secondary response. The mice were treated as in (A), but 5 days after immunization, they received an extra dose of aR3/IgG (i.p.). The mice rested for six weeks before they were challenged with the administration (i.d) of CpG-B (10μg) and NP-OVA(10μg) in the footpads. 7 days after the challenge immunization, the mice were sacrificed and the dLNs and spleen were collected. **(E)** Experimental timeline. **(F)** Percentage of pentamer$^+$ cells (within CD8$^+$ T cells) in the LNs and spleen of IgG/aR3-treated mice. **(G)** Number of pentamer$^+$ cells. **(H)** Percentage of T_{EM}-like (CD44$^+$CD62L$^-$ CD127$^+$) cells in pentamer$^+$ cells.. **(I)** Percentage of MPECs, among pentamer$^+$ cells . **(J)** Percentage of IFN-γ$^+$ and CD107$^+$ cells (within CD8$^+$ T cells) in the spleen of IgG/aR3-treated mice. Data from one experiment (n=5). *p≤0.05, **p≤0.01, by two-way ANOVA followed by Bonferroni posttest (A-D, F-H, J or by two-tailed unpaired Student's t test (I).

Along the same lines, seven days following secondary immunization (Fig. 4.8E), we noted a similar trend for reduced frequency of antigen-specific cells, among total $CD8^+$ T cells, in the LN and spleen of aR3-treated mice (Fig. 4.8F) while the absolute counts of pentamer positive cells in the spleen were almost two-fold lower (Fig. 4.8G). Adding to that, phenotypic analysis revealed that the T_{EM} subset contracted both in the LN (by 29%) and spleen (by 40%) in mice that received the aR3 antibody relative to the IgG-treated ones (Fig. 4.7H). Together with that, the T_{MPEC} compartment among pentamer positive $CD8^+$ T cells was also decreased in the spleen of aR3-treated mice and a similar non-significant trend was observed in the LN (Fig. 4.8I). More importantly, following antigen-specific *ex vivo* restimulation, we observed that the percentage of IFN-γ and CD107 expessing cells (among $CD8^+$ T cells) in the spleen of aR3-treated mice was reduced by 46% and 40% respectively, compared to control-treated mice (Fig 4.8J). Furthermore, similar observations were noted with regard to the expansion capacity, the phenotypic characteristics as well as the functional potential of antigen-specific $CD8^+$ T cells when we employed a bacterial pathogen (*Listeria monocytogenes* – expressing OVA), instead of the subunit vaccine, for the secondary challenge immunization (data not shown).

Collectively, our findings indicate that by using an adoptive transfer model, we did not manage to detect a notable effect of aR3 treatment in the outcome of the primary and secondary antigen-specific $CD8^+$ T cell response following immunization with a subunit vaccine. Instead, studying the endogenous $CD8^+$ T cell compartment suggested that the administration of the aR3 antibody might slightly limit LEC proliferation and subsequently result in a contracted pool of antigen-specific $CD8^+$ T cells with decreased effector function potential upon secondary challenge. Although these studies give us a first hint for the direct immunological role of LEC proliferation, they still need to be repeated in order to confirm our findings. Further investigation is required to better understand how LEC expansion might be linked to antigen-specific $CD8^+$ T cell proliferation and thus, determine the impact of LECs in the generation of adaptive immunity.

Generation of the Prox1-DTR transgenic mouse model in which LECs can be selectively ablated

Our second approach to evaluate the contribution of $CD8^+$ T cell priming by LECs in the induction of an immune response was the generation of a mouse model that would allow selective deletion of LECs. We used the Cre/lox site-specific recombination system to establish and study such a transgenic mouse model. Our system involved the inducible diphtheria toxin receptor (DTR), part of the heparin-binding epidermal growth factor-like growth factor, which has been established as a tool for conditional lineage ablation (30). Unlike primate cells, murine cells are not susceptible to diphtheria toxin (DT) due to the low affinity of DT for rodent heparin-binding epidermal growth factor-like growth factor. Expression of DTR on the cell surface enables endocytosis of DT and subsequently, rapid apoptosis of the target cell. To obtain a model that allows for specific deletion of LECs, we crossed mice with the gene encoding the DTR downstream of a loxP- flanked transcriptional stop element in the Rosa26 locus (31) (Floxed mouse) to Prox1-CreERT2 mice (Cre mouse) (Figure 4.9). Prox1-CreERT2 mice express Cre recombinase under the control of the Prox1 promoter and the Cre enzyme is only active upon treatment with

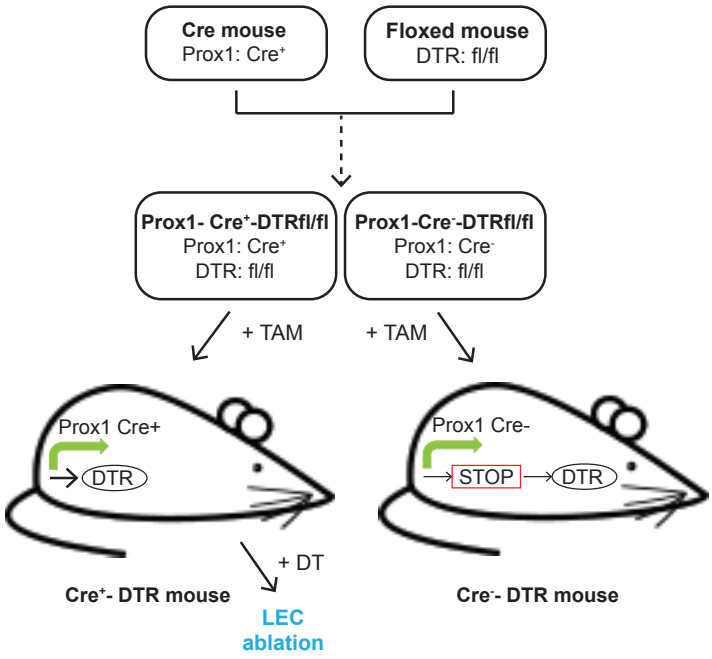

Figure 4.9 Generation of the Prox1-DTR transgenic mouse model in which LECs can be selectively ablated. To evaluate the contribution of $CD8^+$ T cell priming by LECs in the induction of immune responses, we sought to generate a mouse model that would allow selective deletion of LECs. Briefly, we crossed mice with the gene encoding the simian diphtheria toxin receptor (DTR) downstream of a loxP-flanked transcriptional stop element (Floxed mouse) to Prox1-CreERT2 mice (Cre mouse), which express Cre recombinase under the control of the Prox1 promoter. The expression of Cre recombinase in the Cre mouse is an inducible phenotype. The Cre enzyme is only active upon treatment with tamoxifen (TAM). In the progeny of interest, cells bearing the Prox1 promoter (LEC) express the DTR and are prone to toxin-induced apoptosis once exposed to DT (LEC ablation). Administration of tamoxifen is previously required to activate Cre recombinase in LECs. For our studies, we used mice of the Prox1-Cre^+-DTRfl/fl genotype to achieve specific deletion of LECs and used the littermate mice that did not bear the Cre transgene (genotype: Prox1-Cre^--DTRfl/fl) as controls.

tamoxifen (TAM). Therefore, in the progeny of interest (Prox1-Cre^+-DTRfl/fl), cells bearing the Prox1 promoter (LECs) express the DTR and are prone to apoptosis once exposed to DT (LEC ablation). Administration of tamoxifen is previously required to activate Cre recombinase in LECs. For our studies, we used mice of the Prox1-Cre^+-DTRfl/fl genotype (Cre^+-DTR mouse) to achieve specific deletion of LECs while the littermate mice of a Prox1-Cre^--DTRfl/fl genotype, that did not bear the Cre transgene (Cre^--DTR mouse), served as control.

Administration of diphtheria toxin (DT) in Prox1-Cre^+- DTR mice induces selective ablation of LECs but the mice do not survive more than 24-48h

First, we sought to confirm the specific ablation of LECs in the generated Prox1-Cre^+-DTR mice. Cre^+-DTR and the littermate Cre^--DTR (Cre^--DTR) control mice were injected with tamoxifen (TAM, 1mg) intraperitoneally, daily for 3-5 days to induce expression of the Cre recombinase. The mice rested for two weeks before we intraperitoneally administered 100ng of DT. The following day, the Cre^+-DTR mice displayed a sub-lethal phenotype and therefore, we sacrificed all mice and collected

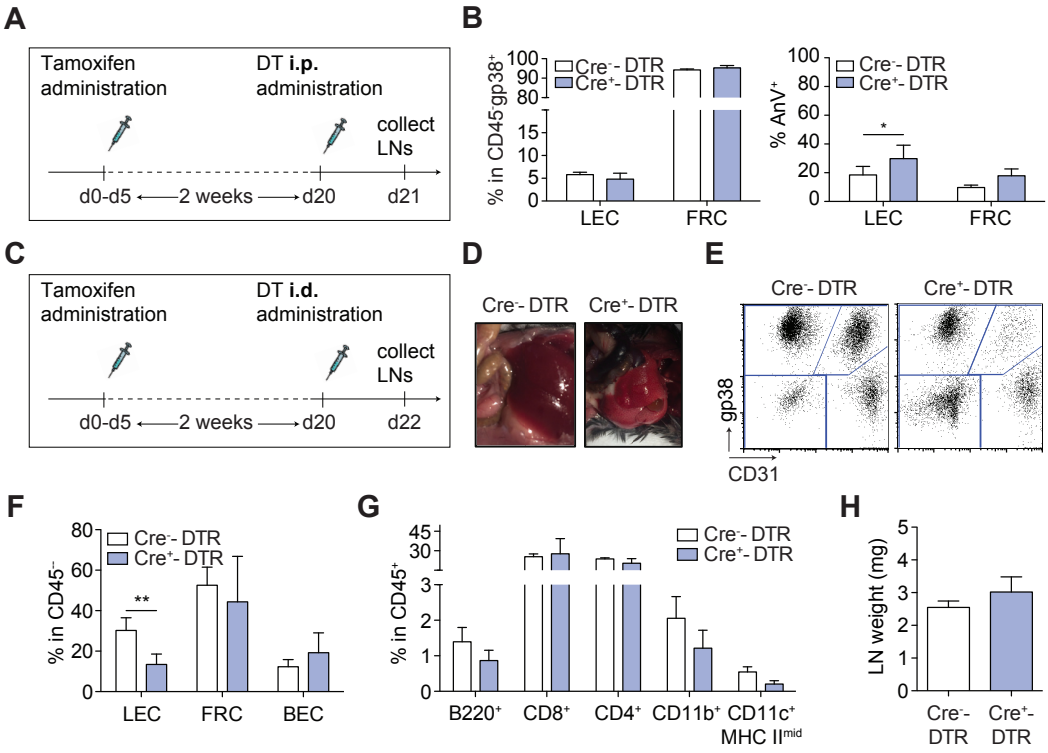

Figure 4.10 Phenotypic changes in the LN following diphtheria toxin (DT) administration in Prox1-Cre^{+}- DTR mice suggest selective ablation of LECs but the mice do not survive more than 24h or 48h following intraperitoneal or intradermal administration of DT, respectively. Cre^{+}-DTR and the littermate Cre^{-}-DTR control mice were administered with tamoxifen (1mg, i.p.) daily for 3-5 days and rested for 2 weeks before they were i.p. injected with DT (100ng/mouse). Up to 24h later, the mice were sacrificed and the skin-dLNs were collected. Cell suspensions were generated and analyzed by flow cytometry. **(A)** Experimental timeline. **(B)** Left, percentage of LECs (defined as gp38^{+}CD31^{+}) and FRCs (gp38^{+}CD31^{-}) among CD45^{-}gp38^{+} cells. Right, percentage of apoptotic cells (AnV^{+}) within LECs and FRCs. The population of LECs was selectively diminished 48h following local administration of DT while the cellularity of other LNSC subsets and hematopoietic cells in the LN was not altered. Two weeks after tamoxifen treatment, Cre^{+}-DTR and Cre^{-}-DTR control mice were (i.d.) injected in the footpads with DT (15ng/mouse). The mice displayed sublethal phenotypes 48h after DT administration; they were sacrificed and the skin-dLNs were collected. Cell suspensions were generated and analyzed by flow cytometry. **(C)** Experimental timeline **(D)** Intestinal hemorrhage and abnormal liver morphology in Cre^{+}-DTR mice. Images of the liver and abdominal contents of Cre^{-}-DTR and Cre^{+}-DTR mice. **(E)** Representative dot plots showing the distribution of LNSC subsets (FRCs gp38^{+}CD31^{-}, LECs gp38^{+}CD31^{+}, BECs gp38^{-}CD31^{+}, DNs gp38^{-}CD31^{-}) gated on CD45^{-} cells. **(F)** Percentage of LECs, FRCs and BECs among CD45^{-} cells in Cre^{-}-DTR (empty bars) and Cre^{+}-DTR (light blue bars) mice. **(G)** Percentage of B cells, CD4^{+} and CD8^{+} T cells and different antigen-presenting cell subsets (CD11b^{+}, CD11c^{+} MHC II^{mid}) within CD45^{+} cells in response to DT treatment. Cell subsets are defined as follows: B220^{+}, CD3^{-}B220^{+}; CD4^{+}, CD3^{+}CD8^{-}CD4^{+}; CD8^{+}, CD3^{+}CD4^{-}CD8^{+}; CD11b^{+}, MHC II^{+}CD11b^{+}; CD11c^{+}MHC II^{mid}, CD11b^{-} CD11c^{+}MHC II^{mid}. **(H)** Weight of LNs in Cre^{-}-DTR and Cre^{+}-DTR mice. Data from one experiment (B, n=4; D-H, n=5). *p≤0.05, **p≤0.01by two-tailed unpaired Student's t test (B, D-H) or two-way ANOVA followed by Bonferroni posttest (G).

the skin-dLNs (Fig. 4.10A). Flow cytometric analysis revealed a slight but insignificant decrease in the frequency of LECs (defined as gp38^{+}CD31^{+}) among CD45^{-}gp38^{+} cells in the LN of mice bearing the Cre transgene (Cre^{+}-DTR) compared to their counterparts in negative littermates (Cre^{-}DTR, Fig. 4.10B left). We further observed an increase in the percentage of apoptotic cells in LN LECs of Cre^{+}-DTR mice, as determined using the annexin V (AnV) marker for apoptosis. We also detected a slight but insignificant increase in the frequency of AnV^{+} FRCs in these mice (Fig. 4.10B, right). In a similar model that had been also developed for the specific ablation of LECs using the LYVE-1 promoter (LYVE-1 - Cre/iDTR mouse), the

authors reported that the mice died without visible edema following systemic administration of DT (18). They discovered that ablation of LYVE-1$^+$ intestinal lacteals destroyed the blood capillaries and deformed the structure of the villi, resulting into severe inflammation of the proximal part of the intestine. We speculated that this phenomenon may have been identically responsible for the poor health of the Prox1-Cre$^+$-DTR mice following systemic DT application, and therefore, we asked whether local administration of DT might induce LEC ablation without distortion of the intestinal barrier. To this end, two weeks after the last dose of TAM, we i.d. injected DT in the upper limbs of Cre$^{+/-}$-DTR mice at a dose of 15ng/mouse (Fig. 4.10C), based on previous publications reporting local ablation in a Cre-DTR system (32). The mice again displayed sub-lethal phenotypes, although this time, the symptoms appeared later, at 48h after DT administration. Examination of the liver and abdominal contents revealed intestinal hemorrhage and abnormal liver morphology in Cre$^+$-DTR mice whereas the organs appeared intact in the control Cre$^-$-DTR mice (Fig. 4.10D). Flow cytometric analysis of the skin-dLNs demonstrated specific ablation of LECs in Cre$^+$-DTR mice (Fig. 4.10E, F). More specifically, the percentage of LECs, among CD45$^-$ cells, was decreased by 56% in Cre$^+$-DTR compared to Cre$^-$-DTR mice, whereas the percentage of FRCs and BECs was not altered (Fig. 4.10F). The specificity of LEC deletion was also confirmed by investigating the hematopoietic cell compartment; no significant changes were detected in the percentage of B cells (B220$^+$), CD4 (CD4$^+$) and CD8 (CD8$^+$) T cells and different antigen-presenting cell subsets (CD11b$^+$, CD11c$^+$ MHC II^{mid}) among live cells following DT treatment in Cre$^{+/-}$-DTR mice (Fig. 4.10G). Adding to that, the weight of the LN was not affected (Fig. 4.10H).

Local ablation of lymphatic vessels in the ear of Prox1-Cre$^+$- DTR mice is achieved by local administration of low-dose DT into the ear skin

Although we achieved specific ablation of LECs in Prox1-Cre$^+$-DTR mice by local DT administration, the mice did not survive, probably due to systemic dissemination of DT and subsequent distortion of the intestinal barrier. We next attempted to minimize adverse side effects on the subject mice by optimizing the administered dose of DT, and opted for a lymphangiography-based approach to assess the presence of lymphatic vessels on a living mouse. This is accomplished by injecting a fluorescent protein into the ear skin, which is easily mounted onto a stereomicroscope, allowing for non-invasive assessment of lymphatic drainage function. This system provides the added advantage of enabling us to minimize the number of animals used, as lymphatic drainage of each ear is independent of the other ear, allowing us to administer multiple doses on the same subject, as well as examine effects in real time as the fluorescent protein was cleared. Two weeks after the last dose of tamoxifen, we injected (i.d.) 1ng of DT in the top of the ear of Cre$^{+/-}$-DTR mice mixed with a fluorescent streptavidin antibody (as the fluorescent protein) and directly performed live imaging of the ear of the anaesthetized mice under a fluorescence stereomicroscope (Fig. 4.11A). Streptavidin fluorescence (shown in green), being rapidly drained, illuminated the network of collecting lymphatic vessels (Fig. 4.11B, left column), demonstrating no differences between Cre$^-$-DTR and Cre$^+$-DTR mice, as expected. The mice received two more doses of DT with a two-day and three-day interval respectively. Administration of DT was always followed by fluorescent streptavidin injection and live imaging. Three days after the second dose of DT, we

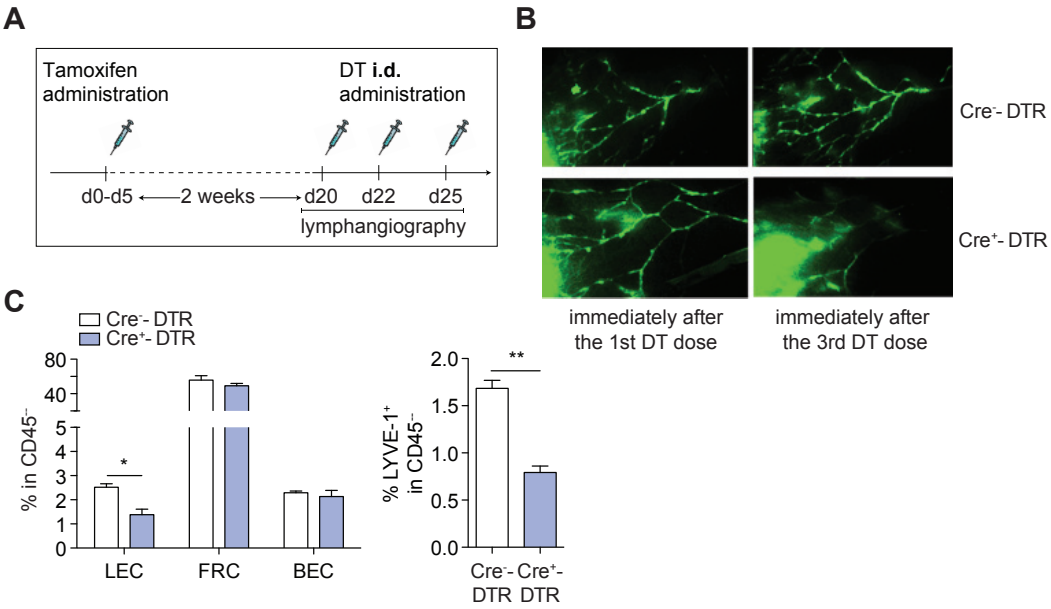

Figure 4.11 Ablation of lymphatic vessels in the ear of Prox1-Cre$^+$-DTR mice by intradermal injection of low-dose DT into the ear skin. Cre$^+$-DTR and the littermate Cre$^-$-DTR control mice were administered with tamoxifen (1mg, i.p) daily for 3-5 days. After 2 weeks, the mice were injected with DT (1ng) in the ear dorsal skin, 3 times with a 2-day and 3-day interval respectively. DT injection was coupled to administration of fluorescent streptavidin and followed by live imaging under the stereomicroscope to assess lymphatic vessel ablation (lymphangiography). 3 days after the last dose of DT, the mice were sacrificed and the ear skin was collected. Cell suspensions were generated and analyzed by flow cytometry. **(A)** Experimental timeline. Ablation of lymphatic vessels in the ear following local administration of low-dose DT in the ear skin. **(B)** Images of the ear skin upon administration of fluorescent streptavidin (green) before DT administration (left column) and 3 days after the second dose of DT (day 25) in control Cre$^-$-DTR (top row) and Cre$^+$-DTR (bottom row) mice. The injection point is marked by increased fluorescence intensity on the bottom left corner of each image. **(C)** Left, percentage of LECs, FRCs and BECs among CD45$^-$ cells in the ear of Cre$^-$-DTR (empty bars) and Cre$^+$-DTR (light blue bars) mice 3 days after the last dose of. Right, percentage of LYVE-1$^+$ cells among CD45$^-$ cells. Data from one experiment (n=3). *p≤0.05, **p≤0.01, by two-tailed unpaired Student's t test.

observed deletion of lymphatic vessels in the ear skin of Cre$^+$-DTR mice while they remained intact in Cre$^-$-DTR mice (Fig. 4.11B, right column, bottom and top images respectively). This was indicated by the absence of drainage visualized by streptavidin fluorescence and its accumulation and leakage at the injection point (bottom left corner in every image). Three days after the last dose of DT, the mice were sacrificed and the ear skin was collected. Flow cytometric analysis validated the observed LEC ablation and demonstrated that the percentage of LECs among CD45$^-$ cells in the ear skin of Cre$^+$-DTR mice was reduced by 45% compared to Cre$^-$-DTR ones, while the frequency of FRCs and BECs was not altered (Fig. 4.11C, graph on the left). Additionally, the percentage of LYVE-1 positive cells among CD45$^-$ cells was diminished in Cre$^+$-DTR mice (Fig. 4.11C, graph on the right), in consistency with our analysis defining LECs as gp38$^+$CD31$^+$. Finally, lymphangiography performed at later time points demonstrated that lymphatic vessels had been completely regenerated 2 weeks after the last dose of DT (data not shown). Although the live imaging assay clearly displayed the ablation of lymphatic vessels in response to DT treatment and the subsequent flow cytometric analysis confirmed our observations, those studies need to be repeated in order to confirm the validity of our findings. Together with our qualitative observations, quantitative analysis of the acquired images at different time

points might provide us with more accurate information with regard to the kinetics of DT-inducible LEC ablation.

Low-dose local DT administration in Prox1-Cre^{+}- DTR mice failed to induce ablation of LECs in the draining LNs

The next step was to evaluate LEC ablation in the dLNs upon local administration of the same low dose of DT that induced deletion of lymphatic vessels in the ear skin. For that purpose, we injected (i.d.) 1ng of DT in the upper limbs of Cre$^{+/-}$-DTR mice, in which the Cre enzyme had been previously activated, and collected the dLNs 24h, 48h and 72h after DT administration (Fig. 4.12A). Flow cytometric analysis revealed no significant differences in the percentage of LECs, as well as FRCs, among gp38^{+}CD45^{-} cells between Cre^{-}-DTR and Cre^{+}-DTR mice at any of the different time points examined (Fig. 4.12B). We also failed to detect any changes in the absolute LEC counts between the two groups (data not shown). Our data show that, at non-lethal DT dose levels that successfully led to local LEC ablation, insufficient DT remains to affect the LECs at the LNs. Therefore, while local depletion of LECs following local DT administration in the Prox1-Cre^{+}-DTR model is feasible, further optimization is required in order to determine non-lethal yet effective doses for deletion of LECs within a greater region, including the injection site and the LN.

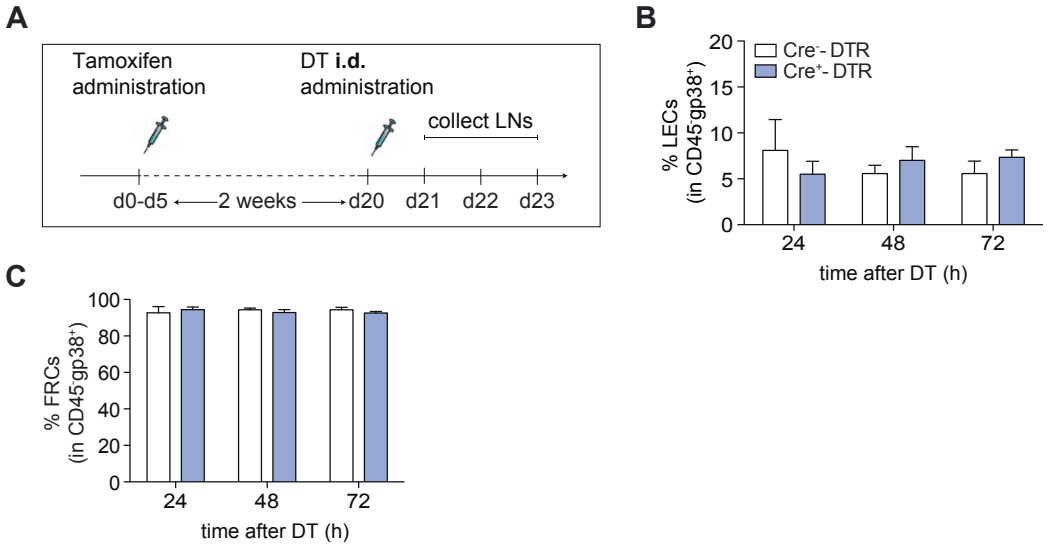

Figure 4.12 Low-dose DT administration in the footpad of Prox1-Cre^{+}- DTR mice failed to induce local ablation of LECs in the draining LNs. Cre^{+}-DTR and the littermate Cre^{-}-DTR control mice were administered with tamoxifen (1mg, i.p.) daily for 3-5 days. The mice rested for 2 weeks before they were i.d. injected with diphtheria toxin (DT, 1ng/mouse) in the footpads. The mice were sacrificed at 24h, 48h and 72h after DT injection and the dLNs were collected. Cell suspensions were generated and analyzed by flow cytometry. **(A)** Experimental timeline. **(B, C)** Percentage of LECs (B) and FRCs (C) among gp38^{+}CD45^{-} cells in the LNs of Cre^{-}-DTR (empty bars) and Cre^{+}-DTR (light blue bars) mice at 24, 48 and 72h following DT administration. Data from one experiment (24h, n=3; 48h, 72h n=7). Two-way ANOVA followed by Bonferroni posttest.

Once the model of LN LEC-specific ablation is established, we speculate it would be a very useful tool to evaluate how the absence of LN LECs might affect the outcome of the primary and secondary immune response.

4.4 Discussion

Our previous studies have demonstrated that LECs can actively scavenge and cross-present exogenous antigens for subsequent MHC I presentation to $CD8^+$ T cells [Chapter 2 and (17)]. LEC-$CD8^+$ T cells interactions under steady-state conditions result in the generation of antigen-experienced cells that remain temporarily inactive, however, they can be functionally reactivated following inflammatory antigenic challenge (Chapter 3). This suggests that, in addition to contributing to the maintenance of peripheral tolerance, antigen uptake by LN LECs might be also directly implicated in the induction of immune responses following infection. Here, we sought to better understand and interpret the impact of LEC-education in the generation of immunity. We first demonstrated that LN LECs can also take up exogenous antigen under inflammatory conditions *in vivo* and evaluated their phenotypic profile in response to inflammatory signals. Then, we showed that LEC-education in the course of inflammation does not alter the phenotype of the educated $CD8^+$ T cells. We employed a subunit vaccine model that triggers robust $CD8^+$ T cell responses while inducing remarkable expansion of the lymph node, characterized by increased LEC proliferation. By using an anti-VEGFR3 blocking antibody, we attempted to inhibit lymphangiogenesis following immunization and thus, assess the impact of LEC-education in the outcome of immune responses. Treatment with anti-VEGFR3 only partially limited LEC proliferation in the lymph node and thus, moderately influenced the expansion capacity, phenotype and functional potential of antigen-specific $CD8^+$ T cells following primary immunization as well as secondary antigenic challenge. In an alternative approach, we generated the Prox1-DTR transgenic mouse model, in which LECs can be selectively ablated. We achieved local ablation of lymphatic vessels in the ear as we tried to optimize the conditions for LEC deletion in the LN, aiming to evaluate the impact of their absence in the induction of immune responses.

LNs can undergo considerable expansion following pathogen infection or immunization, observed already at the early onset and further maintained after the peak of the immune response (11, 15), as well as under various inflammatory conditions, such as chronic inflammatory diseases or tumors (2, 3). Inflammation-induced LEC proliferation, or lymphangiogenesis, is coupled to significant alterations in the lymphatic vessel network and orchestrated by different vascular endothelial growth factors (VEGFs) (4). Here, we exploited a subunit vaccine system, consisting of the model antigen OVA conjugated to our NP platform together with the TLR-9 adjuvant CpG-B. Administration of CpG-B triggered a vigorous expansion of the LN draining the injection site (Fig. 4.1). The size and cellularity of the LN were markedly increased and accompanied by significant alterations in the lymphatic vessel network, as identified by LYVE-1 staining. Similar outcomes have been observed using other adjuvants to trigger LN expansion, such as complete Freund's adjuvant (11), LPS (33, 34) or Montanide (13), as well as following infection with bacterial or viral pathogens (35, 36).

Adding to our previous studies, demonstrating antigen uptake by LECs under steady-state conditions [Chapter 2 and (17)], we showed that LN LECs, in mice previously treated with CpG, took up fluorescently labeled OVA early after intradermal injection *in vivo* (Fig. 4.2). Earlier studies on the presentation of self-expressed

antigens by LNSCs have demonstrated reduced expression of endogenous OVA in FRCs from PolyI:C-treated mice (25). However, here, we observed higher levels of OVA uptake under inflammatory conditions than during homeostasis. Previous studies have also reported that LNSCs, and LECs among them, responded quickly to the co-administration of the TLR-4 adjuvant LPS together with OVA antigen by upregulating the expression of molecules related to antigen-processing and antigen-presentation pathways (34). Along the same lines, our data indicate that LECs can actively perceive and integrate inflammatory signals. Our findings are consistent with a recent study which reported that antigen co-administered with PolyI:C and anti-CD40 was captured by LECs and persisted for more than three weeks following vaccination (16). Interestingly, antigen persistence was dependent on the TLR agonist used.

The phenotype of LECs was altered following CpG administration. This might be attributed to direct sensing of the danger signal, since LECs express various members of the TLR family (25, 37, 38) as well as to indirect inflammatory signals released from $TLR9^+$ cells. Treatment with CpG or *in vitro* stimulation with inflammatory cytokines, that are present in the CpG-inflamed LN, induced identical changes in the phenotype of LECs (Fig. 4.3). Following CpG treatment, we observed upregulation of the MHC class II receptor, the inhibitory ligand PD-L1 and VEGF receptor 3 in LN LECs. The increase in MHC II and PD-L1 is consistent with similar studies showing upregulation of the same molecules under various inflammatory settings (25, 34, 39-41). Inflammation-induced NF-κB signaling has been previously shown to activate VEGFR-3 transcription in cultured LECs (10). These data suggest that LECs are poised to sense inflammatory triggers and actively regulate the expression of key components of the antigen presentation machinery. However, the levels of costimulation in LN LECs remained low and were only slightly affected by CpG treatment, as previously reported following treatment with polyI:C (25) or in the presence of IFN-γ and TNF-α (39).

The balance of costimulatory and coinhibitory molecules in LECs was not reversed under inflammatory conditions. This was reflected on the outcome of antigen-specific LEC-$CD8^+$ T cell interactions in the presence of CpG or inflammatory cytokines; LEC-educated $CD8^+$ T cell retained their activation status and displayed high levels of CD62L (Figure 4.4), as observed under steady-state conditions *in vitro*. Taken together, our findings indicate that LN LECs constantly scavenge exogenous antigens, under both homeostatic as well as inflammatory conditions and thus, support the hypothesis for a dual role of LEC-mediated antigen presentation.

The capacity of LN LECs to generate antigen-experienced $CD8^+$ T cells might be directly linked to the previously discussed LEC proliferation, and subsequent LN expansion, following pathogen infection. We have mentioned earlier that CpG administration might increase VEGFR3 expression on the surface of LECs (Fig. 4.3). With the use of the anti-VEGFR3 blocking antibody (mF4-31C1), we attempted to inhibit LN lymphangiogenesis following immunization with a subunit vaccine and thus, evaluate the effect of the contracted LEC population in the elicited immune response. Treatment with the anti-VEGFR3 antibody is known to block exclusively the new lymphatic growth without abrogating the function of existing lymphatic structures (42). The cellular composition of the stromal cell compartment was not

greatly affected by anti-VEGFR3 treatment (Fig. 4.5). While we observed a consistent trend for a slight contraction of the LEC population among the independent experiments performed, which was not observed for the other stromal cells or the different cell subsets of the hematopoietic compartment, there were no statistically significant effects noted. This might be attributed to decreased efficiency of the blocking antibody with respect to our experimental setup. Alternatively, the inflammatory effects induced by the adjuvant portion of our subunit vaccine might have induced too strong a magnitude of a lymphangiogenic response that the selected dose or administration frequency of the anti-VEGFR3 antibody were unable to counteract. Despite being very effective in abrogating lymphangiogenesis in the context of a tumor at the same dose, as determined by studies performed in our laboratory [(26) and unpublished data], the setting of CpG-induced inflammation might require more radical treatment. More importantly, in addition to VEGFR3, VEGFR2-signaling has also been associated with inflammatory LN lymphangiogenesis (1, 7, 11) and the processed form of VEGF-C can also bind VEGFR2 (43). Additionally, B cells, as well as macrophages and neutrophils have also been associated with the expansion of the lymphatic network following immunization via expression and regulation of VEGF-A, which signals through VEGR2, or VEGF-D (1, 8, 11). Furthermore, medullary FRCs, which come to close contact with LECs have been suggested to promote the expansion of the lymphatic network by providing VEGFs (13). Therefore, other growth factors might also be implicated in CpG-induced inflammatory lymphangiogenesis and combinatory blocking might be required in order to impede it in a more potent way. However, anti-VEGFR2 treatment can also inhibit angiogenesis and possible collateral effects should be taken into consideration. Additionally, Yang et al. recently demonstrated that expansion of FRCs in the LN following immunization was primarily determined by naïve lymphocyte trapping induced by DCs, while homeostatic T-cell proliferation efficiently induced FRC growth (13). Therefore, other than several growth factors, different features of the immune response might be also associated with the enlargement of the LN.

We tried to evaluate how the observed mild contraction of LN LEC upon treatment with anti-VEGFR3 might influence the induction and the functional outcome of the primary and secondary $CD8^+$ T cell immune response (Fig. 4.6, 7, 8). We first employed an adoptive transfer system for our studies presuming that it would allow for detection of antigen-specific $CD8^+$ T cells to a greater degree and thus, enable us to better evaluate the impact of anti-VEGFR3 treatment. Treatment with anti-VEGFR3 only slightly influenced the functional outcome of the primary and secondary immune response using the adoptive transfer model (Fig. 4.6, 7). We failed to detect any significant alterations in the expansion and phenotype of OT-I cells with respect to anti-VEGFR3 administration. However, we did observe a moderate decrease in the frequency of IFN-γ positive cells in the spleen following primary immunization (Fig. 4.6), as well as slightly lower IL-2 positive cells following secondary challenge (Fig. 4.7). Although the impact of anti-VEGFR3 treatment appeared quite moderate, those findings might be attributed to a smaller, or less competent, pool of early antigen-specific $CD8^+$ T cells following the shrinkage of LECs' population. Fewer proliferating LECs would mean fewer $CD8^+$ T cells being educated by LECs. This would, in turn, result in fewer IFN-γ positive cells upon

primary immunization and subsequently, in the establishment of a smaller memory compartment and thus, fewer IL-2 producing cells upon secondary challenge. Under this view, one would expect the effector subsets to be also negatively influenced during the secondary immune response. We noticed a trend for lower IFN-γ and TNF-α positive cells in the LN and spleen of aR3-treated mice, which was, however, not statistically significant. We retrospectively considered that the advantage of the adoptive transfer system might actually smooth out the effects of anti-VEGFR3 treatment in the establishment of immune responses; the abundance of antigen-specific $CD8^+$ T cells, being readily available in the LN and spleen following transfer, might actually decrease the sensitivity of our system. We turned to a non-adoptive transfer experimental setup, to evaluate the impact of blocking VEGFR3 signaling to the endogenous antigen-specific $CD8^+$ T cell population (Fig. 4.8). We observed a lower frequency of the memory effector subset (T_{EM}) upon subunit vaccination in the LN, as well as both in the LN and spleen following challenge immunization for the anti-VEGR3 – treated mice. More importantly, we also noted a decrease in the levels of cytolytic, IFN-γ and CD107a-expressing, effector cells in the spleen of anti-VEGR3 – treated mice during the secondary immune response. Although these studies need to be repeated in order to confirm our observations, the data are consistent with our findings from the adoptive transfer setup while similar trends were observed when a bacterial pathogen was used for the challenge immunization. Most of the alterations in antigen-specific $CD8^+$ T cell cellularity and phenotypic profile in response to aR3 treatment were detected in the spleen; this is consistent with our current hypothesis for the generation of an early pool of antigen-specific $CD8^+$ T cells. At the time points investigated in our studies, which are typically thought to model the peak rather than the early stages of the immune response, the antigen-experienced cells educated by LECs must have been reactivated by professional APCs giving rise to effector cells that exit the LN and head to the periphery. Also, corroborating evidence has recently emerged attributing more active roles to LECs in the generation of protective immunity. Tamburini et al. have recently demonstrated that vaccine-elicited antigen persistence in LN LECs was dependent on LEC proliferation and resulted in immune protection by circulating memory $CD8^+$ T cells (16). Further investigation is required in order to conclude about the effect of limiting lymphangiogenesis on the generation of $CD8^+$ T cell responses following immunization. Our studies indicate that the endogenous model appears more suitable to address the questions posed while the investigation should be extended to different time points upon vaccination.

While blocking VEGFR3 might allow us to interpret the effect of LEC expansion following immunization and its contribution in the outcome of the immune response, it might also entail some side effects that could cloud the clarity of our observations. VEGFR3 is known to be expressed in activated macrophages (28) as well as other $CD11b^+$ monocytic populations (29). Although, here, we have not detected any noticeable alteration in the $CD11b^+$ subset in response to anti-VEGFR3 treatment, as well as to any other subset of the hematopoietic compartment, it is likely that our observations might have been indirectly affected by VEGFR3 blocking. Previous studies have demonstrated that blockade of VEGF-C/D dramatically reduces the infiltration of $CD11b^+$/$Gr\text{-}1^+$ macrophages in the dLN in the course of LPS-induced dermal acute inflammation while it downregulates lymph flow and inflammation resolution (7). Following infection or immunization, the afferent lymphatic vessels

expand to accommodate the increased migration of APCs (15) while HEVs increase in size and quantity to allow for the efficient circulation of naïve T cells (44). Alterations on those main routes for immune cell recruitment upon VEGFR3 blockade will affect trafficking in and out of the LN and might influence our observations in terms of T cell cellularity at specific time lapses during the immune response. In a model of chronic inflammation in obliterative airway disease (OAD), inhibition of VEGFR3 signaling inhibited lymphangiogenesis and reduced infiltration of $CD4^+$ T cells (45). Furthermore, the expression of VEGFR-3 on macrophages has been recently suggested to serve as a negative feedback mechanism to prevent excessive reaction following bacterial infection by regulating proinflammatory cytokine production (28). This suggests that ablation of VEGFR-3 ligand binding on macrophages might impact the microenvironment and thus, influence the phenotype and function of the elicited antigen-specific $CD8^+$ T cells. Therefore, aside from limiting the extensive expansion of LECs, the usage of VEGFR3 might directly affect the function of immune cells as well as indirectly modify the kinetics of the elicited immune response. Those side effects should be taken into careful consideration when interpreting our findings with regard to LECs' contribution in the initiation of adaptive immunity.

In addition to abrogating inflammation-induced lymphangiogenesis in the course of an immune response, we also sought to specifically ablate LECs in order to assess their precise contribution in the development of immune responses. Lineage specific ablation has been a very useful means to investigate the role of FRCs in antiviral T cell responses and revealed an unprecedented function of FRCs in regulating B cell immunity (32). We generated the Prox1-DTR mouse model that allows for conditional LEC ablation *in vivo* (Fig. 4.9) by administration of diphtheria toxin. Systemic administration of DT in the Prox1-Cre^+-DTR mice, as well as high dose of DT via intradermal injection, led to death 24h later while examination of the abdominal contents revealed intestinal hemorrhage and abnormal liver morphology (Fig. 4.10). There was no sign of systemic toxicity induced by DT per se, since the littermate control mice did not display any sign of disease. In a similar model, in which Cre recombinase is directed by the LYVE-1 promoter, administration of diphtheria toxin led to ablation of the intestinal lymphatic vessels and resulted in septic shock and death after 24h, due to dissemination of intestinal pathogens into the circulation (18). Taking into consideration that Prox1 is expressed by various cell types in different organs, including the lacteals and collecting vessels of the ileum and the liver (46), we sought to explore low-dose local administration of DT in order to achieve LEC ablation while preventing intestinal barrier distortion and subsequent death. Intradermal administration of DT in the ear skin resulted in successful deletion of lymphatic vessels in the ear (Fig. 4.11), which reappeared after two weeks with the mice displaying normal phenotypes during this time period. We have not yet managed to optimize local DT administration in the footpads to induce effective deletion of LECs in the dLNs (Fig. 4.12). However, the inducible selective ablation of lymphatic vessels in the ear is a very useful tool for functional assays involving lymphatic drainage and could be harnessed for our purposes of studying the immunological role of LECs in future studies. Our plan would be to immunize the mice with our subunit vaccine, following LN LEC-specific ablation, and subsequently assess the frequency, phenotype and functional potential of the antigen-specific

$CD8^+$ T cells at different time points, early after vaccination as well as after the establishment of memory. As an alternative to this approach, we are currently considering the generation of a LEC-specific MHC I conditional knockout, in which the function of MHC I antigen presentation in LECs would be abolished, or specific antigen targeting to LECs coupled with the elimination of professional APCs in the LN.

Adding to this, it would be challenging to further investigate how the anatomical location of LECs might reflect potential alterations in their immunological role. It has been already reported that LECs in the skin display phenotypic and functional differences compared to LECs in the LN (34, 47). In the context of endogenous self-antigen presentation, Cohen et al. have shown that LN resident LECs display greater tolerogenic potential compared to LECs from peripheral tissues (48), as identified by the variability in PD-L1 expression as well as the levels of the tissue-restricted tyrosinase antigen. Variations have also been detected among the different anatomical subsets of LECs in the LN. Therefore, the microenvironment might actively control the diverse immunomodulatory aspects of LECs. This also introduces the possibility of diverse dedicated LEC subsets, which display plasticity and shape their immunological function depending on localization. Other than the diversity of environmental factors with respect to location, the anatomical positioning is also coupled to differential interactions with immune cells. Thus, location might actively influence the impact of immunological modulation by LECs.

Taken together, we explored two different approaches aiming to illuminate the physiological role of antigen-presentation by LN LECs and its impact in the establishment of adaptive immunity following inflammatory antigenic challenge. Our studies were focused on a setting of acute inflammation, with direct LN hyperplasia following immunization and resolution of the response later on. We have demonstrated that LN LECs can actively scavenge exogenous antigen in an inflammatory setting integrating signals from their microenvironment and we have some first evidence about how limiting LN LEC proliferation in the course of subunit vaccine immunization might affect the immunological outcome of the elicited response. However, our findings might be altered in the setting of a chronic inflammatory disease; it is well established that LEC expansion might have different functional consequences with respect to the site and time frame during inflammation. The developed Prox1-Cre-DTR mouse model provides an additional tool in determining the direct role of LECs in the generation of immunity and the establishment of immunological memory. Integrating the knowledge acquired here in the implementation and design of our ensuing studies will allow us to fully address the questions raised with potentially valuable implications for the design of future vaccines.

4.5 References

1. Halin, C., N. E. Tobler, B. Vigl, L. F. Brown, and M. Detmar. 2007. VEGF-A produced by chronically inflamed tissue induces lymphangiogenesis in draining lymph nodes. *Blood* 110: 3158–3167.
2. Alitalo, K. 2011. The lymphatic vasculature in disease. *Nat. Med.* 17: 1371–1380.
3. Lund, A. W., and M. A. Swartz. 2010. Role of lymphatic vessels in tumor immunity: Passive conduits or active participants? *J Mammary Gland Biol Neoplasia* 15: 341–352.

4. Tan, K. W., S. Z. Chong, and V. Angeli. 2014. Inflammatory lymphangiogenesis: cellular mediators and functional implications. *Angiogenesis* 17: 373–381.
5. Liao, S., and P.-Y. von der Weid. 2014. Inflammation-induced lymphangiogenesis and lymphatic dysfunction. *Angiogenesis* 17: 325–334.
6. Jussila, L., and K. Alitalo. 2002. Vascular growth factors and lymphangiogenesis. *Physiological Reviews*.
7. Kataru, R. P., K. Jung, C. Jang, H. Yang, R. A. Schwendener, J. E. Baik, S. H. Han, K. Alitalo, and G. Y. Koh. 2009. Critical role of CD11b+ macrophages and VEGF in inflammatory lymphangiogenesis, antigen clearance, and inflammation resolution. *Blood* 113: 5650–5659.
8. Tan, K., S. Chong, F. Wong, M. Evrard, and S. Tan. 2013. Neutrophils contribute to inflammatory lymphangiogenesis by increasing VEGF-A bioavailability and secreting VEGF-D. *Blood*.
9. Kaipainen, A., J. Korhonen, and T. Mustonen. 1995. Expression of the fms-like tyrosine kinase 4 gene becomes restricted to lymphatic endothelium during development. In.
10. Flister, M. J., A. Wilber, K. L. Hall, C. Iwata, K. Miyazono, R. E. Nisato, M. S. Pepper, D. C. Zawieja, and S. Ran. 2010. Inflammation induces lymphangiogenesis through up-regulation of VEGFR-3 mediated by NF-kappaB and Prox1. *Blood* 115: 418–429.
11. Angeli, V., F. Ginhoux, J. Llodrà, L. Quemeneur, P. S. Frenette, M. Skobe, R. Jessberger, M. Merad, and G. J. Randolph. 2006. B Cell-Driven Lymphangiogenesis in Inflamed Lymph Nodes Enhances Dendritic Cell Mobilization. *Immunity* 24: 203–215.
12. Soderberg, K. A., G. W. Payne, A. Sato, R. Medzhitov, S. S. Segal, and A. Iwasaki. 2005. Innate control of adaptive immunity via remodeling of lymph node feed arteriole. *Proc. Natl. Acad. Sci. U.S.A.* 102: 16315–16320.
13. Yang, C.-Y., T. K. Vogt, S. Favre, L. Scarpellino, H.-Y. Huang, F. Tacchini-Cottier, and S. A. Luther. 2014. Trapping of naive lymphocytes triggers rapid growth and remodeling of the fibroblast network in reactive murine lymph nodes. *Proceedings of the National Academy of Sciences* 111: E109–18.
14. Halin, C., and M. Detmar. 2006. An Unexpected Connection: Lymph Node Lymphangiogenesis and Dendritic Cell Migration. *Immunity* 24: 129–131.
15. Tan, K. W., K. P. Yeo, F. H. S. Wong, H. Y. Lim, K. L. Khoo, J.-P. Abastado, and V. Angeli. 2012. Expansion of cortical and medullary sinuses restrains lymph node hypertrophy during prolonged inflammation. *The Journal of Immunology* 188: 4065–4080.
16. Tamburini, B. A., M. A. Burchill, and R. M. Kedl. 2014. Antigen capture and archiving by lymphatic endothelial cells following vaccination or viral infection. *Nat Comms* 5.
17. Hirosue, S., E. Vokali, V. R. Raghavan, M. Rincon-Restrepo, A. W. Lund, P. Corthésy-Henrioud, F. Capotosti, C. Halin Winter, S. Hugues, and M. A. Swartz. 2014. Steady-state antigen scavenging, cross-presentation, and CD8+ T cell priming: a new role for lymphatic endothelial cells. *The Journal of Immunology* 192: 5002–5011.
18. Jang, J. Y., Y. J. Koh, S.-H. Lee, J. Lee, K. H. Kim, D. Kim, G. Y. Koh, and O. J. Yoo. 2013. Conditional ablation of LYVE-1+ cells unveils defensive roles of lymphatic vessels in intestine and lymph nodes. *Blood* 122: 2151–2161.
19. Jat, P. S., M. D. Noble, P. Ataliotis, Y. Tanaka, N. Yannoutsos, L. Larsen, and D. Kioussis. 1991. Direct derivation of conditionally immortal cell lines from an H-2Kb-tsA58 transgenic mouse. *Proc. Natl. Acad. Sci. U.S.A.* 88: 5096–5100.
20. Hirosue, S., I. C. Kourtis, A. J. van der Vlies, J. A. Hubbell, and M. A. Swartz. 2010. Antigen delivery to dendritic cells by poly(propylene sulfide) nanoparticles with disulfide conjugated peptides: Cross-presentation and T cell activation. *Vaccine* 28: 7897–7906.
21. van der Vlies, A. J., C. P. O'Neil, U. Hasegawa, N. Hammond, and J. A. Hubbell. 2010. Synthesis of Pyridyl Disulfide-Functionalized Nanoparticles for Conjugating Thiol-Containing Small Molecules, Peptides, and Proteins. *Bioconjugate Chem* 21: 653–662.
22. Fletcher, A. L., D. Malhotra, S. E. Acton, V. Lukacs-Kornek, A. Bellemare-Pelletier, M. Curry, M. Armant, and S. J. Turley. 2011. Reproducible isolation of lymph node stromal cells reveals site-dependent differences in fibroblastic reticular cells. *Front. Immunol.* 2: 1–15.
23. Link, A., T. K. Vogt, S. Favre, M. R. Britschgi, H. Acha-Orbea, B. Hinz, J. G. Cyster, and S. A. Luther. 2007. Fibroblastic reticular cells in lymph nodes regulate the homeostasis of

naive T cells. *Nat. Immunol.* 8: 1255–1265.

24. Broggi, M., M. Schmaler, and N. Lagarde. 2014. Isolation of Murine Lymph Node Stromal Cells | Protocol. *JoVE (Journal of ….*
25. Fletcher, A. L., V. Lukacs-Kornek, E. D. Reynoso, S. E. Pinner, A. Bellemare-Pelletier, M. S. Curry, A. R. Collier, R. L. Boyd, and S. J. Turley. 2010. Lymph node fibroblastic reticular cells directly present peripheral tissue antigen under steady-state and inflammatory conditions. *J. Exp. Med.* 207: 689–697.
26. Lund, A. W., F. V. Duraes, S. Hirosue, V. R. Raghavan, C. Nembrini, S. N. Thomas, A. Issa, S. Hugues, and M. A. Swartz. 2012. VEGF-C promotes immune tolerance in B16 melanomas and cross-presentation of tumor antigen by lymph node lymphatics. *Cell Rep.* 1: 191–199.
27. Rutkowski, J. M., J. E. Ihm, S. T. Lee, W. W. Kilarski, V. I. Greenwood, M. C. Pasquier, A. Quazzola, D. Trono, J. A. Hubbell, and M. A. Swartz. 2013. VEGFR-3 neutralization inhibits ovarian lymphangiogenesis, follicle maturation, and murine pregnancy. *The American Journal of Pathology* 183: 1596–1607.
28. Zhang, Y., Y. Lu, L. Ma, X. Cao, J. Xiao, J. Chen, S. Jiao, Y. Gao, C. Liu, Z. Duan, D. Li, Y. He, B. Wei, and H. Wang. 2014. Activation of vascular endothelial growth factor receptor-3 in macrophages restrains TLR4-NF-κB signaling and protects against endotoxin shock. *Immunity* 40: 501–514.
29. Hamrah, P., L. Chen, C. Cursiefen, Q. Zhang, N. C. Joyce, and M. R. Dana. 2004. Expression of vascular endothelial growth factor receptor-3 (VEGFR-3) on monocytic bone marrow-derived cells in the conjunctiva. *Exp. Eye Res.* 79: 553–561.
30. Saito, M., T. Iwawaki, C. Taya, H. Yonekawa, M. Noda, Y. Inui, E. Mekada, Y. Kimata, A. Tsuru, and K. Kohno. 2001. Diphtheria toxin receptor-mediated conditional and targeted cell ablation in transgenic mice : Abstract : Nature Biotechnology. *Nat. Biotechnol.* 19: 746–750.
31. Buch, T., F. L. Heppner, C. Tertilt, T. J. A. J. Heinen, M. Kremer, F. T. Wunderlich, S. Jung, and A. Waisman. 2005. A Cre-inducible diphtheria toxin receptor mediates cell lineage ablation after toxin administration. *Nat. Methods* 2: 419–426.
32. Cremasco, V., M. C. Woodruff, L. Onder, J. Cupovic, J. M. Nieves-Bonilla, F. A. Schildberg, J. Chang, F. Cremasco, C. J. Harvey, K. Wucherpfennig, B. Ludewig, M. C. Carroll, and S. J. Turley. 2014. B cell homeostasis and follicle confines are governed by fibroblastic reticular cells. *Nat. Immunol.* 15: 973–981.
33. Kang, S., S. Lee, K. Kim, H. Kim, S. Mémet, and G. Koh. 2009. Blood Journal | Toll-like receptor 4 in lymphatic endothelial cells contributes to LPS-induced lymphangiogenesis by chemotactic recruitment of macrophages. *Blood*.
34. Malhotra, D., A. L. Fletcher, J. Astarita, V. Lukacs-Kornek, P. Tayalia, S. F. Gonzalez, K. G. Elpek, S. K. Chang, K. Knoblich, M. E. Hemler, M. B. Brenner, M. C. Carroll, D. J. Mooney, S. J. Turley, Immunological Genome Project Consortium. 2012. Transcriptional profiling of stroma from inflamed and resting lymph nodes defines immunological hallmarks. *Nat. Immunol.* 13: 499–510.
35. McLachlan, J. B., J. P. Hart, S. V. Pizzo, C. P. Shelburne, H. F. Staats, M. D. Gunn, and S. N. Abraham. 2003. Mast cell-derived tumor necrosis factor induces hypertrophy of draining lymph nodes during infection. *Nat. Immunol.* 4: 1199–1205.
36. Kumar, V., E. Scandella, R. Danuser, L. Onder, M. Nitschké, Y. Fukui, C. Halin, B. Ludewig, and J. V. Stein. 2010. Global lymphoid tissue remodeling during a viral infection is orchestrated by a B cell-lymphotoxin-dependent pathway. *Blood* 115: 4725–4733.
37. Pegu, A., S. Qin, B. A. Fallert Junecko, R. E. Nisato, M. S. Pepper, and T. A. Reinhart. 2008. Human lymphatic endothelial cells express multiple functional TLRs. *J. Immunol.* 180: 3399–3405.
38. Wang, P., and Y. Cheng. 2011. Gene expression profile of lymphatic endothelial cells. *Cell. Biol. Int.* 35: 1177–1187.
39. Nörder, M., M. G. Gutierrez, S. Zicari, E. Cervi, A. Caruso, and C. A. Guzman. 2012. Lymph node-derived lymphatic endothelial cells express functional costimulatory molecules and impair dendritic cell-induced allogenic T-cell proliferation. *FASEB J.* 26: 2835–2846.
40. Tewalt, E. F., J. N. Cohen, S. J. Rouhani, C. J. Guidi, H. Qiao, S. P. Fahl, M. R. Conaway,

T. P. Bender, K. S. Tung, A. T. Vella, A. J. Adler, L. Chen, and V. H. Engelhard. 2012. Lymphatic endothelial cells induce tolerance via PD-L1 and lack of costimulation leading to high-level PD-1 expression on CD8 T cells. *Blood* 120: 4772–4782.

41. Dubrot, J., F. V. Duraes, L. Potin, F. Capotosti, D. Brighouse, T. Suter, S. LeibundGut-Landmann, N. Garbi, W. Reith, M. A. Swartz, and S. Hugues. 2014. Lymph node stromal cells acquire peptide-MHCII complexes from dendritic cells and induce antigen-specific $CD4^+$ T cell tolerance. *Journal of Experimental Medicine* 211: 1153–1166.
42. Pytowski, B., J. Goldman, K. Persaud, Y. Wu, L. Witte, D. J. Hicklin, M. Skobe, K. C. Boardman, and M. A. Swartz. 2005. Complete and specific inhibition of adult lymphatic regeneration by a novel VEGFR-3 neutralizing antibody. *J. Natl. Cancer Inst.* 97: 14–21.
43. Joukov, V., T. Sorsa, V. Kumar, M. Jeltsch, L. Claesson-Welsh, Y. Cao, O. Saksela, N. Kalkkinen, and K. Alitalo. 1997. Proteolytic processing regulates receptor specificity and activity of VEGF-C. *EMBO J* 16: 3898–3911.
44. Girard, J.-P., C. Moussion, and R. Förster. 2012. HEVs, lymphatics and homeostatic immune cell trafficking in lymph nodes. *Nat. Rev. Immunol.* 12: 762–773.
45. Krebs, R., J. M. Tikkanen, J. O. Ropponen, M. Jeltsch, J. J. Jokinen, S. Ylä-Herttuala, A. I. Nykänen, and K. B. Lemström. 2012. Critical role of VEGF-C/VEGFR-3 signaling in innate and adaptive immune responses in experimental obliterative bronchiolitis. *The American Journal of Pathology* 181: 1607–1620.
46. Truman, L. A., K. L. Bentley, E. C. Smith, S. A. Massaro, D. G. Gonzalez, A. M. Haberman, M. Hill, D. Jones, W. Min, D. S. Krause, and N. H. Ruddle. 2012. ProxTom lymphatic vessel reporter mice reveal Prox1 expression in the adrenal medulla, megakaryocytes, and platelets. *The American Journal of Pathology* 180: 1715–1725.
47. Amatschek, S., E. Kriehuber, W. Bauer, B. Reininger, P. Meraner, A. Wolpl, N. Schweifer, C. Haslinger, G. Stingl, and D. Maurer. 2007. Blood and lymphatic endothelial cell-specific differentiation programs are stringently controlled by the tissue environment. *Blood* 109: 4777–4785.
48. Cohen, J. N., E. F. Tewalt, S. J. Rouhani, E. L. Buonomo, A. N. Bruce, X. Xu, S. Bekiranov, Y.-X. Fu, and V. H. Engelhard. 2014. Tolerogenic properties of lymphatic endothelial cells are controlled by the lymph node microenvironment. *PLoS ONE* 9: e87740.

Chapter 5

Conclusions, implications and future directions

Throughout this thesis, we explored the immunological role of lymphatic endothelial cells (LECs) with regard to their direct involvement in the induction of immunity and tolerance. We focused on the presentation of exogenous antigens on MHC I by LECs and investigated the immunological outcome of their subsequent interactions with $CD8^+$ T cells. Our findings reveal previously unknown roles of LECs in $CD8^+$ T cell immunity and highlight the diverse aspects of LECs' contribution in immunomodulation.

5.1 Deciphering the physiological significance of antigen presentation by LECs and reconciling their seemingly contradictory functions

When we sought to investigate the immunological role of LECs, the dominant perspective and emerging evidence strongly implicated LECs in the impairment of immune responses. First, various LEC-driven inhibitory mechanisms, mostly indirect, were demonstrated to abrogate the induction of effector $CD8^+$ T cells under steady state or inflammatory conditions. The endogenous expression of peripheral tissue-restricted antigens (PTAs) in LECs and more importantly, their presentation to $CD8^+$ T cells for the induction of deletional tolerance (1) was reported around the same time, to establish LECs as mediators of peripheral tolerance. Subsequently, the ability of LECs to cross-present tumor-derived antigen, resulting in suppression of anti-tumor $CD8^+$ T cell responses, was revealed, opening new questions about a similar role for LECs during homeostasis.

Different pieces of evidence support the concept of LECs as complementary gatekeepers of peripheral tolerance via the presentation of exogenous antigens. Their anatomical position renders LECs as very suitable candidates for

immunological sampling. The lymph, which constantly drains from the periphery to the lymph nodes (LNs), contains peptides and proteins, derived from tissue homeostatic turn-over (2, 3). We hypothesized that LECs, being the first to encounter those antigens upon their arrival in the LN, might be able to capture and cross-present them to subsequently tolerize self-reactive $CD8^+$ T cells. Medullary and cortical LECs come to close contact with naïve T cells as they enter and exit the LN lumen, while subcapsular sinus LECs might intimately interact with naïve T cells reaching the LN via afferent lymphatics. Thus, we speculated that LECs might mimic the function of immature DCs under non-inflammatory conditions and, similarly to other non-hematopoietic antigen presenting cells (APCs), safeguard the uninterrupted preservation of peripheral tolerance.

Our findings were in agreement with our hypothesis; LEC-educated $CD8^+$ T cells proliferated, bearing features of an activated state, but displayed early-generation apoptosis and failed to produce effector cytokines. This indicates that antigen presentation by LECs under steady state conditions might assist peripheral tolerance against draining peripheral self-antigens. In agreement with the earlier studies, our observations reaffirm the concept of LECs' implication in the regulation of immunity, this time via the cross-presentation of exogenous antigens.

Supplementation of the LEC- $CD8^+$ T cell cocultures with exogenous IL-2 did not reverse the dysfunctionally activated phenotypes, indicating that LEC-educated $CD8^+$ T cells are not merely exhausted. Motivated by relevant findings with liver sinusoidal endothelial cells (LSECs), showing that initially "tolerized" $CD8^+$ T cells, primed by cross-presenting LSECs, were reactivated under viral challenge (4), we asked whether LEC-educated $CD8^+$ T cells could exit the non-responsive state. In depth investigation of the functionality of LEC-educated $CD8^+$ T cells demonstrated that the cells can survive in an inactive state with the ability to escape and become functional upon antigenic inflammatory challenge. More specifically, the antigen-specific $CD8^+$ T cells, educated by LECs under steady state conditions, displayed phenotypic and functional memory-like features and gave rise to cytotoxic effector cells following secondary antigen encounter. Importantly, in the setting of a bacterial infection, LEC-educated $CD8^+$ T cells participated in host's protection and further preserved a secondary-memory persistent population. Our data point to an additional role of antigen-presentation by LECs; that of a potential safety mechanism which might complement immune responses when required. These unexpected findings do not contradict our earlier observations for the contribution of LECs in the maintenance of peripheral tolerance. The reactivated cells only gave rise to cytotoxic effectors when stimulated under inflammatory conditions and failed to do so in the presence of immunosuppressive molecules. Our studies indicate that the requirements for the functional reactivation of LEC-educated $CD8^+$ T cells are similar to the ones for naïve cells, preventing the possibility of harmful responses and the induction of autoimmunity. Additional mechanistic studies are needed in order to better characterize, qualitatively and quantitatively, the reactivation threshold in LEC-educated compared to conventional antigen-experienced or naïve $CD8^+$ T cells. Furthermore, we still cannot predict what would be the outcome of $CD8^+$ T cell education against self-antigens, which might also drain to the LN during inflammation and how tolerance would be maintained in this setting.

While our studies have been mainly focused on $CD8^+$ T cell education by LECs under steady state conditions, an evident question is whether LECs alter their behavior during inflammation, induced by pathogen infection or immunization. We demonstrated that LN LECs can also take up exogenous antigen under inflammatory conditions *in vivo.* Their phenotypic profile, in terms of immunological marker expression, was altered suggesting that LECs are prone to sense inflammatory triggers. We observed higher levels of per cell expression of MHC class I, however, we did not observe any significant alterations on the phenotypic profile of LEC-educated $CD8^+$ T cells in response to inflammatory or danger signals.

In light of our findings, we suggest a model in which LECs can constantly sample peripheral antigens present in the lymph, both in the steady-state as well as during inflammation. Due to their advantageous location in the LN, LECs might actually be the first to do so, and they are not expected to discriminate with regard to the origin of the antigen. Following antigen uptake, LECs may interact with naïve $CD8^+$ T cells patrolling the LN in search of their cognate antigen. This interaction would lead to the generation of antigen-experienced $CD8^+$ T cells that would either be apoptotic and die, or survive but remain inactive. In case of homeostasis, presentation of harmless self-antigens would result in the generation of a small pool of antigen-experienced $CD8^+$ T cells, which could not display effector function and would contract over time. In contrast, in case of infection, these cells would be reactivated by professional APCs that have encountered the antigen in the presence of danger signals.

Although further investigation is required to undoubtedly establish the observed double function of antigen-presentation by LECs, it is tempting to speculate on the different roles that it might serve and the different gaps it might fill in the big picture of adaptive immunity. First, it might prevent the induction of autoimmunity without completely eliminating T cell receptor (TCR)-specific $CD8^+$ T cells from the T cell repertoire. This safety mechanism might be very important in case of systemic antigen dissemination before the onset of innate immunity. Several pathogens, such as poxviruses, Hepatitis A and C, and *Salmonella*, have been shown to deploy mechanisms to overcome innate immunity (5). Antigen presentation by immature DCs under non-inflammatory conditions is known to induce tolerance and therefore, LECs' function might rescue pathogen-specific cells from deletion. Secondly, the generation of antigen-experienced $CD8^+$ T cells may supplement and enhance the magnitude of immune responses. The fast drainage of foreign antigen from the periphery, following infection, may lead to the early development of antigen-experienced $CD8^+$ T cells by LECs, which can in turn be amplified once the migrating DCs bearing the antigen reach the LN. Additionally, the unique differentiation state of LEC-educated $CD8^+$ T cells suggests that LECs might also contribute to the development of immunological memory and therefore, contribute to protection in future pathogen infection. The observed persistence of a secondary memory-like subset in LEC-educated $CD8^+$ T cells following pathogenic challenge further supports this notion. Moreover, it is intriguing to think that LECs may be able to sense and integrate signals, such as cytokines and chemokines, in their microenvironment, which in turn, would allow them to direct their diverse functions.

LECs' contribution to the induction of both immunity and tolerance might also help explain the seemingly contradictory roles of lymphangiogenesis in different settings.

On one hand, lymphangiogenesis has been reported to favor suppression of efficient anti-tumor immune responses and promote tumor growth, whereas in the setting of chronic inflammatory disorders, lymphangiogenesis has been linked with deterioration of the disease (6, 7). Through the scope of our findings, these observations can be reevaluated; Antigen presentation by LECs in the tumor-draining LN (-dLN) or in the tumor stroma would result in the induction of inactive $CD8^+$ T cells with non-immediate effector function, as it has been previously reported (8). The possibility that those LEC-educated $CD8^+$ T cells would be reactivated in the immunosuppressive microenvironment of the tumor is very low. Thus, in the context of a tumor, education by LECs would not lead to effective anti-tumor responses but rather be exploited by the tumor to facilitate its progression. In contrast, in a microenvironment rich in inflammatory cytokines and danger signals, as the one usually observed in the setting of chronic inflammation or following transplants, LEC-educated cells would be more prone to reactivation, generating cytotoxic effectors and thus, result in disease aggravation or transplant rejection.

Although our understanding for the immunological role of LECs has grown and we can now better evaluate their implication in the regulation of immune responses, there is still more work to do in order to illuminate the relative significance of their contribution. Earlier reports have underlined the importance of antigen presentation by non-hematopoietic stromal cells in $CD8^+$ T cell expansion using chimeric mice and several infection models (9-11). Those studies suggest that the relevance of antigen presentation by non-hematopoietic stromal cells may be pathogen-dependent as well associated to the kinetics of the immune response. In order to interpret the impact of LEC-education in the generation of immunity, we employed a subunit vaccine model that triggers remarkable expansion of the lymph node coupled to increased LEC proliferation and combined it to treatment with a vascular endothelial growth factor receptor 3 (VEGFR3) blocking antibody. We speculated that by inhibiting lymphangiogenesis and therefore, limiting the number of LECs, we could determine how LEC-education might affect the outcome of immune responses. Treatment with anti-VEGFR3 only partially restricted LEC proliferation in the lymph node and therefore, slightly influenced the expansion capacity, phenotype and functional potential of antigen-specific $CD8^+$ T cells following primary immunization as well as secondary antigenic challenge. Further studies and the development of more elaborate models are required in order to precisely determine the relative importance of LEC versus professional APC antigen presentation.

5.2 Acknowledging the limitations towards the development of more sophisticated tools to study the immunological role of LECs

While our studies have revealed previously unknown functions of LECs, there is still a long way before we truly understand the relative physiological significance of their contributions in the establishment of adaptive immunity. In the absence of a suitable *in vivo* model to study uptake, processing and presentation of exogenous antigens in LECs, we have employed an *in vitro* coculture system using mainly sorted LN LECs from primary cultures and TCR-transgenic $CD8^+$ T cells. The use of cultured LECs cannot exclude the possibility of alterations in their gene expression profile, as it has

been previously observed (12). While keeping this limitation in mind, this 2D system allowed us to study the pathways implicated in antigen trafficking and processing in LECs, to evaluate their phenotypic profile in the presence of T cells, as well as to determine the mechanisms implicated in LEC-$CD8^+$ T cells interactions under different conditions. Furthermore, the established cocultures provided us with satisfying numbers of LEC-educated $CD8^+$ T cells with a reproducible phenotype for subsequent *in vivo* transfer to further investigate their function in the mouse.

Whenever possible, we have exploited approaches in our means to study directly the role of antigen presentation by LECs *in vivo*. We have generated $\beta2m^{-/-}$ BM chimeric mice in order to confirm the *in vitro* observed antigen-specific $CD8^+$ T cell proliferation under steady state-conditions. While this approach enabled us to discriminate between the contribution of hematopoietic versus non-hematopoietic APCs in antigen presentation and subsequent T cell education, it has its own limitations; it requires extensive attention in order to eliminate the effect of radioresistant APCs and more importantly, it does not allow us to distinguish the contribution of LECs among the other lymph node stromal cell (LNSC) subsets. An alternative approach to address this issue would be to combine the use of chimeric mice together with a LEC-targeting platform for the delivery of the antigen or similarly, modified antigen formulations allowing for specific LEC targeting. The mannose receptor is almost exclusively expressed in LECs, among LNSCs ((13) and the Immunological Genome Project Consortium), and thus, this might be an interesting element to exploit. We are currently planning to perform such experiments using mannose-targeting formulations that have been developed in our laboratory. Along the same lines, instead of the chimeric mice, we also consider the use of the CD11c-DTR mice, allowing for deletion of $CD11c^+$ professional APCs (14, 15), coupled to treatment with clodronate-containing liposomes (16) or with the (macrophage-targeting) anti-CSF-1R antibody (17, 18) in order to ablate both dendritic cells and macrophages. Another option for the study of LEC-induced $CD8^+$ T cell response *in vivo* would be the generation of LEC-specific H-$2k^d$ transgenic mice. Such an approach has been previously engaged to evaluate the induction of the $CD8^+$ T cell response by different APCs *in vivo* (19). It would involve the expression of H-$2k^d$ under the Lyve-1 or the Prox-1 promoter to generate transgenic mice that express H-$2k^d$ only on LECs. Immunization with a peptide or a pathogen expressing an immunodominant H-$2k^d$-restricted $CD8^+$ T cell epitope would then allow us to characterize the induction of the $CD8^+$ T cell response by LECs *in vivo*. The expression of Lyve-1 and Prox-1 by other cell types, such as macrophages or hepatocytes, respectively, should be taken into consideration (20, 21).

To assess the precise contribution of LECs in the development of immune responses, we generated the Prox1-DTR mouse model that allows for conditional LEC ablation *in vivo*. Lineage specific ablation has been previously employed to investigate the role of other LNSCs subsets in adaptive immunity (22, 23) leading to revolutionary findings. While we achieved selective ablation of lymphatic vessels in the ear, the Prox1-DTR mouse model displayed several complications; the most important being that systemic administration of diphtheria toxin (DT) resulted in death due to Prox-1 expression in other cell types in several organs, similar to the previously developed Lyve-1 – driven DTR model for LEC ablation (21). We are currently trying to optimize the conditions for local deletion of LECs in the LN, while

keeping in mind that LEC ablation is very likely to trigger significant alterations in the architecture of the LN, which might add another layer of complexity in the interpretation of the observed immunological effects. Under this view, a mouse model that would allow knocking-out specifically the antigen-presentation machinery in LECs would be a more useful tool to investigate their immunological role. We are currently considering the generation of a LEC-specific MHC-I conditional knockout model by crossing the Prox1-CreERT2 mice with the β2m-flox mice, which can be performed in two steps (24). This would allow us to precisely evaluate the contribution of antigen presentation to $CD8^+$ T cells by LECs in adaptive immunity.

Although developing tools to target LECs is not trivial, it would facilitate not only the *in vivo* investigation of their immunological function but also, their therapeutic exploitation. The few approaches that have been explored involve ligands that bind to molecules expressed on LECs, such as hyaluronic acid (25), which can bind to Lyve-1 on LECs, and the LyP-1 peptide, which can bind to p32 protein on tumor associated lymphatics and tumors (26, 27). The LyP-1 peptide has been shown to contain motifs that can bind to neuropilin-2 (NRP-2) on the target cells, while NRP-2–blocking antibodies have recently been shown to reduce tumor lymphangiogenesis (28, 29). Therefore, this is another potential interesting target. Although these approaches present different limitations, combining those with the poly(propylene sulfide) (PPS) nanoparticle (NP) platform that has been widely used in our laboratory for efficient targeted delivery to the LN, might result in the development of a valuable tool for studying LECs *in vivo*. Our laboratory has been actively investigating these different options. Furthermore, a wide range of receptors, such as scavenging, Fc or complement receptors, are expressed on LECs (13, 30) which have not been explored yet as potential targets for LEC-specific engagement.

Another approach to bridge the current gap between *in vivo* and *in vitro* studies would be to take advantage of the emerging systems that try to recapitulate different aspects of the physiological microenvironment and architecture of the LN. It is widely established that the way the cells are cultured, the biochemical and biophysical interactions with their neighboring cells, as well as fluid flow can greatly influence their function (7, 31, 32). Although these systems are not technically simple to develop and still bear the limitation of using primary sorted cells, they can incorporate some of the missing physiological aspects. Our laboratory has been actively working on the development of such a 3D system (33), which can, at least partly, mimic the physiological conditions of mechanical tension and flow, as well as the relevant cell-cell interactions in the context of the LN. We are currently investigating whether by using this system we can replicate our findings derived from the conventional 2D coculture setup.

5.3 Exploiting the immunomodulatory function of LECs for therapeutic applications

Although many questions remain to be answered, our growing perception of the complex immunological role of LECs already prompts us to speculate on whether and how we could exploit their function to modulate immune responses with a therapeutic benefit. Given the diverse impact of LECs in adaptive immunity, as

presented here, different therapeutic interventions could potentially benefit from their immunomodulatory function.

Considering that LECs can generate antigen-experienced $CD8^+$ T cells with a non-terminally differentiated status, which display central memory-like phenotypic and functional characteristics, suggests that they could be usefully integrated in the design of vaccination strategies. It is already well established that the route of administration, as well as the delivery method of the vaccine significantly impact the magnitude of the elicited immune response. Preferential administration via the intradermal route would allow for antigen uptake by LECs, while antigen modification or a specialized LEC-targeting delivery platform could be employed to specifically deliver the antigen to LECs. Antigen presentation by LECs could induce an early pool of antigen-specific T cells with memory-like features while preventing the induction of short-lived effector cells with reduced memory potential, as previously observed in cases of strong inflammatory challenge (34-36). Such a strategy, coupled to a fine-tuned boost immunization might constitute an alternative with beneficial effects in the magnitude and quality of the vaccine-elicited response, providing the required long-lived immunological memory. The design of such vaccines might be more beneficial against pathogens that target lymphoid tissues and harness them for replication, such as HIV or hepatitis (37), or in case of viruses that are known to induce T cell exhaustion (38). Furthermore, this alternative might be worth investigating in case of viruses such as vaccinia virus (VV) or vesicular stomatitis virus (VSV), which infect both hematopoietic and non-hematopoietic cells, and for which LECs have been reported to act as antigen reservoirs (9, 39).

Improved knowledge on LECs immunological function could also aid the development of better strategies for tumor immunotherapy. The direct LEC-driven immunosuppression in the setting of a VEGF-C overexpressing tumor has already been demonstrated and discussed here (8). Different strategies could be employed in order to alter the observed harmful impact of antigen presentation by LECs. Here, we revisit new and previously proposed approaches with respect to LECs' immunomodulatory function. First, the blockade of lymphangiogenesis, which has already been suggested as a therapeutic strategy to eliminate metastasis and tumor progression (6, 40) can be utilized to also limit the scavenging of tumor antigen by LECs and subsequent dysfunctional activation of tumor specific $CD8^+$ T cells. Alternatively, considering that LEC-educated $CD8^+$ T cells can generate cytotoxic effector cells following reactivation under immunogenic conditions, reversing the immunosuppressive microenvironment of tumors might aid in tumor eradication. The targeted delivery of danger signals, as used in adjuvant immunotherapy, and proinflammatory cytokines in the tumor stroma or in the tumor-dLN could be beneficial, since they would turn the dysfunctional LEC-educated anti-tumor $CD8^+$ T cells into CTLs. However, we should bear in mind that LECs themselves are known to produce diverse regulatory molecules implicated in immune suppression, such as TGF-β and IL-10 (30, 41). Switching LEC signaling mechanisms during interaction with $CD8^+$ T cells could be another alternative. Having shown that LEC-$CD8^+$ T cell interactions are primarily governed by the PD-L1 signaling axis, combination therapies of blocking antibodies, which have already being explored for tumor immunotherapy in the clinics (42), might now be re-visited coupled to LEC-targeting or tumor-dLN - targeting platforms. Our laboratory currently explores such strategies.

In the context of chronic inflammation, such as rheumatoid arthritis, inflammatory bowel disease and psoriasis, lymphatic remodeling is known to detrimentally influence disease resolution (43). Similarly, lymphangiogenesis and increased lymphatic density in the grafted tissue has been associated with poor graft survival and rejection. Other than a route of trafficking for APCs and soluble antigen to the LN, along with the enhanced flow of lymph, for the activation of T cells and subsequent immune rejection of the graft, LECs might also directly participate in the induced immune response toward the graft. The use of lymphangiogenic inhibitors, as previously suggested, would be beneficial in these cases by limiting the extent of harmful undesired immune responses.

Although the relative contribution of antigen presentation by LECs in the contexts here discussed has not yet been determined, the therapeutic concept emerging from our studies is that targeting LECs to exploit their immunomodulatory function in combination with other approaches might improve immunotherapeutic strategies and minimize harmful side-effects.

In recent years, the contribution of the lymphatic endothelium in the regulation of immune responses has been gaining appreciation. In this thesis, we established LECs as *bona fide* APCs and revealed their contribution in the maintenance of peripheral tolerance during homeostasis. We unveiled a previously unanticipated role for LN LECs in the modulation of $CD8^+$ T cell responses, including their participation in anti-infectious immunity and the establishment of immunological memory. We developed different tools in order to evaluate the relative significance of LECs' immunological functions and gained valuable insight for their active involvement in the development of adaptive immunity. Collectively, this thesis illuminates the multifaceted immunological role of LECs and further promotes them as major players in several physiological and pathological events, challenging the traditional perception of lymphatics. Hopefully, our findings will be translated into therapeutic advances by exploiting the immunomodulatory features of LECs to enhance the efficacy of future vaccines and immunotherapeutic strategies.

5.4 References

1. Cohen, J. N., C. J. Guidi, E. F. Tewalt, H. Qiao, S. J. Rouhani, A. Ruddell, A. G. Farr, K. S. Tung, and V. H. Engelhard. 2010. Lymph node-resident lymphatic endothelial cells mediate peripheral tolerance via Aire-independent direct antigen presentation. *J. Exp. Med.* 207: 681–688.
2. Clement, C. C., O. Rotzschke, and L. Santambrogio. 2011. The lymph as a pool of self-antigens. *Trends Immunol.* 32: 6–11.
3. Clement, C. C., E. S. Cannizzo, M.-D. Nastke, R. Sahu, W. Olszewski, N. E. Miller, L. J. Stern, and L. Santambrogio. 2010. An expanded self-antigen peptidome is carried by the human lymph as compared to the plasma. *PLoS ONE* 5: e9863.
4. Böttcher, J. P., O. Schanz, D. Wohlleber, Z. Abdullah, S. Debey-Pascher, A. Staratschek-Jox, B. Höchst, S. Hegenbarth, J. Grell, A. Limmer, I. Atreya, M. F. Neurath, D. H. Busch, E. Schmitt, P. Van Endert, W. Kolanus, C. Kurts, J. L. Schultze, L. Diehl, and P. A. Knolle. 2013. Liver-primed memory T cells generated under noninflammatory conditions provide anti-infectious immunity. *Cell Rep.* 3: 779–795.
5. Finlay, B. B., and G. McFadden. 2006. Anti-immunology: evasion of the host immune

system by bacterial and viral pathogens. *Cell* 124: 767–782.

6. Alitalo, K. 2011. The lymphatic vasculature in disease. *Nat. Med.* 17: 1371–1380.
7. Shields, J. D. 2011. Lymphatics: at the interface of immunity, tolerance, and tumor metastasis. *Microcirculation* 18: 517–531.
8. Lund, A. W., F. V. Duraes, S. Hirosue, V. R. Raghavan, C. Nembrini, S. N. Thomas, A. Issa, S. Hugues, and M. A. Swartz. 2012. VEGF-C promotes immune tolerance in B16 melanomas and cross-presentation of tumor antigen by lymph node lymphatics. *Cell Rep.* 1: 191–199.
9. Thomas, S., G. A. Kolumam, and K. Murali-Krishna. 2007. Antigen presentation by nonhemopoietic cells amplifies clonal expansion of effector CD8 T cells in a pathogen-specific manner. *J. Immunol.* 178: 5802–5811.
10. Bassett, J. D., T. C. Yang, D. Bernard, J. B. Millar, S. L. Swift, A. J. R. McGray, H. VanSeggelen, J. E. Boudreau, J. D. Finn, R. Parsons, C. Evelegh, D. Damjanovic, N. Grinshtein, M. Divangahi, L. Zhang, Z. Xing, Y. Wan, and J. L. Bramson. 2011. CD8+ T-cell expansion and maintenance after recombinant adenovirus immunization rely upon cooperation between hematopoietic and nonhematopoietic antigen-presenting cells. *Blood* 117: 1146–1155.
11. Grinshtein, N., T. C. Yang, R. Parsons, J. Millar, G. Denisova, D. Dissanayake, J. Leitch, Y. Wan, and J. Bramson. 2006. Recombinant adenovirus vaccines can successfully elicit CD8+ T cell immunity under conditions of extreme leukopenia. *Mol Ther* 13: 270–279.
12. Amatschek, S., E. Kriehuber, W. Bauer, B. Reininger, P. Meraner, A. Wolpl, N. Schweifer, C. Haslinger, G. Stingl, and D. Maurer. 2007. Blood and lymphatic endothelial cell-specific differentiation programs are stringently controlled by the tissue environment. *Blood* 109: 4777–4785.
13. Hirosue, S., and J. Dubrot. 2015. Modes of Antigen Presentation by Lymph Node Stromal Cells and Their Immunological Implications. *Front. Immunol.* 6: 446.
14. Jung, S., D. Unutmaz, P. Wong, G.-I. Sano, K. De los Santos, T. Sparwasser, S. Wu, S. Vuthoori, K. Ko, F. Zavala, E. G. Pamer, D. R. Littman, and R. A. Lang. 2002. In vivo depletion of CD11c+ dendritic cells abrogates priming of CD8+ T cells by exogenous cell-associated antigens. *Immunity* 17: 211–220.
15. Tittel, A. P., C. Heuser, C. Ohliger, C. Llanto, S. Yona, G. J. Hämmerling, D. R. Engel, N. Garbi, and C. Kurts. 2012. Functionally relevant neutrophilia in CD11c diphtheria toxin receptor transgenic mice. *Nat. Methods* 9: 385–390.
16. Weisser, S. B., N. van Rooijen, and L. M. Sly. 2012. Depletion and Reconstitution of Macrophages in Mice. *J Vis Exp*.
17. MacDonald, K. P. A., J. S. Palmer, S. Cronau, E. Seppanen, S. Olver, N. C. Raffelt, R. Kuns, A. R. Pettit, A. Clouston, B. Wainwright, D. Branstetter, J. Smith, R. J. Paxton, D. P. Cerretti, L. Bonham, G. R. Hill, and D. A. Hume. 2010. An antibody against the colony-stimulating factor 1 receptor depletes the resident subset of monocytes and tissue- and tumor-associated macrophages but does not inhibit inflammation. *Blood* 116: 3955–3963.
18. Ries, C. H., M. A. Cannarile, S. Hoves, J. Benz, K. Wartha, V. Runza, F. Rey-Giraud, L. P. Pradel, F. Feuerhake, I. Klaman, T. Jones, U. Jucknischke, S. Scheiblich, K. Kaluza, I. H. Gorr, A. Walz, K. Abiraj, P. A. Cassier, A. Sica, C. Gomez-Roca, K. E. de Visser, A. Italiano, C. Le Tourneau, J.-P. Delord, H. Levitsky, J.-Y. Blay, and D. Rüttinger. 2014. Targeting tumor-associated macrophages with anti-CSF-1R antibody reveals a strategy for cancer therapy. *Cancer Cell* 25: 846–859.
19. Huang, J., X. Li, K. Kohno, M. Hatano, T. Tokuhisa, P. J. Murray, T. Brocker, and M. Tsuji. 2013. Generation of tissue-specific H-2Kd transgenic mice for the study of Kd-restricted malaria epitope-specific CD8+ T-cell responses in vivo. *J. Immunol. Methods.* 387: 254–261.
20. Truman, L. A., K. L. Bentley, E. C. Smith, S. A. Massaro, D. G. Gonzalez, A. M. Haberman, M. Hill, D. Jones, W. Min, D. S. Krause, and N. H. Ruddle. 2012. ProxTom lymphatic vessel reporter mice reveal Prox1 expression in the adrenal medulla, megakaryocytes, and platelets. *The American Journal of Pathology* 180: 1715–1725.
21. Jang, J. Y., Y. J. Koh, S.-H. Lee, J. Lee, K. H. Kim, D. Kim, G. Y. Koh, and O. J. Yoo. 2013. Conditional ablation of LYVE-1+ cells unveils defensive roles of lymphatic vessels in intestine and lymph nodes. *Blood* 122: 2151–2161.

22. Cremasco, V., M. C. Woodruff, L. Onder, J. Cupovic, J. M. Nieves-Bonilla, F. A. Schildberg, J. Chang, F. Cremasco, C. J. Harvey, K. Wucherpfennig, B. Ludewig, M. C. Carroll, and S. J. Turley. 2014. B cell homeostasis and follicle confines are governed by fibroblastic reticular cells. *Nat. Immunol.* 15: 973–981.
23. Wang, X., B. Cho, K. Suzuki, Y. Xu, J. A. Green, J. An, and J. G. Cyster. 2011. Follicular dendritic cells help establish follicle identity and promote B cell retention in germinal centers. *Journal of Experimental Medicine* 208: 2497–2510.
24. Skarnes, W. C., B. Rosen, A. P. West, M. Koutsourakis, W. Bushell, V. Iyer, A. O. Mujica, M. Thomas, J. Harrow, T. Cox, D. Jackson, J. Severin, P. Biggs, J. Fu, M. Nefedov, P. J. de Jong, A. F. Stewart, and A. Bradley. 2011. A conditional knockout resource for the genome-wide study of mouse gene function. *Nature* 474: 337–342.
25. Jiang, G., K. Park, J. Kim, K. S. Kim, E. J. Oh, H. Kang, S.-E. Han, Y.-K. Oh, T. G. Park, and S. Kwang Hahn. 2008. Hyaluronic acid-polyethyleneimine conjugate for target specific intracellular delivery of siRNA. *Biopolymers* 89: 635–642.
26. Laakkonen, P., K. Porkka, J. A. Hoffman, and E. Ruoslahti. 2002. A tumor-homing peptide with a targeting specificity related to lymphatic vessels. *Nat. Med.* 8: 751–755.
27. Fogal, V., L. Zhang, S. Krajewski, and E. Ruoslahti. 2008. Mitochondrial/Cell-Surface Protein p32/gC1qR as a Molecular Target in Tumor Cells and Tumor Stroma. *Cancer Research* 68: 7210–7218.
28. Xu, Y., L. Yuan, J. Mak, L. Pardanaud, M. Caunt, I. Kasman, B. Larrivee, R. del Toro, S. Suchting, A. Medvinsky, J. Silva, J. Yang, J. L. Thomas, A. W. Koch, K. Alitalo, A. Eichmann, and A. Bagri. 2010. Neuropilin-2 mediates VEGF-C-induced lymphatic sprouting together with VEGFR3. *J. Cell Biol.* 188: 115–130.
29. Caunt, M., J. Mak, W.-C. Liang, S. Stawicki, Q. Pan, R. K. Tong, J. Kowalski, C. Ho, H. B. Reslan, J. Ross, L. Berry, I. Kasman, C. Zlot, Z. Cheng, J. Le Couter, E. H. Filvaroff, G. Plowman, F. Peale, D. French, R. Carano, A. W. Koch, Y. Wu, R. J. Watts, M. Tessier-Lavigne, and A. Bagri. 2008. Blocking neuropilin-2 function inhibits tumor cell metastasis. *Cancer Cell* 13: 331–342.
30. Malhotra, D., A. L. Fletcher, J. Astarita, V. Lukacs-Kornek, P. Tayalia, S. F. Gonzalez, K. G. Elpek, S. K. Chang, K. Knoblich, M. E. Hemler, M. B. Brenner, M. C. Carroll, D. J. Mooney, S. J. Turley, Immunological Genome Project Consortium. 2012. Transcriptional profiling of stroma from inflamed and resting lymph nodes defines immunological hallmarks. *Nat. Immunol.* 13: 499–510.
31. Helm, C.-L. E., M. E. Fleury, A. H. Zisch, F. Boschetti, and M. A. Swartz. 2005. Synergy between interstitial flow and VEGF directs capillary morphogenesis in vitro through a gradient amplification mechanism. *Proc. Natl. Acad. Sci. U.S.A.* 102: 15779–15784.
32. Tomei, A. A., S. Siegert, M. R. Britschgi, S. A. Luther, and M. A. Swartz. 2009. Fluid flow regulates stromal cell organization and CCL21 expression in a tissue-engineered lymph node microenvironment. *The Journal of Immunology* 183: 4273–4283.
33. Pisano, M., V. Triacca, K. A. Barbee, and M. A. Swartz. 2015. An in vitro model of the tumor-lymphatic microenvironment with simultaneous transendothelial and luminal flows reveals mechanisms of flow enhanced invasion. *Integr Biol (Camb)* 7: 525–533.
34. Joshi, N. S., and S. M. Kaech. 2008. Effector CD8 T cell development: a balancing act between memory cell potential and terminal differentiation. *J. Immunol.* 180: 1309–1315.
35. Cui, W., N. Joshi, A. Jiang, and S. Kaech. 2009. Effects of Signal 3 during CD8 T cell priming: Bystander production of IL-12 enhances effector T cell expansion but promotes terminal differentiation. *Vaccine*.
36. Cui, W., and S. M. Kaech. 2010. Generation of effector CD8+ T cells and their conversion to memory T cells. *Immunol. Rev.* 236: 151–166.
37. Trevaskis, N. L., L. M. Kaminskas, and C. J. H. Porter. 2015. From sewer to saviour - targeting the lymphatic system to promote drug exposure and activity. *Nat Rev Drug Discov* 14: 781–803.
38. Wherry, E. J. 2011. T cell exhaustion. *Nat. Immunol.* 12: 492–499.
39. Tamburini, B. A., M. A. Burchill, and R. M. Kedl. 2014. Antigen capture and archiving by lymphatic endothelial cells following vaccination or viral infection. *Nat Comms* 5.
40. Swartz, M. A. 2014. Immunomodulatory roles of lymphatic vessels in cancer progression. *Cancer Immunol Res* 2: 701–707.

41. Podgrabinska, S., P. Braun, P. Velasco, B. Kloos, M. S. Pepper, and M. Skobe. 2002. Molecular characterization of lymphatic endothelial cells. *Proc. Natl. Acad. Sci. U.S.A.* 99: 16069–16074.
42. Nguyen, L. T., and P. S. Ohashi. 2015. Clinical blockade of PD1 and LAG3--potential mechanisms of action. *Nat. Rev. Immunol.* 15: 45–56.
43. Lund, A. W., and M. A. Swartz. 2010. Role of lymphatic vessels in tumor immunity: Passive conduits or active participants? *J Mammary Gland Biol Neoplasia* 15: 341–352.

Efthymia Vokali, MSc

29/01/1986 / Greek nationality
efthymia.vokali@epfl.ch
Chemin des Clochetons 6,
Lausanne 1004,Switzerland
+41 76 23 56 998

EDUCATION

Sep. 2011 – present

PhD candidate in Biotechnology and Bioengineering

Laboratory of Lymphatics and Cancer Bioengineering (LLCB), Swiss Federal Institute of Technology - Lausanne (EPFL) under the supervision of Prof. Melody Swartz

Thesis title: New immunomodulatory roles of lymphatic endothelium and implications for immunotherapy

Expected completion February 2016

Sep. 2009 – July 2011

MSc in Biotechnology and Bioengineering

Swiss Federal Institute of Technology - Lausanne (EPFL)

Master's Project conducted in LLCB under the supervision of Prof. Melody Swartz

Thesis title: Elucidating the mechanisms of Paclitaxel-loaded-Nanoparticle-induced immune response

Sep. 2003 – June 2009

Diploma in Electrical and Computer Engineering

National Technical University of Athens (NTUA)

Specialization: Electromagnetic Waves and Telecommunication

Thesis title: Experimental design for the evaluation of the effects of 3G electromagnetic signals on human brain through EEG and provoked potentials monitoring following auditory stimuli

MAJOR RESEARCH PROJECTS

Sep. 2011 – present

PhD thesis: New immunomodulatory roles of lymphatic endothelium and implications for immunotherapy

-Investigated the role of Lymphatic Endothelial Cells (LECs) on the induction of $CD8^+$ T cell-mediated immunity and tolerance

-Developed expertise in the characterization of stromal cells and in the induction and development of adaptive immunity

-Gained strong experience in animal models and cell culture techniques

-Established collaborations with other research groups in Switzerland

Sep. 2010 – July 2011

Master thesis: Elucidating the mechanisms of Paclitaxel-loaded-Nanoparticle-induced immune response

-Investigated the effects of paclitaxel-loaded-nanoparticles (NPs) on dendritic cells (DCs), with regard to maturation and cytokine production, as well as the potential role of complement in this mechanism

-Worked on the formulation of a nanoparticle-based vaccine for cancer immunotherapy

-Learnt how to synthesize poly(propylene) sulfide (PPS)-core nanoparticles and load them with paclitaxel to target the tumor-draining lymph node

July. 2010 – Sep 2010

iGEM project: Asaia, the pink force against Malaria

-As a member of the EPFL team participating in the international competition of genetically engineered machine (iGEM)

-Engineered a bacterium that naturally lives in the mosquito's gut, to prevent the malaria agent Plasmodium falciparum from infecting the mosquito

PEER-REVIEWED PUBLICATIONS

2014 — Hirosue*, S., E. Vokali*, V. R. Raghavan, M. Rincon-Restrepo, A. W. Lund, P. Corthésy-Henrioud, F. Capotosti, C. Halin Winter, S. Hugues, and M. A. Swartz. 2014. **Steady-state antigen scavenging, cross-presentation, and CD8$^+$T cell priming: a new role for lymphatic endothelial cells.** The Journal of Immunology 192: 5002–5011.

2013 — Thomas, S. N., E. Vokali, A. W. Lund, J. A. Hubbell, and M. A. Swartz. **Targeting the tumor-draining lymph node with adjuvanted nanoparticles reshapes the anti-tumor immune response.** Biomaterials 35: 814–824.

CONFERENCE PRESENTATIONS

2016 — E. Vokali, S. Hirosue, M. Rincon-Restrepo, S.Scherer, A. Mondino, S. Hugues , D. Zehn, M. A. Swartz, **Phenotype and function of CD8$^+$ T cells activated by pMHCI-bearing lymphatic endothelial cells,** poster presented at "Stromal Cells in Immunity" Keystone conference, Keystone, Colorado, USA

2015 — E. Vokali, S. Hirosue, M. Rincon-Restrepo, S.Scherer, A. Mondino, S.Hugues , D. Zehn, M. A. Swartz, **Lymphatic endothelial cells cross-present exogenous antigens to CD8$^+$ T cells to drive a dysfunctional phenotype that can be reactivated upon challenge,** poster presented at ECI conference, Vienna, Austria

2015 — E. Vokali, S. Hirosue, M. Rincon-Restrepo, S.Scherer, P. Courthésy - Henrioud, A. Mondino, S. Hugues , D. Zehn, M. A. Swartz, **Lymphatic endothelial cells cross-present exogenous antigens to CD8$^+$ T cells to drive a dysfunctional phenotype that can be reactivated upon challenge,** poster presented at WIRM conference, Davos, Switzerland

2014 — E. Vokali, S. Hirosue, M. Rincon-Restrepo, W. Lund, V. Raghavan, P. Courthésy-Henrioud, F. Capotosti, C. Halin Winter, S. Hugues , M. A. Swartz, **Lymphatic endothelial cells cross-present exogenous antigens to CD8$^+$ T cells to maintain temporary homeostatic tolerance that can be re-activated upon inflammation,** oral presentation at "Molecular Mechanisms in Lymphatic Function & Disease" Gordon Conference, Lucca, Italy

2013 — E. Vokali, S. Hirosue, M. Rincon-Restrepo, W. Lund, V. Raghavan, P. Courthésy-Henrioud, F. Capotosti, C. Halin Winter, S. Hugues , M. A. Swartz, **Cross-presentation of exogenous antigens by lymphatic endothelial cells drives CD8$^+$ T cell tolerance,** poster presented at the "Tumor microenvironment and Angiogenesis" conference, Ascona, Switzerland

2012 — E. Vokali, S. Hirosue, A. W. Lund, V. Raghavan, P. Courthésy-Henrioud, F. Capotosti, C. Halin Winter, S. Hugues , M. A. Swartz, **Lymphatic Endothelial Cell cross-presentation to CD8$^+$ T cells results in antigen-specific T cell tolerance,** oral presentation at the "Tumor Ecosystem in Cancer Progression and Metastasis" conference, Nice, France

SKILLS

Immunology Techniques	Flow cytometry, immuno-histochemistry, confocal microscopy, ELISA, primary cell isolation, cell culture, small animal handling and experimentation, anesthesia, injections, organ perfusion and collection
Molecular biology and biochemistry	RNA extraction, cDNA synthesis, RT-PCR, DNA and protein electrophoresis, western blot
Software	FlowJo, GraphPad Prism, Adobe Illustrator, Matlab, ImageJ, Ilustrator, Microsoft Office
Languages	English (Fluently spoken and written), French (Proficient), Greek (mother tongue), Japanese (elementary)

OTHER

Interests & Hobbies	Cinema, theater, literature